



Cardiff  
Catalysis Institute

Sefydliad Catalysis  
Caerdydd

---

# **Continuous biomass valorisation with Sn-containing zeolite catalysts**

---

Thesis submitted in accordance with the requirements of Cardiff  
University for the degree of doctor of philosophy by

**Daniele Padovan**

School of Chemistry

Cardiff University

2018

**Supervisor**

Dr. Ceri Hammond

## **Abstract**

This work aims to provide a detailed study of the solid Lewis acid catalyst, Sn-Beta, and particularly focuses on its use as a catalyst for biomass valorisation. Particular emphasis is put on identifying several criteria that are necessary for evaluating the feasibility of the material for intensified operation during the continuous conversion of biomass, such as stability and productivity. The catalyst is tested in continuous flow apparatus for some relevant biomass reactions, such as the valorisation of furfural, and the isomerisation of glucose to fructose. Investigation of the deactivation mechanisms is done by combining kinetic data and characterisation of the material, both fresh and used, in order to relate spectroscopic evidence to catalytic performance. The understanding of deactivation is used to develop countermeasures in order to prevent or mitigate the undesired phenomenon. Important parts of the work are also focused on material synthesis and optimisation, and combinations of different catalysts are also explored, in order to improve the overall performance of the catalytic systems studied within the work.

This thesis begins with a detailed study of the effect of metal loading on the intrinsic activity of Sn-Beta (Chapter 3), where a combination of kinetic experiments and characterisation techniques are presented. This permits identification of the most suitable catalyst for continuous flow catalysis. Continuous flow experiments are then carried out in order to probe the deactivation of the catalyst. A first study of the continuous performance of Sn-Beta focuses on the model reaction of the transfer hydrogenation of cyclohexanone to cyclohexanol (Chapter 4). Following this, the transfer hydrogenation of a more complex system is studied. Particularly, the cascade conversion of furfural to 2-(butoxymethyl) furan, through tandem transfer hydrogenation and etherification over bifunctional Sn-Beta catalysts, is studied (Chapter 5). Having identified the promising stability properties of Sn-Beta during organic phase reactions, the reported “water tolerance” of Sn-Beta is then probed during the continuous isomerisation of glucose to fructose (Chapter 6). Despite showing poor levels of activity and stability in bulk water solvent, excellent continuous performance is observed when solutions of methanol containing small amounts of water (1 – 10 wt. %) are employed. In closing (Chapter 7), the consequences of the findings of this research, in addition to the pertaining challenges these findings open, are also considered.

# Table of contents

## 1. Introduction

1.1 Moving towards a sustainable chemical society.....	1
1.2 Biomass.....	2
1.3 Zeolite catalysts.....	7
1.4 Sn-Beta.....	10
1.5 Reactivity of Sn-Beta.....	12
1.5.1 Baeyer-Villiger reaction.....	13
1.5.2 Meerwein-Pondorf-Verley transfer hydrogenation reduction.....	15
1.5.3 Sugars valorisation.....	16
1.5.4 Bifunctional systems and tandem reactions.....	19
1.6 Sn-Beta synthesis.....	21
1.6.1 Hydrothermal synthesis.....	21
1.6.2 Alternative synthesis of Sn-Beta.....	23
1.7 Process intensification.....	26
1.7.1 Catalyst parameters.....	26
1.7.2 Deactivation during biomass valorisation.....	28
1.7.3 Determine catalyst stability.....	37
1.8 Conclusions.....	39

## 2. Experimental and methods

Abbreviations.....	44
Formula and expressions.....	45
2.1 Catalyst synthesis.....	46
2.2 Kinetic evaluation.....	46

2.2.1 Batch transfer hydrogenation of cyclohexanone and furfural.....	46
2.2.2 Batch etherification of furfuryl alcohol to 2-(butoxymethyl) furan .....	47
2.2.3 Batch glucose isomerisation reaction.....	47
2.2.4 Batch glucose isomerisation reaction with poison molecules.....	48
2.2.5 Continuous flow: transfer hydrogenation and etherification reactions.....	48
2.2.6 Continuous flow: glucose isomerisation and methyl lactate production.....	49
2.2.7 Catalyst regeneration.....	49
<b>2.3 Analytical methods.....</b>	<b>49</b>
2.3.1 Gas chromatography – theoretical background.....	49
2.3.2 Quantification of transfer hydrogenation and etherification products.....	52
2.3.3 High performance liquid chromatography – theoretical background.....	54
2.3.4 Quantification of glucose isomerisation products.....	57
<b>2.4 Characterisation techniques.....</b>	<b>58</b>
2.4.1 Surface area analysis and porosimetry analysis.....	58
2.4.2 Thermo-gravimetric analysis.....	59
2.4.3 Temperature programmed desorption coupled with mass spectroscopy.....	60
2.4.4 Diffuse reflectance infrared Fourier transformed spectroscopy.....	61
2.4.5 Nuclear magnetic resonance.....	62
2.4.5.1 theoretical background.....	62
2.4.5.2 Pulse sequence.....	64
2.4.5.3 Magic angle spinning NMR spectroscopy.....	65
2.4.6 Powder X-ray diffraction.....	67
 <b>3. Identification of active and spectator Sn sites in Sn-Beta and consequences for Lewis acid catalysis</b>	
3.1 Introduction.....	70
3.2 Results and discussion.....	73
3.2.1 Time-online plot as tool to identify the key kinetic parameters.....	73
3.2.2 Activation energy of the process.....	75

3.2.3 Limiting regime of the reaction.....	76
3.2.4 Impact of metal loading on the intrinsic activity.....	78
3.2.5 Characterisation of Sn-Beta.....	82
3.2.6 Textural properties of the catalyst.....	83
3.2.7 Active site characterisation.....	86
3.2.8 Rationalising kinetic data and characterisation.....	92
3.3 Conclusions.....	93

## **4. Intensification and deactivation of Sn-Beta investigated in the continuous regime: cyclohexanone transfer hydrogenation**

4.1	
Introduction.....	95
4.2 Results and discussion.....	97
4.2.1 Continuous flow reactor.....	97
4.2.2 Film diffusion study.....	98
4.2.3 Activation energy of the process.....	100
4.2.4 Preliminary stability study.....	101
4.2.5 Characterisation of used catalyst.....	103
4.2.6 Elemental specific characterisation.....	104
4.2.7 Pore fouling.....	107
4.2.8 Catalyst regeneration.....	111
4.2.9 Optimisation of the system.....	112
4.3 Conclusions.....	116

## **5. Continuous production of 2-(butoxy)methyl furan catalysed by bifunctional Lewis and Brønsted acidic zeolites**

5.1 Introduction.....	118
5.2 Results and discussion.....	121

5.2.1 Preliminary studies of tandem TH/etherification with Sn-Beta.....	121
5.2.2 Study of the etherification step with Lewis and Brønsted acids.....	126
5.2.3 Bifunctional systems.....	130
5.2.4 Synthesis and characterisation of bifunctional catalyst prepared by partial de-alumination.....	132
5.2.5 Continuous performance of physical mixture and bifunctional catalyst.....	136
5.2.6 Identifying deactivation of etherification step during bifunctional continuous catalysis.....	139
5.2.7 Investigation of the lower activity of the bifunctional catalyst.....	141
5.2.8 Solid state incorporation of Al and Sn in a de-aluminate zeolite.....	143
5.2.9 Continuous performance of [2Sn, 0.5Al]-Beta.....	145
5.2.10 Optimisation of the reaction conditions.....	147
5.2.11 Pore volume analysis of used catalyst.....	149
5.3 Conclusions.....	149

## 6. Overcoming catalyst deactivation during the continuous conversion of sugars to chemicals: maximising the performance of Sn-Beta with a little drop of water

6.1 Introduction.....	152
6.2 Results and discussion.....	156
6.2.1 Stability evaluation for glucose isomerisation in water and methanol.....	156
6.2.2 Investigation of the deactivation causes after the reaction in water.....	157
6.2.3 Stability evaluation for glucose isomerisation performed in mixed solvents..	158
6.2.4 Optimal operational window evaluation.....	161
6.2.5 Selectivity as function of water content.....	162
6.2.6 Optimisation of the reaction.....	163
6.2.7 High temperature process: methyl lactate production.....	165
6.2.8 Leaching of Sn during continuous operation.....	167
6.2.9 Understanding the role of water.....	169

6.2.10 Poisoning studies.....	171
6.2.11 TGA and TPD-MS analysis.....	172
6.2.12 Restructuring of active site investigated by $^{119}\text{Sn}$ MAS NMR.....	175
6.2.13 Washing regeneration.....	180
6.3 Conclusions.....	182
 <b>7. Conclusions and pertaining challenges</b>	
7.1 Conclusions.....	185
7.2 Pertaining challenges and final remarks.....	189
 <b>Acknowledgements.....</b>	
	192

# ***1.Introduction***

## **1.1 Moving towards a sustainable chemical society**

Most of the energy produced to sustain human activity in the world is obtained by processing fossil fuel feedstock. Fossil fuels are those that have been formed by natural processes, like anaerobic decomposition of ancient dead organisms.<sup>1,2,3</sup> This slow process began hundreds of millions of year ago, leading to the formation of what today is known as fossil fuel feedstock, found in the form of oil, coal and natural gas. These resources have been exploited since the beginning of the industrial revolution. Since then, the chemical industry was born, and has evolved through modern days in order to exploit, in ever more efficient ways, these resources. First used as source of energy for human activity, from heating sources to power supply for industries, to fuel for transportation, from the second half of the 20<sup>th</sup> century, fossil fuel were widely employed in the newly born polymer industry to make goods that in great part replaced the use of metal and wood. It is clear that fossil fuels are critical for day to day life as it is currently known.

However, many concerns must be raised regarding the usage of fossil resources. Firstly, as the process at the base of their creation involved timescales of millions of years, it is clear



that their synthesis has to be considered non-renewable on a human timescale. As such, there is only a limited quantity of these resources available. Secondly, concerns regarding environmental risk must also be taken into serious consideration. In fact, human activities derived from fossil fuel utilisation largely contribute to the emission in the atmosphere of huge quantities of CO<sub>x</sub> and NO<sub>x</sub>, which are greenhouse gasses that sadly contribute to the global warming effect. Regarding the remaining quantity of fossil fuel feedstock, different estimates about their consumption have been made through the years. Many of these studies indicate that the reservoir of oil could be completely drained within 50-100 years. Since our modern industry and way of life is strictly dependent on this resource and all its derivatives, it is clear that modern research has to increase the effort in finding a solution of this ever-increasing problem. Evidently, optimisation of the current processes and the efficiency of the usage of this resource represents just one way to delay the inevitable ending of the fossil fuel. However, the search for a different raw material in which build a new industry appears to be the most reasonable solution.

On the power front, renewable energies such as solar, geothermic and wind have been proved to possess high potential for supplying energy to most of the anthropogenic activities. Fuel cells, fed by hydrogen derived by electrolysis of water, might also represent an alternative to the modern petrol-powered automotive engine. However, although many alternative energy vectors are possible, the production of polymers and base chemical still require carbon resources. In this light, biomass-based resources represent one of the few realistic solutions regarding the synthesis of chemicals and polymers.

## 1.2 Biomass

Biomass is any material that has an organic origin. It can derive from waste of human activity, or can have both animal and vegetable bases.<sup>4,5</sup> The attractiveness of biomass as an alternative of fossil fuels relays on several factors: i) it is of renewable and/or waste origin, ii) it is delocalised and spread over many parts of the planet, iii) it can be processed for fuel and/or polymer manufacturing, iv) their products can potentially fit into already well established industrial processes, v) the variety of type of biomass allow to obtain a wide arrays of different products, and finally vi) their high functionalisation allow more versatile and completely new molecules to be synthesised. Between all the sorts of biomass, those based from vegetable origin are the most attractive because of their abundance. For

instance, carbohydrates represent 75% of all the renewable biomass feedstock, which is estimated to be produced at  $18 \cdot 10^{10}$  tons year<sup>-1</sup>. Chemists are interested in mainly three way to process vegetable biomass. The first method is its pyrolysis to obtain pyrolysis oil for use in producing heat and energy.<sup>6,7</sup> Another way to process biomass is its conversion to useful products using biological catalysts. Enzymes are generally biological catalysts, and are characterised by very high selectivity for specific reactions. Since they are involved in natural processes, their use with biomass-derived substrates can lead to very efficient and successful processes, such as the fermentation of sugars to produce bio-ethanol<sup>8</sup>. The third method involves the chemical conversion of biomass resulting in the formation of different products, which can be used for several purposes, from the usage for fuel to the synthesis of new classes of chemicals or monomers for the polymer industry.

One of the most abundant types of biomass is lignocellulose, which is the non-edible constituent of the plant cell wall, and thus can be collected as a waste from many activities, such as harvested crops or paper mills industry, for example. However, lignocellulose is not a well-defined homogeneous material. In fact, it has a complex nature, with three main sub-constituents: cellulose, hemicellulose and lignin. They are presents in different quantities, depending of the type of biomass and source of the biomass (Figure 1).

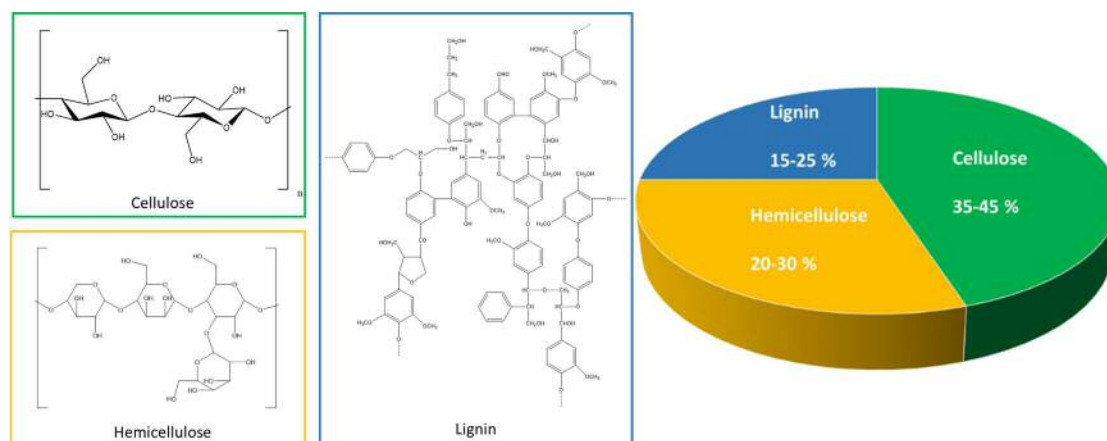


**Figure 1.** (Left) Chemical structure of cellulose, hemicellulose and lignin. (Right) Pie chart graph representing the typical percentages of the lignocellulose constituent.

The diversity of the three components arise from the different building block molecules they are constituted.<sup>9</sup> Lignin is a complex polymer formed mainly of phenolic monomers. The main challenge with respect to the use of lignin is how to break down the bonds between the monomers to obtain the aromatic ring molecules, which are then ready for further

derivatisation. On the other hand, a simpler structure is found for hemicellulose and cellulose. Hemicellulose is an amorphous polymer of various carbohydrates, mainly 5- and 6-carbon rings carbohydrates, such as xylose, mannose, glucose and galactose, only to cite a few. Cellulose, in contrast, is a linear crystalline polymer of glucose units linked by  $\beta(1\rightarrow4)$  bonds. The benefit of using cellulose and hemicellulose is that they are a non-edible source of sugars, in contrast with sugar cane, which is the most common source of sugar and is widely employed in the food industry. The use of such edible feedstock clearly opens an ethical debate, if part of edible resource is used for energy and chemical production.

One of the major challenges of processing lignocellulose in general is that depolymerisation into smaller units is required, so that the constituent parts can be then processed further into final products. For hemicellulose, this is typically achieved by acid catalysis<sup>10</sup>, employing strong mineral acids, such as hydrochloric and sulfuric acid. Amongst all the molecules obtainable after depolymerisation, two sugars are of particularly importance; xylose (aldopentose) and glucose (aldohexose), which are the main constituent monomers of hemicellulose and cellulose, respectively. The chemistry behind these sugars is well established, and their attractiveness relies on the wide range of chemicals that are possible to be obtained by their chemical transformations. In fact, the molecules reachable from these two sugars can cover a wide range of applications, ranging from biofuels to monomers, to bulk commodities such as bio-solvent. Xylose is the main constituent of hemicellulose, and can be readily dehydrated to furfural, a molecule composed of a furanic ring and an aldehyde group.<sup>11</sup> Furfural is produced to a scale of 250 kt y<sup>-1</sup>, and is therefore currently one of the biggest chemicals produced from renewable sources. This molecule is also an important platform. For example, the reduction of the carbonyl group will lead to the corresponding alcohol, which along with its ethers, are promising additives for biofuel applications. In addition, ring-opening products of furfural, such as levulinic acid and its derivatives,<sup>12</sup> occupy a broad area of research. In fact these products can be interested as biosolvents, the most notable of all being  $\gamma$ -valerolactone (Figure 2).<sup>13,14,15</sup>

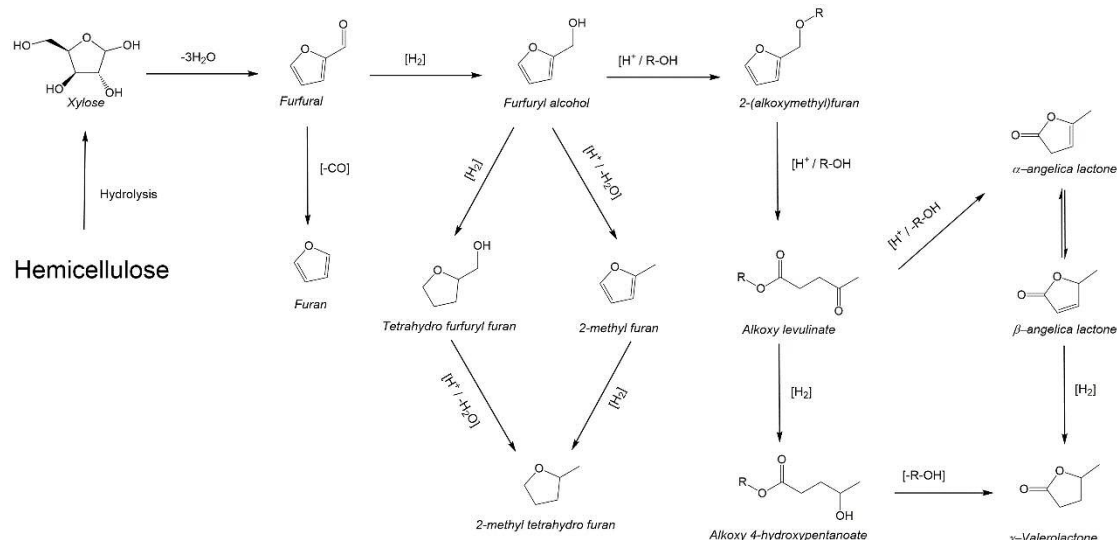


**Figure 2.** General scheme of some of the reaction pathways and products obtainable by hemicellulose valorisation.

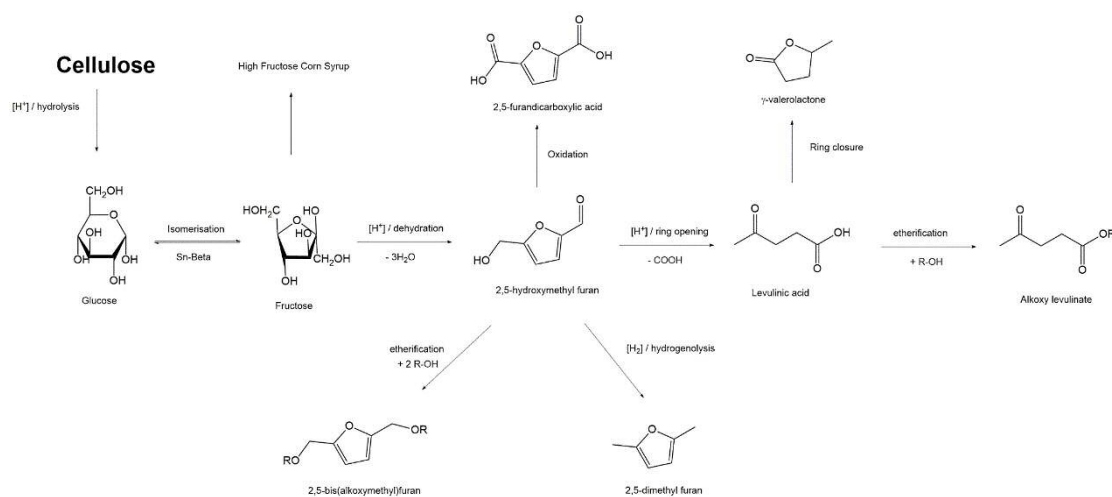


**Figure 3.** General scheme of some of the reaction pathways and products obtainable by cellulose valorisation.

More interestingly again is the valorisation of cellulose (Figure 3), from which glucose can be obtained, as the only constituent monomer of this polymer. Glucose, other than playing a vital role in human metabolism, is also one of the most widely employed substrates in the bio-industry, being the main substrate for the bio-ethanol production *via* fermentation. Another important process, which is the biggest bio-process in the world, is the fermentative isomerisation of glucose to fructose, to make high-fructose corn-syrup (HFCS). Fructose is the ketopentose isomer of glucose, and is much less abundant in nature, hence the need to be industrially obtained by isomerising glucose. Its desirability is due to the fact that is a

much stronger sweetener than glucose. The HFCS produced by this process finds worldwide application, especially in the soft drinks industry. Hence, its currently production is currently about 8 millions t y<sup>-1</sup>. In addition to HFCS production, the isomerisation of glucose to fructose also opens up several potential downstream applications. For example, dehydration of fructose to 2,5-hydroxymethyl furan (HMF) opens up the door to several reaction pathways, which lead to the synthesis of useful products. For examples 2,5-furandicarboxylic acid (FDCA),<sup>16</sup> obtained by oxidation of HMF, is used as bio-monomer for food and drink packaging materials. Due to its similar molecular structure, it is believed to be a possible substitute for terephthalic acid, the primary monomer of polyethylene terephthalate (PET), which is the most widely produced monomer in the bulk chemistry industry, currently produced at over 50 million t y<sup>-1</sup>. If HMF is hydrogenated, 2,5-dimethyl furan (DMF)<sup>17</sup> can be obtained and it is considered a promising biofuel. Levulinic acid and its derivatives can also be produced by ring opening and decarboxylation of HMF, and as it can be seen, these synthetic pathways become analogue to the one obtained by hemicellulose derivatives.

It should be noted that, although fermentative processes allow performing specific reaction with an outstanding degrees of selectivity, they also present some disadvantages. For example, rigid conditions have to be satisfied for the enzyme to operate, not always allowing high productivities to be achieved, nor do they provide much operational flexibility. In addition, the incompatibility of enzymes with many organic solvents or reactants hinders the development of multistep reactions, resulting in a limitation of the type of products obtainable and making the diversification of the chemistry difficult. However, to date many biomass processing have been achieved by enzymatic catalysis, whose costs of the process inevitably rise the cost of the product, limiting their utilisation as commodity chemicals. For these reasons, finding alternatives to the fermentative pathways becomes of crucial importance for developing a sustainable chemistry that uses biomass as starting materials. In this regard, heterogeneous catalysis offers a very good alternative for this kind of chemistry. In fact, the use of heterogeneous catalyst would allow operating under a very broad range of temperatures. They are also compatible with many different organic solvents and the process can be easily engineered in order to obtain a more facile downstream process, such as the catalyst/product separation.

The variety of heterogeneous catalysts employable for biomass valorisation is enormous, so the choice of the class of catalyst must be done following some criteria. Since the fermentative processes suffer most of robustness and low productivity, a heterogeneous

catalyst should have characteristics that allow it to operate intensively at harsher reaction condition, and not be overly influenced by changes in the solvent composition or the presence of different chemicals. Recently, microporous materials, such as zeolites, have been indicated as promising materials to tackle these challenges.<sup>18,19</sup> However, the type of chemistry required to process biomass derived molecule totally differs from the one of fossil fuel origin, in which heterogeneous catalysts, and zeolites in particular, are widely employed. In fact, biomass derived molecules present a high content of oxygenated functional groups, such as carbonyl, alcohol and carboxylic acid, in contrast to fossil fuels where hydrocarbons are the main constituents. Therefore, the chemistry involved in processing this new class of molecules has to be re-thought. Between many class of compound, Lewis acids have proven to be very effective for reaction involving carbonyl group. As such, catalysts possessing this catalytic feature could be good candidates for biomass valorisation. In this context, the Sn-Beta catalyst, belonging to the family of zeolites, has been found to be one of the most successful catalysts for reactions involving biomass-derived substrates. It can be applied to many different reactions, in a very large range of temperatures, it can be used in the aqueous phase as well as with organic media. A more detailed description of this catalyst will follow in the next section.

### 1.3 Zeolite catalysts

As mentioned above, the zeolite Sn-Beta is one of the best candidates for biomass conversion according to the open literature. Zeolites are crystalline aluminosilicate materials, and are characterised by having high surface area and microporous channels. Its constituent unit is a tetrahedral unit, named  $TO_4$ , where T is typically atoms of Si, which represent the main backbone of the silicate structure, and also represents Al in a lower quantities when the material is in its aluminosilicate form. Notably, the small amounts of Al co-present in the structure typically confer the material with catalytic activity. These units are arranged in order to form the so-called building units, like cages and squares. These units are further arranged in the space and their combination forms the final structure of the zeolite, which may vary according to the different arranging of the building units. The zeolite can present a 1D or 3D system of channels whose diameters are within 2 nm, which are defined as micropores. Inside the channels is where the reactions typically take place. Figure 4 shows some of the most common zeolite structures, as adapted from reference 20.

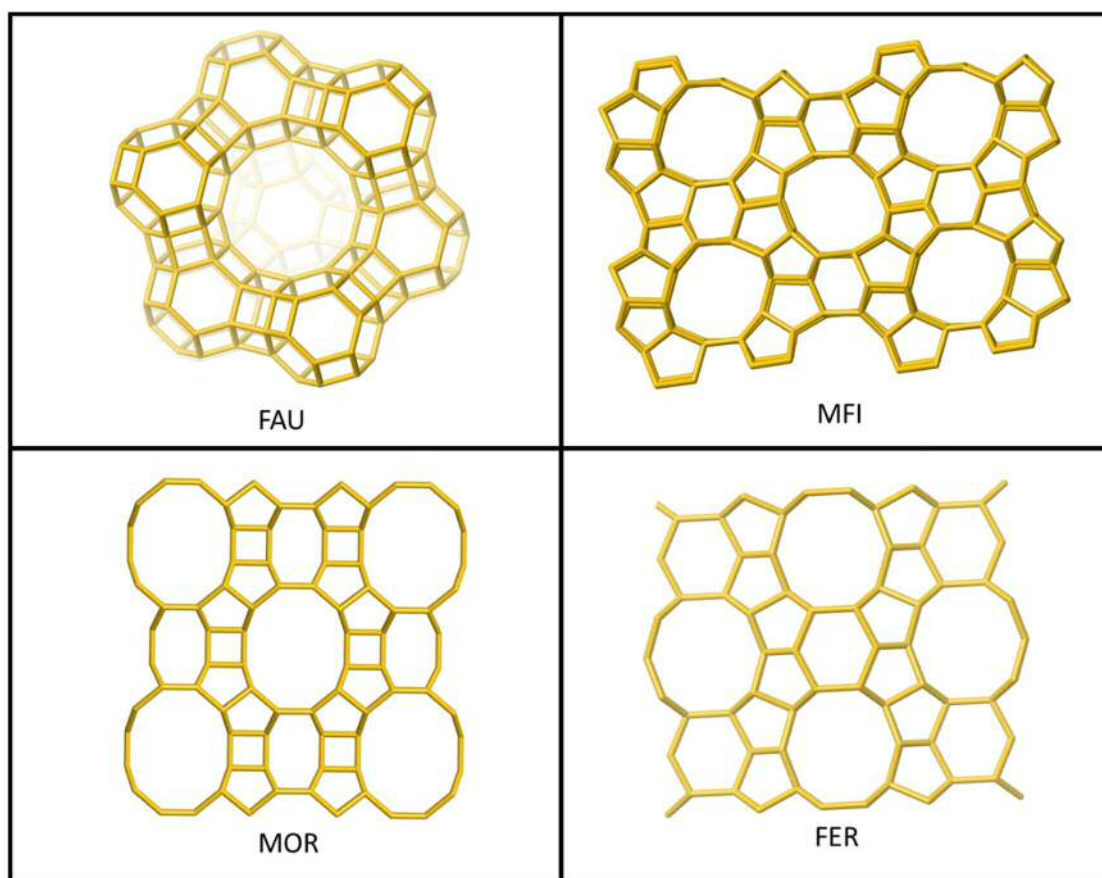


**Figure 4.** Representation of some of the most common zeolite structures. Only the silicon atoms are displayed. From top left to bottom right: Faujasite (FAU), ZSM-5 (MFI), Mordenite (MOR), Ferrierite (FER).

A fully siliceous zeolite would be a crystalline polymorph of silica, and would therefore be a neutrally uncharged solid. When one of the Si atoms is replaced by an Al one, the electroneutrality is lost and a negative charged, centred on the Al atoms, is created. To restore the electroneutrality, a cation is always therefore paired. For example, it could be an alkaline cation, like  $K^+$  or  $Na^+$ , an ammonium ion  $NH_4^+$ , or a proton  $H^+$  (Figure 5). In the case of the proton being the counter-ion, the zeolite exhibits Brønsted acidity. Such protons are highly mobile and easily react with Brønsted bases. This functionality leads to the widespread use of zeolites in the petrolchemical industry. For examples, MFI type of zeolite are employed in the isomerisation<sup>21</sup> or cracking of hydrocarbons.<sup>22</sup> Since the number of protons is proportional to the number of Al, the Si/Al ratio plays a crucial role in tuning the acidity of the material. Interestingly, the reactivity of a particular zeolite does not uniquely depend on the number of Al sites. In fact, the structure of the zeolite also plays a crucial role. The dimension of the channels determines the accessibility of external molecules to the internal structure of the material, in which there is the majority of the surface area and

where the reactions typically take place. This allows zeolites to discriminate based on the shape and dimension of the molecule, a characteristic which results in zeolites also being used as molecular sieves for purification<sup>23</sup> and separation processes.<sup>24</sup>

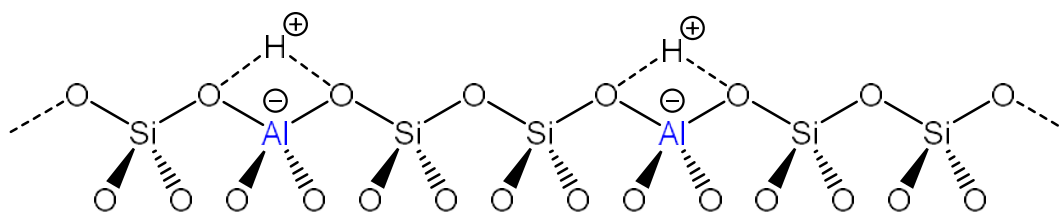


**Figure 5.** Schematic representation of the tetrahedral unit of  $\text{SiO}_4$  and  $\text{AlO}_4$ . A proton is present in the proximity of the aluminium in order to preserve the electroneutrality of the structure.

Conventionally, zeolites are composed of oxygen, aluminium and silicon as main elements. However, in more recent times, aluminium can also be substituted for different metals, known as heteroatoms, which has opened a completely different area in zeolite chemistry. One of the first and iconic heteroatom-containing zeolites is titanium silicalite, more commonly named TS-1.<sup>25,26</sup> In this case, titanium isomorphously occupies a T site in a zeolite possessing a MFI type structure. Being a tetravalent element, electroneutrality in TS-1 is maintained, as shown in figure 6.

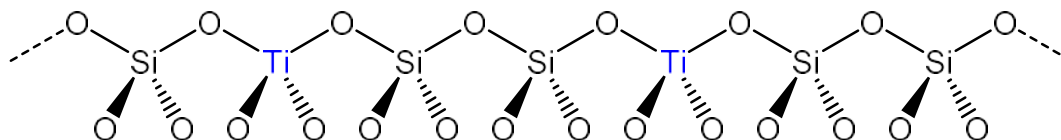


**Figure 6.** Schematic representation of the tetrahedral unit of  $\text{SiO}_4$  and  $\text{TiO}_4$  in TS-1 zeolite. Opposite to conventional zeolite, no cations are needed in the structure in order to preserve the electroneutrality.

TS-1 is the first case of a heteroatom-substituted zeolite that possesses uniquely a Lewis acidic character. By definition a Lewis acid is a species which has an empty orbital and thus can accommodate lone pairs of electrons from a donor, which is then addressed as Lewis base. Typically, TS-1 is employed in liquid phase oxidation reactions involving hydrogen peroxide as green oxidant.<sup>27,28</sup> It can be used for the oxidation of benzene to phenol, or for epoxidation reactions. Since the discovery of TS-1, more effort has been invested in attempting to synthesise new zeolites with improved levels of Lewis acidity, by introducing different heteroatoms in the structure. Amongst many other Lewis acidic elements that can be incorporated into zeolite structures, Sn has been found to be one of the best, rapidly becoming the state-of-the-art of the Lewis acidic zeolites.



## 1.4 Sn-Beta

A Sn containing Beta zeolite was first synthesised by hydrothermal synthesis in 1997 by Mal *et al.*,<sup>29</sup> who were able to synthesise a BEA type zeolite with  $\text{Sn}^{4+}$  atoms tetrahedrally coordinated in the framework. The material later became commonly referred to as Sn-Beta. The BEA topology is actually composed of two different crystalline polymorph structure, commonly named A and B. It is a medium pore type zeolite, with the main member ring being composed of 12 T-atoms, leading to a maximum aperture of 6.7 Å, thus hindering the diffusion of molecules with bigger diameter (Figure 7).

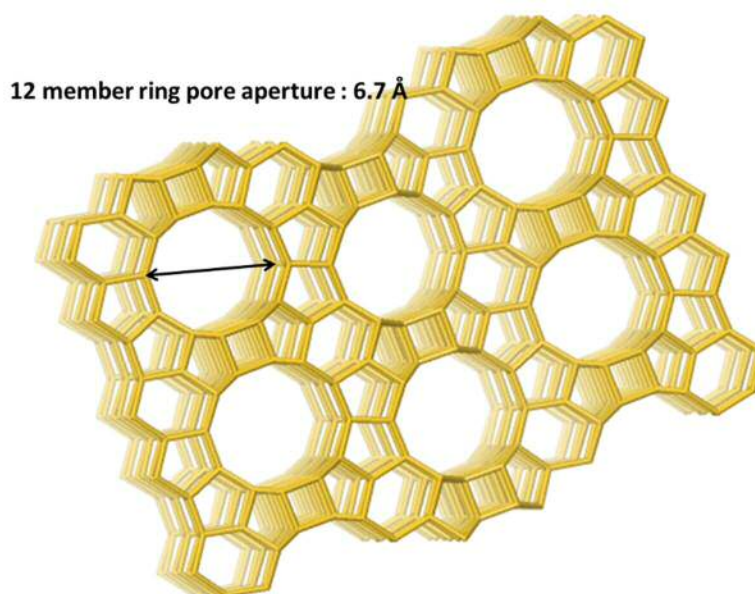


**Figure7.** Representation of the BEA zeolite structure.

Since its first synthesis, different synthetic methodologies have been developed, and different catalytic reactions have also been explored, making Sn-Beta one of the most studied catalyst of its kind in recent years. Sn belongs to the 14<sup>th</sup> group of the periodic table, thus when is tetracoordinated in the zeolitic framework it maintains electroneutrality of the framework, in the same way as Si. Therefore, the structure remains neutral, so no Brønsted acidity is developed upon the insertion of tin, and no cation-exchange sites are formed. Instead, the materials acquire a strong Lewis acidic character, due to the presence of Sn. In particular, there is a strong affinity for Sn to interact with carbonyl groups, thanks to the favourable interactions between a hard acid ( $\text{Sn}^{4+}$ ) and a hard base (carbonyl group), as described by the hard and soft acid and base theory (HSAB). However, not all Sn atoms present in the zeolite are active. In fact, if the Sn atoms do not occupy the T sites, they will

agglomerate to form polymeric  $\text{SnO}_2$ -like species, often called extra-framework species. Such species do not show typical levels of Lewis acidic activity, thus resulting in their inactivity for the reactions in which Sn-Beta is typically employed. Furthermore, it is believed that not all the active sites are the same even if all Sn atoms are within the framework. In this sense, it is possible to differentiate different active site considering at least two different parameters: the T site location and the chemical form of the active site. Within the highly ordered BEA structure, at least nine non-equivalent T sites can be identified.<sup>30,31</sup> Even though they can look similar at first sight, the specific T site in which the Sn is located can greatly affect the accessibility of the reactant molecules and the specific geometry of the Sn-O bonds, having potential effect on the activity of the sites. Another factor that is believed to strongly impact the activity of the Sn sites is the chemical form. In fact, two main species of framework Sn are often proposed in literature, those being the open and closed form. Typically, the first of these is often believed to be the true, and most active, form of the Sn (Figure 8).<sup>32</sup>

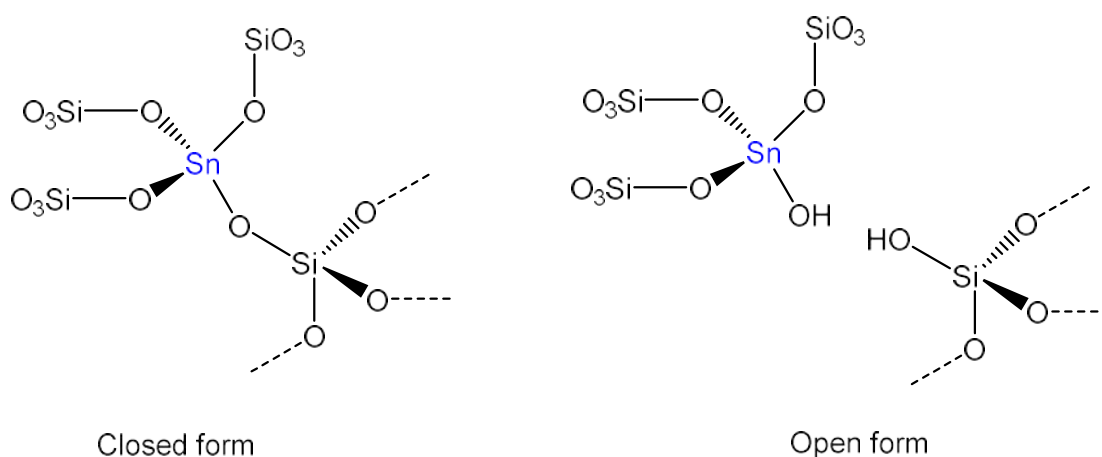


**Figure 8.** Graphical representation of the two proposed Sn active site of Sn-Beta. The closed form is found on the Left, while on the Right the open form is shown. For clarity, all the coordinated molecules (e.g. water) have been omitted and only covalent bonds are shown.

The closed form is a tetrahedrally Sn atom, fully coordinated and enclosed in the zeolite structure. In contrast, the open form presents at least one hydrolysed Sn-O bonds, the simplest of which is the mono-hydrolysed, as shown in figure 8. Notably, weakly coordinated water molecules can also be present on the central Sn atom, resulting in the isomorphously-substituted site obtaining a penta- or hexa-coordinated form.<sup>33</sup> This structure presents a hydroxyl group in the proximity to the active Sn site that is believed to participate directly to the reactions. Some computational studies showed that having a hydroxyl group in the vicinity can significantly lower the activation barrier of a particular reaction undergoing catalysis by Sn-Beta.<sup>34</sup> In this specific case, the isomerisation of sugar was used in the

model.<sup>35,36</sup> Nevertheless, strong and irrefutable experimental evidence that support the existence of these two different forms of active site are yet to be found. In fact, the existence of open and close form was first hypothesised when acetonitrile adsorbed on the material showed two slightly different stretching frequencies following temperature programmed desorption.<sup>37,38</sup> In this case, as the acetonitrile desorbed from the material, a shift in wavenumber was observed, subsequently attributed to interaction with a different forms of Sn. Acetonitrile is often used to probe the strength and numbers of Lewis acid sites, having the ability to coordinate with this active centre and give a specific stretching, detectable by IR spectroscopy. However, it is under debate if that observed shift in stretching frequency is actually due to interaction of acetonitrile with a different Sn site, or it arises from interactions of acetonitrile-Sn adduct and other acetonitrile molecule in the vicinity, thus changing as the coverage of probe molecules vary.<sup>39</sup>

Even though the real form and location of the active site is at the centre of an academic debate, its ability to activate and react with carbonyl moieties has made of Sn-Beta of the most promising catalyst for valorisation of biomass-derived molecules.

## 1.5 Reactivity of Sn-Beta

Along with TS-1, Sn-Beta is one of the most studied and employed heteroatom substituted zeolites. Its success is due to the large number of theoretically “green” processes it can catalyse. Many of the processes that Sn-Beta can efficiently catalyse can have a potentially huge impact in developing sustainable and feasible routes to new types of molecules, such as new bio-polymers, or to substitute existing fossil fuel-derived product. In Figure 9, some of the most important reactions are highlighted and it can be seen that Sn-Beta can be employed as a catalyst for a variety of sustainable chemical transformations. A key example includes the Baeyer-Villiger Oxidation (BVO)<sup>40,41,42,43</sup> for converting ketones to lactones using hydrogen peroxide as green oxidant. Another very import application of Sn-Beta can be found in the transfer hydrogenation (TH) reaction, of the type of the Meerwein-Ponndorf-Verley reduction (MPV).<sup>44,45,46</sup> This consists of the reduction of a ketone or an aldehyde into the respective alcohol, employing a sacrificial alcohol as the hydrogen donor. Considering the high number to oxygenated groups present in typical biomass feedstock, the ability to reduce the substrate is essential for successful processing of these compounds to be achieved. The etherification of alcohols<sup>47,48</sup> and various aldol condensation reactions<sup>49,50</sup> are

also attractive route for growing the carbon chain, and hence decreasing the relative oxidation, of various organic molecules, leading to potential application as bio-fuels or additives. These reactions, in addition to epoxide ring opening, whose 1,2-diols products can found employment as monomers for bio-polymers, are other example, in which Sn-beta can be used as a potential heterogeneous Lewis acid catalysts.<sup>51</sup>

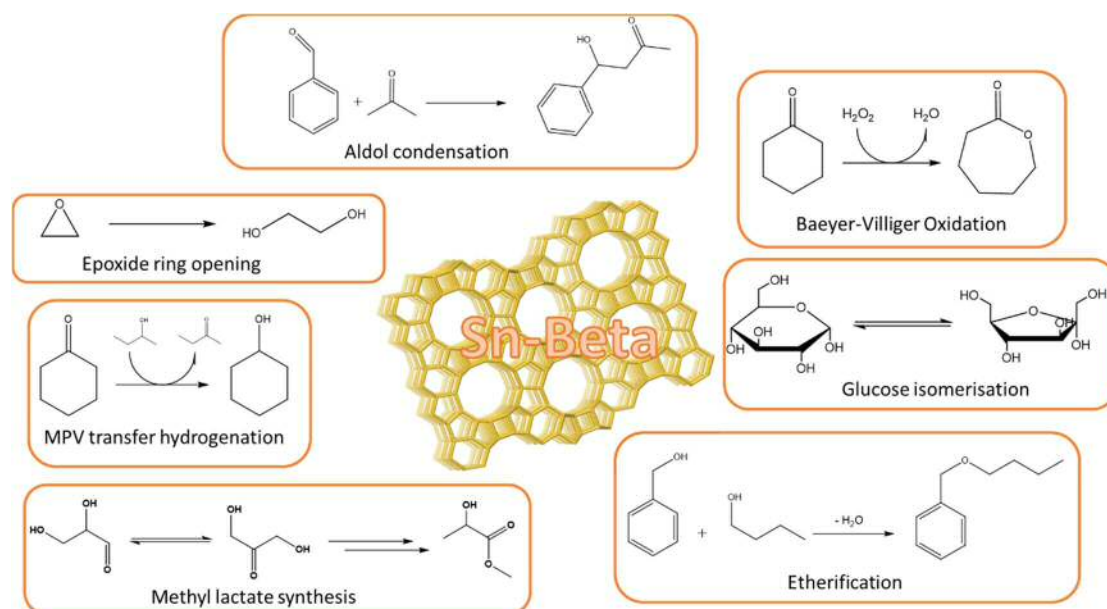


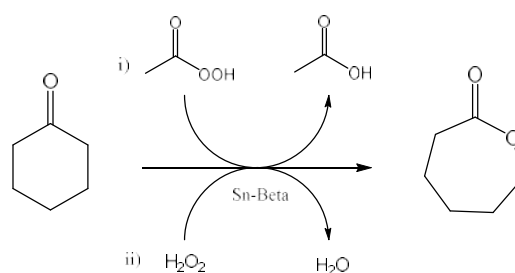
**Figure 9.** Summary of some of the reactions that can be catalysed by Sn-Beta.

However, the largest potential impact of Sn-Beta is realised in the field of sugar upgrading. Indeed, it has been shown that Sn-Beta is able to carry out various sugar valorisation reactions even in the presence of bulk water, something that was considered impossible for a classic Lewis acid catalyst to achieve. Glucose isomerisation and methyl lactate synthesis are the two key reactions that rapidly become of industrial interest, and to date, Sn-Beta has been shown to be the best candidate for an eventual commercialisation of these process.<sup>52,53</sup> The following section presents a more detailed description of some of the most interesting reactions mention above, and in particular how TH of ketones and sugars isomerisation shows a very similar mechanistic pathways.

### 1.5.1 Baeyer-Villiger reaction

First reported by Corma *et al.* in 2001, Sn-Beta has been employed as selective catalyst for the BVO reaction of cyclohexanone to caprolactone with  $\text{H}_2\text{O}_2$  as green oxidant.<sup>54,55</sup> The BVO reaction is classically used to convert a ketone into a lactone or ester, by oxidation with a

peracid. An extremely important example is the BVO of cyclohexanone to caprolactone, industrially achieved by BVO using peracetic acid or meta-chloroperoxybenzoic acid (mCPBA) as oxidant. Caprolactone is the monomer of polycaprolactone, and a key precursor to caprolactam, and is produced in a scale of 4 million t y<sup>-1</sup>. Unfortunately, the use of stoichiometric quantities of the peracid leads to equimolar production of the corresponding organic acid as by-product. This necessitates additional downstream operations in order to neutralise the solution and separate the product, and lowers the atom efficiency of the reaction. The use of Sn-Beta as catalyst for BVO with H<sub>2</sub>O<sub>2</sub> would lead to production of water as by-product, without the need of any complication from the point of view of downstream operations. In figure 10 the two processes are compared.

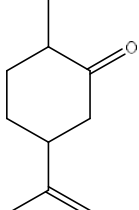
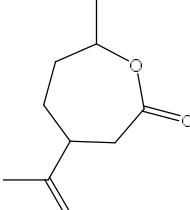
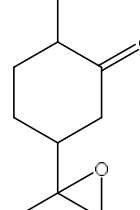
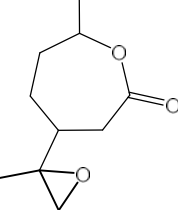


**Figure 10.** BVO reaction for cyclohexanone conversion into caprolactone by i) classical route using peracetic acid and ii) alternative route using H<sub>2</sub>O<sub>2</sub> catalysed by Sn-Beta.

Sn-Beta has shown an outstanding selectivity for the BVO oxidation. Typically, when a substrate with more than one functionality amenable to reacting with peroxide is present in a molecule, multiple products can form. However, Corma *et al.* showed that for 2-methyl-5-(prop-1-en-2-yl)cyclohexan-1-one, a molecule containing both a carbonyl group and a C=C double bond, was reacted over Sn-Beta, Ti-Beta and mCPBA, only Sn-beta showed 100 % of selectivity on the BVO reaction (Table 1). Although Ti-beta was able to produce the epoxide product, no BVO reaction products were detected. Similarly, the peracid formed a mixture of BVO and epoxidation products. This reflects the substantial difference in the reaction mechanism between Sn and Ti, and nicely highlights the unique reactivity of Sn-Beta. Ti, when tetrahedrally incorporated into a zeolite lattice, instead of activating the organic substrate, strongly activates the peroxide through formation of a metal-hydroperoxo or metal-hydroperoxo intermediate. In doing so, hydrogen peroxide becomes more reactive, with the consequence that it reacts with the double bond to form epoxide. On the other hand, Sn-Beta strongly binds to the carbonyl oxygen atom, making the carbon more electrophilic and then susceptible to react with a nucleophile. In other words, Sn-beta does not activate the oxidant through formation of active metal-hydroperoxo species, thus

resulting inactive for the BVO reaction.<sup>55</sup> The understanding of Sn-Beta mechanism of the BVO reaction pushed researchers to explore different reactions in which the carbonyl-activating ability of this catalyst could be further exploited.

**Table 1.** Summary of reaction of 2-methyl-5-(prop-1-en-2-yl)cyclohexan-1-one with different system under the same experimental conditions. Table adapted from reference 26.

Catalyst	Reactant Conversion / %	Products selectivity / %		
				
Sn-Beta / H <sub>2</sub> O <sub>2</sub>	68	100	0	0
Ti-Beta / H <sub>2</sub> O <sub>2</sub>	48		80	
mCPBA	85	11	71	18

### 1.5.2 Meerwein-Pondorf-Verley transfer hydrogenation reduction

Following the search of other potential applications of Sn-Beta, Corma *et al.* showed that such stannosilicate zeolites are able to performed TH reactions of carbonyl group. In fact the reduction of cyclohexanone (CyO) to cyclohexanol (CyOH) was successfully accomplished as shown in figure 11.

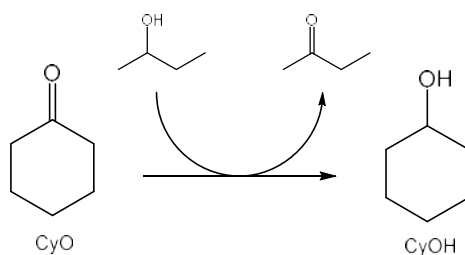


**Figure 11.** Scheme of the MPV cyclohexanone transfer hydrogenation to cyclohexanol.

This particular reaction is a transfer hydrogenation (TH) type of reaction, in which a nominal hydrogen molecule is used to reduce a ketone or aldehyde to its respective alcohol. The main advantage of TH reaction is that the reduction is carried out without using gaseous molecular hydrogen, thus avoiding the high risks associated with its flammability. To achieve this, a sacrificial molecule is used as hydrogen source. Secondary alcohols are amongst the

best option. In these cases, the alcoholic group is co-oxidised into a carbonyl. Sn-Beta has shown to be an order of magnitude more active than Ti-Beta and Al-Beta for the TH of cyclohexanone to cyclohexanol in 2-butanol under the same conditions. Indeed, turn over frequencies ( $\text{mol}_{\text{conv.}} \text{mol}_{\text{metal}}^{-1} \text{h}^{-1}$ ) of 130, 6 and 12 were calculated for Sn-Beta, Ti-Beta and Al-beta, respectively.<sup>44</sup> In Figure 12, an exemplified scheme of the catalytic cycle of MPV of cyclohexanone to cyclohexanol is shown.

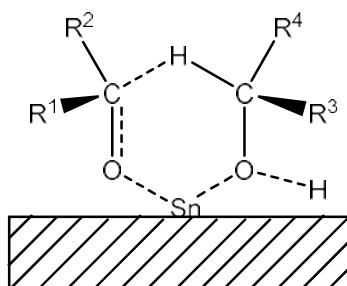


**Figure 12.** General scheme of the proposed 6-membered ring transition state of the MPV reduction of ketone to alcohol.

Regarding the mechanism of the TH reaction, it is generally accepted that the oxygen of the ketone and of the alcohols are simultaneously coordinated to the Sn atom to form a 6-membered ring intermediate, as shown in figure 12. The strong polarisation that the Sn exercises on the carbonyl group makes the carbonylic carbon more electrophilic, favouring the transfer of one hydrogen atom, formally as hydride, from the alcoholic carbon to the carbonylic carbon. It is believed that the open form of Sn in Sn-Beta can help the reaction pathways by moving around the hydrogen atoms with the hydroxyl group that are in the proximity of the active site. Remarkably, it was demonstrated that this reaction could happen in the presence of water, probably thanks to the hydrophobic environment of the zeolite. In fact, upon the introduction of 10 wt.% of water in the solution, high levels of activity were still observed. Since many biomass-derived molecules possess carbonyl group, and water is almost always present in biomass-derived solutions, Sn-Beta can potentially be exploited for the conversion of biomass derived molecules.

### 1.5.3 Sugars valorisation

The main breakthrough on the use of Sn-Beta is its ability to act as Lewis acid even when water is present. Water is known to suppress Lewis acid activity. From the moment that Sn-Beta was discovered to be able to perform TH reaction in the presence of water, many researchers saw the opportunity to employ Sn-Beta for the valorisation of biomass-derived

molecules. In particular, researchers at Haldor Topsøe were the first to prove that Sn-Beta can successfully perform triose sugar isomerisation.<sup>56</sup> In this case, dihydroxyacetone (DHA) was converted to glyceraldehyde (GLA) in solutions of water or methanol at mild temperature (80-100 °C). Surprisingly, it was found that the reaction further proceeded to form lactic acid (LA) and methyl lactate (ML), depending on the nature of the solvent employed. In particular, ML and LA are both precursors of polylactic acid (PLA), a biodegradable plastic polymer that can be used to replace petrol-derived polymers. Other than replacement of existing polyester material used for packaging, PLA has found its own employment as feedstock in 3D printing technology. To date, LA is industrially produced *via* enzymatic process<sup>57</sup> with a scale of 150 kt y<sup>-1</sup>. As such, an alternative catalytic route is highly desirable.<sup>58,59</sup> ML can be obtained by processing sugars at higher temperatures at which the retro-aldol reaction occurs.<sup>60</sup> For examples, it was shown that reacting hexose sugars (glucose, fructose and sucrose) at 140 °C with Sn-Beta, lead to the formation of ML in yields ranging from 40 to 60 %.<sup>53</sup> The synthesis was believed to proceed by breaking the hexose sugars into triose sugars (DHA and GLA) *via* retro-aldol reaction, and subsequently reacting the C<sub>3</sub> units with the catalyst to make ML (Figure 13). Further studies have found that the introduction of alkali salts, like K<sub>2</sub>CO<sub>3</sub>, can further improve the production of ML from glucose or fructose, leading to yields as high as 70 %.<sup>61</sup>

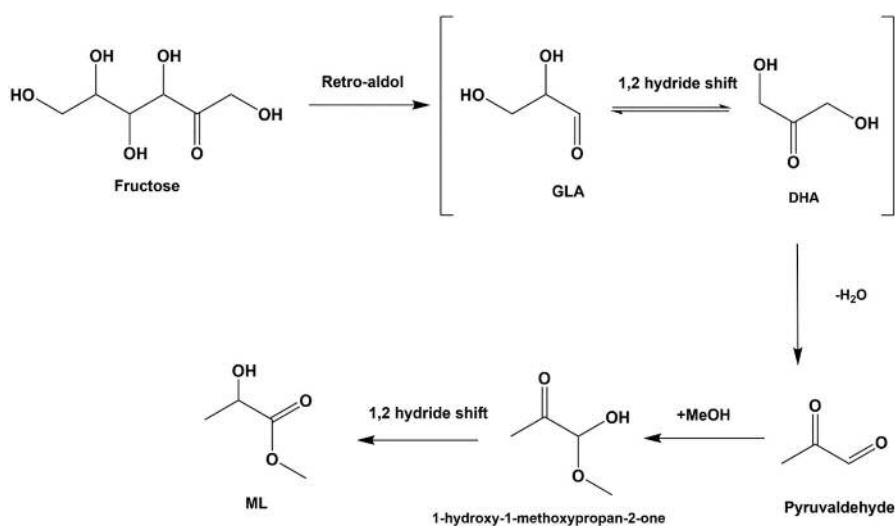


**Figure 13.** Scheme of the sugars conversion to methyl lactate.

A further breakthrough in Sn-Beta research was delivered by the discovery of its ability to catalyse the isomerisation of glucose to fructose in aqueous phase.<sup>52,62,63</sup> This reaction is not only important for the production of high-fructose corn syrups (HFCS), which is abundantly used in the soft drink industry as sweeteners, but is also a key reaction for furanic-derived



compounds. The enzymatic process, mediated by xylose isomerase, typically produces an equilibrium mixture of *ca.* 50 % of glucose, 40 wt.% of fructose and 10 wt% of others saccharides, which mannose being the main of these other by-products.<sup>64</sup> The reaction catalysed by Sn-Beta also produces a similar equilibrium mixture, pointing out how the selectivity of this catalyst resemble very much the enzymatic one. Along with the isomerisation, which is the main reaction, epimerisation to mannose is also present with Sn-Beta (Figure 14).

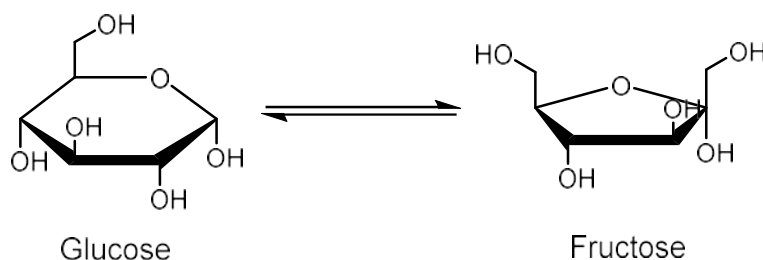


**Figure 14.** Scheme of the glucose isomerisation for HFCS production

The isomerisation of glucose is reportedly to proceed likely *via* 1,2 hydride shift, between the hydrogen on C-2 to C-1 (Figure 15).<sup>65,66</sup> This mechanism can be also seen as an intra-molecular analogue of a classical intermolecular TH reaction. In fact, the same 6-membered transition state as proposed for the TH reaction has also been proposed for this reaction.

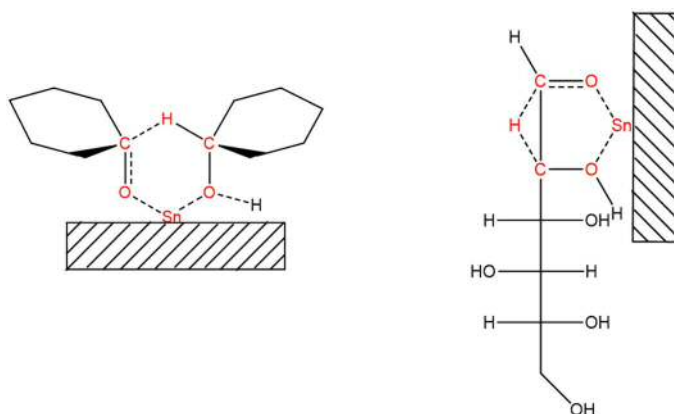


**Figure 15.** Proposed 6-member ring transition state of MPV mechanism for cyclohexanone transfer hydrogenation (Left) and glucose isomerisation (Right).

On the other hand, the epimerisation of mannose seems to proceed via 1,2- carbon shift. Although mannose is typically present as secondary product, observed at a selectivity lower than 20 %, it has been observed that introduction of borate salts<sup>67</sup> or alkali cations<sup>32,68</sup> dramatically increases the selectivity to mannose, albeit at the expense of fructose. This effect is believed to originate from an ion-exchange of the proton located on a proximal

silanol group, which may switch off the isomerisation pathways in favour of the epimerisation. This brings an important indirect evidence of the fact that different active sites can be present in Sn-Beta and they can be modified post-synthesis by changing the reaction conditions.

#### 1.5.4 Bifunctional systems and tandem reactions

As said earlier, the isomerisation of glucose to fructose is not only important for HFCS production. It is also the key step towards opening routes to furanic-derived molecule. In fact, fructose more readily dehydrates than glucose, resulting in the formation of 5-hydroxymethyl furfural (HMF), from which a plethora of downstream products can be produced (Figure 3). Production of HMF is of particular importance because many of its derivatives can find employment in different field.<sup>69</sup> For example, oxidation of HMF lead to production of FDCA, which is used in the co-polymerisation with ethylene glycole to produce polyethylene furanoate (PEF). Reduction of HMF will produce 2,5-bis(hydroxymethyl)furan (BHMF) that could be employed for polymers production, and DMF, which is a promising biofuel and green solvent. Ultimately, ring-opening reaction of HMF is used to obtained levulinic acid, interesting platform molecule from which GVL is obtained (Figure 16).

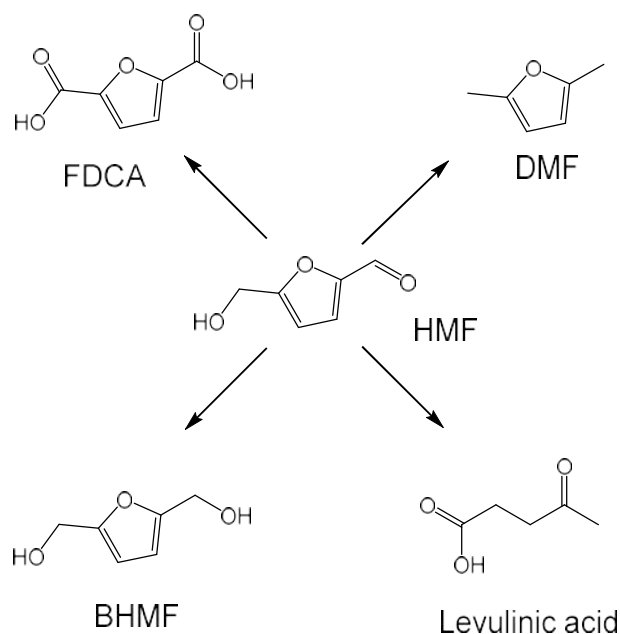


**Figure 16.** Scheme of some of the key products obtainable from HMF valorisation.

Unfortunately, being a Lewis acid means that Sn-Beta does not show high activity for the dehydration of fructose to HMF, which is a fundamental step necessary for all the following processes to take place. On the other hand, Brønsted acids can readily dehydrate fructose into HMF. For this reason, developing bifunctional systems capable of catalysing the multi-step processes required for biomass valorisation is a key point in order to expand the potential of this field. For instance, HMF production from glucose with yield as high as 60 %, has been obtained by using a biphasic system composed of an aqueous solution of Sn-Beta and HCl (pH = 1) and a tetrahydrofuran as organic extracting phase.<sup>70</sup> In an equivalent way, FF can be obtained directly from xylose by isomerisation to xylulose and successive dehydration in one pot reaction, by employing Sn-Beta and the Brønsted resin Amberlist-15.<sup>71</sup>

Another process in which the cooperation of Lewis and Brønsted acids has been shown to be beneficial is the one-pot conversion of FF into GVL. GVL has gained attention for its use as solvent in bio-processing and as possible fuel additive. Figure 17 shows a series of consecutive Lewis and Brønsted catalysed TH and ring opening steps. Here, FF was converted into GVL in a one-pot reaction at around 80 % of yield. In this case, different solid Brønsted acid catalysts, such as Al-MFI, zeolites were used in cooperation with Lewis Sn- and Zr-Beta.<sup>72</sup>

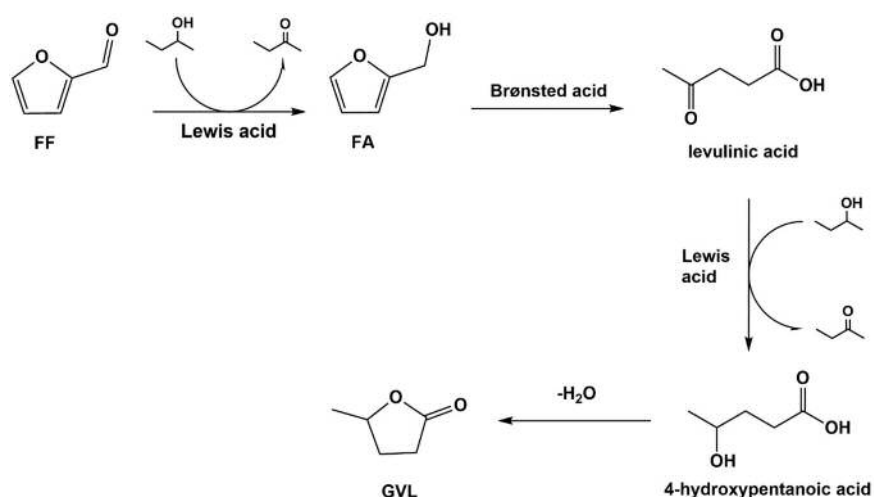


**Figure 17.** Scheme of GVL synthesis from furfural performed by Lewis and Brønsted acids cooperative

Etherification of furanic derived molecules, like furfural and HMF, has also been studied, and once again, cooperation of Lewis and Brønsted molecules were used. In a case reported by Lew *et al.*, sulfonated resins, such as Amberlyst 131 has been used in cooperation with Sn-Beta for the one pot reaction of glucose to 5-(ethoxymethyl)furfural obtaining a yield of 31%

on the ether (Figure 18).<sup>73</sup> Ethers of these molecules are prove to be effective additives for fuels, and may also possess potentials as fuels directly.<sup>74</sup> Although etherification has been observed to occur even in the presence of Lewis acid catalysts alone, intensification of the process has been demonstrated to be not very effective as the etherification step quenches rapidly, as demonstrated by the continuous TH/etherification of HMF in ethanol performed with several Lewis acid catalyst, one of which was Sn-Beta.<sup>75</sup>

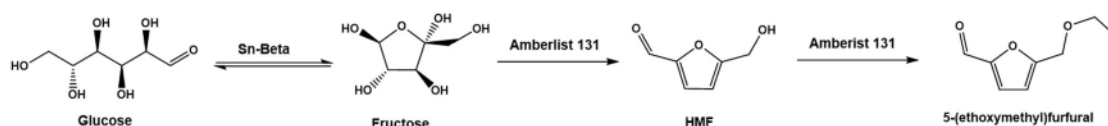


**Figure 18.** Tandem TH/etherification of glucose to 5-(ethoxymethyl)furfural performed by Sn-Beta and Amberlist 131.

In this section, it has been clearly shown the reasons why Sn-Beta has attracted so much attention, and has rapidly become one of the best catalysts for many biomass conversion processes. However, there are currently no commercial processes that employ this catalyst to date. In fact, despite its excellent catalytic performance, the synthesis of this catalyst is characterised by several difficulties and disadvantages that have, so far, discouraged its production, and thus, its commercial employment. In the following paragraph, a brief overview of some of the synthesis approaches for this material are covered, highlighting some of the limitations that exist and how they continue to be overcome.

## 1.6 Sn-Beta synthesis

### 1.6.1 Hydrothermal synthesis

The synthesis of Sn-Beta represent one of the main bottlenecks regarding its industrial implementation, and has strongly slowed down its widespread utilisation and commercialisation. Indeed, other than having the desirable catalytic activity, a promising heterogeneous catalyst has to be obtainable through a viable synthetic route.

The first synthetic method employed to synthesised a fully Lewis acidic Sn-Beta was the hydrothermal synthesis. Hydrothermal synthesis represents the established method to prepare conventional aluminosilicate zeolites, and involves several steps.<sup>76</sup> The synthesis

begins by dissolving the main components of the zeolite, which are silicon and aluminium precursors, in an aqueous solution. Great importance is based on the ratio between the two components, because it will determine the final Si/Al ratio in the zeolite, the parameter that defines the acid strength and acid site density of the material. A mineralising agent is also needed, for the formation of T-O-T bonds. Typically, inorganic anions ( $\text{OH}^-$ ) are used, but sometimes fluoride anion ( $\text{F}^-$ ) must be used instead. Another key component of the synthesis is the structure direct agent (SDA), whose role is direct the synthesis toward a precise zeolite structure. When the gel is formed, it is then transferred into autoclave and treated at high temperature and under autogenic pressure until the crystallisation of the zeolite is completed. After filtration and washing the crystallised zeolite with clean solvent, the powder is calcined in order to remove residues of the SDA from the inorganic porous crystalline material. Similarly, Sn-Beta it is also predominantly synthesised by hydrothermal synthesis (Figure 19), with use of tetraethylammonium hydroxide (TEAOH) as SDA, and tin tetrachloride pentahydrate ( $\text{SnCl}_4 \cdot 5\text{H}_2\text{O}$ ) as tin precursor.

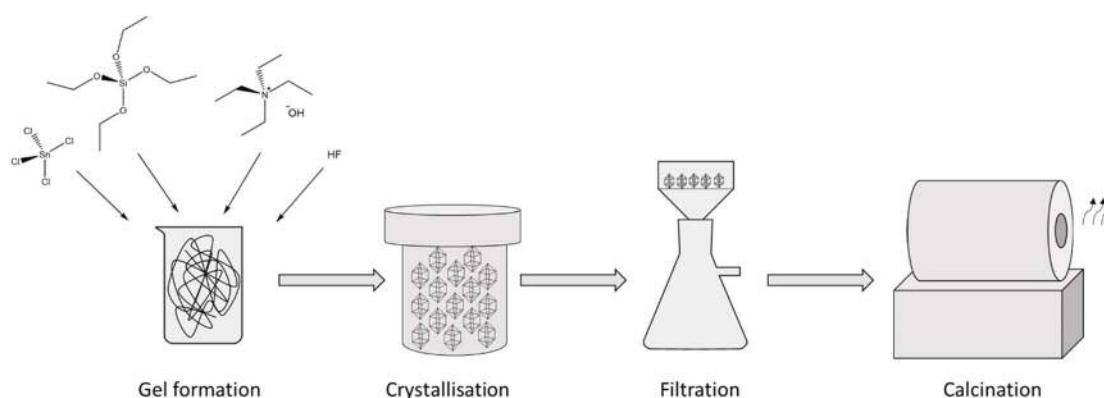


**Figure 19.** Graphical representation of the hydrothermal synthesis of Sn-Beta.

The procedure first involves the formation of the gel by mixing the appropriate amount of tetraethyl orthosilicate (TEOS) and tin tetrachloride pentahydrate ( $\text{SnCl}_4 \cdot 5\text{H}_2\text{O}$ ) as a source of Lewis acid. Tetraethylammonium hydroxide (TEAOH) is used as SDA and HF is required as mineralising agent. To favour the crystallisation, ultra crystalline de-aluminated seeds of zeolite Beta are added to the mixture. Once the gel is formed, it is transferred into an autoclave and heated at high temperature under autogenic pressure for between 10-40 days, after which time the crystals are recovered by filtration and the catalyst is calcined to remove the SDA.

However, the hydrothermal synthesis of Sn-Beta presents many disadvantages. Primarily, it is not possible to obtain incorporation of Sn into a BEA structure by using  $\text{OH}^-$  as mineralising agent. As such, fluoride media is necessary, enhancing the risk of the process due to highly toxic HF. In addition to toxicity, the presence of HF means that dedicated acid resistant apparatus must be employed. Additionally, extremely long synthesis times are required. Crystallisation time as long as 20 days are regularly reported in order to achieve sufficient grade of crystallinity of the materials, and the crystallisation time is proportional to the amount of Sn present in the gel.<sup>77</sup> However, the crystallisation times reduced to 2 days were recently reported by Chang *et al.*, after introduction of a suspension of homogeneously dispersed highly crystalline de-aluminated-Beta seeds into the synthesis gel.<sup>78</sup> Besides these disadvantages, large crystals are often obtained, having consequences on the catalysis, especially representing an issue for internal diffusion. Another big limitation of this synthesis is the low amount of Sn that it is possible to incorporate. In fact, the rate of crystallisation decreases dramatically at increasing Sn contents, to the point that when the Sn is present in quantities higher than 2 wt. %, crystallisation cannot occur.

### 1.6.2 Alternative synthesis of Sn-Beta

For all these reasons, many different alternatives to the hydrothermal synthesis have received increasing attention. Generally, these can be grouped into two categories: bottom-up and top-down methods. An example of the first includes steam assisted conversion method, which shares some similarities with hydrothermal synthesis.<sup>79,80</sup> Indeed, in this case, a SDA, mineralising agent, and silicon and Sn precursors are mixed together in order to form the initial gel. The dry gel as obtained is converted to Sn-Beta upon steam treatment. Thus, the gel is not treated in the liquid aqueous phase as typically occurs during hydrothermal synthesis. Conversion of the gel into a crystalline stannosilicate material was observed between 3-6 h of steam treatment. Although bottom-up methods avoid the use of HF and shorten the synthesis time, the catalytic properties of the materials were significantly lower when compared to the conventional hydrothermally synthesised materials. In particular it has been found that the catalytic activity of the dry gel steam assisted synthesised material is only 25 % of the original Sn-Beta.

A totally different synthetic approach is followed in the so-called top-down methods. These methods, also named post-synthetic, all start from already made (lab synthesised or commercially available) aluminosilicate zeolite of the desired structure (BEA in this case). To

these readily made materials, the aluminium is extracted, typically by acid treatment, and Sn is successively insert (Figure 20).

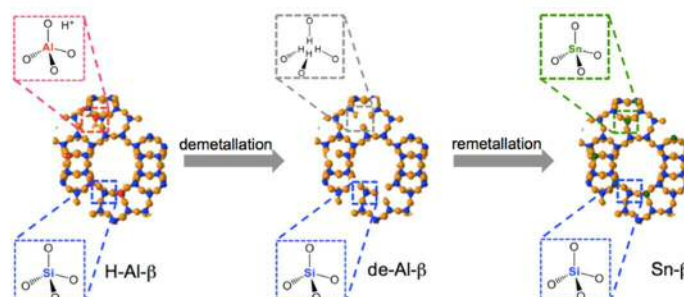


**Figure 20.** Graphical representation of the synthesis of Sn-Beta via post-synthetic de-metallation and re-metallation.

The extraction of aluminium, carried out under acid conditions,<sup>81,82,83</sup> leaves in the framework some vacancies, called silanol nest, into which other atoms can be accommodated. Sn can be successfully inserted into these vacancies following different methods. For example, gas-solid, liquid-liquid and solid-solid have all been exploited for the synthesis of the Sn-Beta. Chemical vapour deposition of  $\text{SnCl}_4$  into a de-aluminated Beta zeolite was performed in order to obtain Sn-Beta with up to 6 wt.% Sn.<sup>84,85</sup> The material as obtained showed a visible amount of extra-framework species by UV-Vis technique. Despite this, the material was shown to exhibit comparable activity to the hydrothermal synthesised analogous when it was employed for the BVO reaction. An alternative post-synthetic method can be found with liquid-solid types of synthesis. For these, it has been shown that Sn can be incorporated in the de-aluminated zeolite framework by grafting Sn(IV) chloride pentahydrate in the zeolite vacancies, by refluxing the material in dry isopropanol.<sup>36,86,87,88</sup> The Sn-Beta catalysts obtained through this method possessed a metal loading ranging from 0.3 to 8.6 wt.% Sn-Beta. Notably, at low metal loadings and when employed for glucose isomerisation, the catalyst showed TOF higher than the hydrothermal catalyst, showing that this technique can be a valid alternative to the classical method. At this point, it is worthy of mention that alternative method to make vacancies in the zeolite can be used, other than de-alumination. In fact, de-silication can also be employed. In this case, silicon atoms are extracted from the framework in order to form vacancies where different heteroatom can be successively inserted. In contrast to de-alumination, de-silication is obtained by treating the zeolite in alkaline solution, and generally milder conditions are sufficient. Dapsens *et al.* used this methodology to successfully insert Sn in a MFI structure that was previously desilicated

in a solution of 0.2 M of NaOH at 65 °C.<sup>89</sup> The catalyst as obtained was shown to be active for the isomerisation of glyoxal, even though it showed 3-times lower intrinsic activity with respect to the hydrothermally synthesised Sn-MFI analogue. De-silication is used also to make hierarchical zeolites, which also expands then the porosity range, from the domain of micropore to the mesopore. This methodology proved to be very effective for the synthesis of hierarchical Sn-containing zeolite able to process bulkier molecules.<sup>90,91,92</sup>

Although the methods mentioned above offer a valid alternative to hydrothermal synthesis, they also suffer of some limitation. For example, metal vapour deposition methods required the use of a dedicated gas-apparatus and higher temperature of synthesis (500 °C), while liquid phase grafting required the use of anhydrous solvents. In this regards, solid state incorporation (SSI) has been proven to offer several advantages. This method, which will be used to make the catalyst employed in this work, and is thus described in more detail in the next chapters, allows one to obtain a catalyst with a high loading of Sn, up to 10 wt.%.<sup>93</sup> A suitable Sn precursor, in this case Sn(II)acetate is mechanically mixed with the de-aluminated zeolite, in order to form homogeneous solid-solid precursor of Sn-Beta. After the solid-solid mixture is prepared, a heat treatment at 550 °C is performed to obtained the final Sn-beta. The advantages of having a solid-solid process are numerous. For example, no dedicated synthesis equipment is required. Indeed, the mechanochemical synthesis simply requires mortar and pestle, in which the Sn precursor and the de-aluminated zeolite are grinded and mixed together. The time of the synthesis is also greatly reduced, with the length of Sn incorporation lying in the temporal scale of hours instead of days. Also the safety of the process is greatly increased, in fact dealing with only powder it does not required any particular equipment of containment, as in cases where liquids are involved. This methodology has also been successfully used to incorporate several metals other the Sn, such as Ti and Zr.<sup>94</sup>

For many years the synthesis of Sn-Beta represented the main bottleneck to its employments. For this reason many efforts have been put in researching alternative ways to the classical hydrothermal synthesis, leading to development of post synthetic methodologies that have been proved to represent valid alternatives for a more facile and intensive production of the catalyst. However, even though the issue of the synthesis of the catalyst in partly solved, several other question remained unsolved, one above all being that of the stability of the catalyst.



## 1.7 Process intensification

### 1.7.1 Catalyst parameters

It is clear that biomass conversion represents a huge challenge that modern chemistry, and catalysis in particular, is facing. However, the number of publications on this field is enormous and yet, the current chemistry manufactory is dominated by chemical processes based on fossil fuel feedstock. It is then clear that something is missing if new processes based on renewable feedstock encounter difficulties in replacing the well established petrochemical processes, despite all the advantages that renewable feedstock offer.<sup>95</sup> Without taking into account the economic evaluation, but only focusing merely on chemical analysis of the reasons why renewable routes have not taken over most of the conventional chemistry, it looks clear that a big piece is missing. In fact, examining the open literature on biomass catalysis, it looks evident that very few works have focused their attention to the actual engineering aspect of this chemistry. Whilst most of the catalytic system are fully explored in term of their most fundamental parameters, such as activity and selectivity, very few works make a step forward to an actual intensification of the process. The two parameters mentioned above are certainly the most easily known and easily obtainable descriptors of a catalyst. Notably, activity is an arbitrary unit. In fact, it is often defined as the amount of substrate converted per unit time per unit of amount of catalyst, and is expressed by a parameter called conversion, defined as follows:

$$\text{Conversion (\%)} = \frac{[R_0] - [R_t]}{[R_0]}$$

Where  $[R_0]$  and  $[R_t]$  are the concentrations of the reactant before the reaction occurs, and at a certain time of the reaction (t), respectively.

Despite this parameter being widely employed, it does not provide intrinsic information of the activity of the catalyst. In fact, as can be seen from the equation, the value of conversion is strongly dependent on the initial concentration of the reactants and on the amount of catalyst. For instance, performing a two reactions with the same amount of catalyst but in one having half of the concentration of the reactant it will be found that the conversion

doubles in that case, even though the catalyst performance, in term of activity, are exactly the same for both systems. For this reason comparison of different catalysts solely based of conversion are incomplete, if not incorrect. Another parameters to evaluate intrinsic activity is then preferred, and is called turn over frequency (TOF).

$$\text{TOF} = \text{moles}_{(\text{converted})} \text{ moles}^{-1}_{(\text{active site})} \text{ hour}^{-1}$$

TOF takes in account the number of substrate converted per unit time per active site, giving a normalised value of activity to the concentration of substrate and the amount of catalyst/active sites. However, it is not always possible to determine the exact amount of active site. For this reason, it is often preferred to take into account the total number of moles of the metal, regardless of its actual active/non-active form. Determination and quantification of active sites often relies on use of characterisation techniques involving probe molecules; to cite some examples: CO chemisorption, temperature programmed reduction/oxidation, acetonitrile adsorption, pyridine adsorption etc. On the other hand, determination of the total number of metal sites simply requires elemental analysis that can be done by ICP-MS or by SEM-EDX for example. Despite this, the TOF measurement still permits a more direct comparison between different catalysts and systems.

Although it is desirable having a catalyst with the highest activity possible, in many case this is not a crucial parameter for the commercialisation of a catalyst. In fact, in the economy of an industrial process, downstream operations, like product separation and purification, normally represent one of the most cost-demanding steps. In this regards it is essential that the process has a high selectivity, even if it comes at the expenses of activity. Selectivity means the ability of the catalyst to direct the reaction to yield a particular product rather than others. In industrial processes, high selectivity in a product means easier separation and purification of the crude mixture of reaction, drastically pulling down the overall cost. Selectivity can be express by the following equation:

$$\text{Selectivity (\%)} = \frac{\text{moles of desired product}}{\text{moles of all products}} \times 100$$

Along with activity and selectivity, which certainly are central parameters of a catalyst, stability is another important parameter. This parameter is frequently overlooked in lab-scale research, but often can make the choice on the practicability of an industrial process.<sup>96</sup> The stability of a catalytic process is defined by the ability of the catalyst to perform its catalytic cycles for an extended period of time whilst retaining the initial performance; In other words, without losing its activity and/or selectivity over a certain period. Although is of more immediate picturing when talking about stability, time not always represent the parameters against which the stability is compared. In fact, more indicative, is the number of substrate turnover, which is the number of the catalytic cycles that the catalyst (but more specifically the active sites) can perform without losing a certain extent of its initial activity. This extent is arbitrary and can vary from case to case, and often is determine by the value of the product obtained. Besides, productivity of a process play an important role, also in light of deactivation. Productivity is often define as:

$$\text{Productivity} = \frac{\text{Product}}{\text{Catalyst} \times \text{Time}}$$

It is clear that deactivation and productivity are two parameters strictly interconnected in the evaluation of a process. In fact, a process that suffers of high deactivation but it is also highly productive can still be considered fruitful. In analogous way, a process that is does not have high productivity, but possess a very high degree of stability can be equally feasible. It is important to bear in mind that evaluation of a single parameters cannot provide an exhaustive picture of the whole process viability.

However, while selectivity, activity and productivity data are already mostly available for many reactive systems involving renewable feedstock, stability studies in liquid phase biomass valorisation are almost unexplored and at the very early stage of the research, consequently hindering a thorough analysis of the feasibility of biomass valorisation processes.

### 1.7.2 Deactivation during biomass valorisation

As described above, the stability of a catalytic reaction is vital in determining the success of a process. As the aim of this thesis is the study and intensification of some of the most

important biomass reactions, stability/deactivation studies will be a central point of this work.

Deactivation phenomena can arise for several different reasons, and some deactivation mechanisms are often typical of a determinate class of materials.<sup>97</sup> Since in this work zeolite catalysts are employed, only the most common deactivation processes influencing zeolites will be describe below. Deactivation phenomena are greatly dependant on the reaction conditions and on the phase in which the reaction is carried out. The liquid phase *i.e.* the solvent, in which most biomass valorisation reactions are performed, introduces major differences with respect to the most common gas phase reaction. Deactivation can also be regroup into two different categories: permanent and non-permanent (Figure 21). Deactivation of a reversible nature is, of course, less undesirable, as full or partial activity can be recovered upon particular treatments.

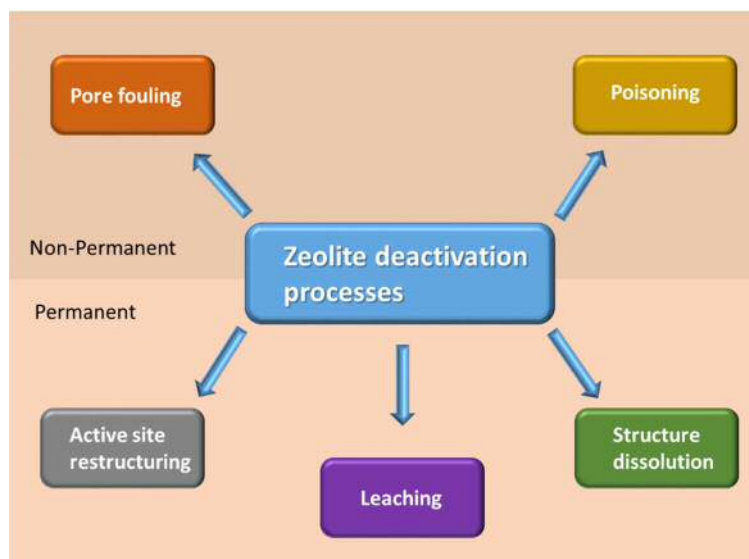


**Figure 21.** Scheme of some of the most common deactivation processes that involve zeolite materials. The processes are divided into permanent and non-permanent phenomena.

One of the most common types of deactivation that zeolites, and more generally porous materials, suffer from is fouling. It consists in deposition of particular materials, often high molecular weight products derived by decomposition or polymerisation of carbon based species, which can be reactants, products, by-product or solvent, into the porous network. Figure 22 is a schematic representation of fouling.

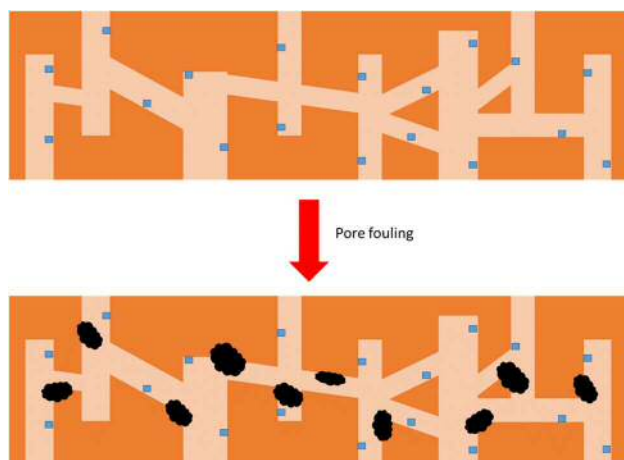


**Figure 22.** Graphic representation of pore fouling caused by carbonaceous deposition (bottom). It can be seen that the coke formation within the pore of the zeolite diminish the internal volume, thus hindering the reachability of the active site (blue square).

Fouling can be present both in liquid and gas phase catalysis, where it is often named as coke deposition. Fouling can deactivate the catalyst mainly through two mechanisms: i) poisoning of active site or ii) blocking of zeolite pore. Given that the majority of zeolite active sites are located inside the pores, fouling can result in dramatic losses of performance if the accessibility to the inner part of the zeolite is restricted. Since carbonaceous deposition is the main cause of fouling, it can be easily diagnosed by performing surface area/porosimetry analysis, and thermo-gravimetric analysis (TGA), on the used catalyst. If fouling is present, a decrease in surface area and total pore volume will be observed. Due to the typically high molecular weight of these depositions, they would mostly be detected by TGA by desorbing only at unusually high temperature. Also coupling TGA with mass spectrometry could help by detecting the chemical nature of these compounds, and a  $\text{CO}_2$  related mass spectroscopy signal is detected by their combustion. It is clear that if the catalyst is treated at a sufficient high temperature in order to burn the organic residue, and at the same time the preserve the physical integrity of the crystalline structure, the activity can be theoretically fully recovered. A way to mitigate pore fouling is to use materials with bigger pore diameter, in order to minimise the impact of having large deposition of carbon. This can be done mainly in two way: i) to use another material with same active site but bigger pore architecture, or ii) to make hierarchical pore structure on the same material (*i.e.* through de-silication) in order to increase the pore aperture.

As mentioned above, poisoning can also contribute to catalyst deactivation. It comes from a strong adsorption between the active site and the poison molecule, which inhibits that site from further participating in the catalytic cycle (Figure 23).

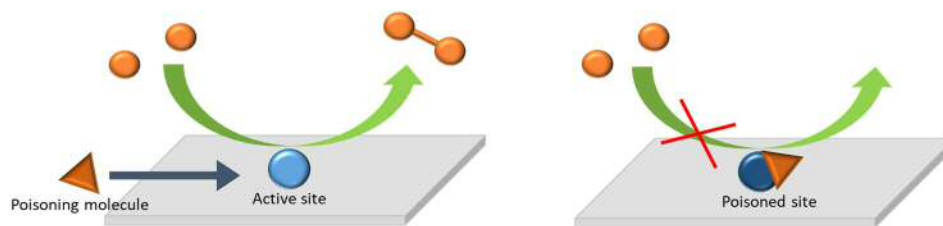


**Figure 23.** Schematic representation of poisoning. On the left it is shown the active site doing is normal catalysis prior being poisoned. After poisoning (on the Right), the active site is unable to react anymore with the substrate.

The poisoning molecule can be of many different natures. It can come from a fouling-derived compound that selectively form around the site, or can be the reactant or the product itself. In many cases, it can be a by-product or an impurity present in the reaction feed, such as electropositive alkaline ion, which are known to be able to exchange with acid proton of the zeolite. In contrast to fouling, poisoning is more subtle and many difficulties can be encountered for a direct observation of the phenomena. In fact, as demonstrated by Mannel *et al.*, poisoning can arise from a stoichiometric ratio between active site and poison, thus the molecule can be present in solution at ppm or even lower level, being sometimes below the detectability limits of some common analytical technique such as liquid and gas chromatography. In some cases, indirect methods can be applied to investigate if the catalyst is amenable to chemical poisoning.<sup>98</sup> In fact, it is possible to perform batch kinetic experiment in which a controlled concentration of the possible poison is introduced from the beginning in the reaction mixture and the kinetic constant is calculated from the initial rate of the reaction. The concentration of the poison is then varied in different experiments and finally a plot of the kinetics constant as a function of the amount of 'poison' added can be obtained. If the molecule introduced in the system act as a poison a decrease of the initial reaction rate will be observed, as the poison concentration will increase. In this way, poison molecules for that catalyst can be discovered and also the level of concentration from which the effect start to be observable can be known. In this way, focused analysis on the real reaction system can be performed in order to attest if that molecule is present and at which concentration. This approach has been used by Yakabi *et al.* during the Baeyer-Villiger oxidation of cyclohexanone to caprolactone with hydrogen peroxide. It has been found that the presence of the hydrolysis product of caprolactone, 6-

hydroxyhexanoic acid (6-HHA), halved the initial rate of the reaction when present in low quantities. One poison that can interest biomass valorisation directly is water. In particular Lewis acidic centres are susceptible of deactivation by water poisoning, as shown by Corma *et al.* There, during the transfer hydrogenation of cyclohexanone, in the presence of 4 wt.% of water the initial activity dropped of the 80 % of the value obtained in the case the catalysis was performed in pure alcoholic solvent.<sup>46</sup> In addition, although glucose isomerisation can be performed in water by Sn-Beta, this system shows a two order of magnitude lower rate than the same system performed in methanol. Poisoning can be of reversible nature if the poison can be removed. In the case of selective polymerisation of by-product around the active site, full activity can occasionally be restored by thermal treatment. However, sometimes the chemisorption between the poison and the active site is so strong that no regeneration is possible. In such cases, mitigation of the phenomena can be attempted by changing the reaction conditions in order to inhibit or decrease the formation of the poison. If the poison is present as an impurity in the reaction feed, careful purification has to be done prior to it being exposed to the catalyst. For instance, alkaline cation can be removed by passing the solution through ion-exchange materials,<sup>99</sup> or water can be removed by trapping it in molecular sieves.<sup>100,101</sup>

Restructuring of the active site can also lead to deactivation of the catalyst. In fact, the metal centre responsible for the catalysis are often active only when determinate conditions, like geometry, oxidation state, location, *etc.*, are satisfied (Figure 24).

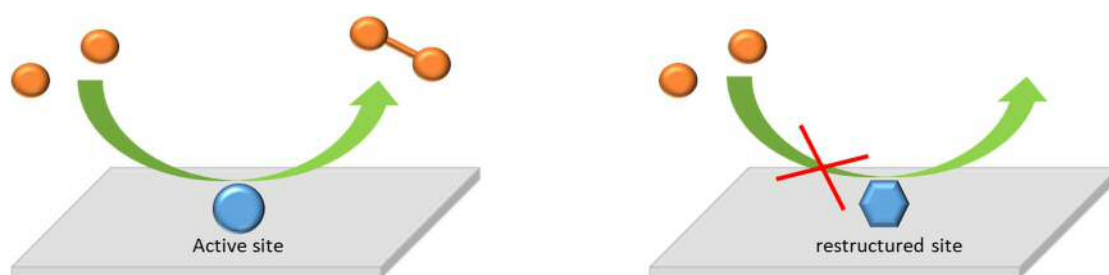


**Figure 24.** Schematic representation of the restructuring process. In this case the active site assuming a certain geometry (Left) is able to catalyse the reaction. When the active site is restructured to another in order to assume a different geometry it loses its catalytic behaviour for that specific reaction.

Especially for Lewis acid zeolite catalyst like Sn-Beta, the incorporation of Sn into the tetrahedral sites of the zeolite structure is a necessary condition for reactivity to be achieved. It has been demonstrated that if Sn is present as its oxide form, like  $\text{SnO}_x$  species, it does not participate to Lewis type catalysis. Restructuring of active site not only can lead

to loss of activity, but it could also change also the selectivity. The causes of restructuring can be of chemical or physical nature. The intrinsic reaction conditions, such as temperature and pressure, can induce changing in the type of active site, even though this mode is more evident in supported nanoparticle catalysts, where temperature can cause agglomeration of the metal dispersed on the surface of the support, decreasing drastically the active surface area. This restructuring phenomenon is commonly referred to as sintering.

To identify if restructuring has occurred, spectroscopic techniques are normally employed. Of course the choice of the technique has to be done according to the type of element the active site is composed of. Moreover, the technique not only has to be able to detect the active site *i.e.* be sensitive, but should ideally also give different signals for different species of active site *i.e.* be selective. In general, UV-Vis, Fourier-Transformed Infrared (FT-IR), Raman, Nuclear Magnetic Resonance (NMR) and X-Ray Absorption Spectroscopy (XAS) are all techniques that can be employed in this regard. FT-IR coupled with adsorption/desorption of probe molecules have been demonstrated to be a useful method to determine if speciation of active site has occurred. In particular, the use of  $\text{CD}_3\text{CN}$  has been proven a very effective method to probe Lewis acid site. In fact, it strongly and selectively binds with Lewis acid sites in the catalyst, resulting in precise signal in the FT-IR spectrum. As such, this technique has been employed to characterise, in addition to quantify, the Lewis acid strength of the sites in Sn-Beta. Lari *et al.* used  $\text{CD}_3\text{CN}$  adsorption to investigate the extent of Lewis acid reorganization on Sn-Beta.<sup>102</sup>

Leaching of active site is an irreversible modality of catalyst deactivation. It consists in the solubilisation of the active species from the solid catalyst to the solvent of the reaction (Figure 25).

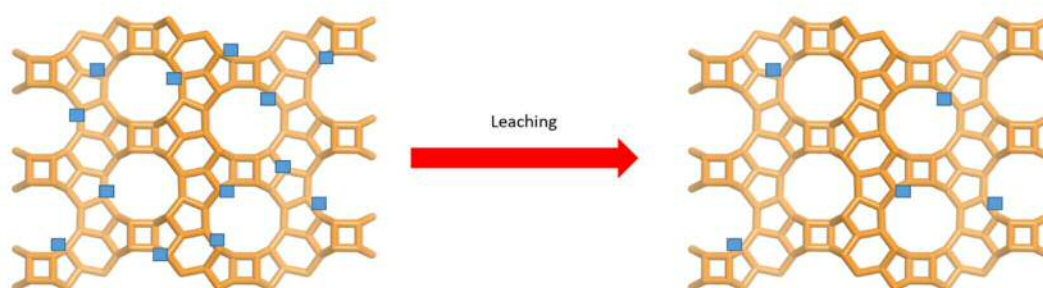


**Figure 25.** Schematic representation of leaching. It can be seen that after leaching (Right) most of the active species (represented as blue square) are stripped away from the zeolite framework.



The consequences of leaching are deleterious, especially for continuous operation. Indeed, even a low rate of leaching can cause, over the long term, the loss of almost all the active components of the catalyst. It has also concerns on the point of view of the environmental safety, since the leached metal compound that might form in solution can be toxic. However, if the reaction has been performed in batch mode, the effect of leaching can be masked by the fact that the same active species, when are present in the solution, can still act as homogeneous catalysts, sometimes resulting in an increase of the rate of reaction. In this case a simple kinetic experiment, called a hot filtration, can be performed to understand if this is happening or not. This experiment consists of starting the reaction normally until a certain point of conversion is reached. After this, the solution and the catalyst are separated through filtration, and the solution is placed back in the reactor without the solid catalyst. At this point, if the reaction continues to proceed even in the absence of the solid catalyst, it is clear that the active phase has passed to the solution and is acting as a homogeneous catalyst (Figure 26). However, particular care must be taken to evaluate this experiment correctly. Indeed, it may be the case in which some heterogeneous active phase leaches in the solution, but once it is solubilised, it loses its catalytic activity, thus showing no conversion after the hot filtration even though leaching has occurred.

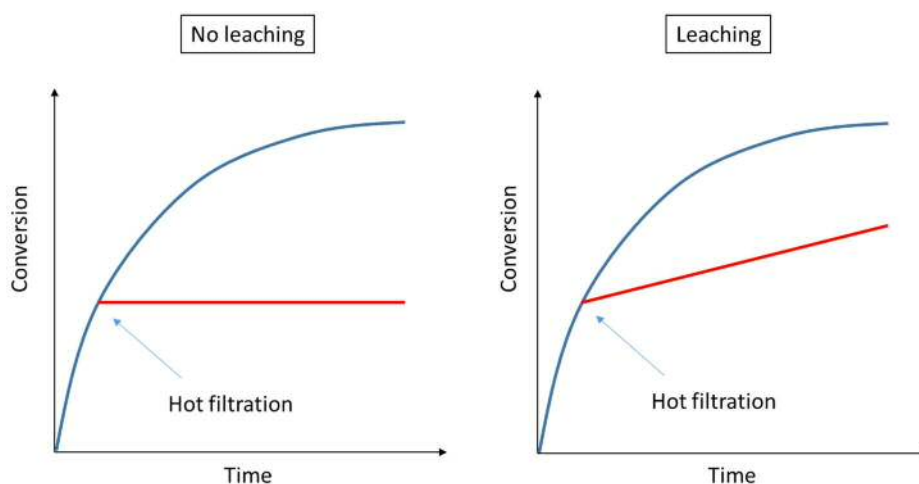


**Figure 26.** Example of hot filtration experiment during batch operation. The blue line represents the conversion vs. time profile of the reaction performed with the solid catalyst in the mixture. The red line represents the kinetic profile after the hot filtration (removal of catalyst). On the left it can be seen that no conversion is observed after the removal of catalyst, suggesting that the reaction is purely heterogeneous catalysed. On the right the catalyst leached some of the active phase in the solution, some extent of conversion is detected during time, meaning that homogeneous catalysis is performed by the leached species.

In this case, direct methods can be used to confirm if some material has leached. For instance, elemental analysis on the solution, performed by Inductively Coupled Plasma (ICP) can detect analytes in solution even at concentrations as low as ppb. Elemental analysis can also be performed on the solid catalyst collected after reaction. If ICP needs to be employed on the solid, the material has to be solubilised. Normally zeolites can be dissolved using strong acids like HF. However, it is possible that during dissolution the active species can react to form insoluble particles, making then impossible the detection by ICP. Alternative techniques can be use, in fact, X-ray photoelectron spectroscopy (XPS) can be employed for elemental analysis, however it can only probe the external part of the material, so if leaching of the species that populate the inner part of the material occurs, it can be difficult to detect. Scanning Electron Microscopy (SEM) coupled with an Energy Dispersive X-ray (EDX) detector can also perform elemental analysis, even though its sensitivity is not as good as ICP.

Lastly, dissolution of the material represents another cause of deactivation, and it is obviously an irreversible kind (Figure 27).

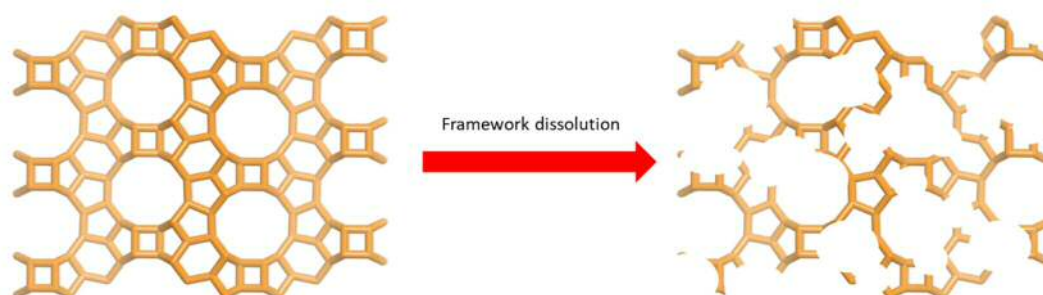


**Figure 27.** Schematic representation of a structural dissolution process. It can be seen that upon dissolution of part of the framework, the material loses crystallinity and surface area, two fundamental characteristics for the catalysis done by zeolites.

If degradation of the structure is severe, XRD analysis should clearly indicate a loss of crystallinity. However, if only part of the structure is damaged, porosimetry analysis might be a better alternative to detect any modification that has occurred to the zeolite. In fact, decrease in the pore volume can be a symptom of partial dissolution of the structure. However, to differentiate between this and pore fouling, this kind of deactivation should be irreversible. As such, if the original porosity cannot be restored by removal of carbon, it is an indication that permanent damage has occurred to the structure. This particular modality of deactivation consist in the physical destruction of the material, and it is of particular

importance during biomass valorisation, since the liquid phase, the presence of water and the high temperatures and pressures employed during continuous operation, can lead the hydrothermal dissolution of the whole or just partial of the zeolite structure. Ravenelle *et al.* compared the stability of FAU and MFI zeolites in liquid water in a temperature range between 150 – 200 °C under autogenic pressure.<sup>103</sup> It was found that while MFI zeolite was completely stable, FAU encountered severe structure amorphisation, showing how greatly the different zeolite structures affect the hydrothermal stability of the material. The acidity and alkalinity of the medium is also important in determining the stability of material. Typically, high Al containing zeolite are more susceptible to hydrothermal dissolution in presence of acids, as shown by West *et al.* during lactic acid production from sugars catalysed by USY with Si/Al = 6, in which it was promptly damaged by the acid product formed during the reaction.<sup>104</sup> Therefore, many efforts must be made to try minimising this effect. If high temperatures are required for the reaction to proceed, then one solution is to do a careful choice of the solvent, which greatly impact the stability of the zeolite. The use of co-solvents can also mitigate the effect, as demonstrated by Aellig *et al.*<sup>105</sup> In this case, an immiscible solvent mixture of water (20%) and methyl isobutyl ketone (80%) was used during the isomerisation and dehydration of xylose performed with a physical mixture of Ga-USY zeolite and an Amberlyst-36 resin. Leaching of the catalyst was reduced compared to the same reaction performed in pure water, and the presence of the immiscible co-solvent further favoured the stability of the system by continuously extracting the unstable reaction product, furfural, into the organic phase, minimising its consecutive hydration. In addition, the choice of the material structure can make a huge impact in the hydrothermal stability. Differences in hydrothermal stability are also found within the same structure, only by changing the synthetic method. For example, the hydrothermal stability of Sn-Beta zeolites greatly differs according to the kind of synthesis they have been made of. Hydrothermally synthesised zeolites are proved to be more tolerant and resistant to water, reflecting in better catalytic performance when water is the medium.<sup>106,107</sup> Their superior resistance is attribute to their higher hydrophobicity. Indeed, post-synthetic Sn-Beta materials typically present many structural defects, such as silanol groups that greatly increase the hydrophilicity of the material, enhancing the interaction with the water molecule.

It appears clear that many way of deactivation are possible, and obviously, only rarely the deactivation of catalyst is due due to only one specific cause. It is a synergy of all these different modalities that make the catalyst deactivate, and this complicates the way to identify them and consequently act in order increase the stability. However, before to asset

which modalities are responsible for catalyst deactivation, it is of critical importance to know which are the best methods in order to determine it experimentally.

### 1.7.3 Determine catalyst stability

In order to get an insight on catalyst deactivation, the choice on how the reaction is performed is crucial. What is required is a method to determine the degree of a decrease of activity or selectivity while the catalyst is performing a catalytic reaction. In liquid phase heterogeneous catalysis there are two main modalities that can be employed to perform such investigations. The first and most common is batch, while the second is in continuous flow.

When the reactions are carried out in batch mode, the solution containing the reactant and the catalyst are confined in the reactor, often a round bottom flask. It is a closed system, meaning that no exchange of matter is observed during the reaction. The kinetic information, conversion and selectivity for example, are normally plotted against time. In this manner, information about stability is usually obtained doing recyclability tests. These tests consist in recovering the catalyst by filtration after one cycle of reaction has finished. Then the recovered catalyst is tested again for another cycle of reaction and so on for several cycles. Evaluation of stability of catalyst is then made by comparison of the final conversion reached at the end of every cycle to that obtained in the first cycle. This method, although giving an initial idea of the stability of the catalyst, present some limitations. Comparing only the final point of conversion means that no insight of the intrinsic kinetics are known, which are often obtained at low conversion. Batch reactions are also often performed at low substrate to metal molar ratio, meaning that the total turnover number of the reaction is rather low.

For this reason, continuous flow operation represents a more realistic and informative method for studying the stability of a catalyst.<sup>108</sup> Differently from the batch, continuous flow reactors are open systems, where the catalyst is confined inside a reactor and the reactant is continuously flown through the column. In particular, packed bed reactors have the catalyst densely packed inside the reactor, often a tubular piece, and the reactant solution is flow through it and the reaction occurs. In contrast to batch operation, the proceeding of the reaction is defined by the spatial coordinate instead of temporal. In fact, the reactant will be converted as it crossed the catalyst bed, so that the conversion is not time dependent but

space dependent. As such, at every position of the catalytic bed it correspond a different concentration of the substrate (Figure 28).

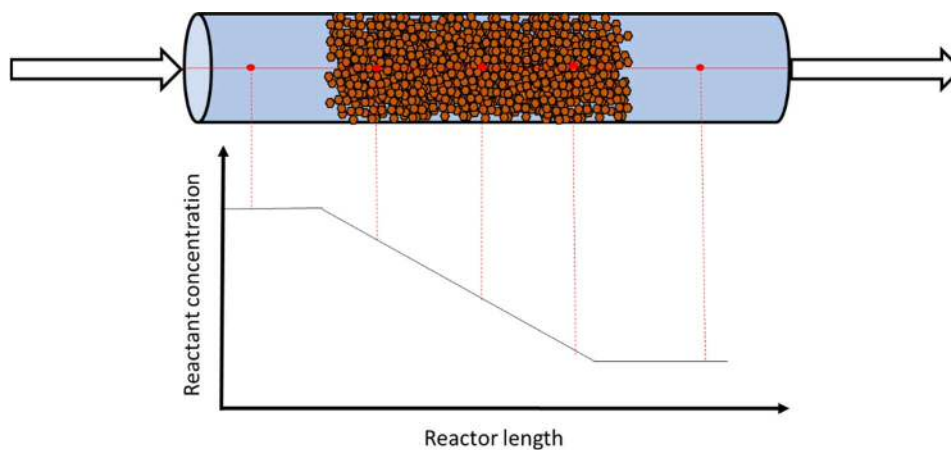


**Figure 28.** Schematic representation of the concentration profile of the reactant during a continuous plug flow reactor. The concentration of the reagent decreases as it moves through the catalytic bed.

Important new parameters must be defined when talking about continuous flow. It is called contact time and it is the ration between the volume of the reactor and the volumetric flow rate of the reactant solution. This unit of measure indicates how much time the reactant stay in contact with the catalyst. Typically, the higher the contact time, the higher the conversion. It then can be compare to the time of the classical batch reaction.

Contact time (min) = \_\_\_\_\_

Between some of the advantages of continuous flow compare to the batch reactor:

- i) improved process- and safety-control,
- ii) higher levels of mass- and heat-transfer,
- iii) faster rates of reaction,
- iv) minimised reactor volumes,
- v) higher levels of scalability and
- vi) improved space-time-yields.

Other than these advantages, it presents one major advantage that makes it a particularly suitable method for deactivation study, that being the possibility to work at steady-state conditions. When the continuous flow works at steady-state condition the concentration along any point of the catalyst bed is theoretically constant with time. Under these conditions, and in the ideal absence of any deactivation, the conversion monitored against the time on stream should not vary with time. Hence, any variation of conversion against time on stream can be attributed to some deactivation phenomena, and hence represents an accurate and direct quantification of the event. This can subsequently be done mathematically by calculating rate of deactivation obtained by monitoring the decrease in conversion determined at the end of the reactor as a function of time on stream.<sup>109</sup> It is then obvious that continuous flow chemistry allows a thorough analysis on the catalyst stability.

### 1.8 Conclusions

Biomass conversion has been shown to be a topic whose attractiveness is as big as it is challenging. However, heterogeneous catalysis has been shown to tick all the boxes needed to engage this challenge. Lewis acid catalysis shows a high potential for biomass valorisation, due to its ability to interact with carbonyl group, which are widely present in the most of the biomass-derived molecules, for example in sugars. Between solid Lewis catalysts, Sn-Beta is one of the most promising material that can be potentially employed for biomass valorisation reactions, as demonstrated by the long record of publications. However, very few processes are based on renewable feedstock even though the basic chemistry behind it is fully understood. One of the reasons why the renewable routes are still not able to compete with the established fossil fuel-derived chemistry has root also on the academic research. In fact, almost no insights are present on the stability of Sn-Beta, and more generally on the heterogeneous liquid phase catalysis. However, it has been shown that combination of characterisation and continuous flow kinetic analysis represents the best experimental tool to study the stability of catalyst during intensified operations. The aim of this thesis is therefore to develop an experimental protocol aimed to study and evaluate the possible employment of Sn-Beta for biomass conversion. The study of the process will start from the very early stage, which is the synthesis of the catalyst. Sn-Beta with different properties will be made and the most suitable according to the need of the moment will be employed for the catalysis. The study of continuous flow reactions, with a particular focus on

the deactivation of the catalyst, will be performed in different system. Starting from a simple model reactions, increasing levels of difficulties will be added whilst the complexity of the substrate study will grow, until facing one of the hottest topics in biomass conversion, which is the valorisation of sugars, such as glucose, in the presence of water.

To summarise, the following topics will be found in this work chapters:

i) in Chapter 3 the effect of metal loading in the zeolite on intrinsic activity and productivity of the catalyst is investigated. Kinetic evaluations are performed through batch experiments of CyO and characterisations on the materials are made in order to gather structure-reactivity information;

ii) in Chapter 4 preliminary investigations on Sn-Beta stability are made by testing the catalyst in the continuous flow reactors for TH of CyO. Study of reaction regime are also made. Deactivation mechanisms are also studied by means of characterisation of used catalyst. The newly acquired knowledge are then use to performed regeneration of the catalyst and mitigation of deactivation;

iii) in Chapter 5 the continuous cascade reaction of TH/etherification of furfural to 2,5(butoxymethyl)furan is studied, having the main aim to develop a stable and selective process for the ether production. High and stable selectivity in the ether are achieved by introducing a Brønsted functionality in the system, therefore different options on how to made a bifunctional catalytic system are explored by modifying the synthesis of the catalyst, to finally developed a bifunctional catalyst that fulfil the desire requisition of stability, selectivity and productivity in the ether;

iv) in Chapter 6 the study of the continuous glucose isomerisation is carried out in methanol and water. Particular emphasis will be made on the effect of the solvents composition (pure and mixture) and how this affect continuous operation. Characterisation techniques, in particular  $^{119}\text{Sn}$  MAS NMR, are employed to investigate how the Sn sites changes according to different operational conditions.

## References

---

<sup>1</sup> N. Abas, A. Kalair, N. Khan, *Futures*, 2015, **69**, 31.

<sup>2</sup> S. H. Mohr, J. Wang, G. Ellem, J. Ward, D. Giurco, *Fuel*, 2015, **141**, 120.

<sup>3</sup> M. Hook, X. Tang, *Energy Policy*, 2013, **52**, 797.

- <sup>4</sup> C. O. Tuck, E. Pérez, I. T. Horváth, R. A. Sheldon, M. Poliakoff, *Science*, 2012, **337**, 695.
- <sup>5</sup> R. A. Sheldon, *Green Chem.* 2014, **16**, 950.
- <sup>6</sup> W. N. R. Wan Ishak, M. W. M. Hisham, M. A. Yarmo, T.-Y. Y. Hin, *Renewable and Sustainable Energy Reviews*, 2012, **16**, 5910.
- <sup>7</sup> T. Kan, V. Strezov, T. J. Evans, *Renewable and Sustainable Energy Reviews*, 2016, **57**, 1126.
- <sup>8</sup> A. V. Bridgewater, *Biomass and Bioenergy*, 2012, **38**, 68.
- <sup>9</sup> C.-H. Zhou, X. Xia, C.-X. Lin, D.-S. Tong, J. Bertramini, *Chem. Soc. Rev.*, 2011, **40**, 5588.
- <sup>10</sup> W. S.-L. Mock, M. J. Antal, *Ind. Eng. Chem. Res.*, 1992, **31**, 94.
- <sup>11</sup> I. Agirrezabal-Telleria, I. Gandarias, P. L. Arias, *Catal. Today*, 2014, **234**, 42.
- <sup>12</sup> E. Ahmad, M. I. Alam, K. K. Pant, M. A. Haider, *Green Chem.*, 2016, **18**, 4804.
- <sup>13</sup> X. Tang, X. Zeng, Z. Li, L. Hu, Y. Sun, S. Liu, T. Lei, L. Lin, *Renewable and Sustainable Energy Reviews*, 2014, **40**, 608.
- <sup>14</sup> K. Yan, Y. Y. J. Chai, Y. Lu, *Applied Catalysis B Environmental*, 2015, **179**, 292.
- <sup>15</sup> E. I. Gurbuz, J. M. R. Gallo, D. M. Alonso, S. G. Wettstein, W. Y. Lim, J. A. Dumesic, *Angew. Chem. Int. Ed.*, 2013, **52**, 1270.
- <sup>16</sup> E. De Jong, M. A. Dam, L. Sipos, G.-J. M. Gruter, *ACS Symposium Series*, 2012, **1105**, 1.
- <sup>17</sup> Y. Roman-Leshkov, C. J. Barret, Z. Y. Liu, J. A. Dumesic, *Nature*, 2007, **447**, 982.
- <sup>18</sup> T. Ennaert, J. Van Aelst, J. Dijkmans, R. De Clercq, W. Schutyser, M. Dusselier, D. Verboekend, B. F. Sels, *Chem. Soc. Rev.*, 2016, **45**, 584.
- <sup>19</sup> A. Jacobs, M. Dusselier, B. F. Sels, *Angew. Chem. Int. Ed.* 2014, **53**, 8621.
- <sup>20</sup> <https://www.iza.org/>
- <sup>21</sup> V. M. Akhmedov, S. H. Al-Khowaiter, *Catal. Rev.*, 2007, **49**, 33.
- <sup>22</sup> E. T. C. Vogt, B. M. Weckhuysen, *Chem. Soc. Rev.*, 2015, **44**, 7342.
- <sup>23</sup> P. S. Goh, A. F. Ismail, *Desalination*, 2018, **434**, 60.
- <sup>24</sup> C. Xu, X. Lu, Z. Wang, *Journal of Membrane Science*, 2017, **524**, 124.
- <sup>25</sup> M. Taramasso, G. Perego, B. Notari, US Patent No. 7081237, 1983.
- <sup>26</sup> G. Bellussi, R. Millini, P. Pollesel, C. Perego, *New J. Chem.*, 2016, **40**, 4061.
- <sup>27</sup> M. G. Clerici, G. Bellussi, U. Romano, *J. Catal.*, 1991, **129**, 159.
- <sup>28</sup> D. Bianchi, L. Balducci, R. Bortolo, R. D'Aloisio, M. Ricci, G. Spanò, R. Tassinari, C. Tonini, R. Ungarelli, *Adv. Synth. Catal.*, 2007, **349**, 979.
- <sup>29</sup> N. K. Mal, A. V. Ramaswamy, *Chem. Commun.*, 1997, **5**, 425.
- <sup>30</sup> S. R. Bare, S. D. Kelly, W. Sinkler, J. J. Low, F. S. Modica, S. Valencia, A. Corma, L. Nemeth, *J. Am. Chem. Soc.*, 2005, **127**, 12924.
- <sup>31</sup> P. Wolf, M. Valla, F. Nunez-Zarur, A. Comas-Vives, A. J. Rossini, C. Firth, H. Kallas, A. Lesage, L. Emsley, C. Copert, I. Hermans, *ACS Catal.*, 2016, **6**, 4047.
- <sup>32</sup> R. Bermejo-Deval, M. Orazov, R. Gounder, S.-J. Hwang, M. E. Davis, *ACS Catal.*, 2014, **4**, 2288.
- <sup>33</sup> A. V. Yakimov, Y. G. Kolyagin, S. Tolborg, P. N. R. Vennestrom, I. I. Ivanova, *J. Phys. Chem. C*, 2016, **120**, 28083.
- <sup>34</sup> T. R. Josephson, G. R. Jenness, D. G. Vlachos, S. Caratzoulas, *Microporous and Mesoporous Materials*, 2017, **245**, 45.
- <sup>35</sup> G. Li, E. A. Pidko, E. J. M. Hensen, *Catal. Sci. Technol.*, 2014, **4**, 2241.
- <sup>36</sup> W. N. P. Van der Graaff, G. Li, B. Mezari, E. A. Pidko, E. J. M. Hensen, *ChemCatChem* 2015, **7**, 1152.
- <sup>37</sup> M. Boronat, P. Concepcion, A. Corma, M. Renz, S. Valencia, *J. Catal.*, 2005, **234**, 111.
- <sup>38</sup> M. Boronat, P. Concepcion, A. Corma, M. Renz, *Catal. Today*, 2007, **121**, 39.
- <sup>39</sup> S. Roy, K. Bakhmutsky, E. Mahmoud, R. F. Lobo, R. J. Gorte, *ACS Catalysis*, 2013, **3**, 573.
- <sup>40</sup> A. Corma, L. Nemeth, M. Renz, S. Valencia, *Nature*, 2001, **412**, 423.
- <sup>41</sup> M. Renz, T. Blasco, A. Corma, V. Fornes, R. Jensen, L. Nemeth, *Chem. Eur. J.*, 2002, **8**, 4708.
- <sup>42</sup> C. Jimenez-Sanchidrian, J. R. Ruiz, *Tetrahedron*, 2008, **64**, 2011.
- <sup>43</sup> R. Otomo, R. Kosugi, Y. Kamiya, T. Tatsumi, T. Yokoi, *Catal. Sci. Technol.*, 2016, **6**, 2787.
- <sup>44</sup> A. Corma, M. E. Domine, L. Nemeth, S. Valencia, *J. Am. Chem. Soc.*, 2002, **124**, 3194.
- <sup>45</sup> M. Boronat, A. Corma, M. Renz, *J. Phys. Chem. B*, 2006, **110**, 21168.
- <sup>46</sup> A. Corma, M. E. Domine, S. Valencia, *Journal of Catalysis*, 2003, **215**, 294.
- <sup>47</sup> A. Corma, M. Renz, *Angew. Chem. Int. Ed.*, 2007, **46**, 298.
- <sup>48</sup> J. Jae, E. Mahmoud, R. F. Lobo, D. G. Vlachos, *ChemCatChem*, 2014, **6**, 508.
- <sup>49</sup> J. D. Lewis, S. Van de Vyver, Y. Roman-Leshkov, *Angew. Chem.*, 2015, **127**, 1.



- <sup>50</sup> S. Van der Vyver, C. Odermatt, K. Romero, T. Prasomsri, Y. Roman-Leshkov, *ACS Catalysis*, 2015, **5**, 972.
- <sup>51</sup> B. Tang, W. Dai, G. Wu, N. Guan, L. Li, M. Hunger, *ACS Catal.*, 2014, **4**, 2801.
- <sup>52</sup> M. Moliner, Y. Román-Leshkov, M. E. Davis, *Proc. Nat. Acad. Sci.*, 2010, **107**, 6164.
- <sup>53</sup> M. S. Holm, S. Saravanamurugan, E. Taarning, *Science*, 2010, **328**, 602.
- <sup>54</sup> A. Corma, M. T. Navarro, M. Renz, *Journal of Catalysis*, 2003, **219**, 242.
- <sup>55</sup> M. Boronat, A. Corma, M. renz, G. Sastre, P. M. Viruela, *Chem. Eur. J.*, 2005, **11**, 6905.
- <sup>56</sup> E. Taarning, S. Saravanamurugan, M. S. Holm, J. Xiong, R. M. West, C. H. Christensen, *ChemSusChem*, 2009, **2**, 625.
- <sup>57</sup> M. A. Abdel-Rahman, Y. Tashiro, K. Sonomoto, *Biotechnology Advances*, 2013, **31**, 877.
- <sup>58</sup> M. Dusselier, P. Van Wouwe, A. Dewaele, P. Jacobs, B. Sels, 2015, *Science*, **349**, 78.
- <sup>59</sup> M. Dusselier, P. Van Wouwe, A. Dewaele, E. Makshina, B. F. Sels, *Energy Environ. Sci.*, 2013, **6**, 1415.
- <sup>60</sup> M. S. Holm, Y. J. Pagan-Torres, S. Saravanamurugan, A. Riisager, J. A. Dumesic, E. Taarning, *Green Chem.*, 2012, **14**, 702.
- <sup>61</sup> S. Tolborg, I. Sabada, C. M. Osmundsend, P. Fristrup, M. S. Holm, E. Taarning, *ChemSusChem*, **2015**, **8**, 613.
- <sup>62</sup> R. Bermejo-Deval, R. S. Assary, E. Nikolla, M. Moliner, Y. Roman-Leshkov, S.-J. Hwang, A. Palsdottir, D. Silverman, R. F. Lobo, L. A. Curtiss, M. E. Davis, *Proc. Nat. Acad. Sci.*, 2012, **109**, 9727.
- <sup>63</sup> N. Rajabbeigi, A. I. Torres, C. M. Lew, B. Elyassi, L. Ren, Z. Wang, H. J. Cho, W. Fan, P. Daoutidis, M. Tsapatsis, *Chemical Engineering, Science*, 2014, **116**, 235.
- <sup>64</sup> S. Bhosale, M. Rao, V. Deshpande, *Microbiol. Rev.*, 1996, **60**, 280.
- <sup>65</sup> Y. Román-Leshkov, M. Moliner, J. A. Labinger, M. E. Davis, *Angew. Chem. Int. Ed.*, 2010, **49**, 8954.
- <sup>66</sup> Y.-P. Li, M. Head-Gordon, A. T. Bell, *ACS Catalysis*, 2014, **4**, 1537.
- <sup>67</sup> W.R. Gunther, Y. Wang, Y. Ji, V. K. Michaelis, S. T. Hunt, R. G. Griffin, Y. Roman-Leshkov, *Nature Communications*, 2012, **3**, 1109.
- <sup>68</sup> J. R. Christianson, S. Caratzoulas, D. G. Vlachos, *ACS Catal.*, 2015, **5**, 5256.
- <sup>69</sup> A. A. Rosatella, S. P. Simeonov, R. F. M. Frade, C. A. M. Alfonso, *Green Chem.*, 2011, **13**, 754.
- <sup>70</sup> E. Nikolla, Y. Roman-Leshkov, M. Moliner, M. E. Davis, *ACS Catal.*, 2011, **1**, 408.
- <sup>71</sup> V. Choudhary, A. B. Pinar, S. I. Sandler, D. G. Vlachos, R. F. Lobo., *ACS Catal.*, 2011, **1**, 1724.
- <sup>72</sup> L. Bui, H. Luo, W. R. Gunther, Y. Roman-Leshkov, *Angew. Chem. Int. Ed.*, 2013, **52**, 8022.
- <sup>73</sup> C. Lew, N. Rajabbeigi, M. Tsapatsis, *Ind. Eng. Chem. Res.*, 2012, **51**, 5364.
- <sup>74</sup> J.-P. Lange, E. van der Heide, J. van Buijtenen, R. Price, *ChemSusChem*, 2012, **5**, 150.
- <sup>75</sup> J. D. Lewis, S. Van der Vyver, A. J. Crisci, W. R. Gunther, V. K. Michaelis, R. G. Griffin, Y. Román-Leshkov, *ChemSusChem*, 2014, **7**, 2255.
- <sup>76</sup> C. Cundy, P. Cox, *Microporous and Mesoporous Materials*, 2005, **82**, 1.
- <sup>77</sup> S. Tolborg, A. Katerinopoulou, D. D. Falcone, I. Sadaba, C. M. Osmundsen, R. J. Davis, E. Taarning, P. Fristrup, M. S. Holm, *Journal of Material Chemistry A*, 2014, **2**, 20252.
- <sup>78</sup> C.-C. Chang, Z. Wang, P. Dornath, H. J. Cho, W. Fan., *RSC Advances*, 2012, **2**, 10475.
- <sup>79</sup> Z. Kang, X. Zhang, H. Liu, J. Qiu, K. L. Yeung, *Chemical Engineering Journal*, 2013, **218**, 425.
- <sup>80</sup> C.-C. Chang, H. J. Cho, Z. Wang, X. Wang, W. Fan, *Green Chemistry*, 2015, **17**, 2943.
- <sup>81</sup> H. K. Heinichen and W. F. Hoelderich, *J. Catal.*, 1999, **185**, 408.
- <sup>82</sup> A. Omegna, M. Vasic, J. A. Van Bokhoven, G. Pirngruber, R. Prins., *Phys. Chem. Chem. Phys.*, 2004, **6**, 447.
- <sup>83</sup> C. Coutanceau, J. M. Da Silva, M. F. Alvarez, F. R. Ribeiro, M. Guisnet, *J. Chim. Phys.*, 1997, **94**, 765.
- <sup>84</sup> P. Li, G. Liu, H. Wu, Y. Liu, J.-G. Jiang, P. Wu, *Journal of Physical Chemistry C*, 2011, **115**, 3633.
- <sup>85</sup> M. Liu, S. Jia, C. Li, A. Zhang, C. Song, X. Guo, *Chinese Journal of Catalysis*, 2014, **35**, 723.
- <sup>86</sup> J. Dijkmans, D. Gabriels, M. Dusselier, F. de Clippel, P. Vanelderen, K. Houthoofd, A. Maliet, Y. Pontikes, B. F. Sels, *Green Chem.*, 2013, **15**, 2777.
- <sup>87</sup> W. N. P. van der Graaf, C. H. L. Tempelman, E. A. Pidko, E. J. M. Hensen, *Catal. Sci. Technol.*, 2017, **7**, 3151.
- <sup>88</sup> J. C. Vega-Vila, J. W. Harris, R. Gounder, *Journal of Catalysis*, 2016, **344**, 108.
- <sup>89</sup> P. Y. Dapsens, C. Mondelli, B. T. Kusema, R. Verel, J. Perez-Ramirez, *Green Chem.*, 2014, **16**, 1176.
- <sup>90</sup> P. Y. Dapsens, C. Mondelli, J. Jagielski, R. Hauert, J. Perez-Ramirez, *Catalysis Science and Technology*, 2014, **4**, 2302.
- <sup>91</sup> A. Al-Nayili, K. Yakabi, C. Hammond, *J. Mater. Chem. A*, 2016, **4**, 1373.
- <sup>92</sup> K. Yakabi, K. Milne, A. Buchard, C. Hammond, *ChemCatChem*, 2016, **6**, 1.

- 
- <sup>93</sup> C. Hammond, S. Conrad, I. Hermans, *Angew. Chem. Int. Ed.*, 2012, **51**, 11736.
- <sup>94</sup> P. Wolf, C. Hammond, S. Conrad, I. Hermans, *Dalton Trans.*, 2014, **43**, 4514.
- <sup>95</sup> J.-P. Lange, *Catal. Sci. Technol.*, 2016, **6**, 4759.
- <sup>96</sup> J.-P. Lange, *Angew. Chem. Int. Ed.*, 2015, **54**, 13186.
- <sup>97</sup> J. A. Moulijn, A. E. van Diepen, F. Kapteijn, *Appl. Catal. A: Gen.*, 2001, **212**, 3.
- <sup>98</sup> D. S. Mannel, S. S. Stahl, T. W. Root, *Org. Process. Res. Dev.* 2014, **18**, 1503.
- <sup>99</sup> S. Wang, Y. Peng, *Chemical Engineering Journal*, 2010, **156**, 11.
- <sup>100</sup> B. Hunger, S. Matysik, M. Heuchel, E. Geidel, H. Toufar, *Journal of Thermal Analysis*, 1997, **49**, 553.
- <sup>101</sup> A. Jentys, G. Warecka, M. Derewinski, J. A. Lercher, *J. Phys. Chem.*, 1989, **93**, 4837.
- <sup>102</sup> G. M. Lari, P. Y. Dapsens, D. Scholz, S. Mitchell, C. Mondelli, J. Perez-Ramirez, *Green Chem.* 2015, **18**, 1249.
- <sup>103</sup> R. M. Ravenelle, F. Schubler, A. D'amico, N. Danilina, J. A. van Bokhoven, J. A. Lercher, C. W. Jones, C. Sievers, *J. Phys. Chem. C*, 2010, **114**, 19582.
- <sup>104</sup> R. M. West, M. S. Holm, S. Saravanamurugan, J. Xiong, Z. Beversdorf, E. Taarning and C. H. Christensen, *J. Catal.*, 2010, **269**, 122.
- <sup>105</sup> C. Aelling, D. Scholz, P. Y. Dapsens, C. Mondelli, J. Perez-Ramirez, *Catal. Sci. Tech.* 2015, **5**, 142.
- <sup>106</sup> R. Gounder, M. E. Davis, *Journal of Catalysis*, 2013, **308**, 176.
- <sup>107</sup> R. Gounder, M. E. Davis, *AIChE Journal*, 2013, **59**, 3349.
- <sup>108</sup> G. Eigenberger, W. Ruppel, "Catalytic fixed-bed reactors" Ullman's encyclopedia of industrial chemistry, 1.
- <sup>109</sup> O. Levenspiel, *Chemical Reaction Engineering*, John Wiley & sons, New York, 3<sup>rd</sup> edn., ch. 21, pp. 473.

## ***2. Experimental and methods***

### **Abbreviations**

Solid state Incorporation: SSI

Cyclohexanone: CyO

Cyclohexanol: CyOH

Transfer hydrogenation: TH

Furfural: FF

Furfuryl alcohol: FA

2-(butoxymethyl) furan: BMF

Glucose isomerisation: GI

Methyl lactate: ML

Sn-Beta catalysts containing various quantities of Sn are abbreviated as XSn-Beta, where X represents the Sn loading in wt. %

## Formula and expressions

Conversion:

\_\_\_\_\_

Yield:

\_\_\_\_\_

Selectivity:

\_\_\_\_\_

Turn Over Frequency:

Carbon Balance:

\_\_\_\_\_

Contact time:

\_\_\_\_\_

Substrate turnover:

\_\_\_\_\_

Space-time-Yield:

\_\_\_\_\_

## 2.1 Catalyst synthesis

Commercial zeolite Al-Beta (Zeolyst,  $\text{NH}_4$ -form) was de-aluminated by treatment in  $\text{HNO}_3$  solution (13 M  $\text{HNO}_3$ , 100 °C, 20 mL  $\text{g}^{-1}$  zeolite) for a total of 20 hours, if not specified differently in the text.

Solid State Incorporation (SSI) of Sn into de-aluminated zeolite Beta was performed by grinding the appropriate amount of  $\text{Sn(II)acetate}$  with the necessary amount of de-aluminated zeolite for 10 minutes in a pestle and mortar. Sn-Beta catalyst with metal loading of 2, 5, 8 and 10 wt. % were synthesised and named 2Sn-Beta, 5Sn-Beta, 8Sn-Beta and 10 Sn-Beta respectively. Typically, to make 1 g of 2Sn-Beta, 0.0399 g of  $\text{Sn(II)acetate}$  and 0.9800 g of de-aluminate Beta were mixed and grinded together for 10 min. Following this procedure, the sample was heated in a tubular combustion furnace (Carbolite MTF12/38/400) to 550 °C (10 °C  $\text{min}^{-1}$  ramp rate) first in a flow of  $\text{N}_2$  (3 h) and subsequently air (3 h) for a total of 6 h. Gas flow rates of 60 mL  $\text{min}^{-1}$  were employed at all times.

$\text{Sn(O}_2\text{)-Beta}$ , purely containing  $\text{Sn(O}_2\text{)}$  in extra lattice positions were made in the same way but using  $\text{SnO}_2$  as tin precursor instead of  $\text{Sn(II)acetate}$ .

Bifunctional Sn in partially de-aluminated Beta zeolite was made by Sn SSI in a partial de-aluminated zeolite Beta. Partial de-alumination was achieved by performing  $\text{HNO}_3$  treatment for 1 h instead of 20 h. Sn SSI was successively performed in order to obtained the bifunctional catalyst.

Bifunctional Al/Sn-Beta was also made by SSI of  $\text{Sn(II)acetate}$  and  $\text{Al(III)acetylacetonate pentahydrate}$  into a fully de-aluminated zeolite Beta following the same procedure described above. Both metal precursors were ground together with the de-aluminated zeolite powder, and a single calcination procedure was followed.

The proton form of the  $\text{NH}_4$ -form of the Al-Beta zeolites (H-Beta) was obtained after a treatment at 550°C in a tubular furnace for 3h under air flow.

## 2.2 Kinetic evaluation

### 2.2.1 Batch transfer hydrogenation (TH) of cyclohexanone (CyO) and furfural (FF)

Batch TH reactions were performed in a 50 mL round bottom flask equipped with a reflux condenser, which was thermostatically controlled by immersion in a silicon oil bath. The

vessel was charged with a 10 mL solution of the reactant (0.2M) in 2-butanol, which also contained an internal standard (biphenyl, 0.01M). The substrates used vary according to the reaction, with both CyO and FF used for TH reactions. The solution was subsequently heated to the desired temperature (typically 120 °C oil bath temperature, which corresponds to the reflux temperature of 2-butanol *i.e.* 98 °C). The reaction was initiated by addition of an appropriate amount of catalyst, typically corresponding to 1 mol. % Sn relative to the substrate, unless otherwise explicitly stated. The solution was stirred at  $\pm$  800 rpm with an oval magnetic stirrer bar. Aliquots of reaction solution were taken periodically for analysis, and were centrifuged prior to injection into a GC (Agilent 7820, 25m CP-Wax 52 CB). Reactants were quantified against a biphenyl internal standard (for detailed information see section 2.3.1). Batch reactions were repeated at least three times to ensure reproducibility.

### 2.2.2 Batch etherification of furfuryl alcohol (FA) to 2-(butoxy)methyl furan (BMF)

Etherification reactions were performed in an identical way to TH. The only difference was that as substrate FA was used and different catalyst were employed. Along with Sn-Beta, the H-form of Al-Beta (various SiO<sub>2</sub>/Al<sub>2</sub>O<sub>3</sub> ratios between 25-300) and de-Al-Beta were employed. The amount of catalyst used was chosen according to the desired metal to substrate ratio, typically 100 (1 mol. %), but different ratios were also explored. In these cases, the change in metal/substrate ratio is explicitly described in the text. Batch reactions were repeated at least three times to ensure reproducibility.

### 2.2.3 Batch glucose Isomerisation (GI) reaction

D-glucose (Sigma-Aldrich,  $\geq$  99%) isomerisation experiments were performed in 15 mL thick walled glass reactor (Ace pressure tube, Sigma-Aldrich) that was heated in a temperature controlled oil bath. The reactor was charged with 5 mL of an aqueous solution of glucose (10 wt. %, 0.6 1M), and an appropriate amount of catalyst corresponding to a 1:50 Sn:glucose molar ratio (2 mol. %). Once the oil had reached the desired temperature (110 °C), the reaction was initiated by vigorous stirring with a magnetic stirrer bar (800 rpm). The reactor was stirred for an appropriate length of time, and time online samples were obtained by periodically quenching the reaction by rapidly cooling the reactor in an ice bath. Aliquots of solution were extracted with a syringe and centrifuged to remove solid particulates. Prior to injection, 0.1 mL of sample were diluted in 0.4 mL of deionised water and 0.1 mL of aqueous

solution of sorbitol (5 wt. %) as standard. The samples as prepared were subsequently analysed by HPLC (Agilent 1200 infinity II). Compounds were separated with a Ca Hi-Plex column (6.5 x 300 mm, 8  $\mu$ m particle size, Agilent), which was isothermally held at 80 °C. Ultrapure water was used as the mobile phase, at a flow rate of 0.75 mL min<sup>-1</sup>. An Evaporative Light Scattering Detector (ELSD Agilent 1200) was used in order to detect the sugars. Batch reactions were repeated at least three times to ensure reproducibility.

### 2.2.4 Batch glucose isomerisation with poison molecules

GI poisoning studies were performed in a pressurised Ace tubular glass reactor, thermally controlled by immersion into a hot oil bath on an IKA hot plate. The desired amount of reactant solution (5 mL of a solution of 10 wt. % of glucose in water), catalyst and poison were placed inside the reactor in order to fix the molar ratio at 1:50 Sn:glucose and 10:1 glucose:poison. The reaction was initiated by vigorous stirring with a magnetic stirring bar and the stirring rate was set to 800 rpm. Samples were periodically collected after quenching the reaction by cooling the pressure tube in an ice bath. The samples were prepared and analysed by HPLC as described in the previous section.

### 2.2.5 Continuous flow: TH and etherification reactions

Continuous TH reactions were performed in a plug flow, stainless steel, tubular reactor. The reactor was connected to an HPLC pump (Agilent 1200) in order to regulate the reactant flow (typically between 0.4 and 0.5 mL min<sup>-1</sup>) and allow operation at elevated pressures. The catalyst (typically between 30 and 100 mg) was mixed with a diluent material (SiC (particle size of 63-75  $\mu$ m)) in order to avoid back mixing and to minimise the pressure drop, and the bed placed in between two plugs of quartz wool. The diluted sample was densely packed into a ¼" stainless steel tube (4.1 mm internal diameter), and a frit of 0.5  $\mu$ m was placed at the end of the bed in order to avoid any loss of material. The reactor was subsequently immersed in a thermostated oil bath at the desired reaction temperature. Pressure in the system was controlled by means of a backpressure regulator, and the pressure drop was determined by comparison of the HPLC pump pressure to the outlet pressure measured by a pressure gauge. An overpressure of 5-10 bar was typically employed, depending on reactant flow rate and column length, and this allowed operation above the boiling temperature of the solvent (2-butanol, 98 °C). The reaction feed was identical to that used for batch

reactions. Aliquots of the TH reaction solutions were taken periodically from a sampling valve placed after the reactor. TH of FF and etherification of FA were performed under identical reaction conditions. Initial continuous flow reactions were repeated three times to ensure reproducibility.

### 2.2.6 Continuous flow: GI reaction and ML production

Continuous glucose isomerisation and methyl lactate production were performed in the same plug flow reactor described above. GI reaction mixture was analysed by HPLC analysis, while ML product were analysis by GC.

### 2.2.7 Catalyst regeneration

Periodic catalyst regeneration was performed heating the whole reactor in a combustion furnace (Carbolite MTF12/38/400) to 550 °C (10 °C min<sup>-1</sup>) in air (3 h).

## 2.3 Analytical methods

### 2.3.1 Gas chromatography – theoretical background

Gas chromatography (GC) is an analytical technique used for separation and quantification of mixture of components. The requisition for a substance to be analysable by GC is that has to be vaporised without decompose. For this reason, GC developed mainly thanks to petrochemical chemistry expansion, where light-to-medium molecular weight hydrocarbons are the main components, and are readily analysed by GC. In GC, but more generally for all the chromatographic techniques, the analytes are “pushed” through the system by a carrier. In the case of GC, this gas is often an inert gas, with helium typically employed. This constitutes the mobile phase. This phase will pass through the chromatographic column, where a stationary phase is present, normally solid particles or polymers spread as thin layers on the column walls. The molecules transported in the mobile phase interact differently with the stationary phase, leading them to be eluted from the column at different time. This time is often referred as retention time (r.t), and at fixed conditions is characteristic of each compound being eluted from the system (Figure 1).



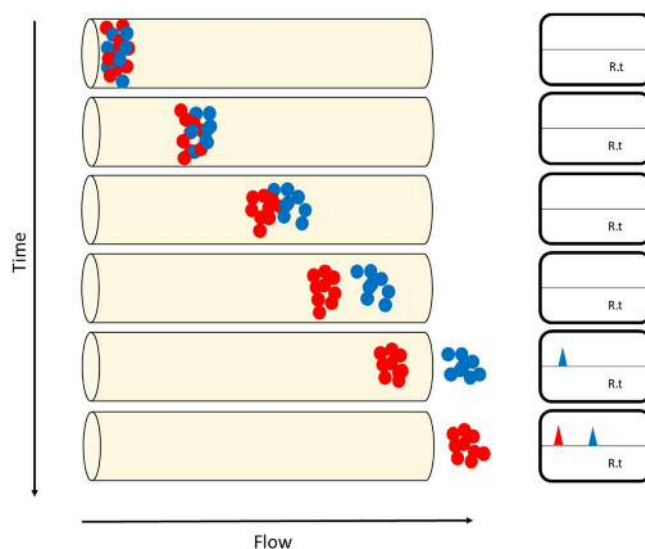


**Figure 1.** Scheme of a chromatographic separation process. The two compounds (in blue and red) interact differently with the stationary phase of the column, resulting in a different elution of the two substances at

The GC instrumentation (Figure 2) is typically constitute by several common elements. The injector is where the sample, gas or liquid, is introduced and vaporised at high temperature (normally between 150 – 300 °C). The carrier gas, whose flow is accurately controlled by the means of a valve or a mass flow controller, carries the analytes into the column that is held inside the column oven. The column oven controls the temperature at which the GC column is working, and during an analytical run it normally varies from room temperature to ca. 300 °C with a set ramp rate, depending on the speed and extent of separation required. The separation of the analytes is strongly dependent from the temperature, in addition to the type of stationary phase, so the control of temperature represents one of the most important parameters in GC. Finally, the eluted analytes will go to the detector, which generates a response that is proportional to the amount of the analyte detected.

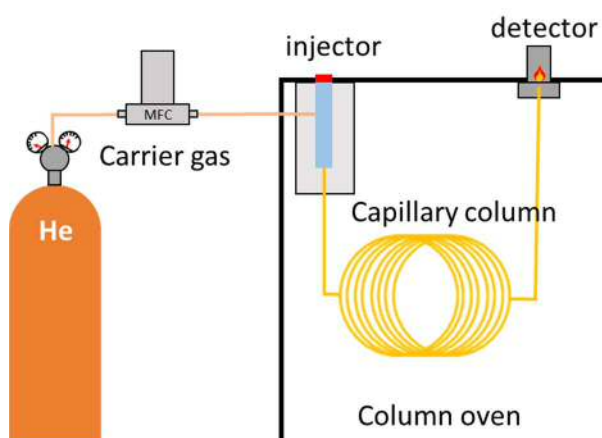


**Figure 2.** Generic schematic representation of a gas chromatographer with a FID detector.

One of the most important parts of the GC is the detector. A wide choice of detectors is available. The choice of detector will determine the feasibility of detecting a compound and the sensitivity of the signal generated. The detection of hydrocarbon or organic molecules containing low quantities of oxygen, such as alcohols, ketones and ethers, is often achieved by the use of a Flame Ionisation Detector (FID). The compounds eluted from the column go into a combustion chamber where a  $\text{H}_2$  flame burns the organic molecules. This combustion generates a flow of ions that are collected by a metal collector. This consequently generates a current that is read by an amperometer and the signal is generated. It has a maximum response for a fully hydrogenated hydrocarbon, while oxygen atoms in the molecule decreases the response. This detector has little or no response to  $\text{CO}$ ,  $\text{CO}_2$  and  $\text{H}_2\text{O}$ , since they are unable to burn, and thus cannot generate a FID signal.

Central part of gas chromatography, but also true for liquid chromatography, is what is commonly called a method. A method is a collection of all the parameters the machine is running to assure the best separation between all the analytes present in a sample. A GC a method normally comprises injector temperature, gas carrier flow rate, temperature ramp profile of the column oven, temperature of the detector (Figure 3).

Injector temperature / °C	Carrier gas (He) flow rate / mL min <sup>-1</sup>	Detector temperature / °C
250	5	250

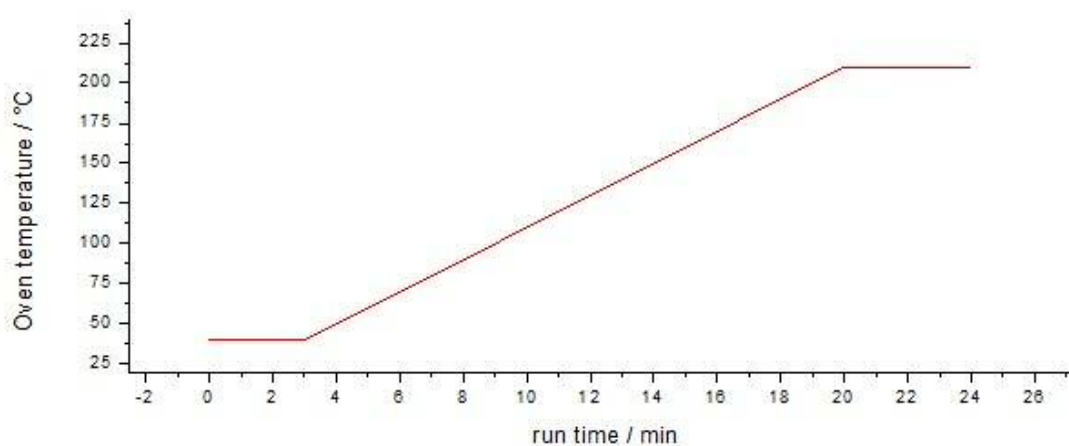


**Figure 3.** GC method parameters such as injectore temperature,carrier gas flow rate, detector temperature and temperature profile of the GC oven used for the separation of the products of TH and etherification reactions.

The method, along with the right choice of the stationary phase, will determine at which retention time a specific component will elute. The response of the detector will generate a plot, called chromatograph, in which intensity of the signal is compared against the retention time. An analyte typically produce a gaussian peak, whose area can be integrated and used for quantification, since the area of the peaks are proportional to the quantity of the compound. Typically precise quantification is achieved by comparing the area of the analytes to calibration curves obtained injecting standard solution of the specific compound. Construction of an accurate calibration curve will be explained later in the text.

### 2.3.2 Quantification of TH and etherification products

In this thesis, the quantification of the products of TH and etherification reactions were performed by means of a GC (Agilent 7820, 25m CP-Wax 52 CB column) equipped with and FID. Biphenyl (bp) has been used as internal standard. Calibration curves have been obtained as follows. Accurate solutions of the analytes have been made, by varying the concentration of the substrate in a particular solvent (Table 1). The concentration of the solutions have been chosen in order to cover all the concentration range that the analyte could possibly assume during the reaction, assuming the reaction going from 0 to 100 % of conversion/yield. In the samples, along with the analyte, a constant amount of internal standard was introduced, normally corresponding to 5 mol. % of the highest concentration of analyte. The area of the analyte and standard were obtained by integration of the corresponding signal in the chromatograph.

**Table 1.** Tables of concentrations and GC area for (top left) CyO and (top right) biphenyl.

n°	Cyclohexanone		Biphenyl	
	Concentration / M	Area	Concentration / M	Area
1	0.206	5861	0.01634	1075.4
2	0.103	2929.7	0.01777	1156.4
3	0.0515	1436.2	0.01621	1036.1
4	0.0206	585.4	0.01673	1121.6
5	0.0103	283.3	0.01718	1140.5

**Table 2.** Table of the ratio between CyO and biphenyl concentrations and area.

n°	[CyO] / [bp]	A <sub>CyO</sub> / A <sub>bp</sub>
1	12.6071	5.4501
2	5.7962	2.5334
3	3.1771	1.3862
4	1.2313	0.5219
5	0.5995	0.2484

The calibration line was subsequently produced by plotting the ratio of the concentration of the analyte and its standard against the ratio of the corresponding area obtained by the chromatogram (Figure 4).

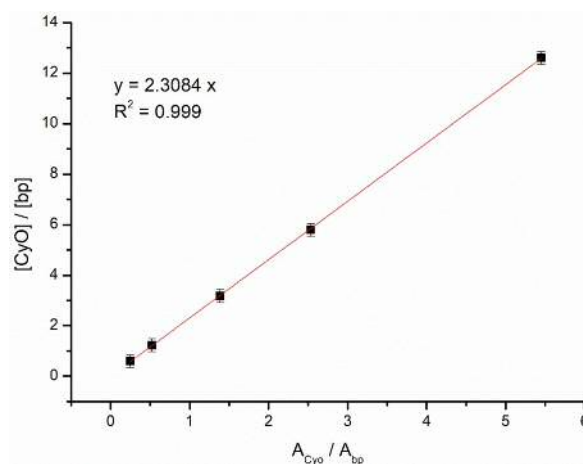


**Figure 4.** Calibration plot to obtain the GC response factor of CyO against the biphenyl internal standard. The ratio of CyO and biphenyl of concentration and GC area are plotted and the slope of the resulting line is taken as calibration factor (CF).

The calibration factor (CF) have been obtaining by calculating the slope of the fitting curve equation of the calibration points, and it is used to obtain the unknown concentrations of the analytes during the reaction.

All the CF and retention time of the analytes studied by GC in this thesis are reported in table 3.

**Table 3.** Table of the calibration factor and retention time of the compounds detectable by GC used in this thesis work.

n°	Analyte	CF	r.t. / min
1	Cyclohexanone	2.31	14.74
2	Cyclohexanol	2.19	16.02
3	Furfural	3.37	14.06
4	Furfuryl alcohol	3.26	16.30
5	2-(butoxy)methyl furan	2.25	15.50
6	2-butoxy levulinate	1.73	18.01
7	Biphenyl	/	22.10

### 2.3.3 High Performance liquid chromatography (HPLC) – theoretical background

HPLC technique is an alternative, and sometimes complementary, analytical methodology to gas chromatography, and as GC, the separation of components present in a mixture is achieved in order to identify and quantify all the analytes by comparison with calibration curves. HPLC technique is preferred to GC when is not possible to vaporise the analytes without decomposing them, *i.e.* where the analytes are either poorly thermally stable, and/or possess low vapour pressure. Therefore HPLC finds wide use in pharmaceutical analysis, where often the analytes are complex and highly functionalised molecules sensitive to heating. Also sugars chemistry is often analysed by liquid chromatography, due to the low decomposition temperature of C<sub>6</sub> saccharides (< 150 °C).

The same theoretical principles of separation described for GC can be applied in HPLC separation; and once again, the separation of analytes is achieved by interaction of the analyte in the mobile phase with the stationary phase. In this case, the mobile phase is a liquid solution of the analyte in a solvent (called eluent). The stationary phase is often a polymeric resin that is densely packed inside a column, which is itself held in a thermostatted compartment. A schematic representation of an HPLC set up is shown in figure 5.

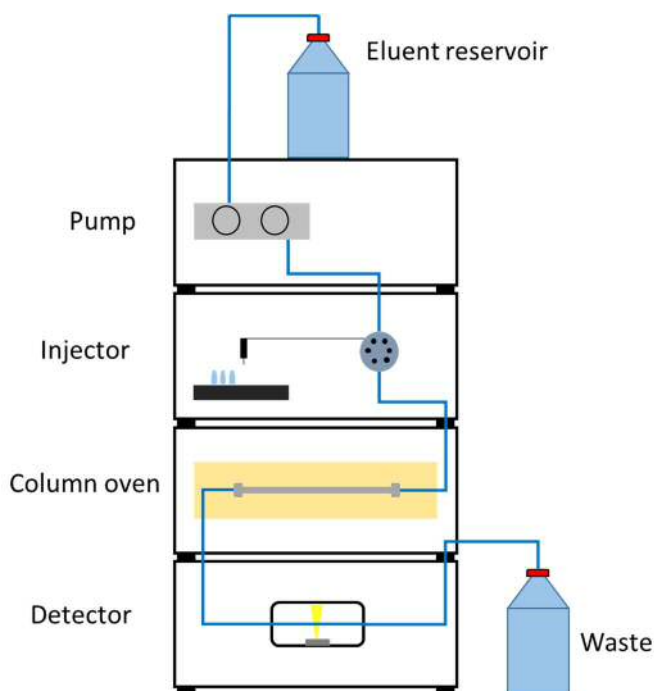


**Figure 5.** Generic schematic representation of a HPLC system. the eluent and the samples are pushed through all the system by mean of the HPLC pump. The separation of the analytes takes place in the column and the eluted compounds are detected by one or more detector modules.

In order to achieved an efficient interaction between mobile and stationary phase and a good separation, the instrument have to run at high pressures, normally between 40 and 100 bar, and in some cases even higher. Therefore, the main component of the instrument is the pump. The role of the pump is to provide an accurate and constant flow of eluent (and analyte) through all the system, and the ability to operate at high pressure arise from the pressure drops caused by the densely packed chromatographic column. The sample is introduced in the system by a six-port valve, in which a calibrated sample loop (typically between 10 and 100  $\mu\text{L}$ ) is filled prior to injection, in the phase that is typically called loading. At the moment of the injection, a valve will switched, allowing the eluent to pull the samples through all the system (Figure 6).

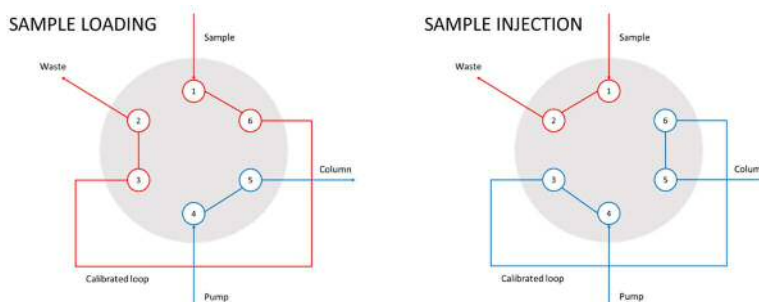


**Figure 6.** Schematic representation of a typical HPLC 6-port valve injection system. On the left the valve is in sample loading position prior the injection. The sample is loaded in the calibrated loop and the valve port are switched in the sample injection position in order to push the samples towards the HPLC column.

The choice of stationary phase ultimately depends from the nature of the analytes being investigated. Analysis in the so-called reverse-phase is very common, in which a hydrophobic stationary phase (normally C<sub>18</sub> polymer) is employed with a polar mobile phase, typically water or similar solvent with good miscibility, like methanol and acetonitrile. This column is typically use to separate hydrophobic compound, like aromatics. Also very common are acidic resins stationary phase for organic acid separation. Typically sulfonated polystyrene is employed for this use. Sugars are analysed with a cation-exchanged version of this sulfonated resin, normally with Ca<sup>2+</sup> ions exchanged to H<sup>+</sup> ions in order to allow a good separation of sugars mixtures. As for GC, the wide choice of the detector is dictated by the nature of the analyte. One of the most widespread detectors is the refractive index detector (RID). The principles of detection is based on the change of the refractive index on the eluent when is passing through the specific flow cell that is irradiated by a light beam. The beam will deflect differently depending on the difference between the refractive index of the eluent containing the analyte, and the reference eluent itself. It has become the most common detector because of its universality. On the other hand, its relative sensitivity is quite limited. The UV-vis detector is also very common. In this case, detection is based on the difference in absorbance between the solution containing the analyte, and the eluent itself. Obviously, in this case the detected molecules need to have a functional group that is UV-sensitive. For this reason this detector is widely employed for organic acids. Sugars typically present very low UV absorbances, and if they are present in low concentration their sensitivity to RID is also limited. For this reason, an Evaporative Light Scattering Detector (ELSD) is the most desirable for sugars detection and quantification. The effluent coming from the column is nebulised and vaporised at low temperature (typically 30 °C) in a nitrogen stream. During this process, the eluent and compounds with low boiling point are vaporised, while solid particle of the analyte with high or no boiling point, like sugars, are formed and hit by a light beam, that is scattered proportionally to the quantity of solid particle present. The extent of the scattering generates a signal. The major advantage of this detector is its specificity to a selected kind of compounds, in this case sugars, while are totally inactive to light molecules. Therefore, the signal related to the reaction solvent is often not detected by the ELSD.

Methods for HPLC are normally simpler than GCs. The column temperature is normally kept constant as defined by the manufacturer because many polymers are susceptible of swelling if they are employed outside a certain narrow temperature range. The eluent composition can be kept constant (isocratic flow), or can vary with time (gradient flow) in order to

improve the separation of certain compounds. Flow rates are normally kept constant during the all method.

### 2.3.4 Quantification of GI products

During this work, glucose isomerisation products were separated and quantified by the means of an Agilent 1200 infinity II high performance liquid chromatography system. The sugars were separated by an Agilent Ca Hi-Plex packed column held at 80 °C and using high purity water as eluent, with a flow rate of 0.75 mL min<sup>-1</sup>. Sugars were detected by an ELSD Agilent 1200 detector. Quantification of sugars has been done by using calibration curves made in a similar way as described in the paragraph above. The only major difference was the sample preparation, since a suitable internal standard could not be found. Accordingly, sorbitol was used as a standard and was added just prior the injection *i.e.* it was employed as an external standard. Reaction samples were thus prepared as followed: a weighted amount of sample (ca. 0.1 g) was diluted in 0.4 mL of deionised water and ca. 0.1 g of aqueous solution of 0.5 wt. % of sorbitol was added. Since the ELSD response was not linear for the concentration range analysed, a power equation was the best fit for calibration curve (Figure 7).

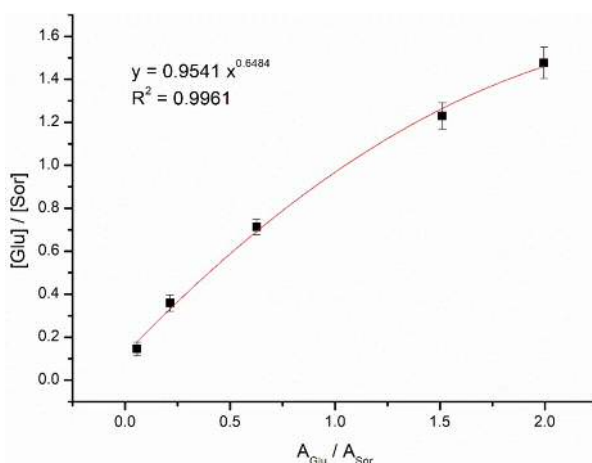


**Figure 7.** Calibration plot to obtain the HPLC response factor of glucose against the sorbitol standard. The ratio of glucose and sorbitol of concentration and HPLC area are plotted and a power function is obtain as descriptor of the response to the ELSD detector.

As such, to calculate the unknown concentration of glucose and other related products in a real reaction solution, the following equation was then employed:



**Table 4.** Table of the calibration factor and retention time of the compounds detectable by HPLC used in this thesis work.

n°	Analyte	CF <sub>a</sub>	CF <sub>b</sub>	r.t. / min
1	Glucose	0.9514	0.6484	10.5
2	Mannose	1.0065	0.6332	11.6
3	Fructose	1.2478	0.7829	12.8
4	Sorbitol	/	/	20.2

## 2.4 Characterisation techniques

### 2.4.1 Surface area analysis and porosimetry analysis

Surface area and porosimetry measurements of a solid material are done by the means of adsorption of gaseous molecules. These methods consist of physically adsorbing an inert gas at its condensation temperature on the material. Many equations can be used to calculate the specific surface area, but the most commonly used is the BET equation.<sup>1</sup> The isotherm obtained is a function of the volume of gas adsorbed ( $v$ ) against the relative pressure ( $p/p_0$ ). The monolayer adsorbed gas quantity ( $v_m$ ) is correlate to the total surface area.

According to BET theory, it should be possible to obtain a straight line if the equation is applied in the partial pressure range of  $0.05 - 0.35 p/p_0$ . The slope calculated by this line contains the value of  $v_m$  and the specific surface area can be calculated.

Where  $N$  is the Avogadro number,  $s$  is the adsorption cross-section of the adsorbing gas,  $V$  is the molar volume of the adsorbing gas and  $a$  is the mass of the solid material. The total pore volume can be directly extrapolated from the isotherm at partial pressure  $p/p_0 = 0.99$ .

In principle, any gas can be used as adsorbate to obtain the isotherm and apply the BET theory. In practice, nitrogen is the most common gas used for surface area analysis, because it is abundant and cheap, and the sample can be kept at 77 K (condensation temperature of nitrogen) by immersing the sample holder in liquid nitrogen.

In this work, specific surface area was determined from nitrogen adsorption using the BET equation, and total pore volume was taken from the total volume of adsorbate at  $p/p_0 = 0.99$ . Nitrogen adsorption measurements were performed on a Quantachrome Quadrasorb, and the adsorption isotherms were obtained at 77 K. The samples were degassed prior the nitrogen adsorption. Two different way of degassing were performed, depending of the kind of sample analysed. When the sample was fresh (not post-reaction) degassing was performed under vacuum (ca.  $10^{-6}$  bar) at 250 °C for 6 h. When the sample was post-reaction they were degassed under milder conditions: 115 °C for 6 h at atmosphere pressure under nitrogen flow. This milder degas treatment was applied in order to remove only physically adsorbed species (gas and moisture) and not possible heavy carbonaceous compounds, whose role in pore fouling needed to be determined.

#### **2.4.2 Thermo-Gravimetric Analysis (TGA)**

TGA is a technique in which the mass of the sample is measured while its temperature is changed over time. The information provided about this technique can regard the thermal stability of the sample, or the species adsorbed on the material. The technique is commonly used to characterise polymers, in which their characteristic decomposition temperatures provide qualitative information about the chemical nature and composition of the material. If coupled to a mass spectrometer, it can provide qualitative information about the species evolved from the material. The instrumentation is made of a combustion chamber in which a balance is constantly measure the mass of the sample that is placed on an alumina crucible. The temperature can be accurately programmed and the atmosphere of the combustion chamber, gas flow and gas composition, can be controlled as well. A plot of the mass of the

catalyst versus time and/or temperature is obtained from this analysis. It is common practice to plot the first derivative of the mass loss against time/temperature; This allows a more clear and visual identification of when, and hence at what temperature, a specific mass loss occurs.

In this work, TGA were performed on a Perkin Elmer system. Samples were held isothermally at 30 °C for 30 minutes, before being heated to 550 °C (10 °C min<sup>-1</sup> ramp rate) in air. A final isotherm of 3 h was subsequently used.

### 2.4.3 Temperature Programmed Desorption (TPD) coupled with Mass Spectroscopy (MS)

TPD experiments consist on the investigation of various phenomena related to temperature changes of a solid sample. Often probe molecule are absorbed at room temperature on the material, and successively are desorbed by gradually increasing the temperature at which the sample is held under a controlled flow of gas. The gas effluent is then analysed in order to obtain information of various nature. For example NH<sub>3</sub>-TPD is typically used to quantify the acid strength of a catalyst by measuring at which temperature, and at which amount, NH<sub>3</sub> is desorbed from the sample upon heating, after its saturation onto the catalyst at room temperature. Other than experiments with probe molecules, TPD methods can also be used to quantify and identify the molecules that are present in a catalyst after it has been used during reaction. The detection of the gas stream can be done with several detectors. The most common detector is the thermal conductivity detector (TCD), in which the thermal conductivity of the effluent is compared to a standard. TCD detector can also be used to quantify the different species if compared with calibration curves. However, no indication of the type of molecules desorbed is obtain by this kind of detector. If a qualitative analysis is desired then TPD can be couple with a Mass Spectrometer (MS) detector. In this way the mass to charge (m/e) of the compounds evolved from the sample can be detect for an easier identification of the gas composition.

In this thesis, TPD-MS measurement were carried out on a home-made system formed by a Bruker Tensor II equipped with a Harrick praying mantis DRIFT cell connected with the MS. The catalyst was placed inside the drift cell and its surface was constantly monitored by the IR spectrometer. The cell was heated from 30 to 550°C (ramp rate 10 °C/min) and a constant flow of air was kept during all the experiment. The outlet of the DRIFT cell was connected to a Hyden QGA mass spectrometer for the online analysis of the gas phase.

#### 2.4.4 Diffuse Reflectance Infrared Fourier Transformed (DRIFT) spectroscopy

Molecules are capable of absorbing IR radiation when the energy of the incident beam matches the energy necessary to excite a particular mode of vibration of the chemical bonds present in the molecule. Exploiting this characteristic, IR spectroscopy is used to determine the type and strength of bonding present in the molecules. In particular, the mid-IR region, cover a range of energies between 600 to 4000  $\text{cm}^{-1}$ , is of particular interest. Many modes of acquiring IR spectra are possible, however diffuse reflectance IR spectroscopy (DRIFT) is particularly suitable for powder analysis, because it does not need any sample preparation, and it is easy to perform *in situ* experiments with a dedicated setup.

In catalysis, the adsorption of probe molecules to the material can give precious information about the type and the strength of the active site, as described above (see 2.4.3, TPD-MS). In addition to this fact, when these molecules are adsorbed on these sites, they give also birth to specific vibrational signal. The strength of this signal can provide useful information on the type of interaction, in addition to the strength of interaction, between the probe and the catalyst surface. These interactions can be tested under different conditions, like temperature, gas composition, vacuum, and the change in intensity can be correlate to the strength of the bond active site-probe molecules. Of particular interest for Lewis acidic material are deuterated acetonitrile and pyridine, which are often used as probe molecules because they give characteristic vibrations when they are bonded to Lewis acid sites. In particular, when acetonitrile forms Lewis acid-base adduct, a vibration at 2310  $\text{cm}^{-1}$  is generated. In contrast, when the molecule is only weakly physisorbed on the catalyst the signal is shifted to 2275  $\text{cm}^{-1}$ . Semi-quantitative comparison of the Lewis acid strength between different materials can be done by measuring the area of the signal at 2310  $\text{cm}^{-1}$  at progressively increased temperatures, in order to remove the contribution of the physisorbed molecules. Likewise, pyridine is often use as a probe molecules. In addition, to provide Lewis acid information, pyridine can interact with Brønsted acid sites; Lewis acid-related vibration can typically be found at 1595 and 1450  $\text{cm}^{-1}$ , while Lewis acid interactions are indicated by the signal at 1643 and 1540  $\text{cm}^{-1}$ .

DRIFT spectroscopy was performed in a Harrick praying mantis cell. The spectra were recorded on a Bruker Tensor II spectrometer over a range of 4000-650  $\text{cm}^{-1}$  at a resolution of 2  $\text{cm}^{-1}$ . In situ  $\text{CD}_3\text{CN}$  and pyridine measurements were performed on pre-treated zeolite powders at higher temperature in order to de-gas the material (550 °C, 1 hour under flowing air, 60  $\text{mL min}^{-1}$  in synthetic air). After the pre-treatment, the samples was let to cool down

to room temperature. Successively, the sample was saturated with the probe molecule vapour at room temperature for 5 minutes. At this point, vacuum was applied to the DRIFT cell (ca.  $10^{-5}$  bar) and the temperature was gradually ramped in through a temperature range between 30 and 250 °C. the IR signal was continuously monitored during this process.

## 2.4.5 Nuclear Magnetic Resonance (NMR) spectroscopy

### 2.4.5.1 Theoretical background

NMR spectroscopy is a technique that probes the local magnetic field around a nuclei of a specific element in a particular sample. This technique has become the primary technique of analysis for organic chemists, in fact detailed structural information about molecule and how their atoms are spatially arranged can be obtained. NMR is conventionally applied to probe  $^1\text{H}$  and  $^{13}\text{C}$  nuclei of the organic molecules and the analysis is done to a solution of the analyte, typically present in a deuterated solvent. The following section describes the fundamental theory of NMR spectroscopy.

When the sum of the protons and neutrons is an odd number, the nucleus possess a property called spin, and is described by the quantum number  $I$  and it is associated a magnetic moment called  $\mu$  and defined as:

$$\mu = I \gamma$$

where  $\gamma$  is the gyromagnetic ratio, a constant property of each nuclei. When a nucleus is immersed in an external magnetic field ( $B_0$ ), the magnetic moment of the nuclei align, either with or against the direction of the external magnetic field,  $B_0$ . In this case, the spin quantum number is called  $m$  and the degenerate nuclear energy level splits, forming different energy levels (Figure 8). This is known as the Zeeman effect. Each single energy level can therefore be defined as:

$$E = \pm m \hbar \gamma B_0$$

When  $m$  is  $\pm\frac{1}{2}$ , two nuclear energy levels are formed and the difference between these levels is expressed as:

$$\Delta E = \hbar \gamma B_0$$

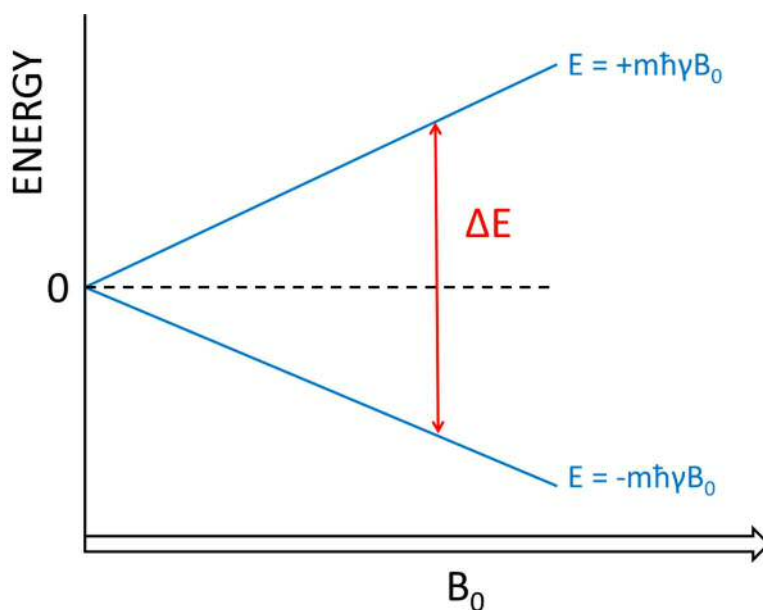


**Figure 8.** Representation of the spin energy level splitting of a nuclei (with  $m = \pm\frac{1}{2}$ ) as function of the external magnetic field  $B_0$ .

When the sample is irradiated by a radiation that has the amount of energy corresponding to  $\Delta E$ , a promotion of nuclei from the lowest to the highest level is observed. Radio-frequency radiation, in the order of hundreds of MHz or GHz, are typically required for the absorption to occur. The exact frequency (called Larmor frequency) depends from the kind *i.e.* the identity, of the nucleus under study, and from the magnitude of the external magnetic field, as determined by:

—

The above reasoning is true for an isolated nucleus. However, in molecules, all the nuclei are surrounded by electrons that orbiting around them. Since these electrons are charged moving particles, they create a local magnetic field,  $B_e$ , which can interact and oppose the external field,  $B_0$ . Since each nuclei has different interactions with the electrons, the extent of  $B_e$  will vary with the different species. As a result, the effective resonance frequency ( $\nu_{\text{eff}}$ ) will be extremely sensitive to the local magnetic surrounding of the nuclei, giving birth to characteristic and unique signals for each species in a sample, even if all species correspond to the same chemical element. The effective resonance frequency will be then re-defined as:

---

The actual NMR signal is built during the so-called relaxation period, which is the reverse phenomena of the absorption. When the radio-frequency is no longer irradiating the sample, the nuclear spins start to relax, thus returning to their thermodynamically stable level of energy. Relaxation processes are complex and can be of different nature, however the two more common relaxation modes are the spin-lattice ( $T_1$ ) and spin-spin ( $T_2$ ) relaxation. The relaxation mode can have different timescale and they are strictly dependent from the nature of the nuclei and their chemical surrounding. As such, two different nuclei of the same element can have a very different relaxation times and mechanisms, depending on the position they occupy in the molecules. In general, the more efficient the relaxation, the faster is time of  $T_1$ , and hence the faster is the time of analysis and consequently, the quality of the signal, since more spectra can be acquired per unit time, increasing the signal to noise (S/N) ratio, resulting in better signal quality and resolution.

The resonance frequency of a particular NMR signal is expressed in terms chemical shift ( $\delta$ ) and have ppm as unit. It is the resonance frequency of a specific nuclei compared to the frequency of the same element nucleus when it is in an arbitrary standard molecule ( $\nu_{ref}$ ). The chemical shift are normalised to the working frequency of the spectrometer, the same chemical shift is observed for the same nuclei in different machines.

---

### 2.4.5.2 Pulse sequence

Modern NMR spectrometers use a pulse sequence in order to acquire the NMR signal. The pulse sequence is composed by three main phases: radio-frequency pulse, Free Induction Decay (FID) recording and recycle delay time (Figure 9).

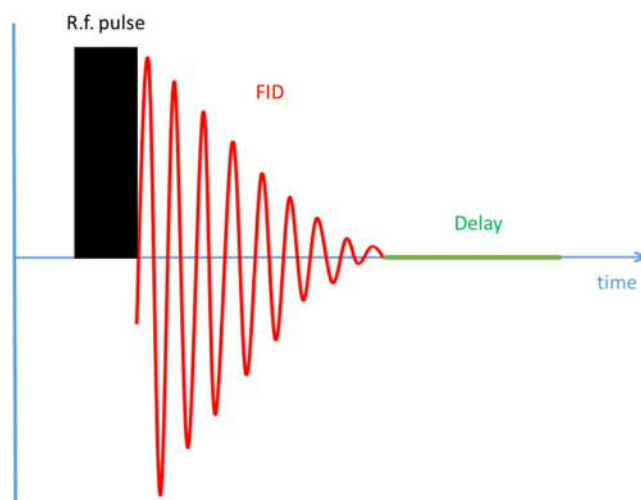


**Figure 9.** Conventional NMR pulse sequence. It is composed by a fast r.f. pulse in which the nuclear spin are excited to a upper energy level. Subsequently the r.f. pulse is stopped and the FID is recorded. A delay time is often employed to allow all the nuclear spin to relax their original level, before to apply again the r.f. pulse.

The pulse is the part in which the radiofrequency (at Larmor frequency) is applied to the sample, thus the spin are excited to the upper nuclear energetic level. After the pulse, a process of precession in the direction of the magnetic field of the excited spin starts, but rapidly fades with time. This process is called FID and is the actual signal that the NMR produces. Lastly, a delay is the time required for all, or a part of the spin to relax back to their equilibrium energy level in absence of any radio frequency excitation. After that, the sequence starts again. The FID is a sinusoidal function in a time dominion, thus the data are processed with the Fourier transform (FT) to transform the signal detected from time-dominion to frequency-dominion, leading to the classical NMR spectra.

#### 2.4.5.3 Magic angle spinning NMR (MAS NMR) spectroscopy

However, when NMR is applied to solid samples, spectra typically possess very poor quality. In fact, the main problem of solid state NMR arises from the anisotropy of the local magnetic field of nuclei present in the solid sample. Whilst in solution the molecules are mobile and anisotropy of the field are averaged by their free motion, the solid state phase constrains molecules motion, “freezing” their local magnetic field and causing anisotropic nuclear spin interactions, resulting in broad signals and poor S/N, producing spectra of very difficult interpretation and assignment. However, after many years of research, it has been found that spinning the solid sample at high frequency (1-50 kHz) around an axis placed at  $54.7^\circ$



respect to the magnetic field  $B_0$  (Figure 10), simulates the random molecular motion that is present in solution and the anisotropic nuclear interaction are greatly reduced, leading to sharper and more defined peaks.

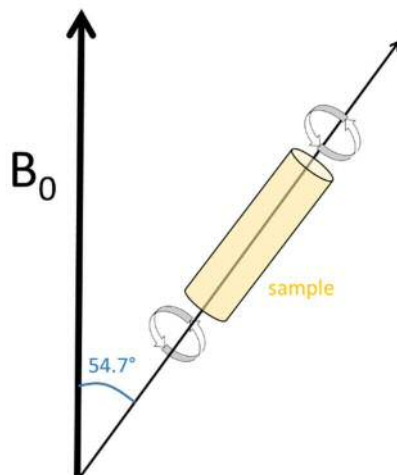


**Figure 10.** MAS NMR spinning rotor placed at  $54.7^\circ$  (magic angle) respect to the applied magnetic field.

The main focus of this thesis is Sn-containing catalysts. Unfortunately, Sn has been proved to be a very challenging element for MAS NMR spectroscopy. In fact, very noisy spectra are normally obtained due to the combination of low Sn loading (between 2 and 10 wt. %), the low natural abundance of  $^{119}\text{Sn}$  isotope (8.59 %) and long relaxation times for Sn,  $T_1$ . For many years, the analysis of  $^{119}\text{Sn}$  MAS NMR has been limited and did not provide accurate information.<sup>2,3</sup> However, recently it has been shown that applying the Carr-Purcell-Meiboom-Gill (CPMG) echo-train acquisition to  $^{119}\text{Sn}$  MAS NMR analysis that the S/N can be substantially improved, permitting a more clear reading and interpretation of the spectra, even though this is achieved at the expense of chemical shift resolution.<sup>4,5</sup>

In this thesis, MAS NMR experiments were performed at Durham University through the EPSRC UK National Solid-state NMR Service with a 400 MHz (9.4 T) solid state NMR spectrometer.

$^{119}\text{Sn}$  MAS NMR spectra in direct excitation were acquiring using a Larmor frequency of 149 MHz, with a recycle delay of 2 seconds. The rotor spinning frequency was set on 10 KHz.  $^{119}\text{Sn}$  MAS NMR spectra in cross-polarisation ( $^1\text{H} \rightarrow ^{119}\text{Sn}$ ) were acquire using a Larmor frequency of 149 MHz and a recycle delay of 1 second. The rotor spinning frequency was set on 10 KHz.

$^{29}\text{Si}$  MAS NMR spectra were acquired using a Larmor frequency of 79 MHz and a recycle delay of 90 seconds. A frequency of 10 KHz was used to spin the sample rotor.

### 2.4.6 Powder X-ray Diffraction (pXRD)

X-ray diffraction technique is widely employed in material chemistry to identify and quantify different crystalline phases, when compared with a data bank database. Crystalline solid materials present characteristic structure in which their constituents, which can be atoms, molecules or ions) are spatially arranged in a highly ordered manner that is repeated in the three dimensions of the space. Crystals can act as a crystalline three-dimensional diffraction grate when there are irradiating with monochromatic X-rays. Therefore, X-rays can be used to study the spatial arrangement of component of the crystal by applying studying the diffracted radiation. When Bragg's law requirements are satisfied, at certain angles of diffraction the constructive interferences of the X-ray provides information about the crystalline lattice like the spacing between the planes.

;      —

Where  $n$  is an integer number,  $\lambda$  is the wavelength of the X-ray radiation and  $\theta$  is the angle between the diffracted beam and the sample. A schematic of the X-ray diffraction process is shown in figure 11.

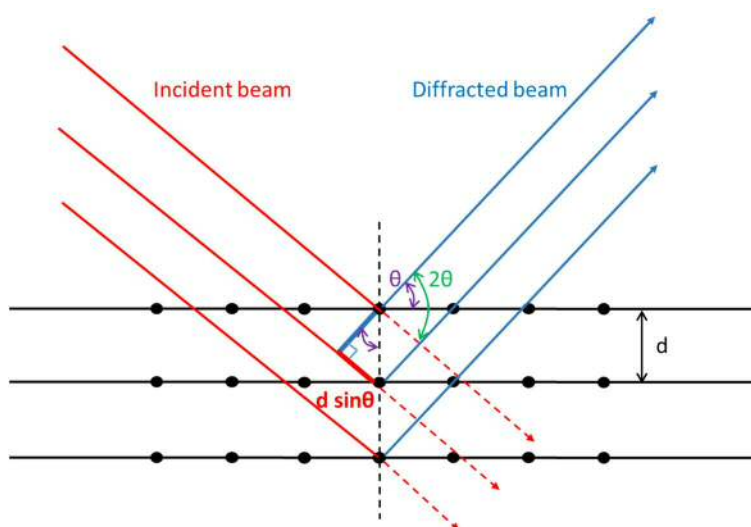


**Figure 11.** Scheme of diffraction phenomenon generated by the incidence of a monochromatic radiation into a crystalline structure according to the Bragg's law. The incident radiation interacting with the different lattice plane place at distance  $d$ , will generate a diffracted radiation at  $\vartheta$  degree.

Other than information of the d-spacing, it is also possible to calculate the crystallite size by using the Scherrer equation:

$$D = \frac{K\lambda}{\beta \cos \theta}$$

Where  $K$  is a dimensionless shape factor (normally between 0.9-1),  $\lambda$  is the wavelength of the X-ray radiation,  $\theta$  is the angle between the diffracted beam and the sample and  $\beta$  is the line broadening at Full Width Half Maximum intensity (FWHM).

The diffractometer is composed by three main components: the X-Ray generator, the sample holder and the detector (Figure 12)

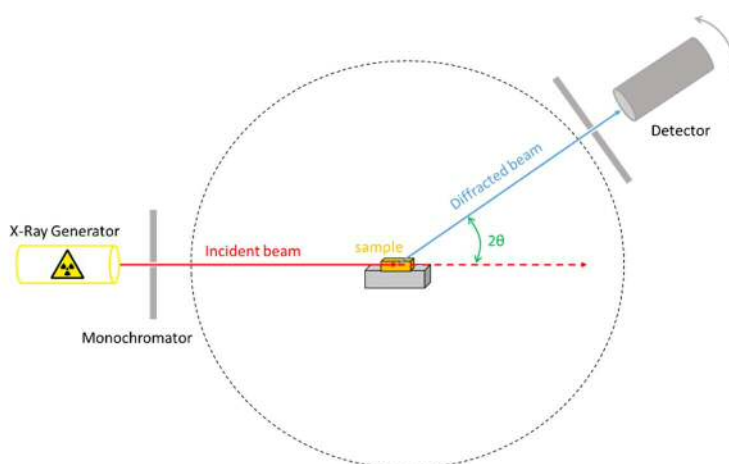


**Figure 12.** Schematic of a classical XRD machine. The monochromatic X-ray is generated by the generator and filter before it hits the sample. A mobile detector moves at different angles to record the intensity of the diffracted beam at  $2\theta$  angle respect to the incident radiation.

The X-ray radiation is generated by irradiating a foil of copper with a high-energy electron beam. An inner core electron of the copper atom will be expelled producing a vacancy that will be filled by one electron of the upper level, generating a cascade of electrons. This movement of electron will give birth to several X-ray radiations that will pass through a monochromator to be filtered into a single monochromatic beam. Only a monochromatic X-ray, typically the  $\text{CuK}\alpha$  radiation ( $1.5418 \text{ \AA}$ ), will be selected and converged to the sample. The detector will move with around an arc and will therefore collect the diffracted radiation at several angles, from ca. 5 to 70  $2\theta$ . As a result from pXRD analysis, a diffractogram is obtained, and intensity of the diffracted beam are plotted against the diffraction angle  $2\theta$ .

In this work, a PANalytical X'PertPRO X-ray diffractometer was employed for powder XRD analysis. A  $\text{CuK}\alpha$  radiation source (40 kV and 30 mA) was utilised. Diffraction patterns were recorded between 6-55°  $2\theta$  (step size 0.0167°, time/step = 150 s, total time = 1 h).

## References

- 
- <sup>1</sup> S. Brunauer, P. H. Emmett, E. Teller, *J. Am. Chem. Soc.*, 1938, **60**, 309.
- <sup>2</sup> S.-J. Hwang, R. Gounder, Y. Bhawe, M. Orazov, R. Bermejo-Deval, M. E. Davis, *Top. Catal.*, 2015, **58**, 435.
- <sup>3</sup> W. R. Gunther, V. K. Michaelis, M. A. Caporini, R. G. Griffin, Y. Roman-Leshkov, *J. Am. Chem. Soc.*, 2014, **136**, 6219.
- <sup>4</sup> Y. G. Kolyagin, A. V. Yakimov, S. Tolborg, P. N. R. Vennestrom, I. I. Ivanova, *J. Phys. Chem. Lett.*, 2016, **7**, 1249.
- <sup>5</sup> A. V. Yakimov, Y. G. Kolyagin, S. Tolborg, P. N. R. Vennestrom, I. I. Ivanova, *J. Phys. Chem. C*, 2016, **120**, 28083.

### ***3. Identification of active and spectator Sn sites in Sn-Beta and consequences for Lewis acid catalysis***

#### **3.1 Introduction**

As described in Chapter 1, stannosilicate zeolites such as Sn-Beta, are highly active catalysts for a variety of catalytic processes involving biomass-derived substrates. Notable examples include the tandem transfer hydrogenation (TH)/etherification reaction of furfural, and the valorisation of sugars, either through isomerisation to fructose, or retro-aldol conversion to C<sub>3</sub> compounds. The aim of this thesis is to study several systems catalysed by Sn-Beta, and particularly investigate their stability and maximise their ability to continuously produce the desired products. To achieve this aim, obtaining a catalyst with a high content of active site is a pre-requisite. In fact, high metal loadings theoretically increase the activity per gram of catalyst. This is essential in order to maximise the space-time-yield (STY), which is one of the main descriptor for productivity of the catalyst, especially for continuous flow processes. It is noted that STY is defined as the number of moles of product produced per unit time per unit of volume. A catalyst with high activity per unit volume (achieved by increasing the loading of active component) will therefore be beneficial in order to achieved a high STY.

Many different methods to synthesise Sn-Beta have been explored in recent years, and important characteristics of the material are determined by the choice of the synthetic methodology.<sup>1,2,3,4</sup> Indeed, factors such as hydrophobicity and metal loading are dramatically impacted by the choice of preparation methodology. Although it is appreciated that classical hydrothermal synthesis of Sn-Beta results in the formation of highly active and hydrophobic catalysts, this method of synthesis does not allow catalysts with Sn loading higher than 2 wt. % to be obtained. For this reason, other methodologies must also be explored. Post-synthetic methods (see Chapter 1 section in 1.6.2), on the other hand, are known to allow faster synthesis of the catalyst, and may present opportunities to achieve metal loadings higher than 5 wt. % of Sn. After a careful evaluation between post-synthetic methodologies presented in literature, solid state incorporation is considered the most suitable method and therefore will be used in this work.<sup>5,6</sup> The choice of this method is based on the following reasons: i) the synthesis procedure is safe (avoiding the use of HF), easy and reproducible; ii) it is characterised by fast synthesis times; iii) it reportedly permits high metal loadings (> 2 wt. % Sn) to be obtained; iv) the catalyst contains very small crystallites (ca. 1  $\mu\text{m}$ ), which may improve transport properties during the reaction. Between all the advantages over the classical hydrothermal synthesis listed above, the higher Sn loadings achievable by SSI is definitely the main attractiveness of this method. Figure 1 summarises the steps necessary for the synthesis of the catalyst.

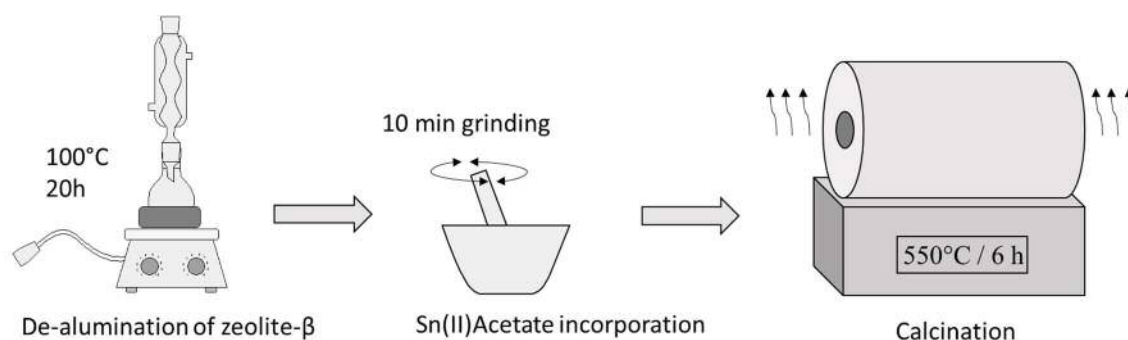


**Figure 1.** Scheme of the solid state incorporation (SSI) methodology for Sn-Beta synthesis.

Starting from a commercial aluminosilicate Beta zeolite, a 20 h treatment in concentrated, aqueous nitric acid is made in order to extract the aluminium atoms from the zeolite framework. Successively, the de-aluminated zeolite is recovered, washed and dried. In the second step, a solid organometallic precursor of Sn, in this case Sn(II)acetate, is added to the de-aluminated powder, and the mixture is grinded together for 10 minutes. The physical

mixture is then placed in a tubular furnace and treated to 550 °C, first for 3h under nitrogen, and then an addition 3 h in air.

Incorporation of Sn into the zeolitic framework by SSI methodology theoretically allows obtaining Sn-Beta with different metal loadings. Nevertheless, few detailed kinetic studies are available for Sn-Beta catalysts made by SSI. As such, prior to performing stability studies in continuous flow, the basic kinetic parameters, such as kinetic constant and activation energies, need to be known. Importantly, the intrinsic activity of the catalyst for TH and glucose isomerisation (GI) also need to be benchmarked. Besides, the impact of metal loading on intrinsic activity is still unexplored in literature, mainly due to the lack of materials with high Sn loading. Therefore, this chapter will investigate the activity of a series of SSI-made Sn-Beta containing different Sn loadings, for two particular reactions, those being the TH of cyclohexanone (CyO) and GI at different metal loadings.

As described in Chapter 1, TH is a useful method to reduce the oxygen content of various oxygenated compounds, through use of a sacrificial hydride donor, in this case the solvent (2-butanol). It is also a useful example of an intermolecular hydride transfer reaction (*Vide Infra*). For this chapter, the TH of CyO to cyclohexanol (CyOH) in 2-butanol as solvent represents a useful model reaction, in which a full kinetic evaluation of the activity of the catalysts can be compared with existing literature data obtained with similar materials.<sup>7</sup> Using 2-butanol both as solvent and reactant also allows one to push the equilibrium of the reaction almost fully towards cyclohexanol, and assuming that its concentration does not vary with time, the reaction can be treated as pseudo-first order to the cyclohexanone.

The GI reaction to form fructose in aqueous media is the second reaction chosen to test the performance of the catalyst. GI is a useful reaction, in that it can be performed in the presence of water, which is an important aspect concerning stability of the catalyst (Figure 2).<sup>8</sup> Moreover, it has also been shown that the mechanism of the reaction can be seen as an intramolecular TH, therefore direct comparison with the kinetics data obtained for GI and the TH of CyO can be made. Importantly, the commercial relevance of this reaction is outstanding; it is the biggest biochemical process in the world catalysed by enzyme and it is used to produce High Fructose Corn Syrups (HFCS), a sweetener used in the soft drinks industry.<sup>9</sup> Besides HFCS, isomerisation of glucose to fructose is a key step for obtaining platform bio-molecules, since fructose can readily be converted in furanic compounds by dehydration. Between many downstream products obtainable by fructose valorisation, the

most relevant are 5-hydroxymethylfurfural, lactic acid,  $\gamma$ -valerolactone and ethers of furanic compounds.

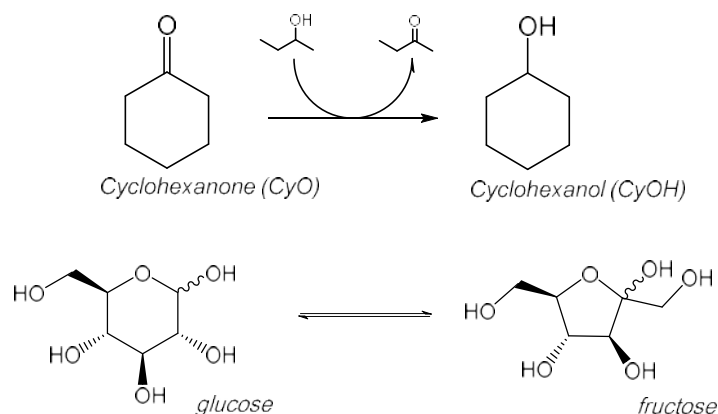


**Figure 2.** Scheme of (Top) the CyO TH to CyOH and (Bottom) GI.

## 3.2 Results and discussion

### 3.2.1 Time-online plot as tool to identify the key kinetic parameters

In order to identify and benchmark the kinetic parameters characteristic of Sn-Beta for TH reactions, batch operations were conducted because they offer an accurate and reproducible method to obtain a set of kinetic data in a relative short period of time. The concentration of the products involved are monitored through the time of the reaction and a typical time-online plot is constructed, in which conversion and yield(s) are plotted as function of time. From this, intrinsic kinetic parameters, such as the kinetic constant and the activation energies, can be calculated. To obtain data that allowed comparison of the intrinsic activity of each catalyst, the molar ratio of CyO and Sn were kept constant in all the experiments, and 1 mol. % of Sn relative to CyO was introduced. It is noted here that catalysts are abbreviated by their metal loading *i.e.* Sn-Beta containing 2 wt. % Sn is denoted as 2Sn-Beta.

A first test of 2Sn-Beta synthesised by SSI for the TH of CyO was carried out and the relevant time-online plot of CyO conversion is shown in figure 3. Firstly, this test showed that Sn-Beta prepared by SSI is active for the TH of CyO reaction. Accordingly, full conversion of CyO in CyOH was achieved in ca. 30 min, with a carbon balance and selectivity > 95 % being observed throughout the reaction period. The intrinsic activity was calculated from the first point of conversion (2 min) by calculation of the turnover frequency (TOF) For 2Sn-Beta, a



value of  $1150\text{ h}^{-1}$  was obtained. When compared to values found in the literature, in this case a hydrothermally-prepared Sn-Beta containing 1.8 wt. % of Sn loading, a value of  $1940\text{ h}^{-1}$  was calculated.<sup>10</sup> Despite the lower absolute value of TOF exhibited by the SSI-synthesised Sn-Beta, it is clear that this method could be successfully used to make Sn-Beta catalysts having the same order of magnitude of activity of the hydrothermally synthesised material.

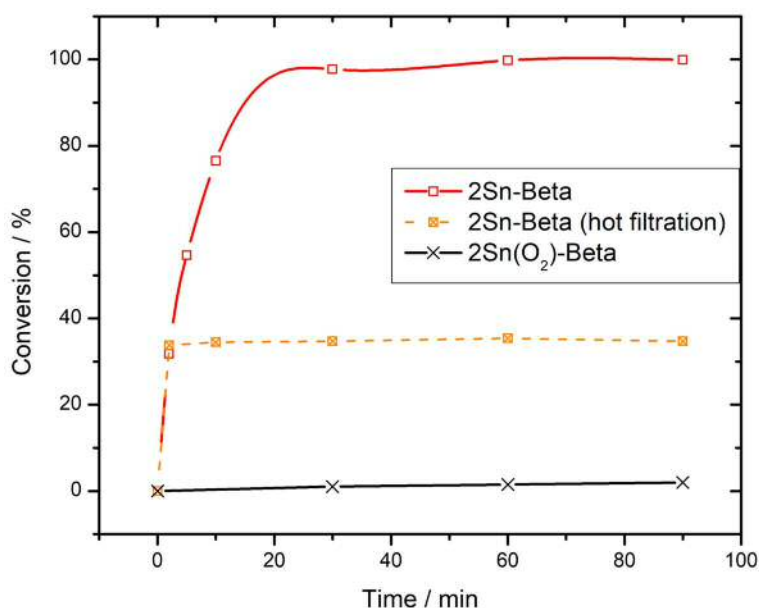


**Figure 3.** Conversion vs. time plot of MPV CyO Transfer hydrogenation in the presence of 2Sn-Beta, 2Sn(O<sub>2</sub>)-Beta and after hot filtration. Conditions: 10 mL of a solution of 0.2 M of CyO in 2-butanol were reacted with the Sn-Beta under reflux (98°C) for 90 min. CyO/Sn=100.

To know if the reaction proceeds purely by heterogeneous catalysis, or if any contribution by homogeneous catalysis is present, a hot filtration experiment was performed. As described in Chapter 1 (see section 1.7.2), this experiment consisted of performing the reaction normally until the first point of conversion is obtained. Then, the reaction solution was quickly filtered through a filter paper and the catalyst removed from the reactant mixture. The resulting solution was then placed back into the reactor, and the reaction was continued. If some level of conversion was observed after the ‘hot filtration’, it could mean that the Sn has possibly leached from the zeolite into the bulk of the solution and act as homogeneous catalyst. As can be seen, the fact that no conversion was observed after the removal of the catalyst clearly demonstrates that the reaction proceeds only *via* heterogeneous catalysis (Figure 3, orange crossed square).

Another parameter to asset is if there are any contributions from extra-framework Sn species, like  $\text{SnO}_2$  species. To achieve this, a 2 wt.%  $\text{Sn}(\text{O}_2)$ -Beta (named 2 $\text{Sn}(\text{O}_2)$ -Beta) was used as catalyst. Such a catalyst was obtained by substitution of  $\text{Sn}(\text{II})$ acetate during the preparation with  $\text{SnO}_2$  as Sn source during the SSI synthesis of the catalyst. The reaction has been carried out under the same identical conditions of the precedent reactions. Figure 3 (black cross) showed that no conversion is detected even after 90 min of reaction, clearly showing that Sn present as (extra-framework)  $\text{SnO}_2$  is inactive.

### 3.2.2 Activation energy of the process

A crucial parameter in catalysis is the activation energy. Activation energy, express in  $\text{kJ mol}^{-1}$ , represents the minimum energy the molecules have to possess for the reaction to occur. Experimentally it can be obtained by studying the temperature dependence of the reaction. In this regard, the Arrhenius expression is the equation that is most routinely used to obtain the energy value.

—

Application of the natural logarithm to the Arrhenius expression gives a linear that can be easily plotted in a graph as with  $\ln(k)$  on the ordinate and  $1/T$  on the abscise.

—

To determine the  $E_a$  of the process, four reactions were performed at different temperatures (temperature range 50 to 100 °C). The apparent kinetic constant has been obtained by each reaction, assuming a pseudo-first order and then used for the Arrhenius plot. The activation energy can be obtain directly by calculating the slop of the resulting line. The calculated activation energy was of  $39.3 \text{ kJ mol}^{-1}$ . Given the relative low value of the activation energy, the possible influence of mass transfer phenomena was evaluated. Indeed, in contrast with chemical reactions, diffusive limited processes have lower energy barriers, normally below  $50 \text{ kJ mol}^{-1}$ . Figure 4 shows the plot of the linear expression of the Arrhenius equation.

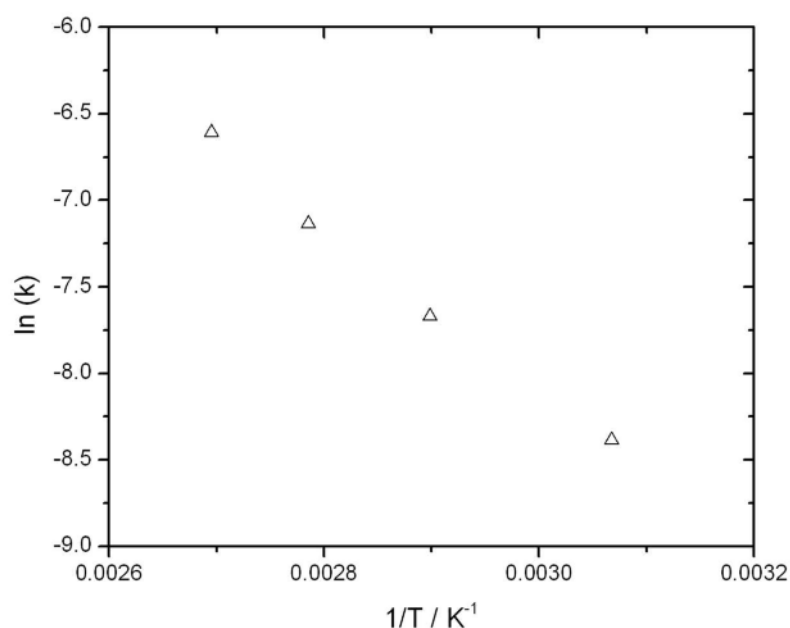


**Figure 4.** Plot of the linear expression of the Arrhenius equation obtained by calculating the relative kinetic constants of the reactions at different temperature (53, 72, 86, 98 °C) .

### 3.2.3 Limiting regime of the reaction

To evaluate the intrinsic catalytic activity, it is important that the reaction is running under kinetic regime, meaning that the rate of reaction should not be limited by diffusion phenomena. For diffusion phenomena, also named mass transfer, is considered all the events that hinder the transfer of the reactant molecules from the bulk of the solution to the active site on the catalyst. In heterogeneous catalysis, diffusion phenomena might play a crucial role in determining the limiting rate of the reaction. Typically, two different types of diffusion can be differentiated: external and internal. The external diffusion concerns the transfer of the reactant molecules from the bulk of the solution to the surface of the catalyst particle. On the other hand, the internal diffusion is the movement of the reactant from the surface of the catalyst to its core. In the case of zeolites, internal diffusion relates to transportation of the reactants and products through the porous network. For zeolites, diffusion can represent a big issue because the active sites are often located inside the micropore rather than in the surface, making even more difficult for the reactant to travel in such narrow cavities. What is important for catalysis science is to be able to determine under which regime the reaction is running, and in case mass transfer is present, find the conditions for which this phenomena can be overcome, if it is possible.

One simple experiment to determine if there is any internal mass transfer limitation is to vary the amount of Sn species in the reaction and see how the rate of reaction change. If the rate of reaction is determined by kinetics, the change in conversion will be proportionally respect to the amount of Sn introduced; *i.e.* if the amount of Sn is doubled, the conversion should double; in contrast, if mass transfer limits the process, increasing the amount of active species will not result in a proportional increase of the rate of the reaction. The experiment illustrated in Figure 4 shows two reactions run with 1 and 2 mol.% of Sn relative to CyO, respectively. It can be seen that by doubling the amount of Sn species introduced, the conversion doubles accordingly, suggesting that no mass transfer is present. Consequently, we can assume that the activation energy found in the previous paragraph was relative to chemical reaction, and that the barrier is relatively low at  $39 \text{ kJ mol}^{-1}$ .

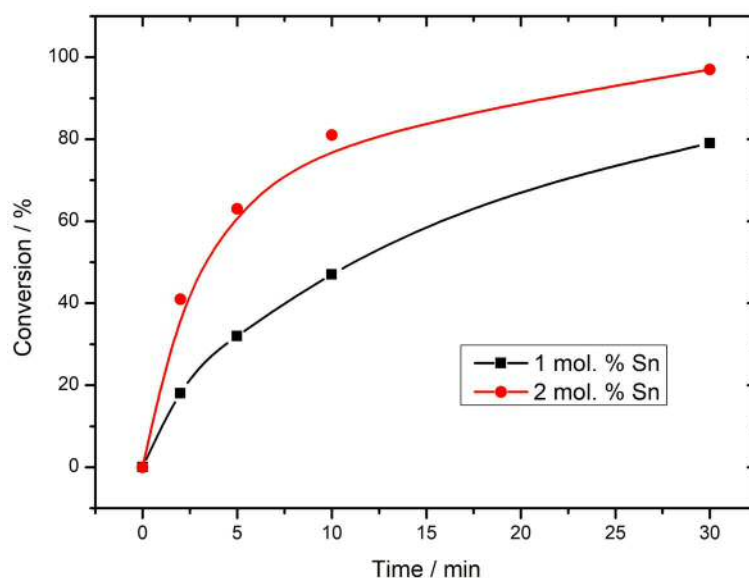


**Figure 5.** Time-online plot of conversion of CyO performed in the presence of different amount of mass of catalyst, therefore at different CyO/Sn.

Another way to test the internal mass transfer is to vary the particle size of the catalyst. Increasing the particle size means to increase the space the molecules have to diffuse into the catalyst. If mass transfer is present, increasing the particle size will lead to a decrease in the observed rate of the reaction. To probe if any external mass transfer is present, reactions at different stirring rate can be performed. If external mass transfer is present, increasing stirring rate will lead to an increment of the observed rate. On the other hand,

when external mass transfer is not present, the observed rate of reaction will be independent from the stirring rate. Figure 6 shows the initial conversion at the same reaction time (5 min) compared at different stirring rate for the 2Sn-Beta. As it can be seen in Figure 6, the reaction does not shows any increase of conversion for stirring rates greater than 600 rpm. Therefore, to assure to work in absence of external mass transfer, the reaction of this work were carried out at 800 rpm. This experiment, combined with the observation that the rate increases linearly with mass charge of catalyst, confirms the reaction to be present in the kinetic regime.

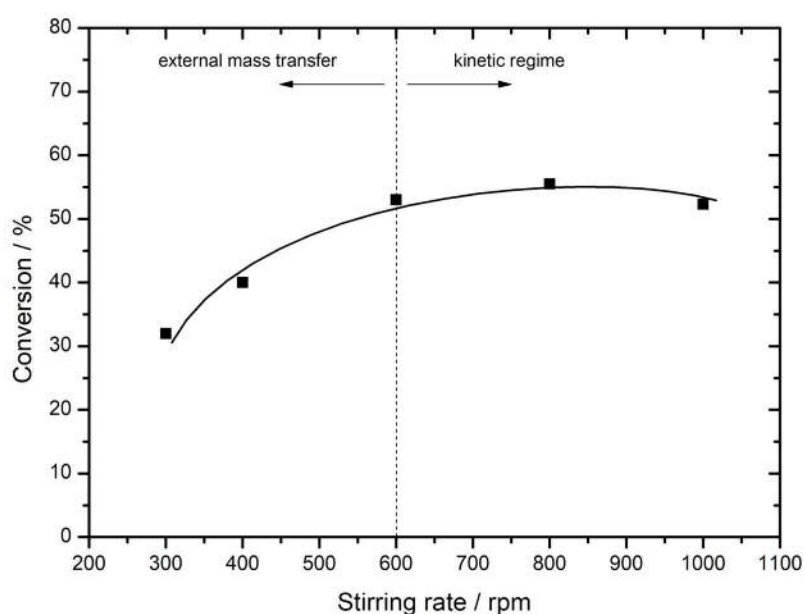


**Figure 6.** Effect of the magnetic stirring rate on the reaction rate for the batch TH of CyO.

In summary, preliminary kinetic studies led to the following conclusions: i) Sn-Beta synthesised by SSI method have comparable activity to the hydrothermal Sn-Beta for the TH of CyO reaction; ii) the reaction proceeds purely *via* heterogeneous catalysis; iii) the process is not mass transfer limited and iv) extra-framework Sn species, such as SnO<sub>2</sub> are not active for TH reaction.

### 3.2.4 Impact of metal loading on the intrinsic activity

Having identified the key kinetic parameters, the study was then focused on the effect of the metal loading on the intrinsic activity of the catalyst. As such, Sn-Beta catalysts with different contents of Sn were synthesised. Loadings of 2, 5, 8 and 10 wt. % were prepared by SSI, and

their activity tested for the TH of CyO in a batch reactor. It is important to highlight that in all tests, the CyO to Sn ratio was kept constant ( $\text{CyO/Sn} = 100$ ) in order to allow a direct comparison of the intrinsic activity of the catalysts at different metal loading *i.e.* the mass charge was adjusted so the same quantity of Sn was present within the reactor in every test. In Figure 7, the time-online plot for the TH of CyO with different catalysts is displayed.

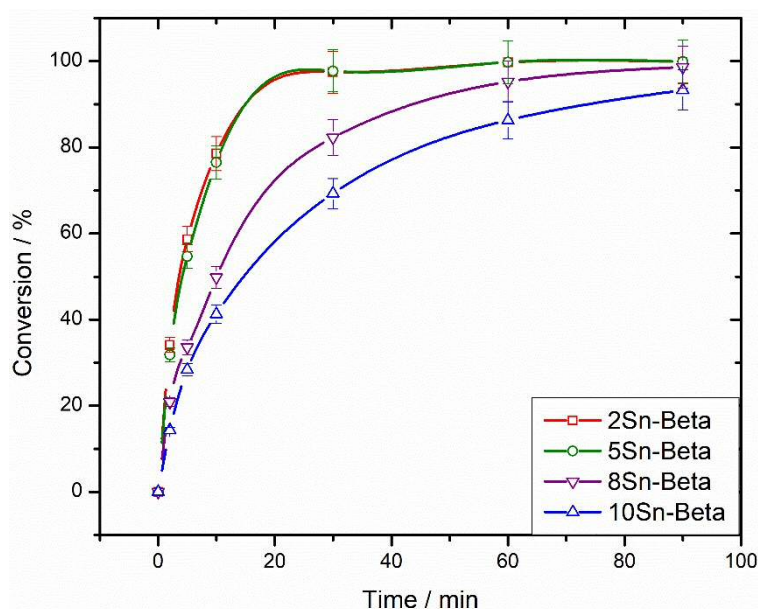


**Figure 7.** Catalytic activity of Sn-Beta catalysts prepared by SSI, and containing different Sn contents, for TH of CyO. 10 mL of a solution of 0.2 M of CyO in 2-butanol were reacted with the Sn-Beta under reflux (98°C) for 90 min. A CyO/Sn molar ratio of 100 was employed.

As can be seen, all the synthesised catalysts were able to convert more than 90 % of the CyO within 90 min. Due to the very fast kinetics, repeated measurements were done in order to improve the accuracy of the points, especially for the first point at 2 min, from which the TOF is calculated. At all level of conversion and for all the catalyst, selectivity in CyOH and carbon balance were > 95 %, in very good agreement with the selectivity values found by Corma *et al.*, indicating that the Sn species in all the catalysts followed the same reaction pathways. However, it is clear that the rate of reaction exhibited by the catalysts series is not uniform through all the series. Indeed, whilst 2 and 5Sn-Beta have same activity, higher loadings Sn Beta (8 and 10 wt.%) are clearly less active at the same CyO/Sn molar ratio. To better understand the impact of loading, the activity of each catalyst is expressed in terms of TOF, calculated at the first point of the time online plot. The resulting TOF values from 2Sn-Beta to 10Sn-Beta were 1150, 1100, 700 and 450  $\text{h}^{-1}$  respectively. It is therefore clear that the metal loading effects the intrinsic activity of the catalyst for the TH of CyO, in particular at higher loadings, where the overall activity of the Sn sites decrease.

To evaluate if the differences in activity observed during TH of CyO were solely related to that specific reaction, or were more general to the material itself, the same series of catalysts were tested for GI in water. As explained in Chapter 1, this reaction can be considered an analogous intramolecular version of the TH reaction. If so, a similar trend in activity along the series would be expected. As for the TH of CyO, the Glu/Sn molar ratio was kept constant for all the reactions, setting it at 2 mol. % relative to glucose, under the conditions of Roman-Leshkov *et al.*<sup>11</sup> Figure 8 shows the time-online plot of the series of catalysts.

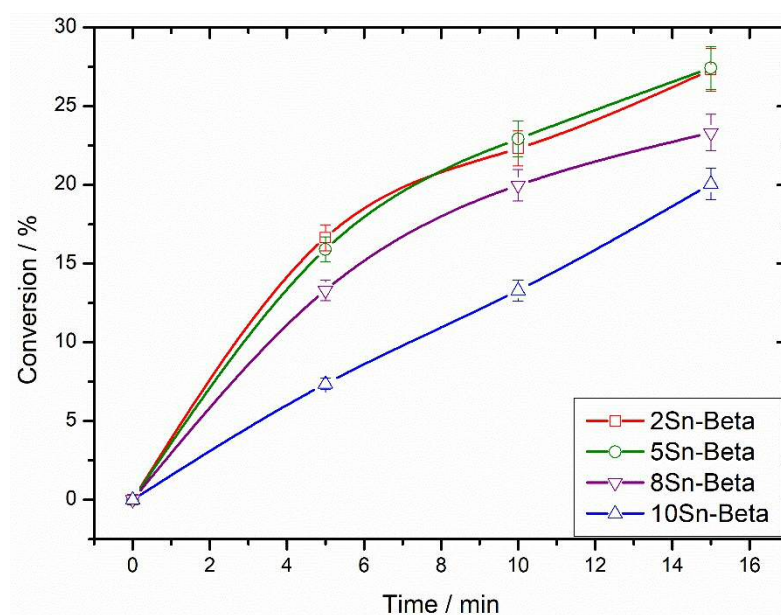


**Figure 8.** Catalytic activity of Sn-Beta catalysts prepared by SSI, and containing different Sn contents, for glucose isomerisation. The reaction was carried out in a sealed thick wall tube at 110 °C using 5 ml of aqueous solution of glucose 0.61M (corresponding to 10 wt.% glucose), at a Glu/Sn molar ratio of 50.

As can be seen, the trend of the activity of the catalyst series is almost identical to the one obtained with the TH of CyO. Indeed, whilst 2 and 5Sn-Beta showed again almost identical intrinsic rate of reaction, the rate decreased when 8 and 10Sn-Beta were employed. Comparison with literature data, in particular between the SSI-made 2Sn-Beta with the 1.8Sn-Beta hydrothermally synthesised and employed for GI under identical condition, revealed that post-synthetic Sn-Beta possess identical activity compared to the analogous material synthesised by hydrothermal synthesis, showing TOF values of 110 and 95 h<sup>-1</sup> respectively.

In Table 1 the results of each reaction are compared at the same level of glucose conversion (so called *iso-conversion analysis*). Yield and carbon balance of the reaction are displayed, showing again that no other products other fructose and mannose are detected (carbon

balance > 95%). The selectivity towards these two products is mainly consistent for all the catalyst (fructose selectivity is about 70 % at *ca.* 20 % of conversion for all the catalysts), showing again that the Sn sites lead to the same final product distribution. These observations suggest that the effect, whereby intrinsic activity is lost at loadings above 5 wt. %, is due to the nature of the catalyst rather than the reactive system considered.

**Table 1.** Kinetic parameters of the GI reaction at same glucose conversion performed with Sn-Beta at different metal loadings. . The reaction was carried out in a sealed thick wall tube at 110 °C using 5 ml of aqueous solution of glucose 0.61M (corresponding to 10 wt.% glucose), at a Glu/Sn molar ratio of 50.

Catalyst	time (min)	$X_{\text{Gluc}}$ (%)	$Y_{\text{Fru}}$ (%)	$Y_{\text{Man}}$ (%)	$\text{Sel}_{\text{Fru}}$ (%)	$C_{\text{bal}}$ (%)
2Sn-Beta	10	22.3	16.4	4.4	73.5	98.6
5Sn-Beta	10	22.9	15.1	3.2	65.9	95.4
8Sn-Beta	10	20.0	13.1	2.9	65.5	96.0
10Sn-Beta	15	20.1	13.8	3.1	68.6	96.7

In order to have a better understanding of the effect of metal loading on the two reactive systems, the initial TOF of the two series of reactions was plotted against the Sn loading of the catalysts. As displayed in Figure 9, in the left Y axis the TOF for GI is reported, while on the right Y axis the TOF of TH is displayed. This plot allows a direct comparison between all the initial TOF calculated for the two reactions along the different loading series of the catalysts. As can be seen from Figure 9, the TOF values stayed substantially constant when 2 and 5Sn-Beta are employed in both reactions. However, when higher loadings were employed, the TOF started to decrease gradually as the metal loading increases. As a consequence, 10Sn-Beta showed the lowest intrinsic activity for both TH and GI systems compared to the other loadings. Thus, detailed kinetic studies clearly indicate that a non-uniform intrinsic activity is observed, and in particular, that this is sensitive to the metal loading. However, although kinetic experiments can provide a lot of information about the reactivity, they cannot provide direct evidence of the chemical nature of the various active site species present in the catalyst. For this purpose, characterisation techniques need to be applied on the catalyst, so that structure-activity-relationship can be efficiently proposed.



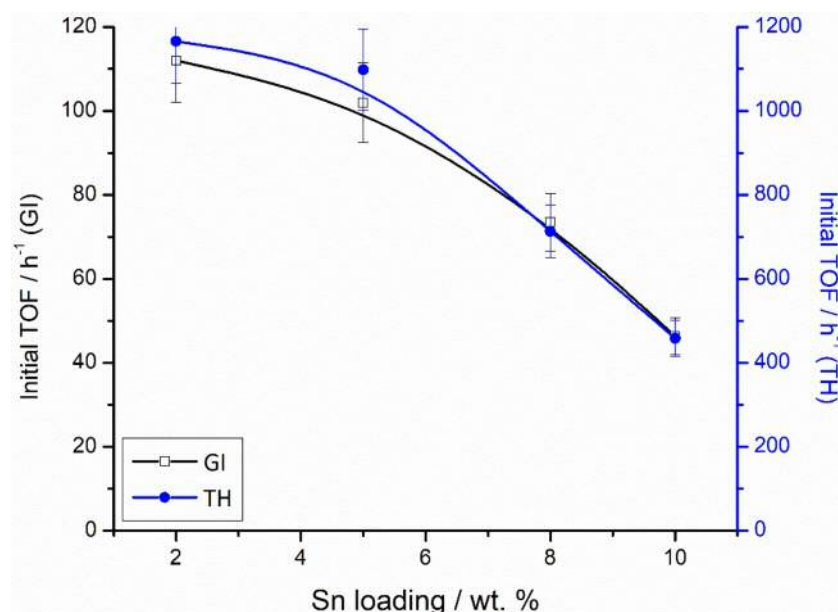


**Figure 9.** Initial TOF for each Sn-Beta catalyst as a function of total Sn loading for both GI (black, left axis, calculated at 5 minutes reaction time) and CyO TH (blue, right axis, calculated at 2 minutes reaction time). TOF calculated as moles (converted)  $\text{mol}^{-1} (\text{Sn}) \text{h}^{-1}$ .

### 3.2.5 Characterisation of Sn-Beta

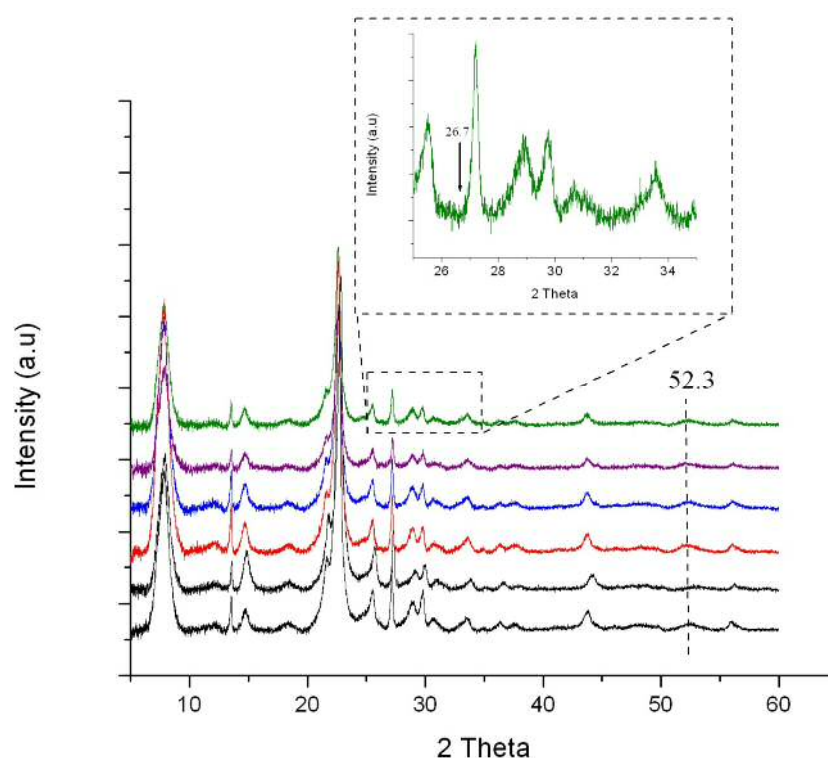
In order to correlate the activity of the catalyst with its structure a series of characterisation techniques have been applied. Although many different aspects of the catalyst need to be characterised, two main characteristics are important in the zeolite catalysts: i) overall textural properties, such as crystalline structure and porosity, and ii) active site structure, *i.e.* in which chemical form is the active element present in the material. From the kinetic observation presented above, some hypotheses can be formulated, and therefore the choice of the techniques and the orders they are applied can be formulated. It is known that the crystalline structure and the micropore channel extension are fundamental requisition for the catalytic activity of zeolite catalysts. Therefore, analysis of the textural properties of the material has to come first. If poor crystallinity and/or a low micropore volume are found, that could be a sufficient reason for poor catalytic performance. On the other hand, if the textural properties are intact, the active site condition must be investigated.

However, it is noted that the precise nature of Sn-Beta active site is at the centre of a big academic debate (see Chapter 1 section 1.4). Despite various different forms being proposed in literature, it is generally accepted that Sn has to be isomorphously substituted into the framework, resulting in high dispersion as a single atom, which can act as a Lewis acid. Different techniques have been developed through the years in order to identify tetrahedral

Sn atoms in the zeolitic framework. Between them,  $^{119}\text{Sn}$  MAS NMR, UV-Vis,  $\text{CD}_3\text{CN}$  DRIFT adsorption have become widespread and routine methodologies to test qualitatively and quantitatively the Sn active sites and their Lewis acidity strength. In contrast, extra-framework Sn species, such as  $\text{SnO}_x$ , do not possess Lewis acidity character, as showed in Figure 2, and their presence can be identified using many different characterisation techniques, such as pXRD,  $^{119}\text{Sn}$  MAS NMR, UV-Vis. As such, great attention should be paid in the identification of the Sn speciation, because Sn can be present in the catalyst either as active and spectator sites.

### 3.2.6 Textural properties of the catalyst

In order to verify the crystallinity of the samples, powder X-ray Diffraction (pXRD) was used. Typical XRD pattern of the Beta structure can be found on online database.<sup>12</sup> Figure 10 shows the pXRD pattern of the series of catalysts. It can be seen that the XRD pattern matches the reference pattern of Beta zeolite found in the database, showing the two main diffraction peak at 8.2 and 23.0  $2\theta$ , indicative of 101 and 311 diffraction plane. The four different loading Sn-Beta catalyst are compared with the parental Al-Beta (which should have a perfect crystallinity) and de-aluminated Beta, prepared by de-alumination in concentrated  $\text{HNO}_3$ . This comparison shows that there are not dramatic differences in the crystallinity of the catalysts despite the different Sn loading, and that high crystallinity is retained through all the steps of the synthesis of the catalyst, starting from the commercial aluminosilicate materials, to the de-aluminated form and eventually, the final Sn-Beta catalysts.



XRD technique is not only useful to examine the crystallinity of a materials, but can also be a

**Figure 10.** pXRD patterns of various Sn-Beta catalysts prepared by SSI, and containing different Sn contents. Black: bottom = Al-beta, top = de-Al-beta; Red; 2Sn-Beta; Blue: 5Sn-Beta; Purple: 8Sn-Beta and Green: 10Sn-Beta.

be invisible to pXRD if the crystal range is limited, which occurs when the crystallite size is too small. Since  $\text{SnO}_2$  was shown to be catalytically inactive for TH reaction its formation at higher loading could lead to the observed decreasing of TOF. Since  $\text{SnO}_2$  possess well-defined diffraction peaks, pXRD could be used to detect any eventual oxide present in the catalyst. In particular, there are two diffraction peaks ( $26.7^\circ$  and  $51.8^\circ$ ) of  $\text{SnO}_2$  that can be used to identify any oxide present in the zeolite, since those peaks do not overlap with any of the Beta structure. From the inset in Figure 11 can be seen that even at the highest Sn loading no diffraction of  $\text{SnO}_2$  can be found. To verify the detectability limits of  $\text{SnO}_2$  in zeolite Beta, physical mixture of bulk  $\text{SnO}_2$  and deAl-Beta were made with  $\text{SnO}_2$  loading of 10, 5 and 2 wt.%. Figure 11 shows that even at low percentages of  $\text{SnO}_2$  the diffraction of  $\text{SnO}_2$  is still well defined. This finding suggests that even in the 10Sn-Beta material the oxide is either not present at loadings above 2 wt. %, or its crystalline structure does not have sufficient long-range to give birth to a detectable XRD signal.

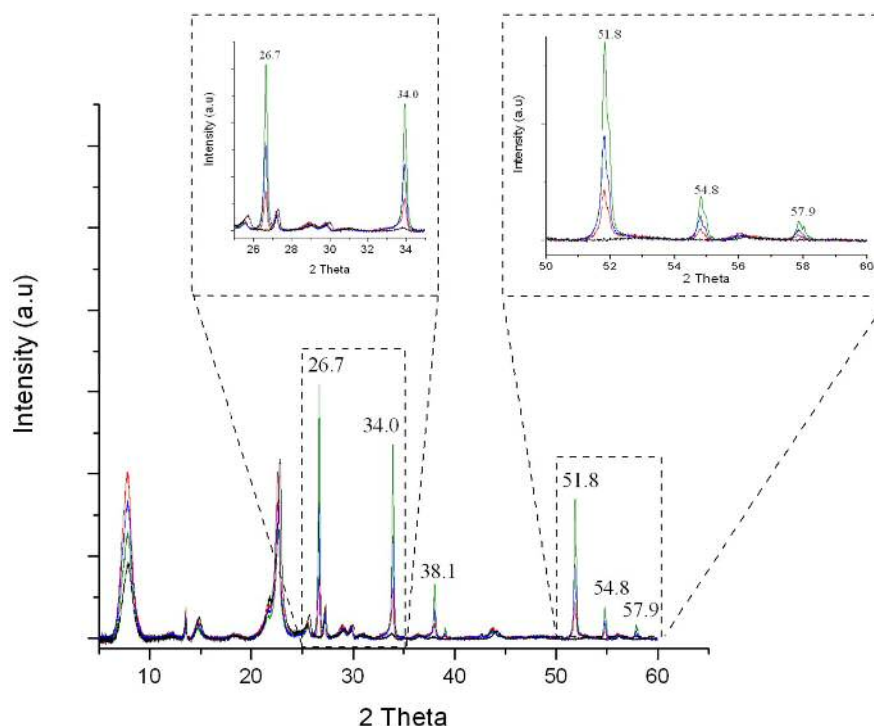


**Figure 11.** pXRD patterns of various  $\text{Sn}(\text{O}_2)$ -Beta catalyst prepared by physical mixing of  $\text{SnO}_2$  and deAl-Beta, and containing different Sn contents. Black: de-Al-Beta, Red:  $2\text{Sn}(\text{O}_2)$ -Beta, Blue:  $5\text{Sn}(\text{O}_2)$  and Green:  $10\text{Sn}(\text{O}_2)$ -Beta.

Another important parameter for zeolitic materials is their surface area and pore volume. In Table 2 the metal content determined by Inductive Coupled Plasma (ICP) elemental analysis, and total pore volume are summarised. It can be seen that the values of total pore volume slightly decreased as the Sn loading increased. However, the decreases in total pore volume is not dramatic, with a difference of 20 % between the highest and the lowest value. Although this small decrease is unlikely to account for the large decrease in activity across the series of catalyst, it can be speculated that some small extra-framework species might partially block the pores, leading to less accessibility to the Sn sites that are most deeply located in the zeolite cavities. However, since the observed decreased in total pore volume is unlikely to be the only cause of the lower activity at high metal loadings, further characterisation were performed with particular focus on the active sites.

**Table 2.** Physical and catalytic properties of Sn-containing zeolites prepared by SSI. <sup>a</sup>Determined by ICP-MS. <sup>b</sup> From reference 3.

Catalyst	Sn wt. % (Si/Sn) <sup>a</sup>	V <sub>micro</sub> (ml g <sup>-1</sup> )
Al-Beta	-	0.23
deAl-Beta	-	0.23
2Sn-Beta	1.8 (75)	0.23
5Sn-Beta	4.5 (29)	0.21
8Sn-Beta	7.3 (18)	0.19
10Sn-Beta	9.2 (15)	0.18
Hydrothermal Sn-Beta <sup>b</sup>	1.5	0.20

### 3.2.7 Active site characterisation

So far, the textural properties of the catalyst showed that the main crystalline structure and extent of crystallinity is comparable for all samples, and that no XRD diffraction peak of Sn<sub>2</sub>O are detected even in the 10Sn-Beta sample. However, porosimetry analysis revealed that the pore volume decreases as the loading of Sn increases. However, the techniques applied so far do not appear to correlate the kinetic behaviour with structure characteristics, and do not give any insight about the active Sn site. Therefore, characterisation methods sensitive to Sn<sup>IV</sup> were carried out.

UV-Vis spectrometry is a technique that can theoretically discriminate between various Sn species, such as framework Sn and SnO<sub>2</sub>-like species. This is possible because these species have very defined ligand-to-metal charge-transfer bands at 220 and 280 nm for framework and extra-framework Sn species respectively.<sup>13</sup> Figure 12 shows the UV-Vis spectra of the four different loading catalysts. Although it was clear that the increasing absorbance at wavelength < 250 nm correlate with the increasing amount of Sn, this technique is clearly not sufficiently sensitive to discriminate between different species of Sn present in these samples. Therefore, different techniques more sensitive to the different Sn species possibly present in the catalyst need to be exploited.

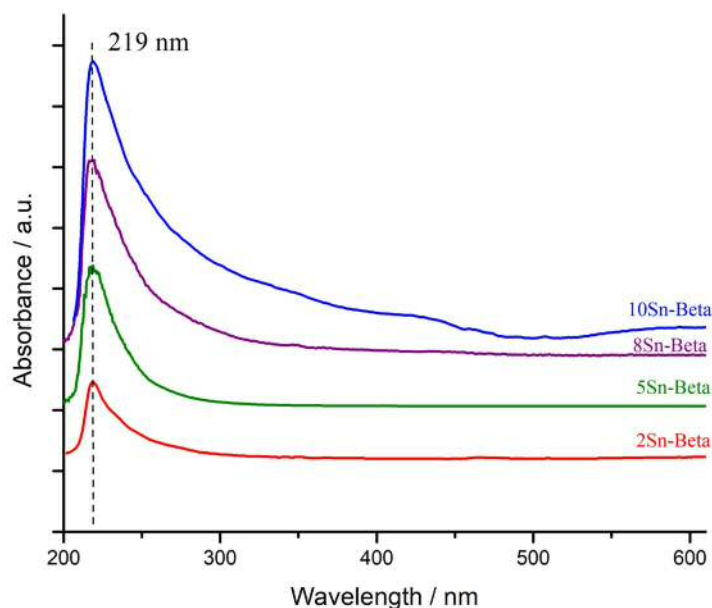


**Figure 12.** UV-Vis spectra of various Sn-Beta catalysts prepared by SSI, and containing different Sn contents.  
 Red: 2Sn-Beta; Blue: 5Sn-Beta; Purple: 8Sn-Beta and Green: 10Sn-Beta

One of the most powerful techniques able to discriminate between different Sn species is  $^{119}\text{Sn}$  MAS NMR. MAS NMR is an element specific technique that is theoretically able to differentiate even the slightest difference between Sn species, since it is sensitive to any electronic change in the proximities of the Sn nucleus. Even though it appears to be an excellent technique its use is still limited, mainly due the low signal to noise ratio (S/N) due to the low natural abundance of the isotope  $^{119}\text{Sn}$ , making the acquisition time for a sample extremely long (typically > 24 h). Another major issue of this technique is the assignment of the NMR signal to precise Sn species, due to the lack of standard compounds to use as comparison. However, many attempts have been made in literature, and a modest library of  $^{119}\text{Sn}$  MAS NMR related to Sn-Beta can be found.<sup>14,15</sup> As such, two major NMR regions have been found related to framework Sn. A region between -350 and -450 ppm is often attributed to tetrahedral framework Sn. It is worthy to notice that these kinds of Sn species are only found when the catalyst is completely dehydrated by high temperature or deep vacuum. When the catalyst is kept under ambient conditions, signals in this region readily shift to lower field, between -650 and -750 ppm. This region is typical of hydrated framework Sn in octahedral geometry, and is the most common and natural form in which Sn can be found in this typology of catalyst. On the other hand, it is possible to assign with a high degree of confidence the resonance of  $\text{SnO}_2$ , since the standard is commercially

available, giving rise to a resonance around -600 ppm. Example of Sn sites and relative chemical shift region is shown in figure 13.

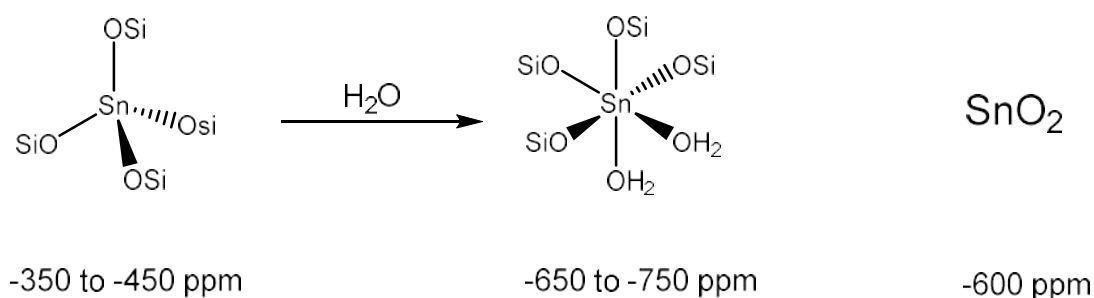


**Figure 13.**  $^{119}\text{Sn}$  MAS NMR chemical shift region of (from left to right) framework hydrated, framework hydrated and extra-framework oxide Sn species.

It is important to clarify that many attempts to assign more precise resonances to specific Sn species, such as close and open forms, have been made. However, as yet no clear experimental evidences are available to support these assignments. Extensive works have been done in order to correlate the synthetic methodology to the typology of Sn sites obtained. As such, a wide array of hydrothermal and post-synthetic Sn-Beta catalysts were analysed and compared by  $^{119}\text{Sn}$  MAS NMR; however, many signals were detected between the range -650 and -750 ppm, so that a not clear pattern between synthetic methodology and Sn site could be seen.<sup>16</sup> Wolf *et al.* also proposed, with the support of computational modelling, that different Sn chemical shifts could arise not only by the different Sn form, but also from the specific T site they occupy in the zeolite framework.<sup>17</sup> It is clear, therefore, that the precise assignation of  $^{119}\text{Sn}$  MAS NMR signal for the Sn-Beta species is one of the biggest on-going challenges in this research field. For this reason, in this thesis it has been chosen to not try to assign more specifically these resonances, but they will only be referred as hydrated or dehydrated framework Sn, and extra-framework Sn presenting as  $\text{SnO}_2$ .

In Figure 14 the  $^{119}\text{Sn}$  MAS NMR spectra of 2, 5, and 10Sn-Beta and 2Sn( $\text{O}_2$ )-Beta are shown,  $\text{SnO}_2$  spectra was also run for comparison and representative of extra-framework Sn atoms. Between all the spectra, two main resonances can be observed, one centred at -602 ppm and the other at -688 ppm. 2 and 5Sn-Beta possess very similar spectra, having a major resonance centred at -688 ppm and a smaller signal around -602 ppm. In contrast, 10Sn-Beta presents a well-defined resonance at -602 ppm, along with the -688 ppm signal. Instead,  $\text{SnO}_2$  and 10Sn( $\text{O}_2$ )-Beta only show a sharp resonance at -602 ppm, and no other signals are detected. With the help of the literature on  $^{119}\text{Sn}$  MAS NMR, the signal at -688 ppm can be

assigned to the hydrated framework Sn species, whilst the -602 ppm is typical of  $\text{SnO}_2$  like species, as confirmed by the sharp signal present in the  $\text{SnO}_2$  spectrum. It is clear from  $^{119}\text{Sn}$  MAS NMR that when the catalyst is made with loading up to 5 wt. % it primarily possesses the same Sn site distribution, since the ratio between the two signals is consistent in the 2 and 5Sn-Beta samples. On the other hand, the 10Sn-Beta presents a higher ratio between the -602/-688 signals, suggesting that at higher loading the Sn speciation changes; in particular, more of the species at -602 ppm are formed. In light of these observations and the trend of the activities observed, it can be seen that the 2 and 5 Sn-Beta possess similar Sn site distribution and they accordingly show similar intrinsic activity. The 10Sn-Beta has a different site distribution, in particular a growth of the signal at -602 ppm is observed and it has lower intrinsic activity. Furthermore, the  $2\text{Sn}(\text{O}_2)$ -Beta shows only the resonance at -602 ppm and no activity is detected for the TH reaction. This strongly proved that extra-framework species are inactive and they are identified by the resonance at -602 ppm. At this point, it can be said with a certain degree of confidence that extra-framework Sn species are only spectator site respect to the TH reaction. Therefore, the lower intrinsic activity exhibits by the 10Sn-Beta compared to the 2 and 5Sn-Beta, can be ascribed to the highest amount of  $\text{SnO}_2$ -like species that are formed during the synthesis of the catalyst but do not participate at the catalysis.

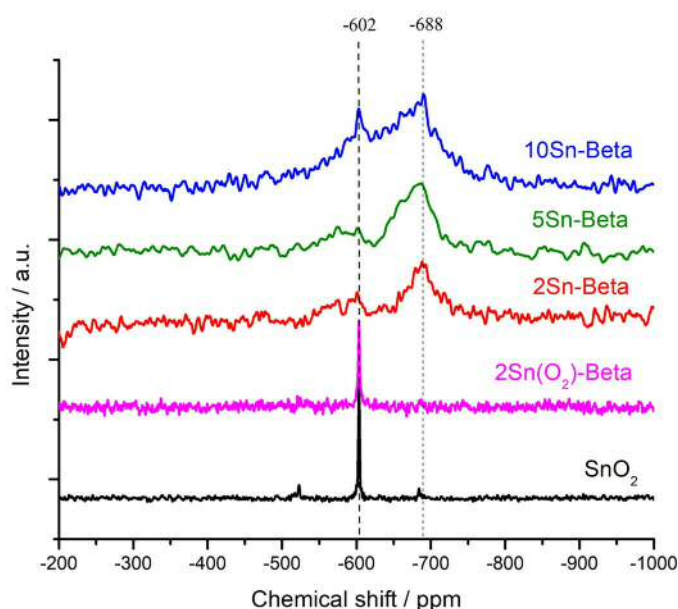


**Figure 14.**  $^{119}\text{Sn}$  MAS NMR spectra of (from bottom to top); bulk  $\text{SnO}_2$ ,  $2\text{Sn}(\text{O}_2)$ -Beta, 2Sn-Beta, 5Sn-Beta and 10Sn-Beta.



After having identified the site distribution between the catalyst series, the Lewis acidity of 2 and 10Sn-Beta, representative of the extreme case that have been shown so far, were evaluated by means of probe molecule, in order to see if the Sn site strength matches the intrinsic activity found during the kinetic tests. To probe the Lewis acidity strength of these catalysts, a CD<sub>3</sub>CN adsorption-desorption experiment under dynamic vacuum at different temperatures has been performed and followed by Diffuse Reflectance Fourier Transform Infrared Spectroscopy (DRIFTS). *d*<sub>3</sub>-acetonitrile (CD<sub>3</sub>CN) is a common probe molecule used for determining the Lewis acidity strength of the acid sites by interacting with the lone pair present on the nitrogen atom. As consequences of this interaction, a typical stretching  $\nu(\text{C}\equiv\text{N})$  is detected and its wavenumber is indicative of the strength of the adduct, while the intensity give an indication of the numbers of the sites. The deuterated form, CD<sub>3</sub>CN, is typically used in order to avoid the splitting of signals caused by the Fermi resonance effect when CH<sub>3</sub>CN is used instead. In many literature works, it has been shown that these molecules interact selectively with framework Sn atom to give a vibration between 2305 - 2320 cm<sup>-1</sup>. On the other hand, extra-framework species do not interact with CD<sub>3</sub>CN or interact very weakly by physisorption, thus no IR signal of chemisorbed molecules is detected in their presence. This technique is also believed to be able to discriminate between different Sn framework species, as suggest by Boronat *et al.*, in which two vibrations at 2316 and 2308 cm<sup>-1</sup> were identify experimentally and supported by simulation, and attribute to the open and closed Sn site respectively on a hydrothermal synthesised Sn-Beta.<sup>18</sup> In contrast, a more cautious approach was adopted by Roy and collaborators, in which they attribute the observed wavenumbers shift to the effect of the presence of additional acetonitrile molecules in the vicinity.<sup>19</sup> Therefore, they suggested that this technique should be used in order to distinguish only between Lewis and non-Lewis sites, rather than try to assign different active sites based on small shift of the vibration position.

For all these reasons, this technique has become a rather established method to probe the Lewis acidic strength of Sn-Beta. Prior the adsorption of the molecules, the materials are dehydrated and degassed (550 °C, 1 h, air flow). Subsequently, CD<sub>3</sub>CN is adsorbed at room temperature, and after saturation, the DRIFT chamber is evacuated by applying vacuum. Desorption of the probe molecule is facilitated by heating the sample in the cell and spectra of the adsorbed molecule were recorded at different temperatures. CD<sub>3</sub>CN that are bounded to the strongest active sites will desorbed at higher temperature, in contrast, signals arising from weaker interactions will desorb at lower temperatures. As such, CD<sub>3</sub>CN only physisorbed on the material surface or weakly bonded to Sn is expected to desorbed at

lower temperatures than  $\text{CD}_3\text{CN}$  strongly coordinated to Lewis acid sites. Besides this, the intensity of the signals can also be semi-correlated to the amount of the species. Figure 15 (Left) shows the desorption profile of  $\text{CD}_3\text{CN}$  followed by DRIFT of 2 and 10Sn-Beta.

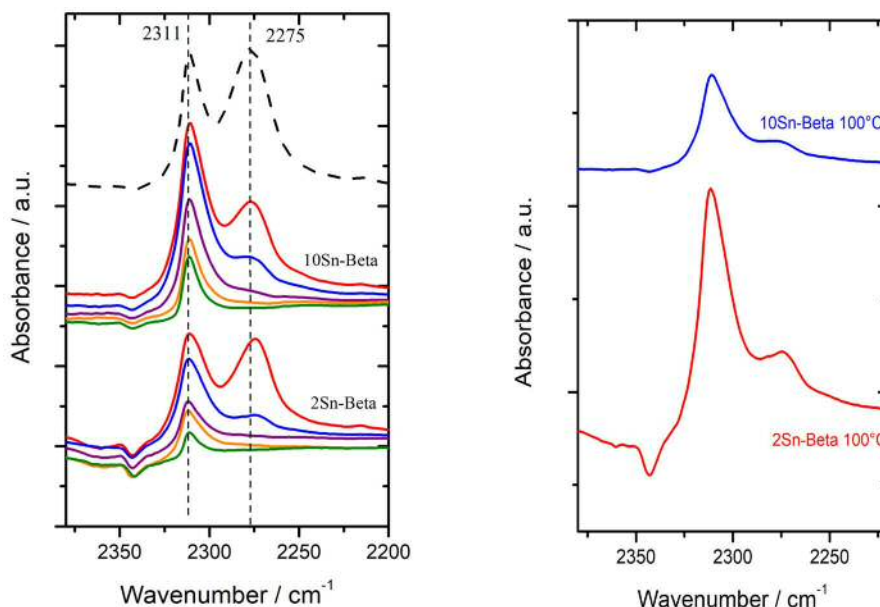


**Figure 15.** (Left) In situ  $\text{CD}_3\text{CN}$  desorption profile for 2Sn-Beta (bottom) and 10Sn-Beta (middle).  $\text{CD}_3\text{CN}$  was desorbed under a dynamic vacuum at various temperature intervals, increasing from top to bottom. A reference spectrum of physisorbed  $\text{CD}_3\text{CN}/2\text{Sn-Beta}$  is provided (dashed line). (Right) Desorption spectra of  $\text{CD}_3\text{CN}$  at 100 °C are normalised against the amount of Sn present in the sample. All spectra are background-referenced against the dehydrated zeolite sample.

For both samples, two main adsorption bands at 2311 and 2275  $\text{cm}^{-1}$  are observed. The band at 2275  $\text{cm}^{-1}$  arises from  $\text{CD}_3\text{CN}$  weakly bonded to the surface silanol groups of the material and readily desorbed when the temperature increases. On the other hand, the band at 2311  $\text{cm}^{-1}$ , which indicates Lewis acid-acetonitrile interaction, is present in both samples, indicating that both samples possess Lewis acidity, and it desorbs slowly upon heating. Although this procedure do not allow a full quantitative calculation of the Lewis acid present in the two samples, some semi-quantitative considerations can still be made. In fact, normalising the adsorption bands at 2311  $\text{cm}^{-1}$  for the quantity of Sn present reveals that the amount of  $\text{CD}_3\text{CN}$  bonded to the Lewis site is higher in the 2Sn-Beta catalyst than in the 10Sn-Beta. This again confirms the highest activity of the Sn sites is obtained a the lower loading materials (Figure 15, Right).

### 3.2.8 Rationalising kinetic data and characterisations

Kinetics data and characterisations provide complementary information to help defining a catalyst under many aspects. The time-online plot for the TH and GI of the series of catalyst revealed that the intrinsic activity of the Sn decreases as the metal loading increases when the Sn wt. % is higher than 5 %. This pointed out to two conclusions: i) the Sn sites are not homogeneously made during the synthesis as the loading increases; ii) the same effect is observed for two different reactions, confirming that is material-dependent, more than reaction-dependent. In particular, it was demonstrated that when the Sn is present as extra-framework species, like  $\text{SnO}_2$ -like species, it is not active for TH reaction. To have an insight of why that was observed, characterisation of the materials were made in order to find structural changes that correlate with the kinetic behaviour. Initially, textural properties of the catalyst, such as crystallinity and porosity were probe by XRD and nitrogen adsorption analysis, respectively, but not convincing evidence were obtained that could correlate well with the kinetic data. Successively, characterisation aimed at discriminating the Sn speciation of the catalyst was carried out. With the help of  $^{119}\text{Sn}$  MAS NMR, it was possible to clearly see a growth of a signal characteristic of  $\text{SnO}_2$  species while the metal loading increased. Accordingly,  $\text{CD}_3\text{CN}$  adsorption on 2 and 10Sn-Beta showed that the lower loaded Sn-Beta possessed higher intrinsic Lewis strength. All this evidence grouped together, lead to the conclusion that the same Sn speciation is obtained during low loadings Sn-Beta synthesis (up to 5 Wt. % of Sn). Afterwards, a higher fraction of the inserted Sn starts to become inactive extra-framework  $\text{SnO}_2$  rather than framework incorporated in the zeolite, leading to a comprehensive decrease in the intrinsic activity, as initially stated by the kinetic data (Figure 16).

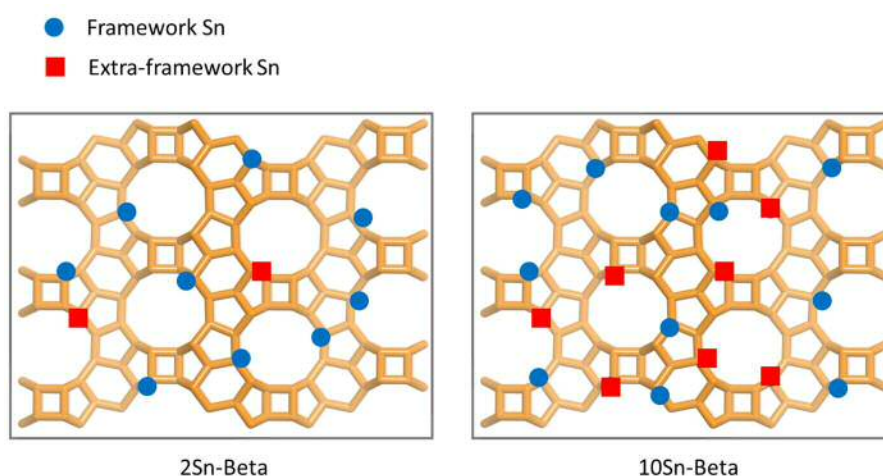


**Figure 16.** Schematic representation of the Sn speciation in 2 and 10Sn-Beta. Active framework and inactive extra-framework Sn sites are depicted as blue circle and red square respectively.

### 3.3 Conclusions

In this chapter, initial catalytic tests of Sn-Beta catalyst have been done for TH and GI. In particular, it has been confirmed that TH reactions proceed through a purely heterogeneous catalysis, and that extra-framework Sn species do not contribute to the reaction. The activation energy has been calculated for the TH of CyO, and due to its relatively low value of  $39.3 \text{ kJ mol}^{-1}$ , reactions with different mass of catalyst have been made to assure the reaction was running under the kinetics regime. Great focus has been made on the effect of the metal loading on the activity of the catalyst. A series of 2, 5, 8 and 10Sn-Beta has been tested in batch mode for TH and GI. A gradual decrease in activity, evaluated as TOF, has been observed for loading higher than 5 wt.%. Characterisation of the materials pointed out that at high loading of Sn, spectator sites are present. These spectators are presumably  $\text{SnO}_2$  like species, as indicated by  $^{119}\text{Sn}$  MAS NMR. Furthermore, the fact that they were not detectable by pXRD suggested they were under the form of short oligomers. Micropore analysis suggested also that at high loading the accessibility of the micropores could partially be hindered. Lastly,  $\text{CD}_3\text{CN}$  adsorption experiments followed by DRIFTS, showed a stronger intrinsic Lewis acidity for the low loading samples.

At this point, a last consideration has to be done about which one is the best catalyst between the series that have been studied in this chapter. In light of the main aim of this work, which is to study the stability of Sn-Beta performing continuous flow processes running at high productivity, hence high STY. It has been evaluated that the 10Sn-Beta, despite it possess the lowest intrinsic activity, is has the highest activity per mass of catalyst, therefore resulted the most promising catalyst for achieving high STY processes. Table 3 summarised the activity normalised on the Sn atoms and on the mass of catalyst.

**Table 3.** Summary of the activity of 2 and 10-SnBeta normalised per Sn content and per mass of catalyst used for the CyO TH.

Catalyst	Activity normalised on Sn atoms ( $\text{moles}_{\text{conv.}} \cdot \text{h}^{-1} \cdot \text{mol}_{\text{Sn}}^{-1}$ )	Activity normalised on mass of catalyst ( $\text{moles}_{\text{conv.}} \cdot \text{h}^{-1} \cdot \text{g}_{\text{cat}}^{-1}$ )
2Sn-Beta	1150	0.175
10Sn-Beta	450	0.360

It is clear that the 10Sn-Beta possess two times higher activity of the 2Sn-Beta when activity per mass of catalyst is evaluate. It is important to clarify that despite the 5Sn-Beta seems to have the highest loading possible until the TOF start to drop (hence the best candidate), it was found that between all the catalysts, it is the hardest to synthesise in a very reproducible way, probably for the fact to be borderline between high loadings and low content of spectators.

The next chapter will then be focused on the development of a continuous flow process for the TH of CyO reaction in 2-butanol, to start studying the stability of Sn-Beta when is employed in continuous operation for organic processes.

## References

- <sup>1</sup> Z. Kang, X. Zhang, H. Liu, J. Qiu, K. L. Yeung, *Chemical Engineering Journal*, 2013, **218**, 425.
- <sup>2</sup> P. Li, G. Liu, H. Wu, Y. Liu, J.-G. Jiang, P. Wu, *Journal of Physical Chemistry C*, 2011, **115**, 3633.
- <sup>3</sup> W. N. P. Van der Graaff, G. Li, B. Mezari, E. A. Pidko, E. J. M. Hensen, *ChemCatChem* 2015, **7**, 1152.
- <sup>4</sup> J. Dijkmans, D. Gabriels, M. Dusselier, F. de Clippel, P. Vanelderen, K. Houthoofd, A. Maliet, Y. Pontikes, B. F. Sels, *Green Chem.*, 2013, **15**, 2777.
- <sup>5</sup> C. Hammond, S. Conrad, I. Hermans, *Angew. Chem. Int. Ed.*, 2012, **51**, 11736.
- <sup>6</sup> P. Wolf, C. Hammond, S. Conrad, I. Hermans, *Dalton Trans.*, 2014, **43**, 4514.
- <sup>7</sup> A. Corma, M. E. Domine, L. Nemeth, S. Valencia, *J. Am. Chem. Soc.*, 2002, **124**, 3194.
- <sup>8</sup> M. Moliner, Y. Román-Leshkov, M E. Davis, *Proc. Nat. Acad. Sci.*, 2010, 107, 6164.
- <sup>9</sup> F. W. Lichtenhaler, "Carbohydrates as organic raw materials" Ullman's encyclopedia of industrial chemistry, 2012, Vol. 6, 583.
- <sup>10</sup> M. Boronat, A. Corma, M. Renz, *J. Phys. Chem. B*, 2006, **110**, 21168.
- <sup>11</sup> Y. Roman-Leshkov, M. Moliner, J. A. Labinger, M. E. Davis, *Angew. Chem. Int. Ed.*, 2010, **49**, 8954.
- <sup>12</sup> <https://www.iza.org/>
- <sup>13</sup> J. Dijkmans, M. Dusselier, W. Janssens, M. Trekels, A. Vantomme, E. Breynaert, C. Kirschhock, B. F. Sels, *ACS Catal.*, 2015, **6**, 31.
- <sup>14</sup> S.-J. Hwang, R. Gounder, Y. Bhawe, M. Orazov, R. Bermejo-Deval, M. E. Davis, *Top. Catal.*, 2015, **58**, 435.
- <sup>15</sup> W. R. Gunther, V. K. Michaelis, M. A. Caporini, R. G. Griffin, Y. Roman-Leshkov, *J. Am. Chem. Soc.*, 2014, **136**, 6219.
- <sup>16</sup> P. Wolf, W.-C. Liao, T.-C. Ong, M. Valla, J. W. Harris, R. Gounder, W. N. P. Van der Graaff, E. A. Pidko, E. J. M. Hensen, P. Ferrini, J. Dijkmans, B. Sels, I. Hermans, C. Coperet, *Helv. Chim. Acta* 2016, **99**, 916.
- <sup>17</sup> P. Wolf, M. Valla, F. Nunez-Zarur, A. Comas Vives, A. J. Rossini, C. Firth, H. Kallas, A. Lesage, L. Emsley, C. Coperet, I. Hermans, *ACS Catal.*, 2016, **6**, 4047.
- <sup>18</sup> M. Boronat, P. Concepcion, A. Corma, M. Renz, S. Valencia, *Journal of Catalysis*, 2005, **234**, 111.
- <sup>19</sup> S. Roy, K. Bakhmutsky, E. Mahmoud, R. F. Lobo, R. J. Gorte, *ACS Catalysis*, 2013, **3**, 573.

## ***4. Intensification and deactivation of Sn-Beta investigated in the continuous regime: cyclohexanone transfer hydrogenation***

### **4.1 Introduction**

Solid state incorporation has been shown to be a promising post-synthetic methodology for making Sn-Beta with high Sn content (up to 10 wt. %). In particular, the impact of the loading on the catalyst activity has been studied in details for the TH of CyO and the GI in batch reactions. As result, it has been shown that at metal loading higher than 5 wt. %, the intrinsic activity gradually decreases as the metal loading increases, making the 10Sn-Beta the less active under this aspect. Characterisation studies, especially with the help  $^{119}\text{Sn}$  MAS NMR spectroscopy, revealed that up to 5 wt. % of Sn the speciation of sites almost homogeneous, but when the loading increases more inactive  $\text{SnO}_2$ -like species are forming, pulling down the intrinsic activity. However, after a more detailed evaluation, despite its lower intrinsic activity, it has been seen that 10Sn-Beta possess a higher activity per gram of catalyst compared to the 2Sn-Beta, in particular approximatively two-times more active. High activity per gram is a desirable characteristic for achieving high space-time-yield (STY) in continuous

flow reactions. Therefore, 10Sn-Beta seems a promising materials compared to the other analogous stannosilicate. However, another parameter of critical relevance for industry is the catalyst lifetime, and is maybe the most important when it comes to decide if a process is viable or not from the economic point of view.<sup>1</sup> However, the lack of academic research about Sn-Beta stability has hindered the process of evaluation of the scalability of Sn-Beta-catalysed processes, such as continuous sugars valorisation. Nevertheless, prior to test Sn-Beta for continuous carbohydrate chemistry, which is likely to possess several major challenges, the intrinsic stability of the catalyst has to be understood for a better-known and simpler reaction. On this regards, TH of CyO is a perfect model reaction to start exploring Sn-Beta stability. The advantage of using the TH is due to the fact that the reaction is relatively simple and the kinetics parameters are fully understood (see Chapter 3). Furthermore, a selectivity approaching 100 % is observed at all levels of conversion, meaning that no major by-products should be present in the reaction mixture, allowing to focus the study only on the catalyst activity. Last but not least, the intermolecular hydride transfer of TH is analogous to the mechanism of sugar isomerisation, firstly hypothesised by Taarning<sup>2</sup> and successively demonstrated by Roman-Leshkov *et al.*,<sup>3</sup> making this reaction a simple, but realistic, model for GI.

In this work, continuous reactions of TH of CyO have been exploited to study the stability of 10Sn-Beta. Successively, characterisation techniques on the used samples have been employed in order to rationalise the mechanism(s) of deactivation of the catalyst. The study of the catalyst deactivation is a key part of the research, since elucidation of the mechanisms of deactivation allow counter-measures to be adopted in order to maximise the lifetime of the material, if possible.

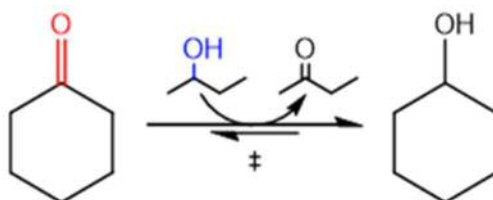


**Figure 1.** Scheme of TH of CyO to CyOH in 2-butanol as solvent and H-donor.

## 4.2 Results and discussion

### 4.2.1 Continuous flow reactor

The best way to probe the lifetime of a catalyst consists of performing catalytic test in continuous flow reactors. Continuous flow experiments allow a truly study of the stability of the catalyst through time. When this is done in batch operation, stability of the catalyst is often evaluated doing repeated cycle of reaction. Often the catalyst is collected, washed and used it again for the successive cycle of reaction, so it can happen that during this step the catalyst can recover some activity, leading to an overestimation of the catalyst lifetime. In contrast, continuous flow reactors allow to evaluate the stability of the catalyst during a single operation, and allow an experimentalist to operate at much higher substrate turnover numbers. In the ideal case of a perfect stable catalyst, the initial conversion should not change with time; this is what is called steady-state operation. However, in most of the cases, catalysts experience deactivation, and that can be evaluate directly by comparing the performance of the catalyst through time with its initial performance. Another advantage is the possibility to change the experimental parameters while the reaction is in progress. In fact changing the flow rate or the temperature when the reaction is already started allows exploring different part of the reaction kinetics. In addition, optimisation of the reaction conditions can be done more easily. Amongst other advantages, continuous reactors also present easier scale-up, improved safety, easier automation of the process, smaller reactor volumes (hence higher STY) and better heat transfer properties. Figure 3 (A) shows a schematic of the reactor used in this work. The main part of the continuous plug flow system is the HPLC pump. Its role is to deliver the reactant solution through all the system, and depending on how densely packed is the catalytic bed, high pressure might be required. The catalyst powder is physically confined inside the reactor (Figure 3 C), in a stainless steel tube of ca. 40 mm of length, and 4.1mm internal diameter. The reactor is placed in oil bath and thermostated at the reaction temperature. The solution with the reactant flows through the catalyst and the reaction take place. The reactor is then connected to a sampling valve, from which the reacted solution is taken and analysed by gas or liquid chromatography. The whole system is kept under pressure by means of a back pressure regulator, in order that the pressure at the back of the reactor can be set to a desired value. Having a back pressure represent an advantage also for the kinetics point of view, in fact allowing operation above the boiling point of the solvent to proceed, hence accelerating the reaction rate.



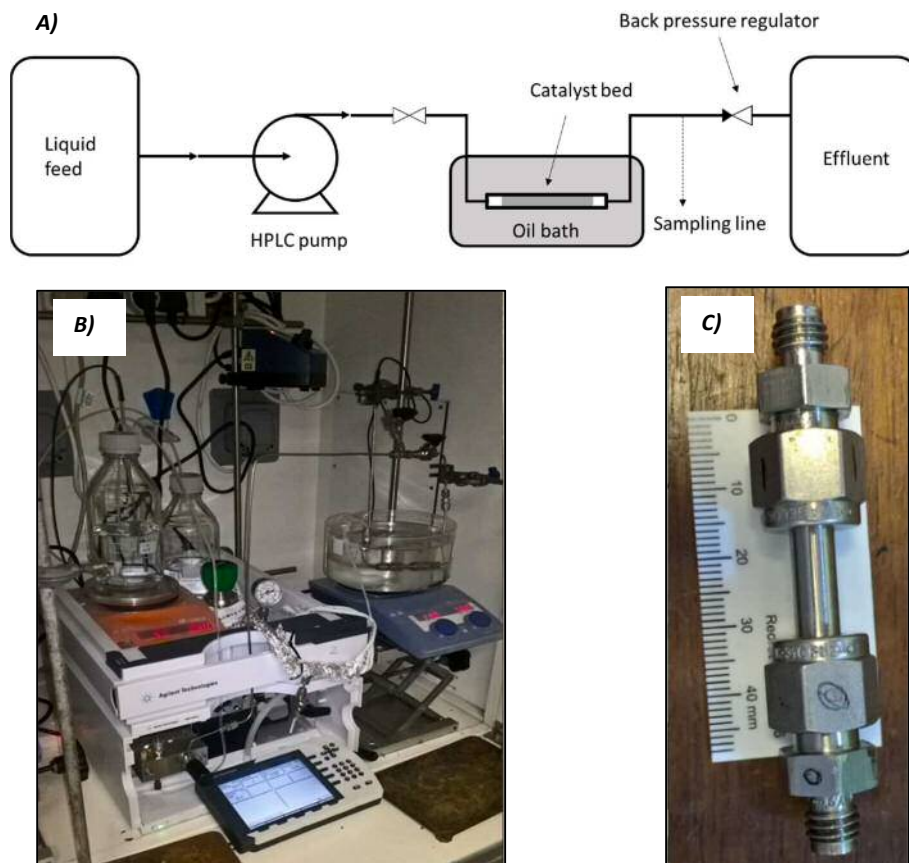


**Figure 2.** (A) Scheme of the continuous flow reactor. (B) Picture of the actual continuous flow system used in this work. (C) Picture of the reactor in which the catalytic bed is packed.

#### 4.2.2 Film diffusion study

Prior performing detailed kinetic studies, it is important to verify that the reactions are running under real kinetic conditions. Therefore, investigation of the regime of the reaction has been performed on the plug flow reactor. To do so, a common and simple test to probe the reaction regime is the so-called linear velocity test. The linear velocity ( $v$ ) is defined as:

Where  $Q$  is the volumetric flow rate and  $S$  is the reactor section. This test comprises set of experiments that allow defining when external diffusion (also named film diffusion) is the limiting regime. In each experiment the amount of catalyst and flow rate of reactant have

been varied proportionally. Doing so, the contact time remains constant, while the linear velocity increases because the section of the reactor is constant. It is important to remind that the contact time defines the conversion, therefore at same contact time, and under kinetic regime, the conversion of the reaction should be the same. Thus, in absence of film diffusion the conversion is independent from the flow rate (at constant contact time). On the other hand, when film diffusion is the dominant regime, the conversion decreases proportionally to the flow rate. Figure 3 summarises how a linear velocity test is carried out. In the three reactors, the mass of catalysts is first doubled and then trebled and the same is done for the flow rate.

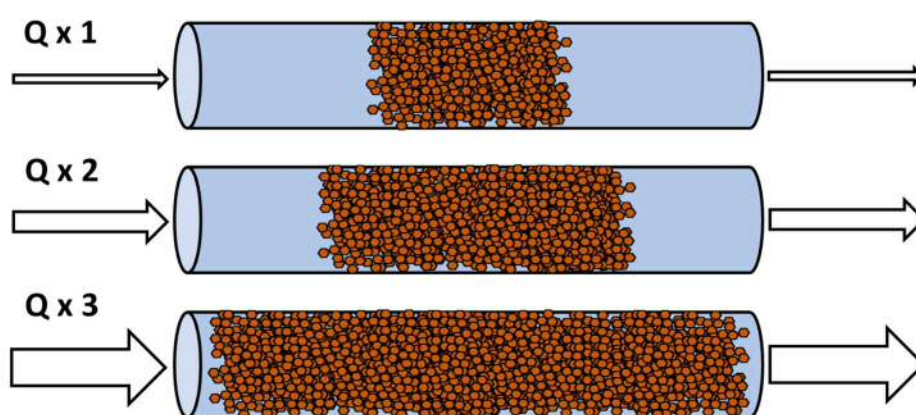


**Figure 3.** Schematic representation of how a linear velocity test is performed experimentally. The mass of catalyst and the flow rate are varied in different flow reaction in order to change the linear velocity and keep constant the contact time. Evaluation of the rate of the reaction as function of linear velocity will tell if film diffusion is present.

In this work, four different flow experiments were carried out by proportionally increasing mass of catalyst and flow rate. In figure 4 it is shown that the conversion is independent from the linear velocity when the reactor operates at flow rates between 0.1 and 0.2 mL min<sup>-1</sup>. Instead, film diffusion is observed when the flow rate was lower than 0.1 mL min<sup>-1</sup>, in this case 0.08 mL min<sup>-1</sup>. Therefore, all the experiments in this chapter were carried out at flow rates higher than 0.1 mL min<sup>-1</sup> in order to maintain true kinetic performance.

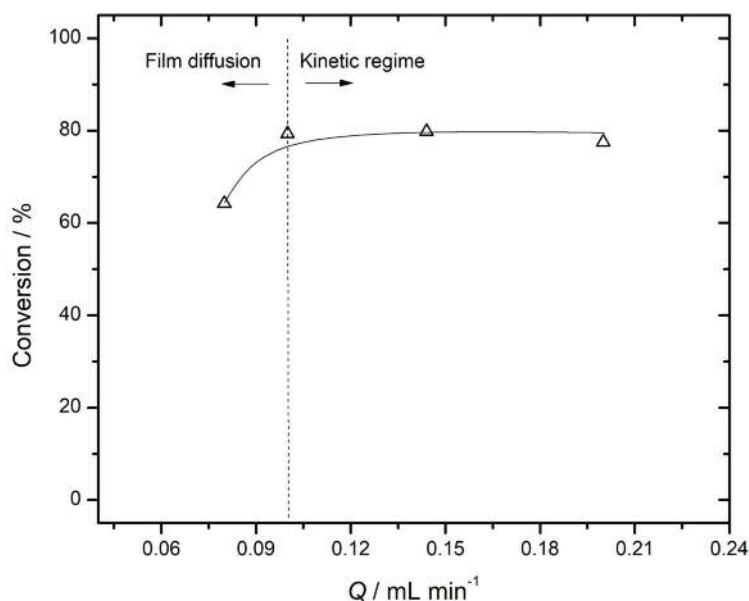


**Figure 4.** Influence of linear velocity on catalytic activity. The CyO reaction has been performed at 100 °C and the mass of catalyst and the flow rate has been varied proportionally in order to keep constant the contact time

#### 4.2.3 Activation energy of the process

To further verify the reaction regime, the temperature dependence of the rate of the reaction when it is performed in the continuous flow need to be studied in order to obtain the activation energy and compare it with the value previously obtained from batch experiments. If true kinetic performance is observed, then a similar temperature dependence should be observed irrespective of the mode in which the reaction is carried out. A set of experiments have been carried out in continuous flow at 80, 90 and 100 °C, as shown in figure 5. In each experiment, the contact time was varied by increasing the flow rate during operation, and the corresponding conversion at each contact time calculated. The activation energy, as calculated by the method described in 3.2.2, was found to be 41.7 kJ mol<sup>-1</sup>. This value is in excellent agreement with the activation energy obtained from the batch experiments (39.3 kJ mol<sup>-1</sup>, chapter 3 section 3.2.2), further confirming that the reaction is under kinetic regime.

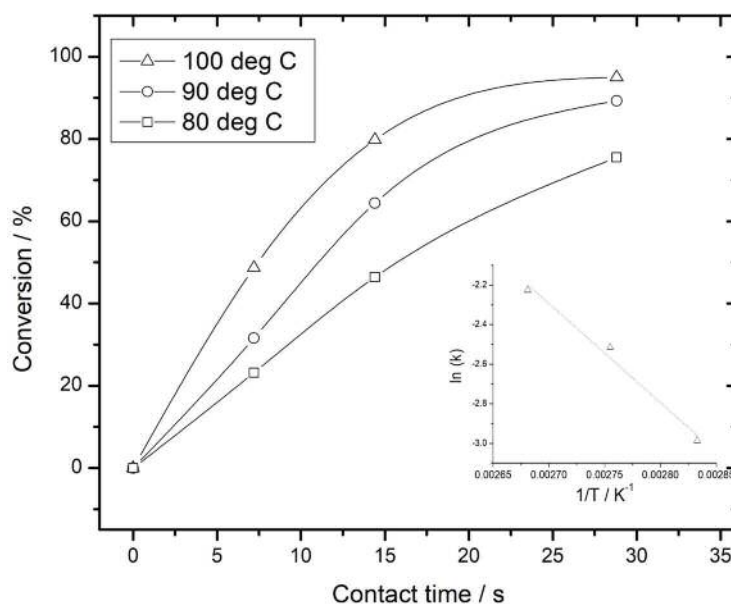


**Figure 5.** Time online data for the MPV transfer hydrogenation of cyclohexanone in continuous mode between 80 and 100 °C. The relevant Arrhenius plot is displayed in the inset.

#### 4.2.4 Preliminary stability study

After having optimised the kinetic parameters of the reaction in continuous flow, preliminary exploration of the long-term stability of Sn-Beta for the TH of CyO could be performed. To do so, the performance of the catalyst, such as conversion, are monitored during time in order that the extent of deactivation could be observed. In order to avoid high pressure drop that could have compromised the practicability of the continuous reaction, an inert material was chosen to dilute the catalyst in order to avoid that possibility that the fine zeolite powder packed during reaction, causing the pressure of the system to rise and eventually to block the system. Therefore, SiC was chosen as diluent to mix with the catalyst in order to form a physical mixture of catalyst and diluent in a weight ratio 1 to 4. On the other hand, the use of the diluent has some drawback, including making characterisation of the catalyst more difficult, due to the difficulty of achieving perfect separation of catalyst and diluent after reaction. Secondly, it leads to a lower STY, since the volume of the catalytic bed is increased by the presence of the inactive phase. Figure 6 reports the kinetic profile of the TH of CyO against time on stream catalysed by 10Sn-Beta at 100 °C.

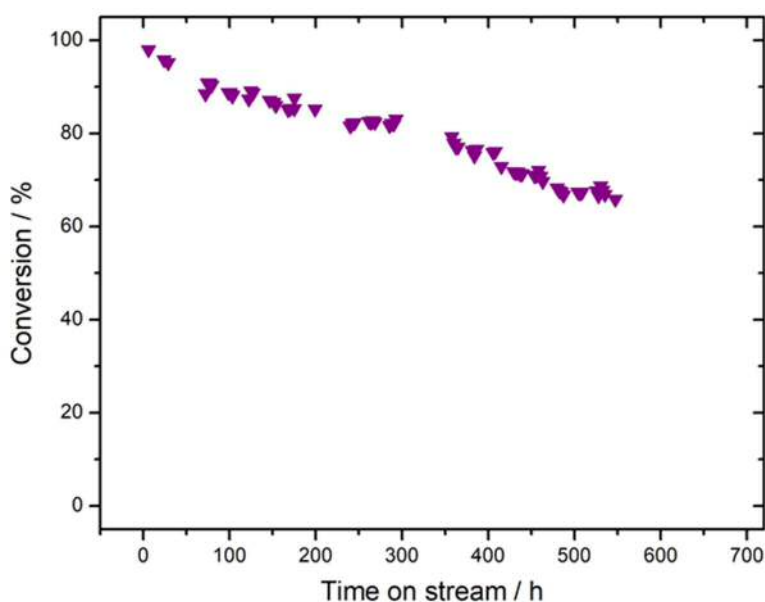


**Figure 6.** Time on stream data vs. conversion of CyO at 100 °C. 0.2 M of CyO solution in 2-butanol are flowed at 0.1 ml min<sup>-1</sup> over 70 mg of 10SnBeta diluted in SiC (1 : 4).

The contact time of the reaction has been set in such a way that the starting conversion was around 98 %, in order to stay below complete conversion of the substrate. This was to ensure that the reaction was not performed in with an ‘excess’ of catalyst, which happens when the amount of catalyst is higher than the minimum amount of catalyst needed to have complete conversion of the substrate. Having an excess of catalyst is a practice quite common in industry because it allow extending the life of the process before strong deactivation phenomena take over; however, it should be added that having excess of catalyst it does not extend the intrinsic life of the material. For the purpose of this work, the use of an excess of catalyst will lead to an over estimation of the life of the catalyst, and does not allow deactivation phenomena to be probed. Hence, for this reason initial conversion below equilibrium level has been preferred. The temperature of the reaction was set to 100 °C, in order to allow comparison with the test performed in batch (reflux temperature of 98 °C). It was found that selectivity in cyclohexanol and total carbon balance were above 95 % through all the duration of the experiment, in perfect agreement with what found during the batch testing. The conversion dropped from the initial value of 98 % to 65 % in about 550 h (ca. 23 days), showing a 1-2 % of decrease in conversion per day. Despite the exceptional stability exhibited by Sn-Beta for continuous TH of cyclohexanone, its stability is clearly not perfect (approximately 30 % deactivation being observed). Hence, the importance of finding the causes of deactivation remains a central challenge of this work.

#### 4.2.5 Characterisation of used catalyst

Although a good level of stability was observed in the preliminary test of 10Sn-Beta for the TH of CyO, the causes of deactivation after the reaction need to be studied. Therefore, characterisation of the used catalytic materials was performed. The approach was analogous to the one followed in the previous chapter. In fact, characterisation techniques are used in order to find differences between the catalyst, in this specific case between a fresh and a used, and then relate them to extent of deactivation. Furthermore, it has to be kept in mind that in here the catalyst has been reacted; therefore, the reaction component has to be taken in account when it comes to choose the right technique and to correlate structural changes with reaction conditions.

Initial studies focused on the textural properties of the zeolite, which could have been compromised by operation in the liquid medium at elevated pressures and temperatures. As such, the crystallinity of the sample after 550h of reaction was compared to that of the fresh one by XRD. From figure 7 it is clear that the crystalline structure of Sn-Beta is still intact after reaction. The decreased in intensity it could be due to the different amount of SiC present after the recovery of the catalyst from the reactor. Since no major differences were found, this is an important evidence that the crystalline structure of the catalyst does not get damage after 550 h of time on stream under reaction conditions.

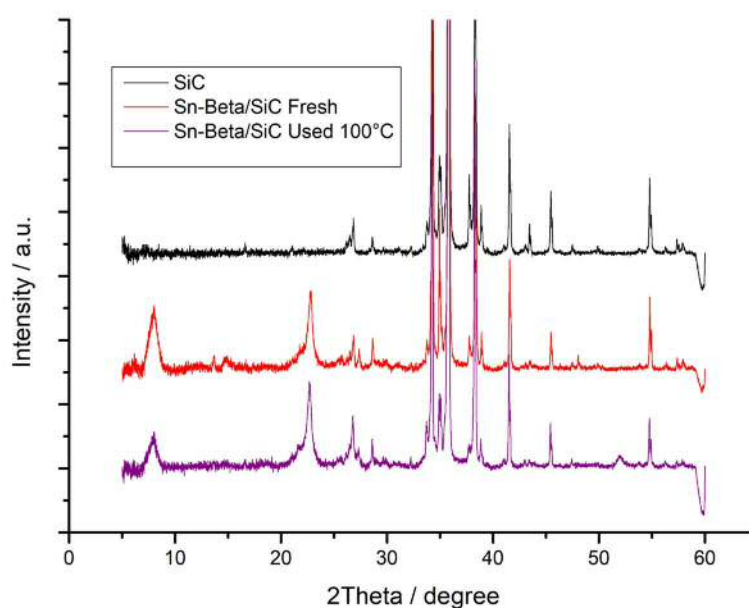


**Figure 7.** A selection of XRD patterns of ex reactor catalyst samples. From top to bottom: SiC (black), Fresh catalyst/SiC mixture (red), used catalyst (purple). The used catalyst was measured after 550 h on stream.

#### 4.2.6 Elemental specific characterisation

Since it appeared that the overall structure of the zeolite did not change after reaction, a closer look to the Sn active sites has been performed through  $^{119}\text{Sn}$  MAS NMR, a technique already used in the previous chapter that provided useful information about the speciation of Sn in the catalyst. Being an element specific technique, the presence of SiC does not interfere with the measurement, but simply results in a lower signal to noise ratio (S/N) due to dilution. The NMR spectra of the used and fresh samples are compared in figure 8.

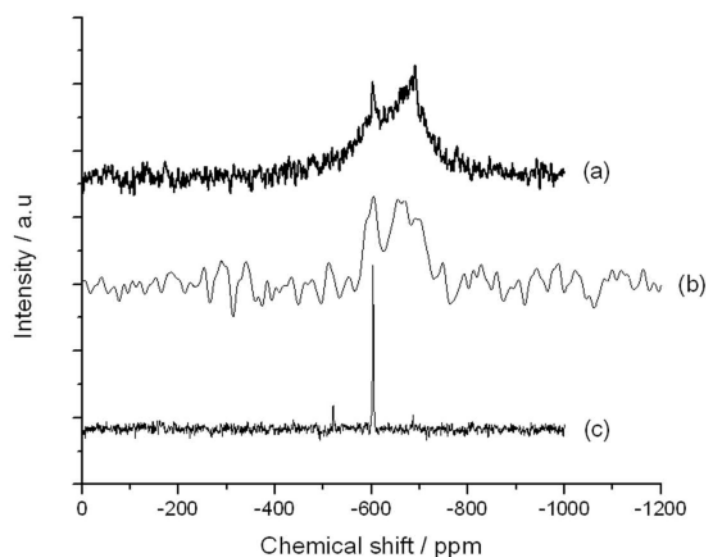


**Figure 8.** MAS NMR spectra of (a) fresh i.e. unreacted 10Sn-Beta, (b) 10Sn-Beta after 500 h on stream, and (c)

The two main features found in the spectra are, as expected from chapter 3, the signals at -602 ppm and -688 ppm, representative of extra-framework and framework tin, respectively. From the comparison of the two spectra, it can be qualitatively seen that the ratio between the -602 and -688 ppm signals is higher for the used sample, suggesting that a growth of the extra-framework species occur during the proceeding of the reaction. Unfortunately, a precise quantitative analysis was not possible mainly for two reasons: the relaxation time of the two species are unknown, which means no quantitative relationship between the area of the signal and the amount of the species can be done; and the integration of the two signals is difficult due to the low S/N.

To try to confirm the extent of extraction of framework Sn, another element specific technique has been applied. X-ray absorption spectroscopy (XAS) has been performed by collaborators at Harwell synchrotron facilities. This technique is one of the most powerful tools that can be used to study to local atomic environment of a specific element. Between all the information that can be acquired there are: the number and type of the neighbour

atoms, the geometry of the element, the oxidation state, and hence the speciation of the active species. Differently from  $^{119}\text{Sn}$  MAS NMR however, XAS is an averaged technique, meaning that all the signal coming from different species are averaged between them. Accordingly, the data analysis is often complicated and a dedicated scientist is needed to achieve sufficient levels of insight. XAS analysis generates a spectrum in which the XAS function is plotted against the energy of the incident radiation. The spectral region is generally divided in two parts, the pre-edge and a post-edge region. The XAS region called EXAFS (Extended X-ray Absorption Fine Structure) is related to the oscillatory part of the XAS spectra and it extends between 50 and 1000 eV after the absorption edge. The main information obtainable from this region is spatial surrounding of the element considered. For example, Corma and collaborators used XAS spectroscopy to try to assign the exact position that the Sn occupy inside the zeolite structure.<sup>4</sup> To allow a more intuitive reading of the spectra, the Fourier transform (FT) is applied to the EXFAS. Doing so, the abscissa axis become a spatial dominion, express in Angstrom. Simplistically, it can be read as the distance at which the Sn-atom scattering occurs. For instance, if an EXAFS signal is found at a certain distance it can be interpreted as the presence of a particular atoms at that particular distance from the Sn that cause that particular scattering. Other than qualitative analysis, EXAFS allows to obtain semi-quantitative information about the species measured because the intensity of the signal is directly proportional to the amount of the element. Prior to measurement of the samples, analysis of standard materials was performed. In this case,  $\text{SnO}_2$  and 5Sn-Beta have been used as standard for extra-framework and framework Sn species respectively, and their FT-EXAFS spectra are shown in figure 9.

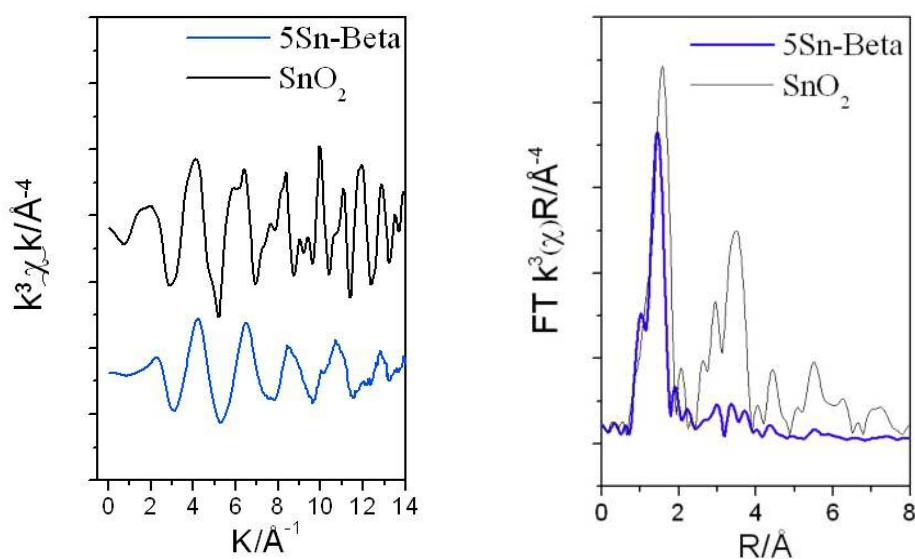


**Figure 9.** (Left) EXAFS  $k^3$  weighted  $\chi$  data and (Right) magnitude of the non phase-corrected Fourier transform, of dehydrated 5Sn-Beta (blue) and  $\text{SnO}_2$  (black).



Two main scattering are present in the  $\text{SnO}_2$ , the first more intense at  $1.5 \text{ \AA}$  is the first shell scattering Sn-O. The second signal around  $3 \text{ \AA}$  arises from Sn-Sn interaction, and is characteristic of  $\text{SnO}_2$ . In Sn-Beta, where ideally all the Sn atoms are isolated, no Sn-Sn should be visible and almost only the Sn-O scattering at  $1.5 \text{ \AA}$  is found.

To achieve sufficient insight, three distinct but identical continuous experiments were therefore performed in continuous flow, each experiment has been terminated at a different time on stream value, 24, 120 and 200 h. In this way the evolution of Sn could be follow during time. Indeed, the local environment of the Sn is of particular importance in determining the presence of extra-framework tin. In Figure 9 the four FT-EXAFS spectra are displayed against time on stream. Overlapping the FT-EXAFS spectra (Figure 10) it can be seen that there are two main peaks, one around  $1.5 \text{ \AA}$  and the other one around  $3 \text{ \AA}$ , indicative of Sn-O and Sn-Sn scattering respectively. Whilst the first signal remains constant through all the time, the signal at  $3 \text{ \AA}$  gradually grows during the reaction. However, the relative increase of Sn-Sn scattering is quite modest, even after 200 h of reaction, suggesting that this only could account for a small contribution in the deactivation process.

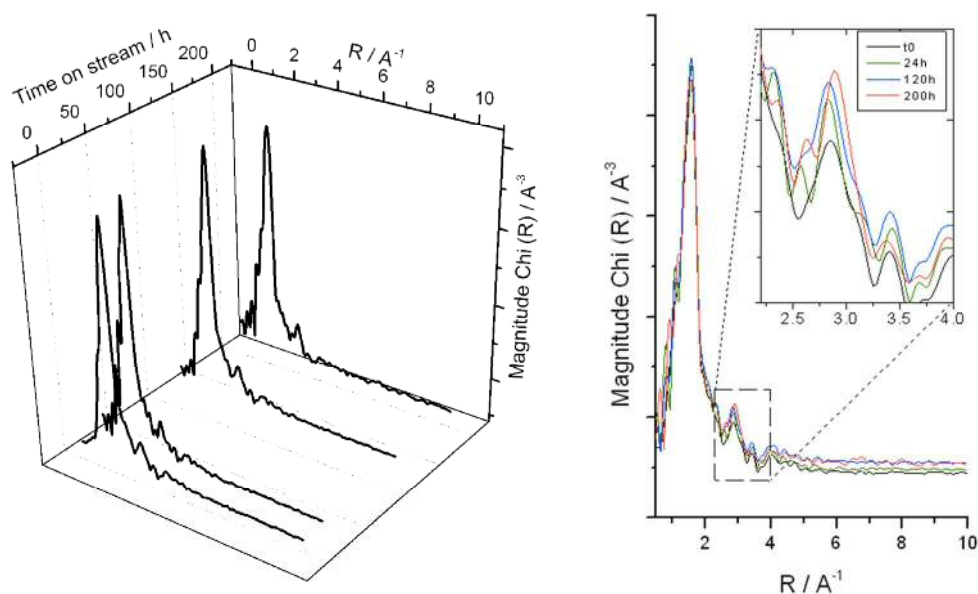


**Figure 10.** (Left) X-ray Absorption spectra of 10Sn-β at various times on stream, and (Right) magnification of the 2.5-4  $\text{\AA}^{-1}$  region of the spectra.

To summarise the findings obtained so far, XRD confirmed that 10Sn-Beta is capable of processing CyO for more than 200 h consecutively without damaging the structure. Successively, two element specific techniques,  $^{119}\text{Sn}$  MAS NMR and XAS, were employed to

probe the speciation of Sn after the continuous TH of CyO. Firstly,  $^{119}\text{Sn}$  MAS NMR analysis shows a growth of the -602 ppm signal relative to the -688 ppm, thus suggesting that some restructuring of framework Sn into  $\text{SnO}_2$  could have occurred. However, the low S/N ratio and the unknown relaxation times of the different Sn species did not permit a clear picture of the phenomena to be achieved. XAS spectroscopy, carried out on used samples at different time on stream, showed that there was an actual increase of the Sn-Sn signal (indicative of  $\text{SnO}_2$ -like species) as the time on stream of the reaction increased. This finding was in excellent agreement to what observe by MAS NMR. However, the extent of the extraction does not appear to be dramatic. Therefore, more characterisation is required in order to explore if other phenomena could contribute to the catalyst deactivation.

#### 4.2.7 Pore fouling

As discuss in Chapter 1 (see section 1.7.2), one of the main causes of deactivation during continuous operations in reactions catalysed by zeolites is the accumulation of carbonaceous species within the micropores, consequently leading to pore blocking and inhibiting access of reactants to the active sites. These species can be formed by particular molecules present in solution (reactant, products, solvent, etc.) or they can arise from the breakage of products during the reaction, and their subsequent polymerisation to form high molecular weight species that are very difficult to desorb from the catalyst at the reaction conditions.

To understand if some carbon deposition has occurred, preliminary studies by Thermo-Gravimetric Analysis (TGA) were performed on the used catalyst. This technique has already been successfully studied for a similar work by Koehle *et al.*, in which the amount of mass lost on a used catalyst was measured and correlate to accumulation of species upon the reaction on the catalyst.<sup>5</sup> The mass loss derivative ( $\text{dTG} / \text{dt}$ ) is plotted against time and is shown in Figure 11.

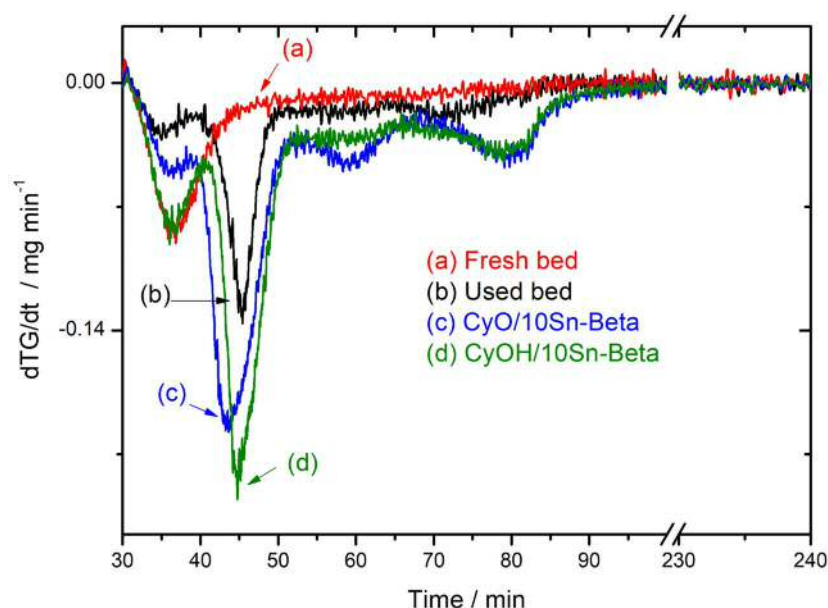


**Figure 11.** TGA data for 10Sn-B. The sample removed after  $\pm 550$  h on stream (b) is compared to a fresh catalyst sample (a), and two reference materials of 10Sn-B doped with CyO (c) and CyOH (d).

For comparison, standard samples were also measured. To do so, a fresh catalyst was stirred separately for 6 h in pure cyclohexanone and cyclohexanol, in order to be able to relate a weight loss signal to a particular molecule. These samples allow a direct comparison between the species that desorbs from the catalyst based on the time of desorption (and hence temperature, as the ramp rate is identical in all experiments). A first peak at 35 min (ca. 60 °C) is present also in the fresh sample, indicating that is probably from the moisture absorbed on the zeolite. At 55 min (275 °C) the used sample presents a major mass loss, and after comparison with the standard samples it can be seen that it match perfectly with the mass loss evolved from the CyOH doped samples. A smaller and broader peak (around 70 min, 425 °C) is also present and could arise from high molecular weight carbonaceous species.

In particular, the great amount of CyOH found is a strong indication that in the used catalyst this particular species is selectively retained over the CyO. In fact, as experiments were performed in continuous flow, CyO and CyOH should be present homogeneously along the x axis of the reactor, as their concentration is space dependent, in contrast to batch reactions where they are time dependent. As such, even if the reactor works at 100 % of conversion, some concentration of reactant and product are found along the axis. Figure 12 is a

schematic of the hypothetical concentration profile of the CyO and CyOH along the plug flow reactor.

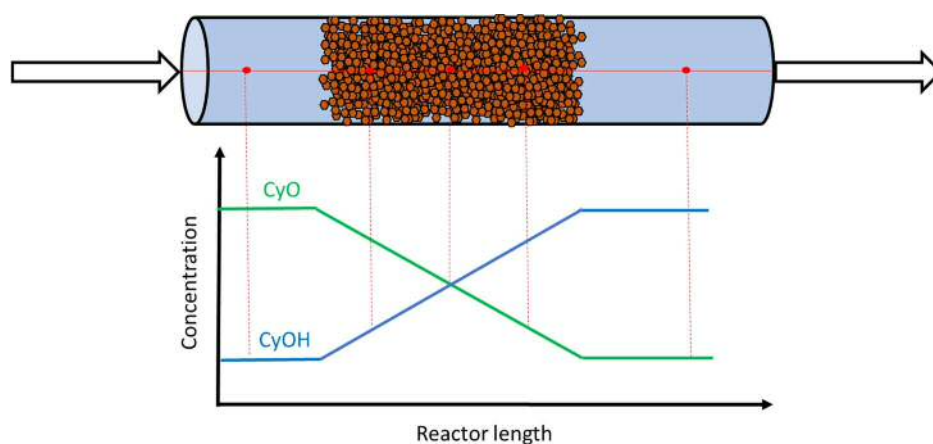


**Figure 12.** Schematic of the plug flow reactor and the CyO and CyOH concentration along the X axis. The concentration of the reactant are space-dependent and time-independent.

Even though TGA of the used and the CyOH-doped controlled samples showed a similar mass loss, the exact nature of the species cannot be readily determine by this technique. For this reason a  $\text{CD}_3\text{Cl}$  extraction at room temperature have been done on the used catalyst and the  $^1\text{H}$  NMR spectra recorded and shown in Figure 13. The spectra appeared very clean and no traces of cyclohexanone could be found, while CyOH and 2-butanol are clearly present, proving once again that the alcohol species in solution are strongly adsorbed to the catalyst during the reaction, which might lead to deactivation. Quite surprisingly, no signal could be attributed to some aromatic or high molecular weight molecule possibly derived from decomposition of the organic substrate. It has been hypothesised that maybe a room temperature extraction was not sufficient to extract heavier compound from the zeolite that might have been strongly absorbed inside the pore, and/or that their solubility in the extraction medium was not sufficient.

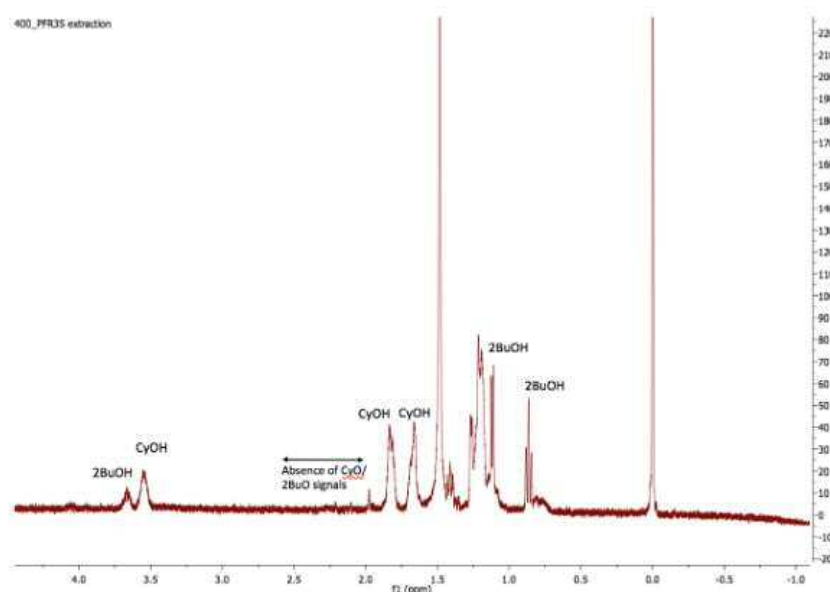


**Figure 13.**  $^1\text{H}$  NMR spectra of the supernatant solution after extraction of the ex reactor catalyst in  $\text{CD}_3\text{Cl}$ . Clear resonances from both alcohol species, 2-butanol and CyOH, are observed, whilst no signals from the corresponding ketones are found.

These techniques provided strong evidences that CyOH and possibly heavier organic compounds are selectively present in the catalyst after the reaction. However, is still unknown if and how they are related to the observed decrease in activity. In fact the species could act either as poison and/or causing fouling. Indeed, a direct consequences of accumulation of products in the zeolite could be the blockage of the micropore, leading then a decrease in the surface area. To prove if any decrease in the surface area and blockage of pore occurred, nitrogen adsorption isotherm analysis were performed on the fresh and used samples to obtained BET area and total pore volume. Particular care have been taken during the degassing step prior the analysis. In fact, a full degassing protocol, often involving deep vacuum and high temperature (250 °C), would have led to a total removal of organic residues based on the TGA measurements, possibly hiding some influence on the surface area. Instead, the samples was heated at 120 °C under ambient pressure and flowed with nitrogen. The surface area and total pore volume obtained are summarised in Table 1.

**Table 1.** Porosimetry data from fresh and used Sn-Beta catalysts.

Catalyst	BET area (m <sup>2</sup> g <sup>-1</sup> )	Total pore volume (cm <sup>3</sup> g <sup>-1</sup> )	Normalised pore volume (cm <sup>3</sup> g <sup>-1</sup> )
Fresh catalyst/SiC	66.5	0.046	0.23
Used catalyst/SiC	26.4	0.022	0.11

Since the analysis have been made on a dilute catalyst and SiC pore volume is negligible compare to the zeolite, the pore volume found have been normalised to the original mass of the catalyst. It can be seen that the total pore volume dropped from 0.23 to 0.11 ml g<sup>-1</sup>, indicating approximatively 50 % loss of the original pore volume, clearly suggesting a that blockage of the pore can be attribute to the loss of activity. Despite the structure and active site are still intact, the impossibility for the reactant to diffuse into the pore is deleterious for the activity.

#### 4.2.8 Catalyst regeneration

Characterisation techniques strongly indicate that fouling is the main cause of deactivation, and changes to Sn *via* extraction and agglomeration, are only a minor cause. It is known that fouling is generally a non-permanent cause of deactivation, therefore if this is actually the case, it should be possible to restore activity of the catalyst, either totally or partially. Since fouling is caused by accumulation of organic compounds, and the zeolite structure and active site are intact, the removal of this carbonaceous species should restore the initial characteristic of the zeolite, with also the initial activity.

To achieve this, the whole reactor has been taken off the system and place in a tubular furnace. A standard calcination protocol for zeolite has been applied, consisting of 550°C in air flow for 3 h. After the thermal treatment the reactor have been re-connected to the reactive system and the reaction has been re-started with the previous experimental settings and the relevant time on stream plot is shown in Figure 14. As can be seen, after the thermal treatment the activity of the catalyst has been completely recovered, indicating deactivation during the first cycle to be non-permanent. Notably, aa similar deactivation rate has been observed during the second cycle, indicating that similar active sites are present during the second cycle. These findings corroborate that deactivation is caused by fouling

and is a reversible phenomenon, something that would not have been possible if collapsing of the structure or Sn restructuring would have been the deactivation cause. It also indirectly shows that the observed extraction of Sn from the framework is only a minor effect; as extra-framework Sn is inactive for TH, no activity can be recovered if this phenomenon became the major form of deactivation.

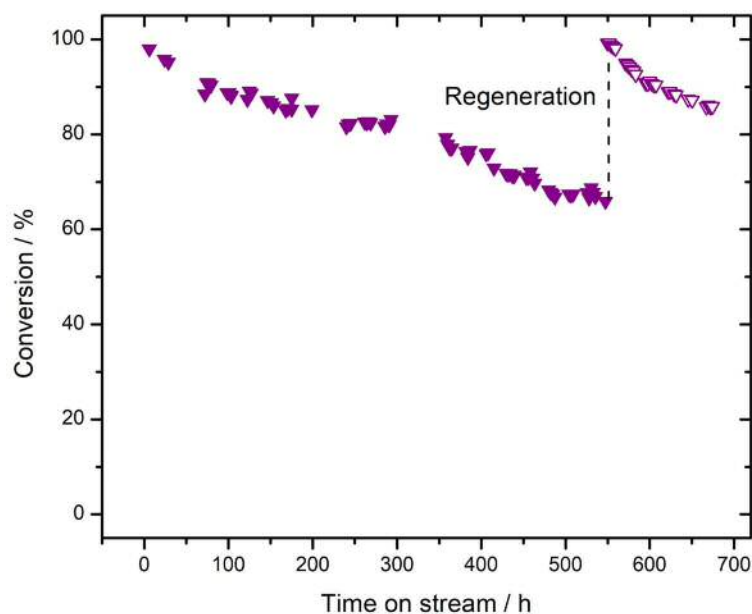


**Figure 14.** Time on stream data for 10Sn- $\theta$  at 100 °C. The regenerated sample data are illustrated by hollow triangles.

#### 4.2.9 Optimisation of the system

All the evidence collected so far pointed as preferential adsorption of the CyOH and heavy carbon residue, as the main cause of deactivation, while not major contribution of Sn restructuring or leaching could be found. To be able to regenerate the catalyst is, of course, desirable. However, the regeneration of the catalyst required the reactor to be removed from the flow system, and heating it for 3 hours prior to re-connection. The time employed for this operation obviously negatively influenced the STY of the whole process. Therefore, more important now could be the use the knowledge gained so far to optimise and extend the intrinsic lifetime of the catalyst. Since strong adsorption of CyOH leads to accumulation of organic products on the catalyst, avoiding the adsorption, or in other words, favouring the desorption of these products, could represents a key point to improve the life of the catalyst. To investigate this further, the TH reaction was performed at higher temperatures. Figure 15 shows the two conversion vs time on stream plots of the reactions performed at 120 and 140 °C, respectively.

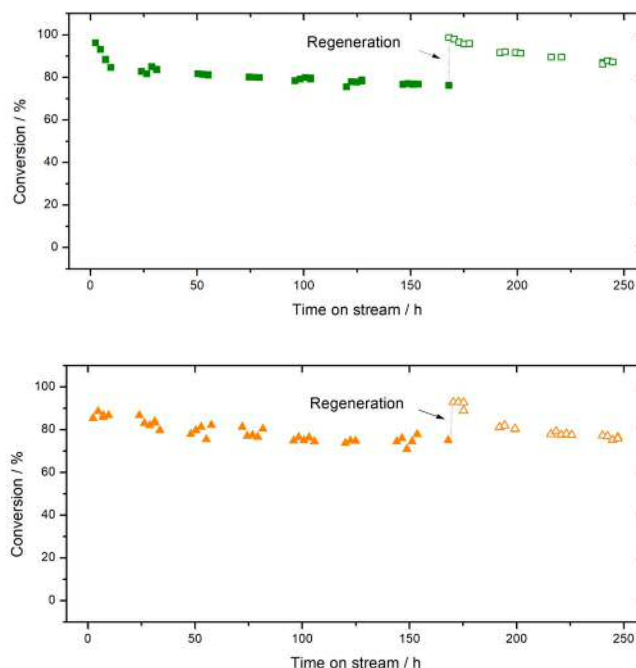


**Figure 15.** Time on stream data for TH of CyO catalysed by 10Sn-Beta at (top) 120 °C and (bottom) 140 °C.

As a consequence of the increase in temperature, the rate of reaction increases accordingly. As such, the flow rate of the reaction was also increased in these tests (so contact time has decreased) in order to have a starting conversion between 85 and 95 % in all cases. Both reactions were carried out for about 170 h. it can immediately be seen that, as in the previous case, no dramatic deactivation is observed even at higher temperatures and higher numbers of substrate turnover. After a first cycle, the reactor was again removed and the same regenerating heat treatment followed, leading to a complete reactivation, as observed in the previous case. This can be considered as indirect evidence that the same deactivation phenomena (fouling) was present in these two systems. However, a more detailed comparison of the kinetic behaviour of the three systems need to be done at this point to evaluate carefully the effect of the temperature on the performance of the reaction. To allow a more direct comparison, the relative performance of the catalysts were plotted against time on stream In figure 16.



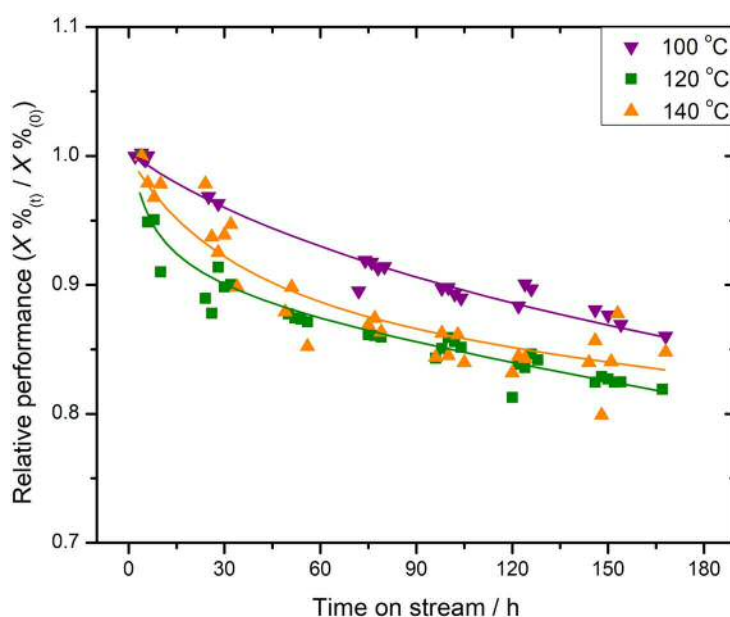


**Figure 16.** Relative catalytic activity of 10Sn-8 over 170 h on stream between 100 and 140 °C. Contact time of the reaction were adjusted in order to start from a similar level of initial conversion.

faster, even though the difference in relative performance between the three reactions after 170 h is within 10 percentage points in all cases. However, it must be pointed out that the increasing the reaction temperature led to an increase of the intrinsic rate of reaction. Therefore, in order to start from a similar level of conversion the contact time had to be decreased. To do so, the flow rate of the reactant solution has been increased, while the volume of the catalyst was kept constant. Increasing the flow rate means, therefore, that the substrate turnover (defined as the number of molecules of substrate that has passed over a mole of Sn at a certain period of time on stream, also increased dramatically, indicating that a more intensive process was being performed.

To have a better insight of the intrinsic activity of the catalyst and how this is effected during continuous operation at different temperature, the effective kinetic constant has been calculated, and the relative decrease has been compared against the substrate turnover. The effective kinetic constant has been calculated assuming a pseudo-first order reaction and is explicated in:

Indeed, it shows the extent of the loss of intrinsic activity of the catalyst act as the reactant molecules pass over it. As such, the relative kinetic constant decrease is plotted against the substrate turnover and showed in figure 17.

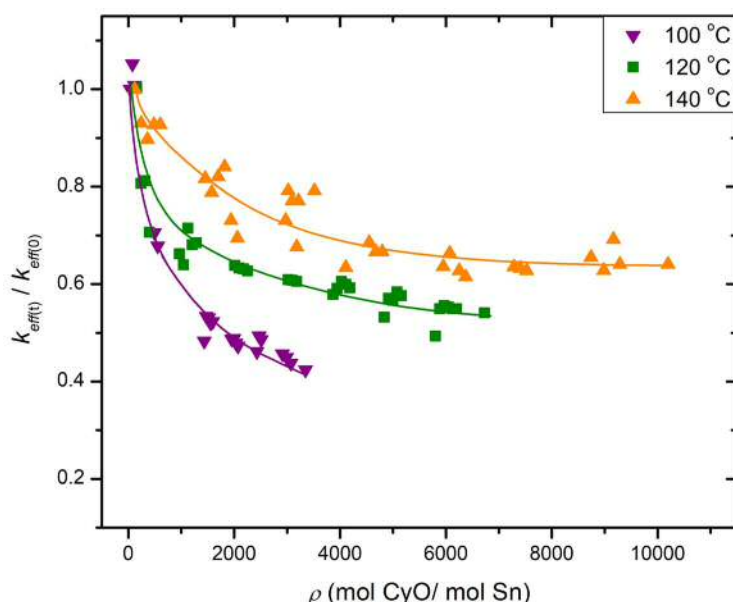


**Figure 17.** Relative effective rate constant of 10Sn-8 with respect to reactor turnover ( $\rho$ ) and temperature between 100 and 140 °C.

It can be seen that the decrease in the rate of reaction is much less dramatic per substrate turnover when the temperature is higher. Furthermore, a *quasi* steady-state is also reached at lower substrate turnover when the reaction is performed at 140 °C. When the continuous TH of CyO is performed at 140 °C, the loss in the reaction rate is approximatively 2-times lower when compared to the reaction performed at 100 °C, at the same substrate turnover (i.e. at 3000 substrate turnover). This clearly demonstrates that operating at higher temperature give an advantage in term of productivity, and helps overcome the slightly higher deactivation that was observed when relative performance of the system were compared against time on stream. In fact, what is important for an industrial process is the ability to produce the highest amount of possible product per mass of catalyst, regardless of this time duration. When the optimised continuous system is compared to the batch the advantage of continuous flow become even more obvious. First of all, the turnover obtained with a single continuous flow experiment correspond to more than 100 batch reactions, demonstrating how rigorous the stability measurements in this chapter are. In addition, the initial space-time-yield of the continuous flow is 40 times higher than the one obtained in batch as shown in table 2.

**Table 2.** Relative performance of Sn-Beta for TH of CyO in batch and flow reactors.

Reactor type	Space-time-yield <sup>1</sup> (kg <sub>CyO</sub> kg <sub>cat</sub> <sup>-1</sup> cm <sub>react</sub> <sup>-3</sup> h <sup>-1</sup> )	Relative STY
Batch	0.76	1
Flow	31.8	41.8

Note: space-time-yield were calculated at maximum conversion as kg of product produced per cm<sup>3</sup> of reactor volume, per hour and per kg of catalyst. <sup>1</sup>Only the liquid volume was used as reactor volume for the batch experiment. <sup>1</sup>Volume of catalyst bed (including diluent) used as reactor volume for the flow experiment

### 4.3 Conclusions

In this chapter, the stability of Sn-Beta zeolite has been studied for continuous TH reaction of CyO to CyOH in organic media. The zeolite has been proved to be very stable in continuous operation and be able to preserve over 70 % of its initial activity for more than 700 h including one short regeneration treatment. Optimisation on the system revealed that operating at 140 °C was beneficial for both activity and stability, and a three-fold =increased in productivity was also achieved by this optimisation. Extensive spectroscopic analysis on the used catalyst bed revealed that the zeolite structure and Sn active site were preserved and almost unchanged after reaction, only a minor extraction of framework Sn could be found. TGA, <sup>1</sup>H NMR, Raman and porosimetry analysis revealed that accumulation of product (CyOH) and higher molecular weight carbonaceous residues lead to fouling of the micropore. In fact, a decrease in volume of approximately 50 % has been attributed to be the main cause of deactivation. However, fouling has proved to be reversible, in fact a simple heat treatment at 550°C in air was able to restore full activity.

The work done in this chapter shows that Sn-Beta performed excellently for the TH of CyO in organic solvent. However, biomass valorisation often involves much more complex reactions. Furthermore, although the catalyst proved to be very stable from the activity point of view, no information through this system can be obtained about long term selectivity changes that may occur. To examine how the catalyst behaves in continuous flow when more reactive substrates and products are possible, a different system has been taken in consideration. In this regards, bio-renewable substrates offer great challenge. An

interesting, useful and sugars-derived class of substrates are furanic compounds, such as furfural, which can be obtained by dehydration of xylose (the key constituent of hemicellulose). When furfural (FF) is reacted with Lewis acids in 2-butanol, two main products are formed; the TH products which is furfuryl alcohol (FA), and the etherification product, which is 2-(butoxymethyl)furan (BMF). Figure 18 shows the reaction pathways of the reaction considered. As it can be seen the reaction is composed of two step. The first step is the TH of FF to FA, and is catalysed by Sn-Beta. The second step is the etherification of FA to BMF with 2-butanol. It has been already demonstrated that Sn-Beta is able to catalyse etherification reactions by Corma *et al.*,<sup>6</sup> while Lewis and collaborators<sup>7</sup> tried to make a continuous TH/etherification of 5-hydroxymethylfurfural, revealing that maintaining high selectivity with only Lewis acids on the etherification products in a continuous flow process is a big challenge. Consequently, in the next chapter the TH/etherification tandem reaction in continuous flow will be studied, with particular attention being paid to the selective production of the ether products. In addition to proving to be a more reactive system possessing multiple reactive steps, the systems also represents a shift towards the continuous upgrading of renewable compounds, which is the major target of this thesis.

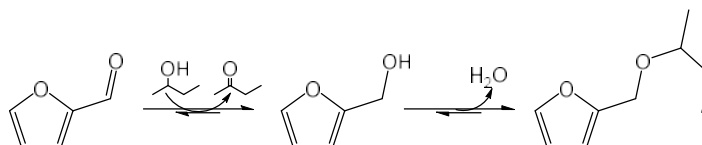


**Figure 18.** Combined TH and etherification of furfural catalysed by Sn-Beta.

## References

- <sup>1</sup> J.-P. Lange, *Catal. Sci. Technol.*, 2016, **6**, 4759.
- <sup>2</sup> E. Taarning, S. Saravanamurugan, M. S. Holm., J. Xiong, R. M. West, C. H. Christensen, *ChemSusChem*, 2009, **2**, 625.
- <sup>3</sup> Y. Román-Leshkov, M. Moliner, J. A. Labinger, M. E. Davis, *Angew. Chem. Int. Ed.*, 2010, **49**, 8954.
- <sup>4</sup> S. R. Bare, S. D. Kelly, W. Sinkler, J. J. Low, F. S. Modica, S. Valencia, A. Corma, L. T. Nemeth, *J. Am. Chem. Soc.*, 2005, **127**, 12924.
- <sup>5</sup> M. Koehle, R. F. Lobo, *Catal. Sci. Technol.*, 2016, **6**, 3018.
- <sup>6</sup> A. Corma and M. Renz, *Angew. Chem. Int. Ed.*, 2007, **46**, 298.
- <sup>7</sup> J. D. Lewis, S. Van der Vyver, A. J. Crisci, W. R. Gunther, V. K. Michaelis, R. G. Griffin, Y. Román-Leshkov, *ChemSusChem*, 2014, **7**, 2255

## ***5. Continuous production of 2-(butoxymethyl) furan catalysed by bifunctional Lewis and Brønsted acidic zeolites***

### **5.1 Introduction**

As described in Chapter 1, when catalytic systems with more than a single potential product are employed, selectivity becomes a critical factor of the reaction. In fact, along with high activity and stability, selectivity represents a key parameter in determining the success of a process. When it comes to evaluating the selectivity towards a product, multiple factors have to be taken in consideration, such as contact time, temperature and catalyst composition. Furthermore, it must be remembered that typically, compromises between activity and selectivity must be found, because whilst one parameter may be favourable for one aspect, it can be detrimental for the second.

The issue of selectivity becomes increasingly important when renewable feedstock is employed. Indeed, the highly functionalised nature of the feedstock drastically increases the possibility and the variety of reaction pathways deriving from a single molecule. If the catalyst and the reaction condition are not carefully chosen, it is likely that a mixture of different products are obtained, resulting in poor yield of the target product, and necessitating energy-demanding downstream operations in order to isolate the target molecule. A perfect example of this complex reaction network is exemplified by furfural (FF) valorisation, shown in figure 1.

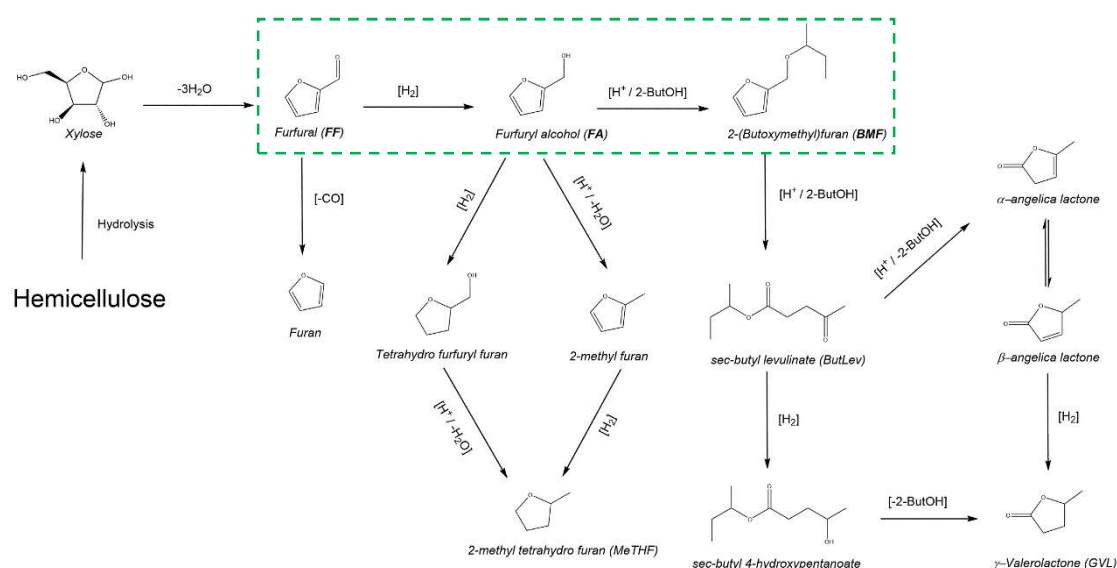


**Figure 1.** Scheme of the reaction network of hemicellulose valorisation. In the dashed box is highlighted the furfural tandem TH/etherification to BMF.

As it can be seen from the scheme, if the reactivity of the system is not finely controlled it can result in a downstream product mixture containing a multitude of products. Even though these products are singularly interesting and potentially useful, the difficult separation would make the process non-economically viable. The raw material from which this synthetic pathway has its origin is hemicellulose, a sugar polymer, whose main constituent is the C-5 sugar, xylose. Therefore, xylose can be obtained by acid depolymerisation of hemicellulose, and its successive dehydration will lead to FF.<sup>1,2</sup> From FF, a wide number of substrates can be obtained, depending on to the reaction conditions and the catalysts used, and they could have a potential employment in several sectors of the chemistry industry. From figure 1, it can also be seen how critical the reduction step of FF to furfuryl alcohol (FA) is, since this step opens up routes to many different products. As such, the FA hydrogenation/deoxygenation route can lead to the synthesis of 2-methyl tetrahydrofuran

(MeTHF), which has been shown to be a promising fuel additive and a good alternative to tetrahydrofuran, which is widely employed as organic solvent and has its origin from fossil fuel substrates. When FA is reacted in the presence of alcoholic solvents and a catalyst that has Lewis and/or Brønsted acidic characteristics, etherification between the two alcohol groups can also occur. Notably, these products are believed to be promising biofuel additives. Both FA and its ether can also undergo further ring-opening, resulting in levulinic acid and the respective ester. These products, other than fuel additive usage, can be converted into  $\gamma$ -valerolactone (GVL),<sup>3</sup> which is a very promising green solvent and bio fuel.

Specifically, ether compounds of FA are of particular interest because they are considered to have application as biofuel, or as biofuel additive. Of great attractiveness is the relative simple synthetic route by which this ether could be obtained. In fact, a one-pot reaction, from FF to the ether can be carried out, saving costs relative to operation of such as reaction with intermediate separation and purification. In fact, as seen in the previous chapters, it can be hypothesised that a reaction pathway in which FF is reduced to FA *via* transfer hydrogenation (TH) and successively etherified with the alcohol; In both steps, the co-reactant can therefore also be the solvent of the reaction. By performing the reduction step by the transfer hydrogenation reaction, then the use of molecular hydrogen is avoided, resulting in a sacrificial alcohol acting as hydrogen donor. Interestingly, the alcohol plays an important role, being simultaneously solvent, hydrogen donor and etherifying agent. Consequently, it is crucial that a catalyst is able to catalyse both TH and etherification reaction.

It has previously been shown that such tandem TH/etherification reactions can be performed with Sn-Beta. For example, Corma *et al.*<sup>4</sup> demonstrated that *para*-methoxybenzaldehyde could be reduced to its respective alcohol and successively to its ethers in the presence of the catalyst at 100 °C. Another interesting study was carried out by Lewis *et al.*,<sup>5</sup> in which 5-hydroxymethyl furan (HMF) was reacted in a continuous flow reactor in order to form 2,5-bis(ethoxymethyl)furan (BEMF) and 2,5-bis(butoxymethyl)furan (BBMF) from ethanol and 2-butanol respectively. In that study, the tandem TH/etherification reaction of HMF was carried out in ethanol and performed by several solid Lewis acid catalyst, such as Hf-, Zr- and Sn-Beta at 120 °C. However, when ethanol was employed as solvent, poor and unstable selectivity to BEMF was obtained. On the other hand, a good level of selectivity to BBMF was observed with Sn-Beta through all the duration of the reaction. However, even in this case a very low total number of substrate turnover were performed (250 turnovers in 100 h of continuous reaction). As such, thorough evaluation of

the stability of the process could not be made. A study conducted by Lew *et al.*<sup>6</sup> also focused on similar tandem TH/etherification reaction processes. In that case, the batch conversion of glucose to 5-(ethoxymethyl) furfural (EMF). In that study, it was shown that the overall process benefits from the introduction of Brønsted acidic species, along with the Lewis acid catalysts that are essential in order to perform the TH step. Indeed, higher yield in EMF were achieved when Sn-Beta and Amberlyst 131 (a Brønsted acid resin) were used in cooperation.

Even though some research has been done, continuous processes of this kind are still a huge challenge. In particular, achieving a stable production of ether is still an unsolved challenge. Although Lewis acid catalysis has been demonstrated to be essential for this type of chemistry, some studies suggest that the employment of a bifunctional catalytic system could bring substantial improvement in term of selective production of a specific compound. Therefore, this chapter will be focused on the study of the continuous tandem TH/etherification of FF to 2-(butoxymethyl) furan (BMF), carried out in 2-butanol as hydrogen donor and solvent. The main aim is to achieve a continuous and stable production of ether, and doing so, explore the potential continuous use of cooperative Lewis/Brønsted acid catalysis.

## 5.2 Results and discussion

### 5.2.1 Preliminary studies of tandem TH/etherification of FF with Sn-Beta

As seen from figure 1, FF valorisation can lead to a multitude of different products. Therefore, the key parameter of this process will be the selectivity to BMF, particularly as a function of conversion and substrate turnover. Despite the main functional group of FF being a ketone, FF substantially differs dramatically from CyO, and is dramatically more reactive, as demonstrated by the complicated reaction network. For this reason, prior to continuous flow testing, thorough understanding of its reactivity has to be explored in batch. In chapter 3 and 4, the catalyst activity and stability have been evaluated in details for the TH of CyO, and 10 Sn-Beta has been demonstrated to be the best catalyst in term of activity per unit mass of catalyst. However, during FF TH/etherification process, given to wider array of by-products obtainable, selectivity becomes the most important parameters. Thus, to gain better understanding of the kinetic and selectivity parameters for the FF tandem TH/etherification reaction, 2 and 10Sn-Beta catalysts are compared again to determine the potential impact of metal loading on both the selectivity and activity of the process.



Preliminary batch tests were carried out under identical conditions to the TH of CyO, in order to compare the TH activity of the catalysts simply as a function of substrate. Therefore, reactions were carried out at 98 °C and the molar ratio between FF and Sn was set to 100 (identical to chapter 4) and kept constant in all the tests, allowing a comparison of intrinsic activity and selectivity to be made. Figure 2 shows FF conversion as function of time over both catalysts.

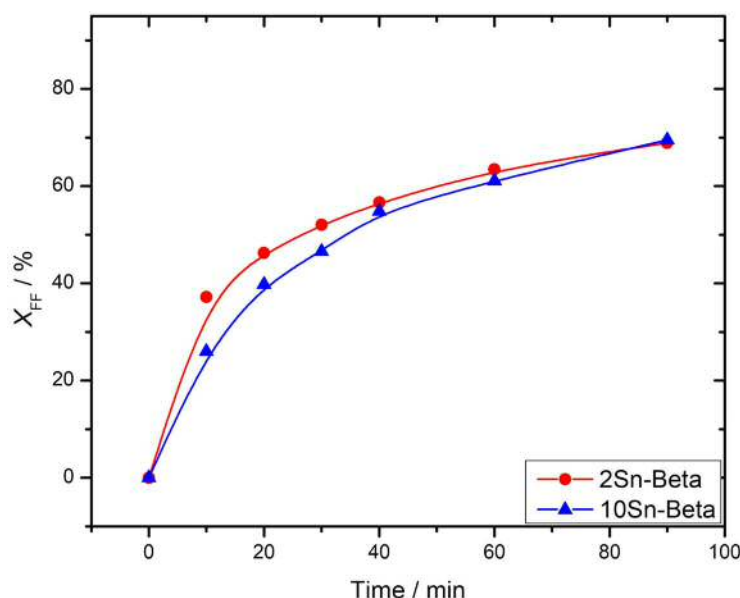


**Figure 2.** Rate of FF conversion over Sn-containing Beta zeolites. A 10 mL solution of FF (0.2 M) in 2-butanol have been reacted with 2 and 10Sn-Beta under reflux temperature (98°C) for 90 min. A FF / Sn = 100 molar ratio was employed for both reactions.

In good agreement with what observed for the TH of CyO, both catalysts showed a good level of activity, reaching approximately 70 % of conversion in 90 min. In further agreement to the work presented in Chapter 3 and 4, 2Sn-Beta possess approximately 30% higher initial TOF than 10Sn-Beta (234 vs. 173 h<sup>-1</sup>, respectively). Even though the difference in initial activity is less marked than for TH of CyO, it is still clear that 2Sn-Beta present the highest intrinsic activity, likely due to the presence of a more uniform active site distribution (Chapter 3.2.4).

Qualitative analysis of the reaction mixtures by GC and HPLC revealed that only FA, BMF and butyl levulinate (ButLev) were present as reaction products. Quantification of these products allowed a more detailed analysis of the reaction pathways to be made. ButLev was found only in traces, with yield lower than 1 % at every points. Carbon balance of the system was above 98 % in all the analysis, leaving then the only two major products FA and BMF

detectable and well quantifiable. For sake of clarity, only the BMF selectivity will be displayed in the figures, while the selectivity of FA can be calculated for difference, being FA and BMF the only two products. The selectivity to BMF as a function of FF conversion is displayed in figure 3.

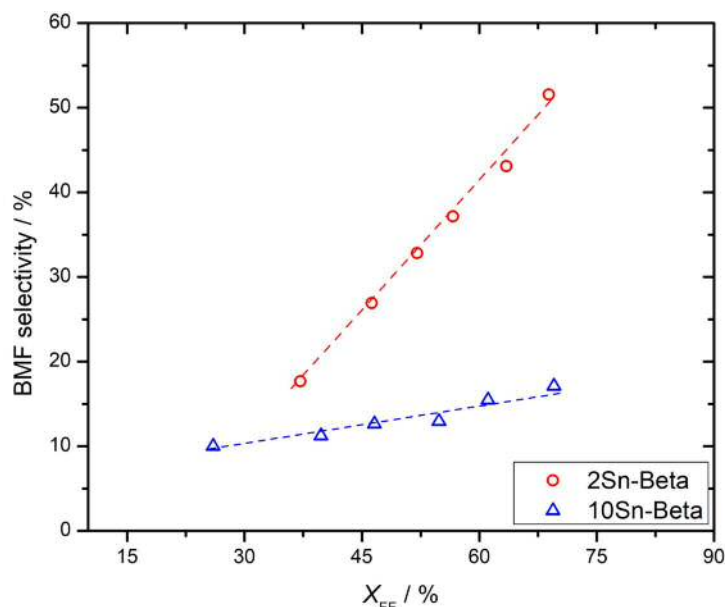


**Figure 3.** Selectivity to BMF as a function of FF conversion during tandem TH/etherification reaction of FF to BMF in 2-butanol performed with 2 and 10Sn-Beta.

As it can be seen, the differences in selectivity are much more remarked than the observed difference in activity for the two different loading catalysts. At a particular level of conversion (70 % FF conversion), 10Sn-Beta exhibits only 15 % of selectivity to BMF, with FA being the major product. At the same level of FF conversion, however, 2Sn-Beta shows approximately 55 % selectivity to BMF. It is therefore clear that although the metal loading has a modest impact on the activity of the catalyst for the conversion of FF, a much more pronounced effect on the selectivity on BMF is observed. Furthermore, the gradual and constant increase of BMF selectivity at increasing FF conversion indicates that the etherification is actually a consecutive step.

Batch kinetic data of the process performed with 2 and 10 Sn-Beta showed that FA and BMF are the two main products obtained, and the ether is a consecutive reaction product. 2Sn-Beta has also been found to be much more selective towards BMF than 10Sn-Beta. However, no information on the stability of the BMF product can be obtained from batch reactions. Therefore, the tandem TH/etherification reaction was investigated in the continuous reactor. Given the different activity per mass of catalyst, the reactant flow rates were adjusted in order to start from a similar level of conversion. In doing so, the reactant

turnovers per unit time of the two system are different, which can evidently impact the stability of the catalyst where reactant- and/or product-induced deactivation processes occur. As such, to have a direct evaluation of the stability of both catalysts, the kinetics parameter, such as relative performance and selectivity, were compared at the same number of substrate turnover numbers rather than time on stream (see Chapter 2 “Formula” for details). The continuous kinetic plot of the TH/etherification process is shown in figure 4.

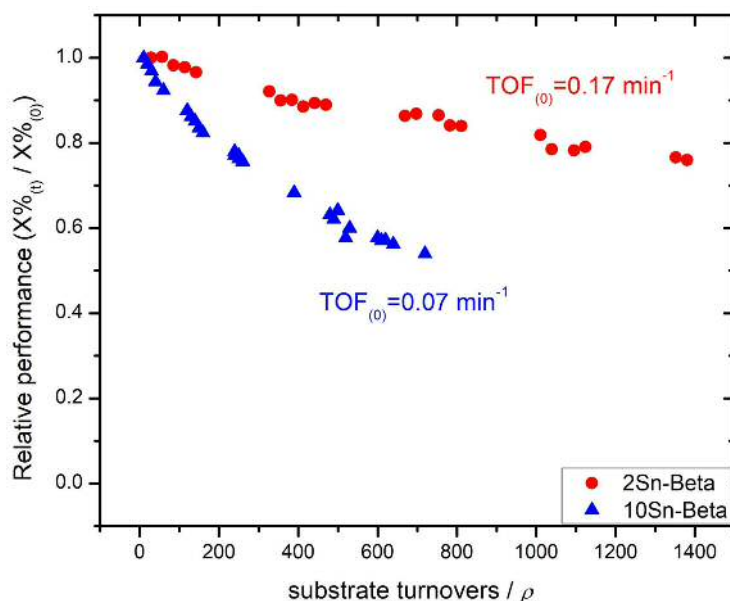


**Figure 4.** Relative performance displayed by 2- and 10Sn-Beta as a function of substrate turnover for the tandem TH/etherification reaction in continuous flow. The contact time of the two reactions was set independently in order to start from a similar level of conversion. Initial conversion of 80 and 71 % were found for 2 and 10Sn-Beta respectively.

Initial conversions of 80 % and 71 % were obtained when 2 and 10Sn-Beta were employed in the continuous flow with a contact time of 2.4 and 2.2 min, respectively. The higher initial TOF calculated when the 2Sn-Beta was used is a further confirmation that lower metal loadings lead to a higher intrinsic activity, independently from the reaction or from the modality that the reaction is carried out. Interestingly, the stability of 2Sn-Beta was also found to be higher than 10Sn-Beta. In fact, the relative performance of 2Sn-Beta, calculated at approximately 750 substrate turnovers was found to be 90 % of the initial conversion, while 10Sn-Beta, at the same numbers of FF turnovers, shows a decrease of almost half of the initial value. To gain an insight of the products distribution, and their relative evolution

during continuous operation, the selectivity of the catalyst as a function of substrate turnovers was also investigated (Figure 5).

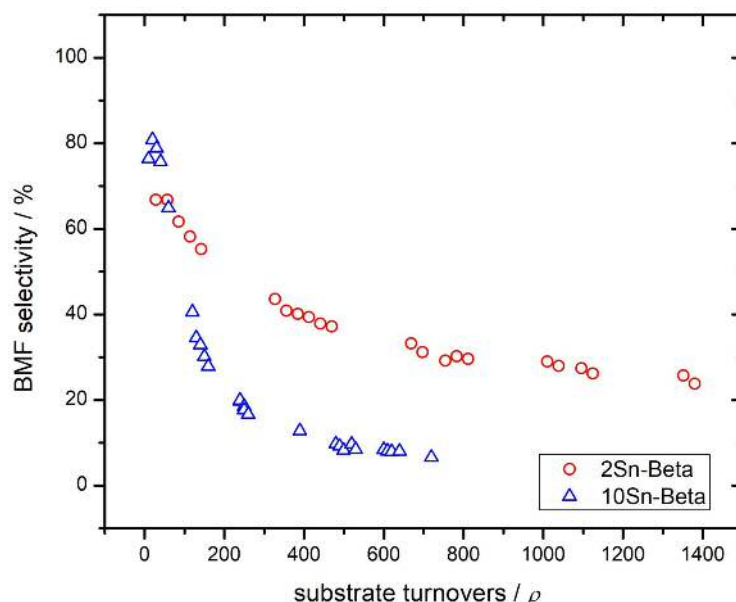


**Figure 5.** BMF selectivity displayed by 2- and 10-Sn-Beta as a function of substrate turnovers for the tandem TH/etherification reaction in continuous flow.

This clearly shows, once again, a remarkable difference in the selectivity of the two catalysts towards the ether product. Indeed, 2Sn-Beta showed a much higher degree of BMF selectivity during continuous FF valorisation. In fact, it loses half of its initial selectivity to BMF (68 %) after approximately 475 substrate turnovers. In contrast, 10Sn-Beta loses half of its initial BMF selectivity after just 120 substrate turnovers, almost four times faster than 2Sn-Beta. It is important to say that no by-products other than FA are detected, and the carbon balance stays > 95 % for the duration of the reaction. As such, these preliminary kinetic experiments confirm that 2Sn-Beta is a more active, stable and selective catalyst during tandem TH/etherification than 10Sn-Beta.

However, despite the improved performance of 2Sn-Beta for BMF production compared to 10Sn-Beta, the rapid deactivation of the etherification step, compared to the TH step, makes exploitation of this catalyst for the production of ether very challenging. Indeed, the deactivation of the etherification step is approximately five times faster than the deactivation of the initial conversion, calculated at 475 substrate turnovers. This fast deactivation of the etherification step will clearly result in a continuous process whose main

product is FA. To have a better understanding of this behaviour, the etherification step alone must be study, in order that a more suitable catalytic system for continuous BMF production can be designed.

### 5.2.2 Study of the etherification step with Lewis and Brønsted acids

To gain a better understanding of the ability of Lewis acids to catalyse the specific etherification step of the reaction, a solution of FA, instead of FF, has been reacted in 2-butanol, in order to obtain BMF. The same reaction conditions used for the tandem TH/etherification of FF to BMF in a batch reactor were applied, so that a direct comparison between the two reactions could be made. In addition to testing the two Lewis acid catalysts (2Sn-Beta and 10Sn-Beta), a de-aluminated Beta zeolite (de-Al-Beta) has also been tested for this reaction. This was done in order to verify if some silanol groups, present as a consequence of the extraction of Al during de-alumination, can make any contribution for the etherification step. The mass charge of de-aluminated Beta was the same as that of 2Sn-Beta, in order that these two catalysts could be compared directly per mass of catalyst. The kinetic data of the etherification of FA is shown in figure 6.

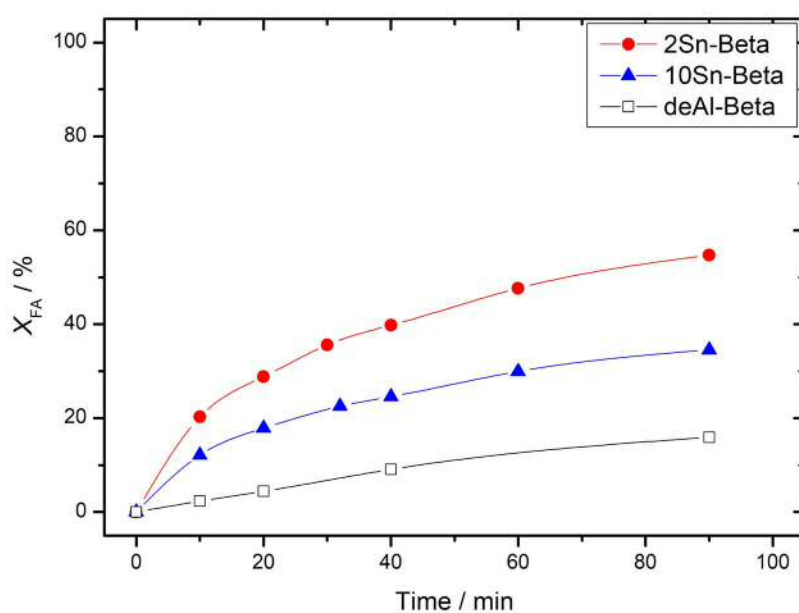


**Figure 6.** Time online plot of the FA conversion obtained with 2Sn-Beta, 10Sn-Beta and deAl-Beta in batch reactor. A solution 0.2 M solution of FA in 2-butanol have been reacted with 2 and 10Sn-Beta, at 98 °C. FA/Sn = 100; the amount of de-Al-Beta was the same 2Sn-Beta.

Both stannosilicate zeolites were able to perform efficiently the etherification of FA to BMF, with a maximum BMF yield of 53 % achieved over 2Sn-Beta over 90 minutes. In line with the data presented above, 2Sn-Beta again exhibits the highest TOF values (118 h<sup>-1</sup> versus 72 h<sup>-1</sup>

for 10Sn-Beta). Interestingly, however, it has been found that de-aluminated-Beta also possesses the ability to catalyse FA etherification, though with a lower rate than the stannosilicate system. This is an important evidence that silanol groups, present following the de-alumination protocol, can participate in the reaction. This is in good agreement to the observations of Lanzafame *et al.*,<sup>7</sup> who also observed that silanols group, present as defect sites in MFI-type silicalite, can act as active site for the etherification of HMF. It is noted here that at 2 wt. %, the Sn introduced in the framework of 2Sn-Beta is lower than the theoretical number of silanol nest that should be formed upon extraction of Al (Sn present in 2Sn-Beta occupied only the 20 % of the theoretical silanol nests created upon de-alumination). However, most of the activity of 2Sn-Beta can be attributed to the presence of Sn in the framework, as can be seen from the higher levels of conversion achieved by that catalyst at any time of the reaction.

Even though this experiment proves that Lewis acids are active for etherification reactions, it is well-known from classical organic chemistry that Brønsted acids are normally preferred as catalysts for the synthesis of ethers. Therefore, their possible employment in the reaction could bring some improvements the whole process, especially in the etherification step. The choice of type of acid that can be very wide, therefore in this work only aluminosilicate zeolites of BEA topology were employed, in order to base the evaluation purely on the effect of the active site and not also on the structure. To have an initial insight of the activity of Brønsted zeolite, a commercial H-Beta (38) with  $\text{SiO}_2/\text{Al}_2\text{O}_3 = 38$  have been reacted with FA under the same conditions. The Al/FA ratio was fixed to 100, in order to be able to directly compare the intrinsic activity of the Lewis and Brønsted acidic sites. The time online plot of FA conversion mediated by H-Beta (38) and 2Sn-Beta is displayed in figure 7.

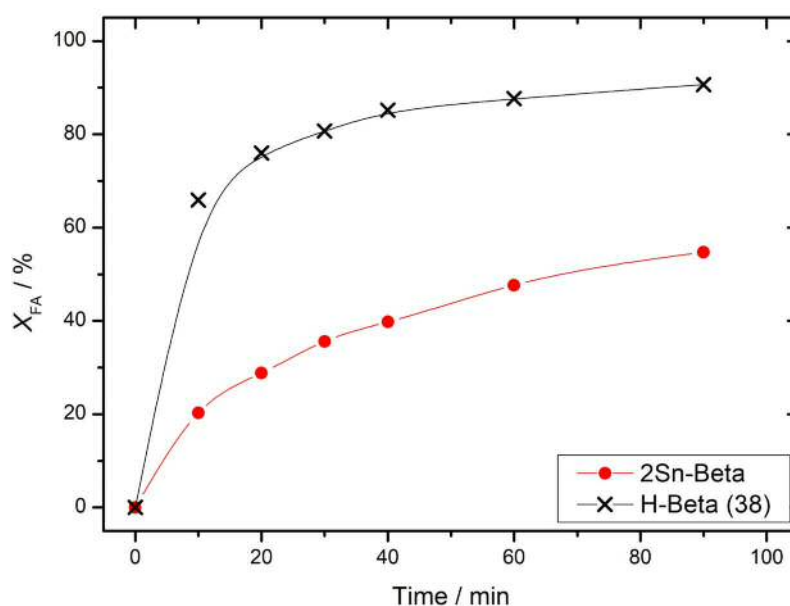


**Figure 7.** Time online plot of the FA conversion obtained with 2Sn-Beta and H-Beta in batch reactor. A 10 mL solution 0.2 M of FA in 2-butanol have been reacted at 98 °C for 90 min. FA/Sn and FA/Al molar ratio have been fixed at 100.

As can be seen from the level of FA conversion obtained for the two catalysts, the intrinsic activity of the aluminosilicate is dramatically higher than the stannosilicate material, reaching a FA conversion of 70 % in 10 min, against the 50 % obtained when 2Sn-Beta was employed over 90 minutes. Furthermore, both systems showed very similar level of selectivity of 80 % in BMF, showing that the reaction pathway is similar for both types of acidic sites. It is clear that introduction of H-Beta catalyst could be helpful for improving the etherification step of the reaction. Accordingly, different commercial H-Beta catalysts with various  $\text{SiO}_2/\text{Al}_2\text{O}_3$  ratios were tested, so that the effect of the strength of the Brønsted acid site on the FA etherification activity and BMF selectivity could be explored, in order to select the best Brønsted acid catalyst. H-Beta with  $\text{SiO}_2/\text{Al}_2\text{O}_3$  of 25 and 300 were reacted with the FA/Al kept constant at 100, FA conversion as function of time and BMF selectivity as function of FF conversion are shown in figure 8.

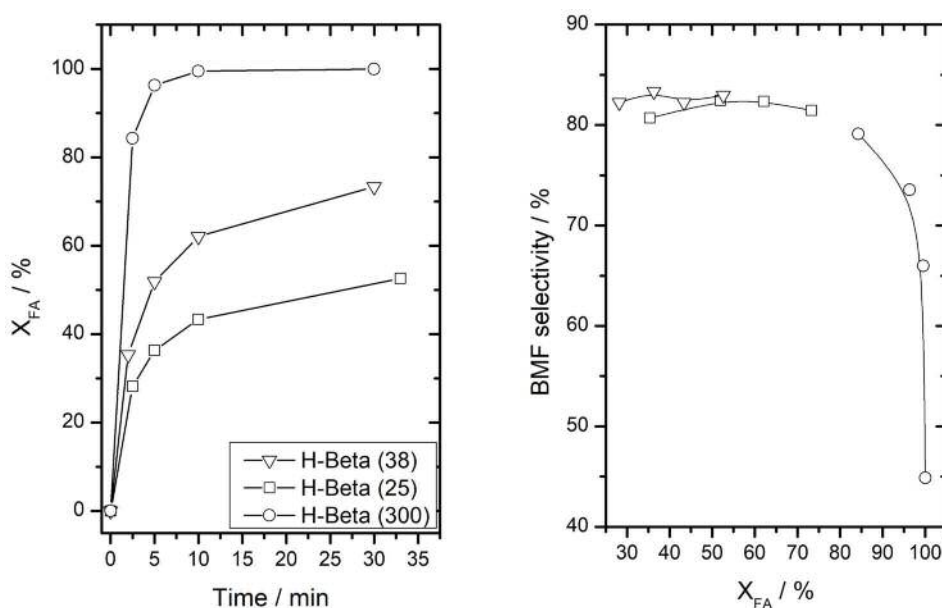


**Figure 8.** Time online plot of the (Right) FA conversion and (Left) BMF selectivity obtained with H-Beta at different Al content in batch reactor. A solution 0.2 M solution of FA in 2-butanol have been reacted at 98 °C. FA/Sn and FA/Al have been fixed at 100.

As can be seen from the conversion of FA with different H-Beta, there is a clear trend of increasing activity as the loading of Al within the zeolite decreases, even when the same moles of Al are present in each reaction. It can be immediately seen that the H-Beta (300) possess the highest intrinsic activity between all the H-Beta tested. In fact, after only 2 min

of reaction, the conversion of FA achieved is already 85 %. All the catalyst showed a very good selectivity on BMF, with value around 80 % until the conversion reached 85 %, only reached by the most active H-Beta (300) within 30 min. This indicates that the stronger Brønsted acid sites present in this material are favourable for the reaction. For H-Beta (300), it can be seen that when complete conversion is approached, the selectivity to BMF drastically decreases, specifically for FF conversion values between 95 and 98 % the BMF selectivity drastically drop to values as low as 45 %. Analysis of the reaction mixture found increasing concentration of ButLev and other products that remained unidentified. These findings strongly suggested that ButLev is formed as a consecutive ring-opening reaction of BMF as one of the possible reaction that take over at high FA conversion. Given the high activity of the H-Beta (300), a correct evaluation of the initial activity of the catalyst could not be made, since almost full conversion was reached after only 2 minutes. Therefore, in order to obtain true kinetic information, the FA etherification catalysed by H-Beta (300) was repeated with a lower amount of catalyst, in order to obtain points at lower values of conversion. The comparison is shown in figure 9.

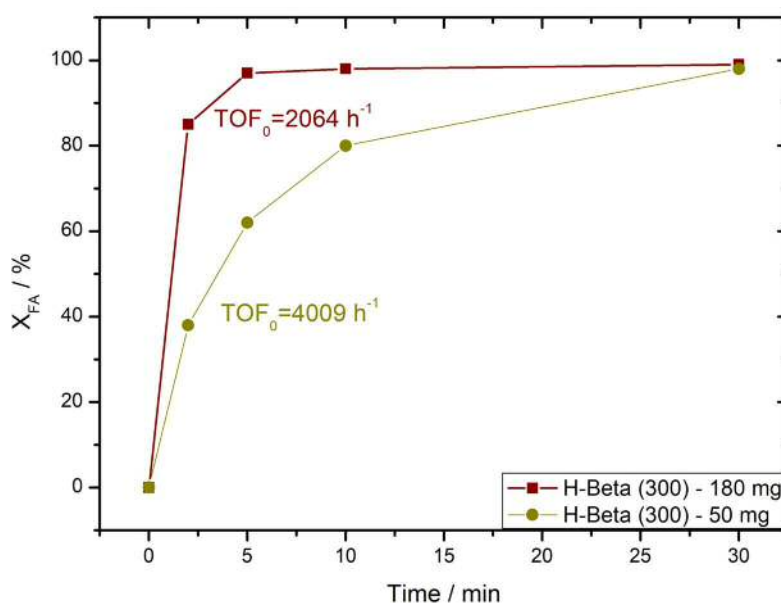


**Figure 9.** Conversion of FA to BMF as a function of time using H-Beta (300) at different mass loading. Initial TOF is displayed for the two different loadings.

As expected, decreasing the catalyst concentration to 50 mg clearly decreases the level of substrate conversion achieved. However, the decrease in conversion is not linear with the decrease in catalyst mass. As such, by normalising the activity of the catalyst per mole of  $\text{Al}^{3+}$ , it can be seen that decreasing the catalyst loading increases intrinsic reactivity dramatically, revealing a much higher TOF value (4009 vs 2064  $\text{h}^{-1}$ ). This means that at high



loadings of catalyst, transport phenomena are present, indicating the reaction to be outside the kinetic regime, and hence, underestimating the true activity of H-Beta (300).

The highest activity showed by H-Beta in the FA etherification made this catalyst a promising partner of Sn-Beta to perform a better tandem TH/etherification reaction of FF to BMF. In fact, it can be hypothesised that a tandem reaction can take benefits from the presence of a Brønsted acid, to perform the etherification in a more efficient way, while the Lewis acid site is necessary for the TH step of FF to FA. Several possibilities can be explored in order to obtain such a reactive system, in which both Lewis and Brønsted acids are present. This can be achieved in two ways: i) by using a physical mixture of Lewis and Brønsted acids and ii) by using a bifunctional catalyst, in which Lewis and Brønsted acid centre are present in the same material.

### 5.2.3 Bifunctional systems

The study of the etherification step alone showed that Brønsted acid catalysts, such as H-Beta zeolites, are more active than Lewis acid catalysts. Thus, their employment in the continuous TH/etherification reaction of FF to BMF might bring an improvement on the selectivity on BMF. As mention above, two ways to introduce the Brønsted functionality are possible, and both differs substantially.

The physical mixture is at first sight the easiest way to introduce Brønsted acidity. In fact, it can be done by simple mixing together the two materials optimised in the previous section (2Sn-Beta and H-Beta (300)). However, the FA etherification batch studies also revealed that the high activity of the aluminosilicates at high conversion level led to ring opening and other consecutive reactions, lowering the overall selectivity. Hence, caution has to be taken in choosing the right proportion between the Lewis and the Brønsted catalysts to ensure maximum activity and selectivity is achieved. Therefore, to identify the right proportion between Lewis and Brønsted acidity, a fixed amount of 2Sn-Beta was employed as catalyst, and to this a variable mass of H-Beta 300 was added. This was done to ensure that similar rates of FF conversion were obtained through TH, allowing the impact of the Brønsted acid on the ether selectivity of the reaction to be clearly understood. Specifically, three physical mixtures of [2Sn-Beta + H-Beta 300] with the composition of [120 + 30 mg], [120 + 60 mg] and [120 + 120 mg] were reacted in batch for tandem TH/etherification. Figure 10 shows the

time on line plot of the conversion as a function of time, and the selectivity to conversion dependence of the mixtures.

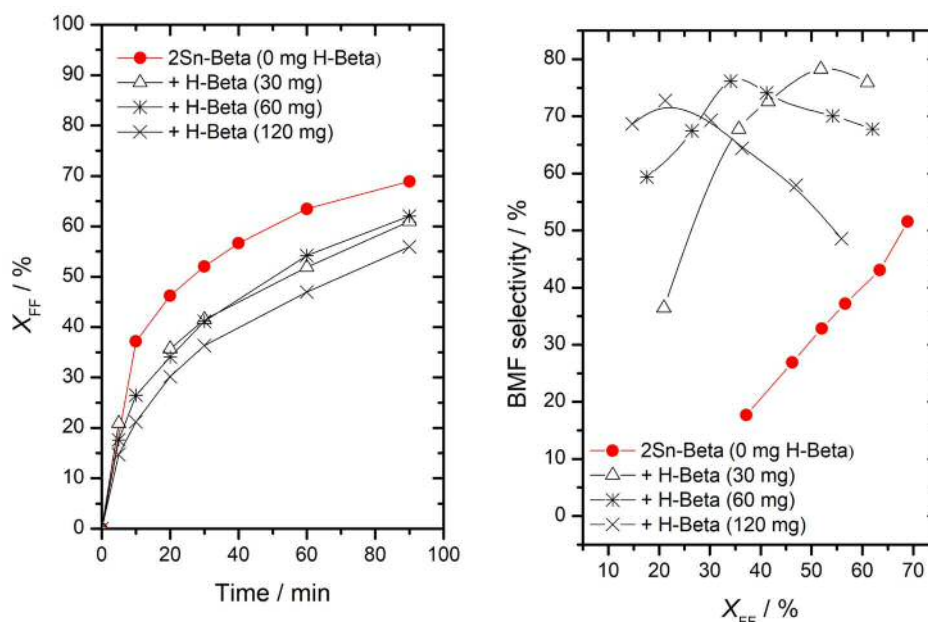


**Figure 10.** (Left) Rate of FF conversion as a function of time and (Right) BMF selectivity as a function of FF conversion, over 2Sn-Beta in the co-presence of H-Beta (300).

From the conversion vs. time plot it can be seen that none of the mixture exhibits the same rate of FF conversion. Indeed it is notable that the decrease of activity correlates with the increment of mass of H-Beta 300. Despite this decrease in activity, analysis of the BMF selectivity as function of FF conversion showed an outstanding improvement of the selectivity to BMF at almost every level of conversion. While the employment of 2Sn-Beta alone produces a linear increase of selectivity as conversion increases, in good agreement with the consecutive nature of the etherification reaction at high FF conversion, the introduction of the Brønsted acid produces a volcano plot, where the selectivity to BMF reaches a maximum at a certain level of conversion, and then decreases, likely due to the ring opening reaction. Interestingly, the position of the maximum is shifted to lower conversion value when more H-Beta is used. Since high masses of H-Beta decrease both the overall rate and BMF selectivity, it is clear that the best combination is found when the 30 mg of H-Beta is added to the Lewis acid, reaching 77 % of selectivity at 60 % of conversion. 2Sn-Beta alone, at the same level of conversion showed around 53 % of BMF selectivity. Consequently to this study, the mixture with 180 mg of 2Sn-Beta and 30 mg of H-beta (300) was chosen as optimal amount to test in the continuous flow reactor (see section 5.2.5).

#### 5.2.4 Synthesis and characterisation of bifunctional catalyst prepared by partial de-alumination method.

Alternatively to the physical mixture, a different strategy can also be followed in order to have Lewis and Brønsted acid functionality present in the system. The synthesis of a fully Lewis acidic stannosilicate requires total de-alumination of a parental zeolite prior the solid state incorporation of Sn. It is reasonable to assume that if the de-alumination is not completed, Sn can still be incorporated and a material containing both Lewis and residual Brønsted acid sites. Notably, a similar material was recently obtained by Dijkmans *et al.*,<sup>8</sup> who achieved a Lewis/Brønsted acid material by grafting  $\text{SnCl}_4 \cdot 5\text{H}_2\text{O}$  in dry isopropanol to a partially de-aluminated beta zeolite. To partially de-aluminate H-Beta (38), with an initial Al content of 2.26 wt. %, a treatment with 13 M solution of nitric acid for 1 h, instead of the conventional 20h, was done. Al elemental analysis, achieved by ICP-MS, found that the amount of metal left after the 1 h treatment was 0.16 wt. %. Since just after 1 h of treatment greater than 90 % of the initial Al was removed, no longer acid treatments were done. Following partial de-alumination, 2 wt.% of Sn was incorporated under otherwise standard conditions by SSI, and the catalyst was called [2Sn, 0.16Al]-Beta.

In order to verify the textural and acidic properties of the bifunctional material, preliminary characterisation was performed. In order to assure that the crystalline structure is preserved when Sn is inserted in the co-presence of Al, XRD analysis was done (Figure 11).

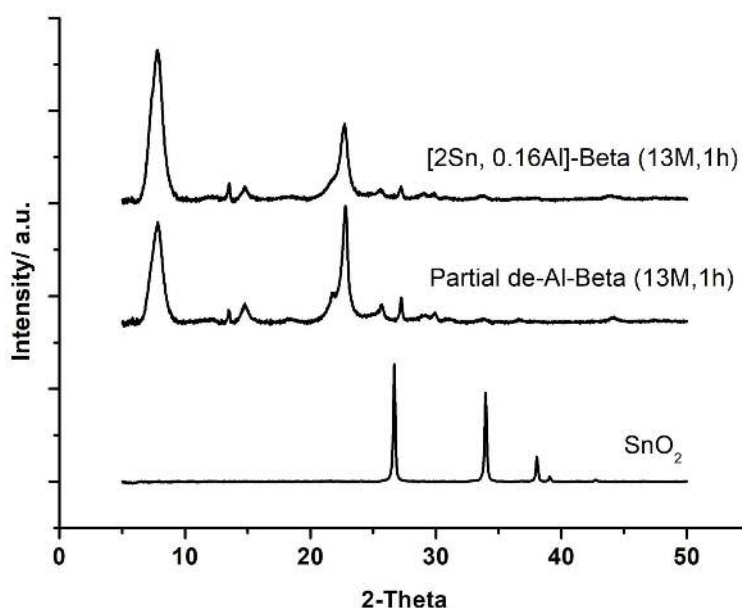


**Figure 11.** XRD patterns of zeolites treated at different conditions. The de-alumination time and concentration of the  $\text{HNO}_3$  solution are in parentheses.

When compared with the crystalline structures of Lewis acidic 2Sn-Beta and  $\text{SnO}_2$ , it is clear that the 1h partially de-aluminated material possesses the expected crystalline structure. Furthermore,  $\text{SnO}_2$  cannot be detected by XRD in all the samples, meaning that, if  $\text{SnO}_2$  is formed upon SSI in the co-presence of Al, the particles do not possess a sufficient long-range ordered structure to give birth to XRD pattern.

Even though ICP analysis confirmed that the material contains Al, the presence of this metal alone is not a sufficient condition for having Brønsted acidity. Indeed, Al needs to be tetrahedrally coordinated in the framework to act as a Brønsted acid. Otherwise, if it is present as extra-framework species, assuming six-fold coordination, it will not have any contribution at the catalysis. As such, it is important to verify that the Al present in the zeolite is still tetrahedrally incorporated in the framework, and is not present as extra-framework species, which is a likely transitory condition that can be hypothesised happening during the acid treatment, before it leaves completely the material. To verify the coordination of  $\text{Al}^{3+}$  in the 1h de-aluminated material,  $^{27}\text{Al}$  MAS NMR was run on the [2Sn, 0.16Al]-Beta and the resulting spectrum is shown in figure 12.

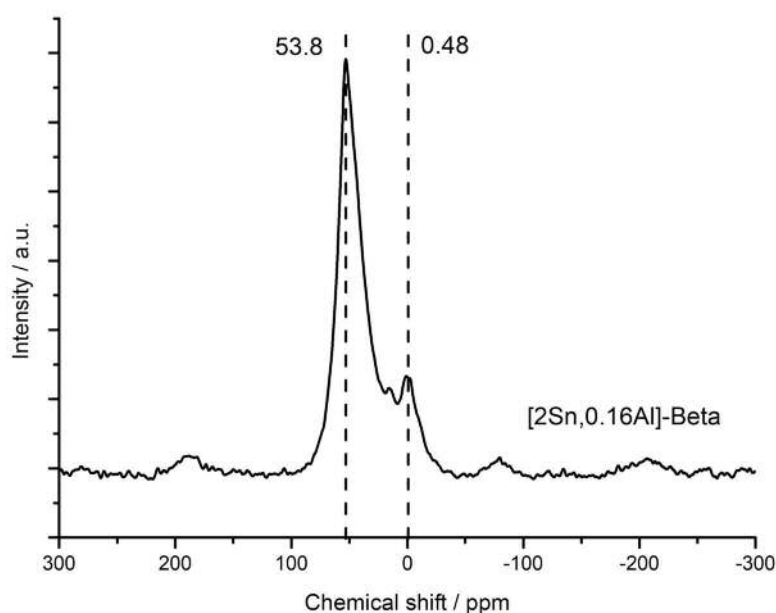


**Figure 12.**  $^{27}\text{Al}$  MAS NMR spectrum of [2Sn, 0.16Al]-Beta. Resonance of tetrahedral and octahedral species are indicated at 53.8 and 0.48 ppm respectively.

Two main resonances are found, one around 0 ppm and one around 54 ppm. The first signal is typical of octahedral Al species, generally indicative of extra-lattice species. On the other hand, the signal at 54 ppm is assigned to tetrahedral coordinated Al atom, which possess the Brønsted acidity characteristic<sup>8</sup>. This analysis confirmed that most of the Al left is still tetrahedrally incorporated in the framework, despite the acidic pre-treatment, and thus possess the right properties to give birth to Brønsted acidity, as desired for this material. It can be noticed that a small fraction of Al signal is present at 0 ppm upon de-alumination, showing that some extra-framework Al species are also present. However, it was shown by Omega *et al.* that extra-framework species were present in the H-form of Beta zeolite prior de-alumination, suggesting that the presence of extra-lattice Al species does not strictly relate with de-alumination process.<sup>9</sup>

Now that preliminary study have stated that most the Al is tetrahedrally coordinated, thus generating Brønsted acidity, it must be verified that also Lewis acidity has been introduced in the catalyst upon Sn incorporation. To do so, the adsorption/desorption of CD<sub>3</sub>CN followed by DRIFT, was performed, as shown previously in Chapter 3. If Lewis acidic species are present, a specific C-N stretching mode will be visible at around 2310 cm<sup>-1</sup>. The experiment is shown in figure 13.

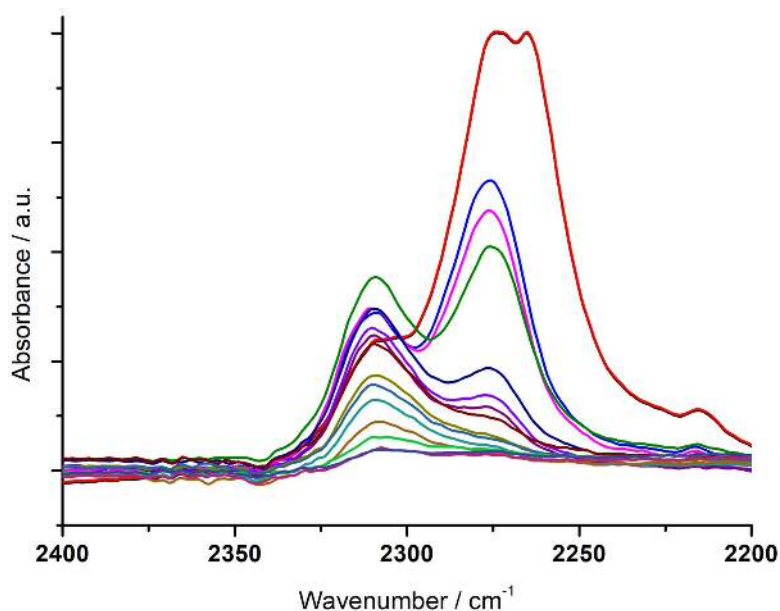


**Figure 13.** CD<sub>3</sub>CN adsorption/desorption on [2Sn,0.16Al]-Beta follow by DRIFT. Evacuation of acetonitrile is made by progressive increment of the temperature.

Figure 13 shows the desorption profile of CD<sub>3</sub>CN after its saturation over the bifunctional catalyst, [2Sn,0.16Al]-Beta. CD<sub>3</sub>CN is evacuated by increasing the DRIFT cell temperature under mild vacuum. It can be seen that just after adsorption the dominant signal is found at

ca.  $2270\text{ cm}^{-1}$ , typical of weak bonding between acetonitrile and external silanols.<sup>10</sup> However, a clear signal at approximately  $2309\text{ cm}^{-1}$  is also observed, indicative of Lewis acidic species present in the catalyst. As the temperature increases, the feature at  $2270\text{ cm}^{-1}$  decreases dramatically. However, the signal at  $2309\text{ cm}^{-1}$  stays visible even at high temperature ( $250\text{ }^{\circ}\text{C}$ ). The feature at  $2309\text{ cm}^{-1}$ , as seen previously in Chapter 3, is indicative of C-N stretching of acetonitrile molecules bonded to Lewis acid centres. The presence of this adduct even at high temperatures clearly demonstrates that the Lewis acidic species present are able to strongly coordinate Lewis bases, such as  $\text{CD}_3\text{CN}$ .

The characterisation techniques used to characterise the material obtained after SSI of Sn into partially de-aluminated Beta framework suggest that Sn and Al are both present in the lattice, hence giving genesis to both Brønsted and Lewis acidity. In order to explore the kinetic behaviour of this new material, batch kinetic experiments for the tandem TH/etherification reaction of FF were made, and the results compared to those obtained for the pure Lewis acid material 2Sn-Beta. The conversion of FF as a function of time, and BMF selectivity as a function of FF conversion, are shown in figure 14.

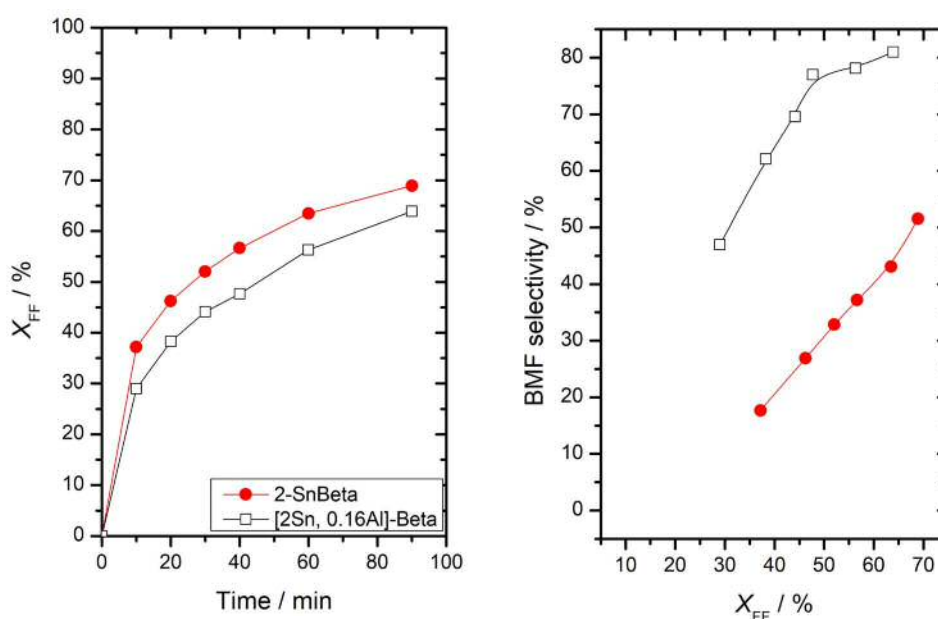


**Figure 14.** (Left) Rate of FF conversion as a function of time and (Right) BMF selectivity as a function of FF conversion, over [2Sn, 0.16Al]-Beta and 2Sn-Beta.

From the rate of FF conversion as function of time (Figure 14, Left), it can be seen that the bifunctional catalyst exhibits a lower activity compared to the fully de-aluminated analogue, which is purely Lewis acidic. This lower activity was already observed when the physical

mixture of Lewis and Brønsted material where employed. These results suggest that the co-presence of Al can somehow lead to lower performance in terms of TH activity. However, more encouraging results were found comparing the BMF selectivity as function of FF conversion. Indeed, the bifunctional catalyst showed higher selectivity to BMF than 2Sn-Beta at every level on FF conversion, reaching 80 % of BMF selectivity at 65 % FF conversion. At the same level of FF conversion, 2Sn-Beta reached only 40 % of BMF selectivity. These batch tests clearly underline the superior BMF selectivity of the bifunctional material compare to the purely Lewis acidic one, albeit at the expense of some intrinsic activity.

At this point, the two bifunctional systems catalytic systems (physical mixture and bifunctional [Sn,Al]-Beta), could be tested for the continuous tandem TH/etherification of FF to BMF, in order to see if the introduction of Brønsted acidity can bring benefits in term of selectivity and stability of the BMF product.

### 5.2.5 Continuous performances of physical mixture and bifunctional catalyst

To determine the continuous performance of the two bifunctional systems, continuous flow experiments of the tandem TH/etherification of FF were carried out under the same conditions employed for the purely Lewis acid system (5.2.1). Due to the complexity that two consecutive reactions bring to the system, the analysis of TH and etherification step will be done in separate sections for the sake of clarity. Figure 15 shows the relative performance of the catalysts in terms of conversion, as function of substrate turnovers, for the three systems (2Sn-Beta, and both bifunctional catalytic systems)

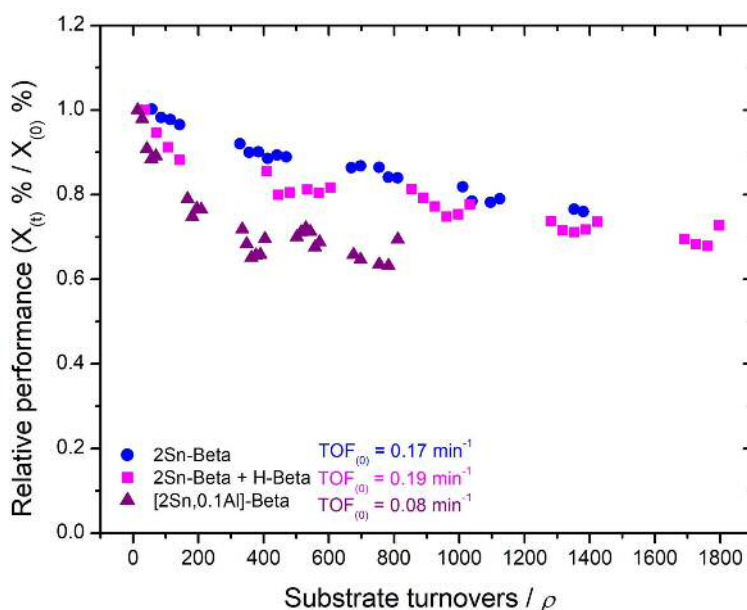


**Figure 15.** Relative performance displayed by 2-Sn-Beta, 2-Sn-Beta/H-Beta and [2Sn,0.16Al]-Beta as a function of substrate turnovers. Contact time of the systems are set in order to start from a similar value of conversion between 80 and 70 %.

The contact time of the system was varied in order to start in a similar range of conversion, between 80 and 70 %. Since the differences in the contact time, evaluation of the performance in terms of substrate turnovers instead of time on stream have been made (*Vide Supra*). From the value of the initial TOF calculated for the three systems, it is immediately evident that the physical mixture (2Sn-Beta + H-Beta) and the Lewis acid alone (2Sn-Beta) showed an almost identical initial activity, with TOF values of 0.19 and 0.17 min<sup>-1</sup> respectively. Surprisingly, the initial TOF of the [2Sn, 0.16Al]-Beta was found to be 0.08 min<sup>-1</sup>, ca. 50 % less than that of 2Sn-Beta. Even though a lower activity compared to 2Sn-Beta was observed in the batch reaction, the difference observed in the continuous flow is more remarked. All the systems exhibited a relatively stable performance in terms of conversion, which reflects the stability of the TH step. While the decrease in relative performance of the physical mixture and 2Sn-Beta were almost identical (20 % of initial activity lost after 800 substrate turnovers), [2Sn, 0.16Al]-Beta experienced a slightly larger extent of deactivation with a loss of 40 % activity observed after 800 substrate turnovers. Despite the differences in activity (as TOF), the three systems show a relatively good stability for the TH step of the tandem reaction.

Analysis of the stability of the etherification step is done by plotting the BMF selectivity as a function of the number of substrate turnovers, as shown in figure 16. The analysis of the two bifunctional systems revealed a completely different behaviour. On one side, the physical mixture system showed that, similarly to the 2Sn-Beta-only system, BMF selectivity could not be retained during continuous operation. Indeed, after 800 substrate turnovers, the BMF selectivity dropped from 75 to 35 %. On the other hand, the [2Sn, 0.16Al]-Beta showed an exceptionally stable etherification step. Indeed, after 800 substrate turnovers, the BMF selectivity is still around 75 %, showing a remarkable difference with the two other systems studied. In all cases, the decrease in BMF selectivity was compensated for by FA production, and only traces (between 0 – 1 mol. % of yield) of ButLev could be found, maintaining the carbon balance over 95 % in all the three systems. Having Al and Sn in the same material, or having them confined in two different phases, clearly impacts dramatically the stability of the etherification step.



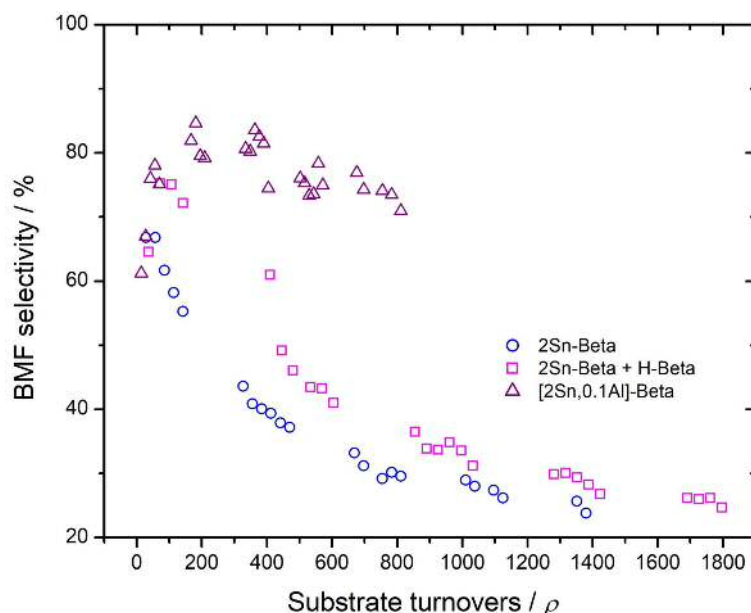


**Figure 16.** BMF selectivity displayed by 2-Sn-Beta, 2-Sn-Beta/H-Beta and [2Sn,0.16Al]-Beta as a function of substrate turnover.

To elucidate if the rapid deactivation of the etherification step observed with the physical mixture was due to the poor stability of H-Beta (300) itself during continuous operations, the stability of this catalyst for the etherification step alone was studied in the continuous flow reactor. To mimic the conditions observed during the tandem TH/etherification reaction with the physical mixture catalytic system, the amount of H-Beta (300) was kept the same, but the concentration of FA in the feed was based on the concentration of FA expected as a product at 80 % of FF conversion, in order to have the same initial molar ratio of FA and Al atoms present in the first part of the reaction. The conversion as function of time on stream is shown in Figure 17. It is clear that severe deactivation is experienced by H-Beta (300) during continuous etherification. Indeed, the initial high conversion and yield rapidly dropped and within 24 h the catalyst has already lost almost its initial activity. It is therefore unsurprising that in the physical mixture, no benefits are found in term of selectivity after approximately 24 h on stream, given that H-Beta (300) loses almost its entire activity in the very first part of the continuous reaction. The rapid loss of activity in this range of time

seems to match well with the observed loss of BMF selectivity exhibited by the physical mixture system during the first 24 h.

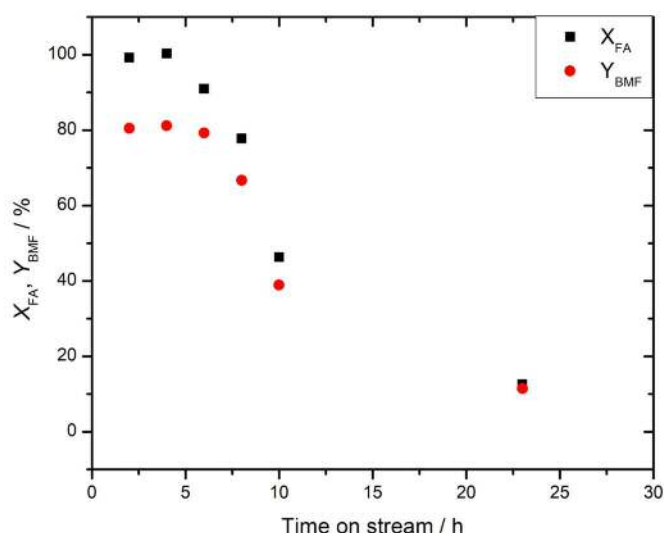


**Figure 17.** Conversion vs. time on stream of H-Beta (300) during continuous FA etherification under the same conditions used during the tandem TH/etherification reaction.

### 5.2.6 Identifying deactivation of the etherification step during bifunctional continuous catalysis

From the continuous kinetic performance of the three systems analysed it appears clear that the TH step (identifiable by conversion per time on stream) does not deactivate much, with only a 15 % of decrease in the case of 2Sn-Beta and the physical mixture, while 35 % of decrease was observed with [2Sn, 0.16Al]-Beta. However, a fast and extended deactivation of the etherification step was observed for 2Sn-Beta alone and the physical mixture system, where a decrease of BMF production of some 50 % was observed in both cases, while in the case of the bifunctional catalyst made by SSI of Sn into a partially de-aluminated zeolite almost no loss of BMF selectivity was observed after the same substrate turnovers, thus showing a very stable etherification step.

To determine the causes of deactivation for the etherification step, TGA measurements on the used samples were performed. As observed in Chapter 4, TGA was able to give strong indication about product adsorption and deposition on the catalyst, which has been proven to greatly contribute to pore fouling and lead to the deactivation of the catalyst during TH of

CyO to CyOH. In figure 18, the derivative of the TGA profile of fresh [2Sn, 0.16Al]-Beta, used [2Sn, 0.16Al]-Beta, the used physical mixture (2Sn-Beta + H-Beta (300)) and used H-Beta (300) are presented.

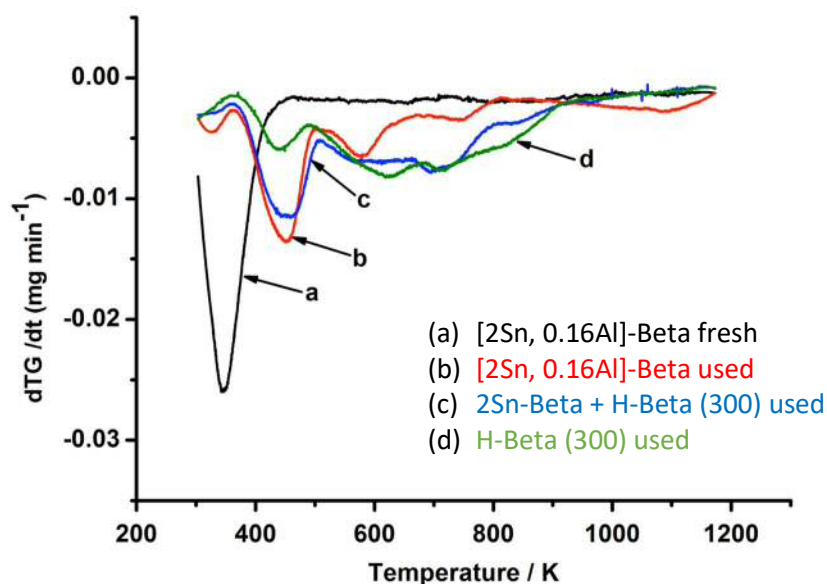


**Figure 18.** Derivative of the TGA of different used catalyst and a fresh sample as function of temperature. RGA were performing on ca. 50 mg of materials. Data have been recorded in a temperature range of 30 - 900 °C and under air flow (30 mL min<sup>-1</sup>). A ramp rate of 5 °C min<sup>-1</sup> have been employed.

The fresh catalyst shows only a mass loss around 70 °C, which can be attributed to adsorbed moisture on the catalyst. A second mass loss is present around 180 °C for all the three used samples and it is not found in the fresh one. Since it is common to the three samples it can be suggested that it might arise from strongly adsorbed solvent or from adsorbed FF, FA and/or BMF, as these are the compounds that are common to the three systems. Substantial differences between the used samples start to be observed at higher temperature. In fact, used [2Sn, 0.16Al]-Beta showed only two minor mass losses at 300 and 480 °C. On the other hand, both the physical mixture and H-Beta (300) showed a quite similar and broad mass loss, covering a temperature range from 300 to 650 °C, which is clearly composed of many substance desorbing at different temperatures. It has to be noticed that this broad accumulation of mass loss is present in the two samples that contain H-Beta 300 (alone and in a mixture with Sn-Beta), while it is not seen when the [2Sn, 0.16Al]-Beta is used. This suggests that the presence of H-Beta (300) leads to formation and accumulation of a wide range of high temperature desorbing compounds. Noticeably, this effect is even more

dramatic for the H-Beta (300) alone, in fact the reaction time was only of 24 h, and the intensity of the broad mass loss observed is found almost at the same of the one in the physical mixture, which has run for a much longer time of reaction (100 h). The nature of this product is unknown, but FA is known to be susceptible to polymerisation in the presence of Brønsted acid species, and these long chain products might lead to deactivation. It can be possible to see a correlation between this broad mass loss present only in the H-Beta (300) and in the physical mixture and their rapid deactivation of the etherification step. Accordingly, in the [2Sn, 0.16Al]-Beta that does not show extensive deactivation of the etherification step, also it does not possess that broad mass loss feature between 300 and 650 °C.

From the TGA it seems that the presence of H-Beta (300) promote the formation of high molecular weight species, that can likely lead to deactivation of the etherification step specifically. On the other hand, having Sn and Al present in the same framework seems to mitigate this effect, resulting in a more stable etherification step. If this is the case, it means that having H-Beta in the system will not allow a continuous TH/etherification process to be performed without the extensive use of regeneration procedures. Therefore, the possibility of performing continuous tandem reactions with physical mixtures of two different materials seems not to be a practicable route. Consequently, more efforts will be put on designing a better Sn and Al containing material that has been proved promising for achieving high selectivity in BMF.

### 5.2.7 Investigation of the lower activity of the bifunctional catalyst

From the kinetic studies presented above, and the characterisation studies of the used catalytic beds, it is clear that having the two functionalities present in the same material is the only way to permit the continuous tandem TH/etherification of FF to BMF without the need of numerous regeneration cycles. The employment of the partial de-aluminated Sn-Beta led to a dramatic improvement of the BMF selectivity, which was one of the targets of this work. However, this clearly occurs at the expense of TH activity, which is obviously important when parameters like productivity or STY become central. Even though preliminary analysis with Lewis acidic probe (see section 5.2.4) showed that Lewis acidity was developed upon the insertion of Sn, it is clear from the kinetic data (particularly the lower initial TOF) that those sites do not shown the expected high activity. To elucidate the

reason behind the lower levels of Lewis acidity of this material, more characterisation focused on the Sn sites were carried out in order.

XRD analysis showed that the structure of the partial de-aluminated zeolite was intact (see section 5.2.4), therefore a subtler effect must account for the lower activity of this catalyst. Since the dominant effect is in terms of activity (hence conversion), a major focus on the Sn sites has been made by investigation with  $^{119}\text{Sn}$  MAS NMR. The spectrum of the bifunctional catalyst, in addition to reference spectra of  $\text{SnO}_2$  and a conventional 2Sn-Beta, are displayed for comparison in figure 19.

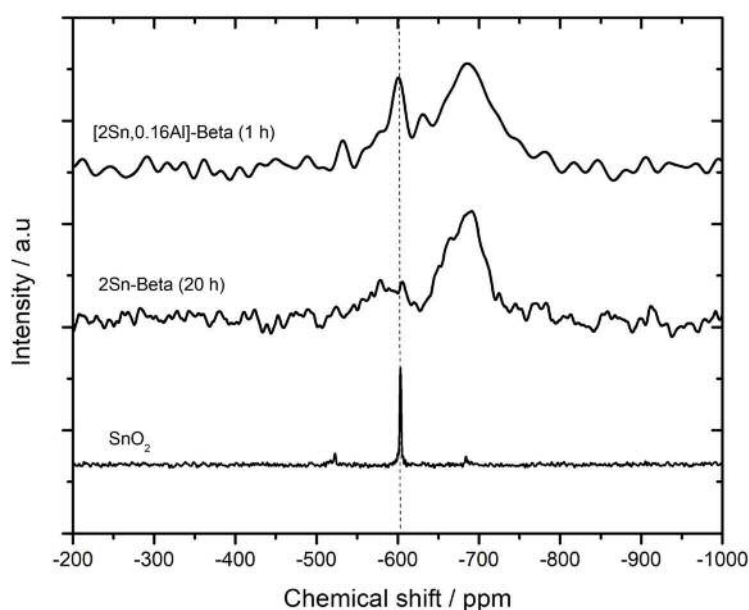


**Figure 19.**  $^{119}\text{Sn}$  MAS NMR spectra of bifunctional [2Sn, 0.16 Al]-Beta and 2Sn-Beta and reference  $\text{SnO}_2$ . Each zeolite contains 2 wt. % Sn, and the time of de-alumination for each sample is added in parenthesis.

The spectra show a clear correlation between time of de-alumination and an increasing ratio of extra-framework/framework Sn signals, respectively at -602 and -688 ppm. Indeed, the quantity of  $\text{SnO}_2$  observed clearly increases when residual  $\text{Al}^{3+}$  species remain in the framework. This strongly suggests that the higher is the amount of Al left in the framework, the harder is to incorporate Sn in the framework, and bigger amount of inactive extra-framework Sn is formed. This observation is in perfect agreement with the lower initial activity of the catalyst. However, the higher selectivity experienced when both Al and Sn are present prompt to search for an alternative way to make a bifunctional material.

### 5.2.8 Solid state incorporation of Al and Sn into a fully de-aluminated zeolite

The low activity of the partial de-aluminated Sn-Beta was believed to arise from the difficulties to insert Sn into the Beta framework when Al was already present in the structure. To avoid this issue, it has hypothesised that both Al and Sn could be re-inserted into a fully de-aluminated beta zeolite by using the SSI method. Omegna *et al.* previously showed that re-incorporation of Al into a de-aluminated Beta framework is possible, although in that case the re-metallation was carried out by stirring the de-aluminated material in a solution of Al isopropoxide in dry hexane.<sup>9</sup> In this work, SSI has been used to incorporate the two metals in the framework. As solid precursors, Sn(II)acetate and Al(III)acetyl acetonate have been used, and the synthesis followed the same procedure that has been used and extensively described in Chapter 2 (section 2.1). An initial bifunctional catalyst, with Sn and Al loadings of 2 and 0.5 wt. % respectively, was made. The material is henceforth named [2Sn, 0.5Al]-Beta.

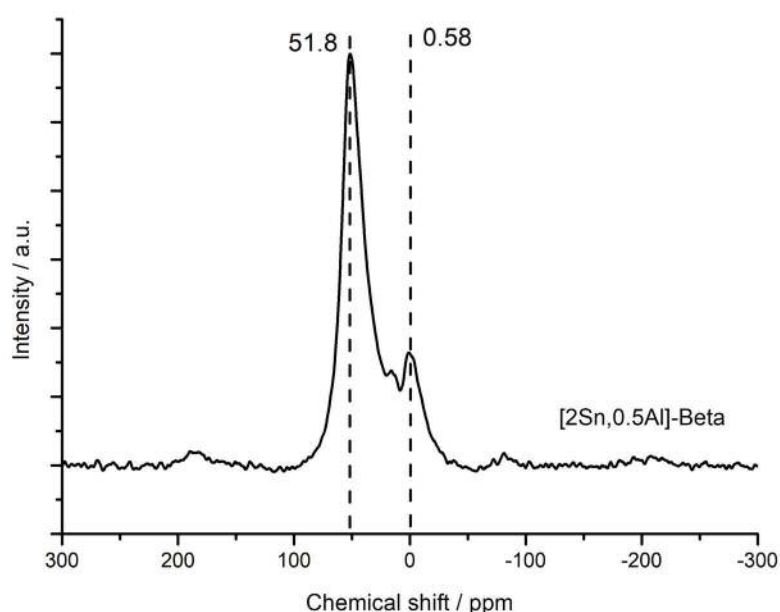


**Figure 20.**  $^{27}\text{Al}$  MAS NMR spectrum of [2Sn, 0.5Al]-Beta. Resonance of tetrahedral and octahedral species are indicated at 51.8 and 0.58 ppm respectively.

In order to verify that the Al was tetrahedrally incorporated in the framework after SSI,  $^{27}\text{Al}$  MAS NMR was carried out, as displayed in figure 20. The intense signal at 51.8 ppm is indicative of tetrahedrally incorporated Al species, while a much less intense signal at 0 ppm indicates the presence of some octahedral Al species, showing that reincorporation of Al can be achieved by SSI.

To prove that both Lewis and Brønsted acids were present in the catalyst following double metallation, pyridine desorption experiment followed by DRIFT spectroscopy were carried out. This experiment was performed in a similar way of the  $\text{CD}_3\text{CN}$  desorption, but with pyridine as probe molecule. Pyridine is a useful molecule able to probe both Lewis and Brønsted acid sites at once. In fact, it is able to interact differently with the two sites, giving birth to distinct vibrations, characteristic of each functionality. In figure 21, the desorption DRIFT spectra of pyridine at different temperatures is displayed.

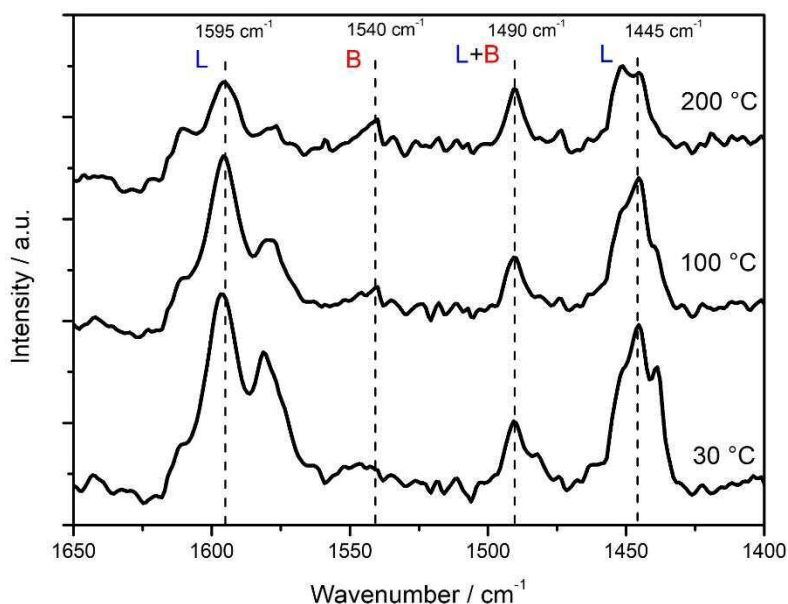


**Figure 21.** DRIFT studies of  $[2\text{Sn}, 0.5\text{Al}]\text{-Beta}$  with pyridine as probe molecule. Pyridine have been adsorbed at room temperature until saturation. Following adsorption the system have been evacuated under vacuum and by stepwise increment of the temperature. Vibrational feature of the pyridine interacting with Sn-Beta at different temperature are show in the figure and are indicated by L if deriving from interaction with Lewis acid sites and by B if the site of interaction is Brønsted.

Interpretation of pyridine adsorption is exhaustively presented in the literature and examples of its use to probe the acidic properties of Sn-Beta catalysts are also known.<sup>11</sup> An absorption band and 1540  $\text{cm}^{-1}$  corresponds to Brønsted sites and it arises from a protonated pyridine molecule. It can be seen that this feature, despite being low in intensity, is well visible at increasing temperature. On the other hand, the bands found at 1595 and 1445  $\text{cm}^{-1}$  correspond uniquely to the interaction between pyridine and Lewis acid sites, thus indicating the Lewis character of the material. It can be noticed also a band is present at 1490  $\text{cm}^{-1}$ , this particular band can be either associated to a protonated pyridine and also to an adduct with a Lewis site, not playing a crucial role in order to assign the type of site. This

technique clearly shows that the material, as synthesised, possess both Lewis and Brønsted acid characteristic. Following this preliminary characterisation, the catalyst has been tested for the continuous tandem TH/etherification of FF, in order to prove if this new synthetic route is able to produce an effective bifunctional catalyst.

### 5.2.9 Continuous performance of [2Sn, 0.5Al]-Beta

In order to verify if the bifunctional catalyst [2Sn, 0.5Al]-Beta, made by SSI of Sn and Al, is able to performed an improved FF to BMF process, the reaction have been performed in the continuous flow system under the same experimental condition at which the 2Sn-Beta catalyst have been run. The relative performance of the catalyst as function of substrate turnover is shown in figure 22. For comparison, the relative performance of 2Sn-Beta over a similar range of substrate turnovers is also presented.

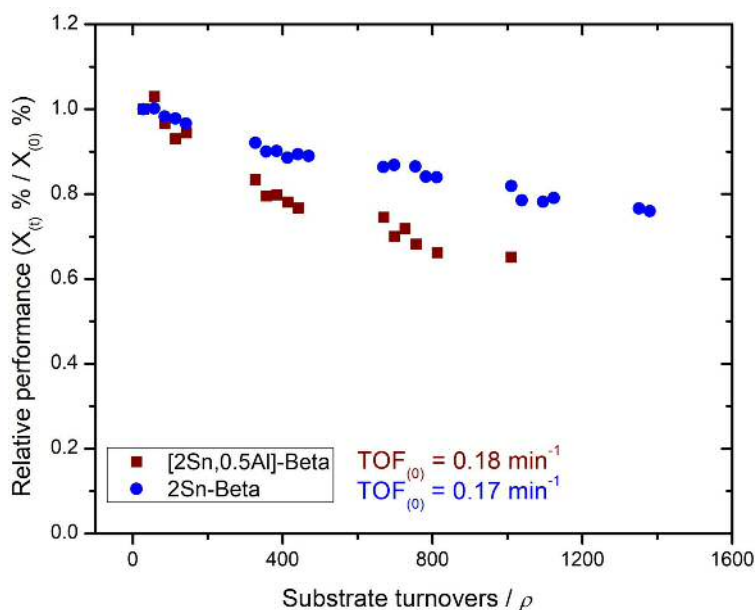


**Figure 22.** Relative performance as function of substrate turnovers displayed by 2Sn-Beta and [2Sn,0.5Al]-Beta. Contact time of the two reaction have been set in order to start from an initial conversion of 75 %.

Starting from a conversion around 75 % in both cases, the activity of the bifunctional catalyst was found to be almost the same of the 2Sn-Beta. Accordingly, a TOF value of  $0.18 \text{ min}^{-1}$  compared the  $0.17 \text{ min}^{-1}$  of the original 2Sn-Beta was calculated. This is an indication that



this methodology, where Sn and Al are incorporated together into a fully de-aluminated framework, allows a more efficient insertion of the Sn, probably resulting in less formation of extra-framework species. The new bifunctional material showed also good TH stability, with a decrease of 35 % of its initial performance after 1000 substrate turnover. At the same numbers of turnovers the fully Lewis acidic 2Sn-Beta showed a lower decrease in relative performance, with a value of the 20 %, suggesting that the presence of Al can somehow accelerate the deactivation of the TH step. In order to evaluate the stability of the etherification step, BMF selectivity as function of substrate turnover have been plotted, and the two systems, bifunctional and only-Lewis acid, have been compared in figure 23.

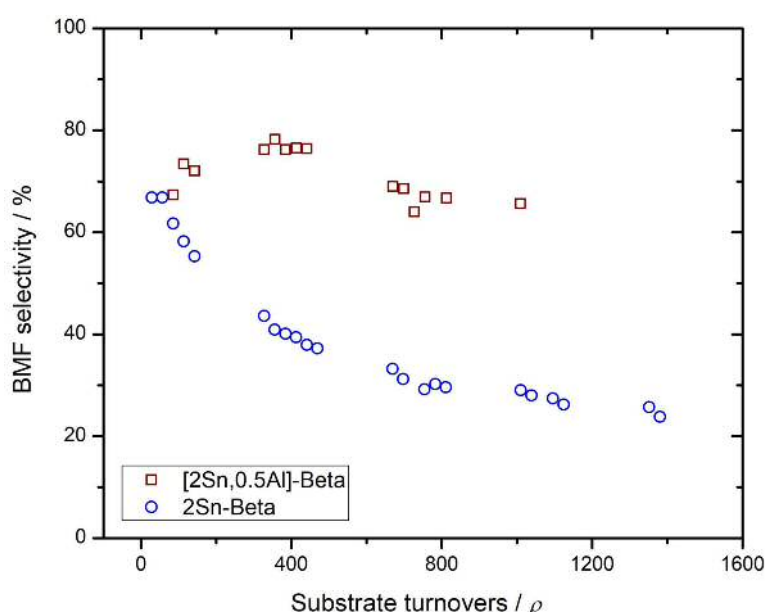


**Figure 23.** Relative performance as function of substrate turnovers displayed by 2Sn-Beta and [2Sn,0.5Al]-Beta.

In addition to high activity for the TH step, this catalyst showed a comparable BMF selectivity to the partial de-aluminated Sn-Beta material ([2Sn,0.16Al]-Beta), even at higher substrate turnovers. Indeed, it can be seen from the plot that the BMF selectivity is still at 70 % after around 1000 substrate turnovers (equivalent to 3 days of reaction). This clearly showed that not only is Sn efficiently inserted in the framework, but also Al showed high activity and selectivity, as shown by the excellent stability of the etherification step. Following these results, that clearly indicate the suitability of this material for tandem TH/reaction of FF to BMF, intensification of the process were attempted in order to optimised the productivity and extend further the lifetime of the catalyst.

### 5.2.10 Optimisation of the reaction conditions

In order to increase the production of BMF, optimisation of the reaction conditions has been attempted by increasing the operating temperature from 100 to 120 °C. As such, the relative performance as function of substrate turnovers of the systems at 100 and 120 are compared in figure 24. As a consequence of the enhancement of the rate of reaction, the flow rate has been increased in order to start from a similar initial conversion (70 %). This led to a substantial increase in TOF, which increased from 0.18 min<sup>-1</sup> (at 100 °C), to 0.33 min<sup>-1</sup> at 120 °C. Moreover, increasing the temperature of the reaction did not negatively effect the stability of the catalyst for either step (TH or etherification). Indeed, the reaction could run for 2300 substrate turnovers maintaining 60 % of its initial activity.

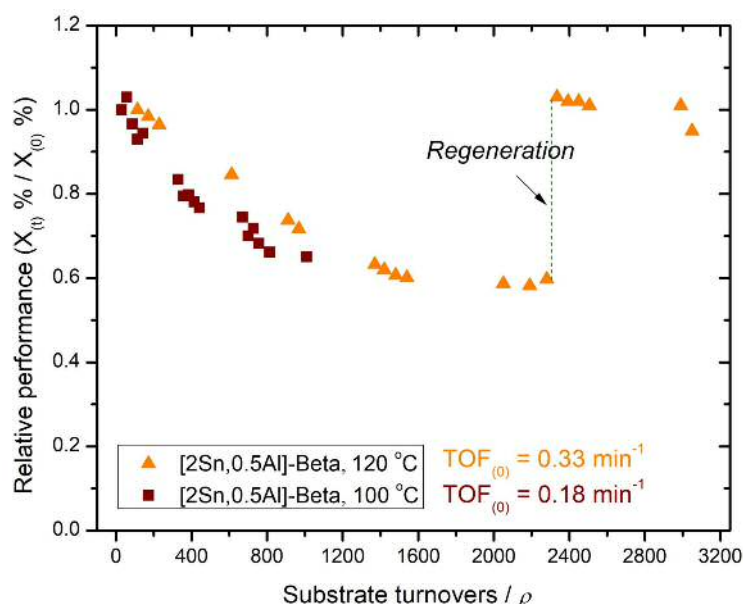


**Figure 24.** Relative performance displayed by [2Sn,0.5Al]-Beta at 100 and 120 °C as a function of substrate turnovers. Contact time of the two reaction has been adjusted in order to start from a similar level of conversion, specifically 75 and 70 % for the systems at 100 and 120 °C respectively. Thermal regeneration of the reactor performing the reaction at 120 °C has been done after 2300 substrate turnovers.

After that point, regeneration of the catalyst was carried out by heating the reactor at 550 °C for 3 h in air. Upon regeneration, a full recovery of the initial activity was observed, suggesting a reversible nature of the mechanism of deactivation. The increase of temperature from 100 to 120 °C clearly showed to have a beneficial effect on the TH step, showing an almost two fold higher intrinsic activity and a comparable stability over the reaction period. Follow these findings, BMF selectivity was calculated as function of

substrate turnovers to investigate how the increase of the temperature could affect the etherification step and the comparison with the system at 100 °C is shown in figure 25.

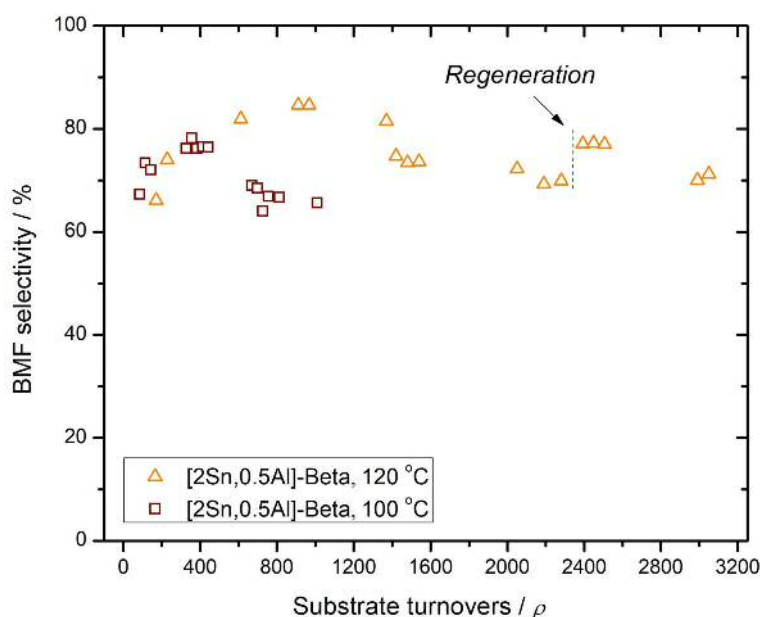


**Figure 25.** BMF selectivity displayed by [2Sn,0.5Al]-Beta at 100 and 120 °C as a function of substrate turnovers. After thermal regeneration (2300 substrate turnovers) no loss of BMF selectivity was detected.

With temperature increased from 100 to 120 °C it can be observed that an even better BMF selectivity could be obtained. In fact, BMF selectivity levels approaching 85 % of were detected at 1000 substrate turnovers, while the maximum selectivity calculated for the system at 100 °C was around 80 % at 400 substrate turnovers. Additionally, very good stability of the etherification step was observed, with BMF selectivity of 70 % after 2300 substrate turnovers. High selectivity (80 %) was also retained after thermal regeneration. Analysis of the reaction mixture found FA to be the main by-product (with selectivity between 35 and 15 %) throughout all the reaction periods, while only small amounts of ButLev were produced, with yields no higher than 1 %. To prove the high selectivity of the catalyst, the calculated carbon balance was found to be above 95 % all the time. The improved selectivity and activity of the bifunctional catalyst at 120 °C led to double the STY

compared to the value obtained at 100 °C, making this catalyst a promising candidate for tandem TH/etherification reactions of biomass substrate.

### 5.2.11 Pore volume analysis of used catalyst

Although dramatic improvements in activity (TOF) and selectivity are achieved at 120 °C, some deactivation is still prevalent. Indeed, after 2300 substrate turnovers, the conversion dropped to approximately 60 % of the initial value. To investigate the possible cause of deactivation, surface area and porosimetry analysis were carried out and showed in Table 1.

**Table 1.** Porosimetry data of fresh, used and regenerated of [2Sn, 0.5Al]-Beta catalyst. Brunnet-Emmett-Teller surface area calculated from BET method, and total pore volume.

Catalyst	BET area (m <sup>2</sup> g <sup>-1</sup> )	Total pore volume (cm <sup>3</sup> g <sup>-1</sup> )
[2Sn, 0.5Al]-Beta / SiC fresh	112	0.049
[2Sn, 0.5Al]-Beta/SiC used	53.4	0.022
[2Sn, 0.5Al]-Beta/SiC regenerated	93.5	0.043

As evidenced in Table 1, after 2300 substrate turnovers the surface area and pore volume decreased of the 43 and 49 % respectively, suggesting that once again, fouling can lead to the deactivation of this material. Following the same regeneration procedure employed in Chapter 4 (550 °C, 3 h, air), the catalyst shows to be able to be regenerated and recover full activity. Furthermore, after regeneration, the initial surface area and pore volume were almost completely recovered, strongly suggesting that deactivation of the material, also in this system, is caused mainly by fouling.

## 5.3 Conclusions

In this chapter, a more complicated reaction network has been investigated with the Sn-Beta catalyst. In fact, the TH of furfural it has been shown to introduce many more challenges respect the simple TH of cyclohexanone. Whereas in the previous chapter only the activity of the catalyst was considered, a more functionalised substrate like furfural can lead to multiple products. On one hand this represents an opportunity because of the bigger pool of useful products obtainable from one molecule. On the other hand, the selective production of a specific target molecule is hard to achieve. It has also been shown that when two or

more reactive step are present, they might have different level of stability during continuous operation, then strategies to favouring one respect to another had to developed. Normally, two approaches are possible in order to select the desire reaction: changing the operational condition, or introducing new kind of reactivity. In this chapter, it has been shown that the etherification step is carried out more efficiently by Brønsted acid catalyst, whilst the Lewis acidity accounts mainly for the TH step of the reaction. Therefore, two bifunctional systems have been studied: physical mixture of Sn-Beta and H-Beta, and bimetallic zeolite containing both Lewis and Brønsted acids. The second approach resulted in a more efficient catalytic system, even though the activity of the material was strongly affected by the type of synthesis of the material. At the end, SSI of Al and Sn into a fully de-aluminated zeolite demonstrated to be the most efficient way to obtain a catalyst able to perform continuous tandem TH/etherification reaction with high selectivity and stability to the ether product. The best result was obtained using [2Sn, 0.5Al]-Beta, prepared by SSI, which exhibited an initial TOF of  $0.33 \text{ min}^{-1}$ , and a selectivity greater than 80 % to BMF over 2500 of substrate turnovers. This result has no precedent in literature and for the first time it has been shown that continuous production of biomass-derived ether substrates can be achieved at high substrate turnovers in organic media.

Even though remarkable results have been achieved in this study, this system still has scope for improvements. For example, some parameters of the synthesis of the bifunctional catalyst have not be fully explored, such as how the ratio of Sn and Al affect the performance and stability of the system and their optimisation could led to an even more favourable production of the ether.

However, most of the bio based platform molecules are derived from biomass feedstock. For example, furfural is obtained from hydrolysis and dehydration of hemicellulose. In almost all of the cases, water is used as reaction solvent. It appears clear now that the ability to operate in the presence of water become a strong requisition. Even more desirable would be to operate having water as reaction solvent, that ideally would allow to perform the process starting from the raw material to the final platform molecule.

So far, it has been shown that Sn-Beta is stable and very active for reactions carried out in organic media. However, it was shown in chapter 3 that one of the strongest point of Sn-Beta is its ability of performing TH reaction with water as solvent, indicated by the glucose isomerisation reaction to make fructose. However, no information about the stability of such processes are available yet. Therefore, in the next chapter the challenge of continuous

glucose isomerisation will be tackled, as this represents an important reaction where the presence of water is likely to play a critical role.

## References

- 
- <sup>1</sup> V. Choudhary, A. B. P. Stanley, I. Sandler, D. G. Vlachos, R. F. Lobo., *ACS Catal.*, 2011, **1**, 1724.
  - <sup>2</sup> J. M. R. Gallo, D. M. Alonso, M. A. Mellmer, J. H. Yeap, H. C. Wong, J. A. Dumesic, *Top Catal.*, **56**, 1775.
  - <sup>3</sup> L. Bui, H. Luo, W. R. Gunther, Y. Roman-Leshkov, *Angew. Chem. Int. Ed.*, 2013, **52**, 8022.
  - <sup>4</sup> A. Corma, M. Renz, *Angew. Chem. Int. Ed.*, 2007, **46**, 298.
  - <sup>5</sup> J. D. Lewis, S. Van der Vyver, A. J. Crisci, W. R. Gunther, V. K. Michaelis, R. G. Griffin, Y. Román-Leshkov, *ChemSusChem*, 2014, **7**, 2255.
  - <sup>6</sup> C. M. Lew, N. Rajabbeigi, M. Tsaptsis, *Ind. Eng. Chem. Res.*, 2012, **51**, 5364.
  - <sup>7</sup> P. Lanzafame, K. Barbera, S. Perathoner, G. Centi, A. Aloise, M. Migliori, A. Macario, J. B. Nagy, G. Giordano, *J. Catal.*, 2015, **330**, 558.
  - <sup>8</sup> J. Dijkman s, M. Dusselier, D. Gabriels, K. Houthoofd, P. C. M. M. Magusin, S. Huang, Y. Pontikes, M. Trekels, A. Vantomme, L. Giebler, S. Oswald, B. F. Sels, *ACS Catalysis*, 2015, **5**, 928.
  - <sup>9</sup> A. Omegna, M. Vasic, J. A. Van Bokhoven, G. Pirngruber, R. Prins, *Phys. Chem. Chem. Phys.*, 2004, **6**, 447.
  - <sup>10</sup> M. Boronat, P. Concepcion, A. Corma, M. Renz, S. Valencia, *J. Catal.*, 2005, **234**, 111.
  - <sup>11</sup> J. W. Harris, M. J. Cordon, J. R. Di Iorio, J. C. Vega-Vila, F. H. Ribeiro, R. Gounder, *J. Catal.*, 2016, **335**, 141.

## ***6. Overcoming catalyst deactivation during the continuous conversion of sugars to chemicals: maximising the performance of Sn-Beta with a little drop of water***

### **6.1 Introduction**

The work carried out so far indicates that Sn-Beta is highly active for several TH reactions. Moreover, the stability of the catalyst during continuous operation has also been explored, and very promising results were achieved. It has been shown that during the transfer hydrogenation (TH) of cyclohexanone (CyO) that Sn-Beta could be used for more than 20 days on stream, losing only 35 % of its initial activity over this extended period of operation. Characterisation techniques were used to identify the main cause(s) of deactivation and strategies to mitigate or to regenerate were also developed. TH of CyO was chosen because

it represent a simple, but realistic model of TH reaction type, the same kind of reaction to which GI belongs. Indeed, has been demonstrated that the GI reaction mechanism involves an intramolecular hydride shift,<sup>1</sup> analogous to the intermolecular hydride shift that occurs between CyO and the solvent (2-butanol) during TH.

Much academic and industrial interest is currently focused on the valorisation of glucose (Figure 1). However, although interest in in both the academic and industrial research sectors is high, to date very little information is available about the continuous potential of these processes catalysed by heterogeneous catalysts. Several possible reactions starting from glucose are of interest. For example, glucose isomerisation (GI) is the biggest biochemical process in the world, and from to this reaction, High Fructose Corn Syrups (HSFC) is produced for use in the soft drink industry, with a production of 8.5 million tons being produced only in the USA in 2015.<sup>2</sup> However, the great interest in the glucose isomerisation reaction relies also on the fact that is a key step for the production of many platform molecules, such as 5-hydroymethyl furan (HMF) and derivatives, which are believed to represent the future of the chemical industry. In figure 1, part of the complex reaction network obtainable following GI is shown.

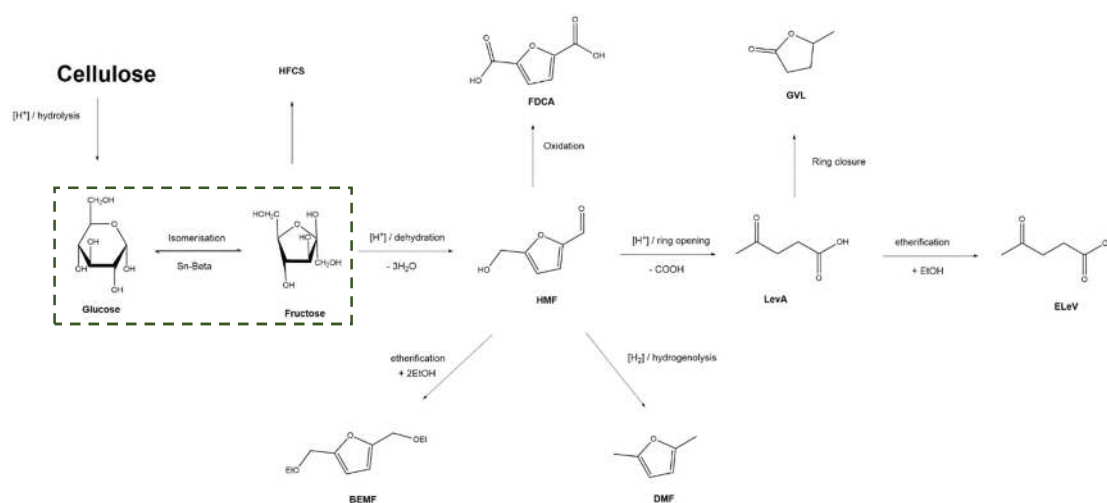


**Figure 1.** Reaction network of most of the products obtainable from the depolymerisation of the cellulose. The key step of glucose isomerisation is indicated by the dashed square.

Glucose can readily be obtained by the depolymerisation of cellulose in acidic media, of which it is the major constituent.<sup>3,4</sup> On the contrary, the natural abundance of fructose is very scarce. Therefore, the most efficient way to obtain this molecule is through isomerisation from glucose, which can be achieved by Sn-Beta.<sup>5</sup> The importance of obtaining



fructose is because many key molecules can be readily obtain by its consecutive reaction. Between them, great attention has been focused on (HMF), easily obtainable by dehydration of fructose. As can be seen, HMF is a platform molecule from which many useful molecules can be derived.<sup>6</sup> For instance, Avantium is producing furan-2,5-dicarboxylic acid (FDCA), in order to copolymerise it with ethylene glycol to obtain polyethylene furanoate (PEF) used for soft drink packaging.<sup>7</sup> Also from HMF, promising biofuel or fuel additive can be synthesised, for example the product of etherification with ethanol results in the production of 2,5-bis(ethoxymethyl)furan (BEMF),<sup>8</sup> whilst the hydrogenolysis lead to the formation of dimethylfuran (DMF).<sup>9</sup> Ring opening of HMF lead to the formation of levulinic acid (LevA), which can be esterified with ethanol to give ethoxy levulinate (ELev), a promising biofuel. As alternative, LevA can be converted in  $\gamma$ -valerolactone (GVL), that could find employment either as fuel additive and as bio-solvent.

Given the plethora of products that can feasibly be attained, it is clear now why the isomerisation of glucose to fructose is a reaction that has gain the attention of the academic and industrial scientific community. Its successful realisation could open the door to a huge supply of new chemicals that can cover wide areas from polymers to solvents and to fuel. It is been found that Sn-Beta can catalyse this reaction when is employed at relatively low temperature ( $< 130\text{ }^{\circ}\text{C}$ ), and the reaction can be carried out in water or alcohol media. Of course, due to the low solubility of glucose in organic solvents, the aqueous route is preferable from an intensification perspective.

On a related aspect, at the same reaction conditions, epimerisation of glucose to mannose can also be observed, though which much lower selectivity. However, with specific modifications to the catalyst, the selectivity of the epimerisation can increase dramatically. Other than isomerisation to fructose, glucose can also be employed for the production of methyl lactate (ML). ML is obtained by retro aldol cleavage of glucose,<sup>10</sup> which occur at elevated temperatures ( $> 140\text{ }^{\circ}\text{C}$ ) and its production is favoured by the presence of alkali cations, such as  $\text{K}^+$  (Figure 2).<sup>11</sup>

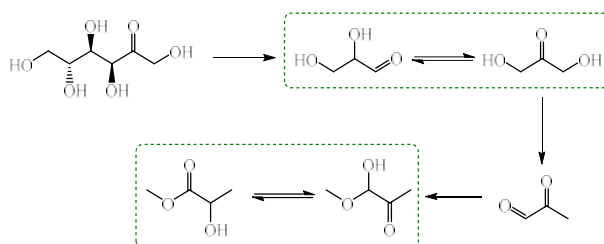


**Figure 2.** Catalytic conversion of glucose to methyl lactate. The reaction steps catalysed by Sn-Beta are highlighted by the dashed boxes. Figure reproduced by permission of Ref 10.

At higher temperature, other products can also be formed during this process, many of which have potential in the bio-polymer industry. Examples include methyl vinyl glycolate (MVG)<sup>12</sup> and *trans*-2,5,6-trihydroxy-3-hexenoic acid (THM), along with direct dehydration-products of glucose, such as furanic molecules (FUR). This shows how the precise temperature plays a key role in determining the type of chemistry that is obtainable from one substrate, a simplified scheme is shown in figure 3.

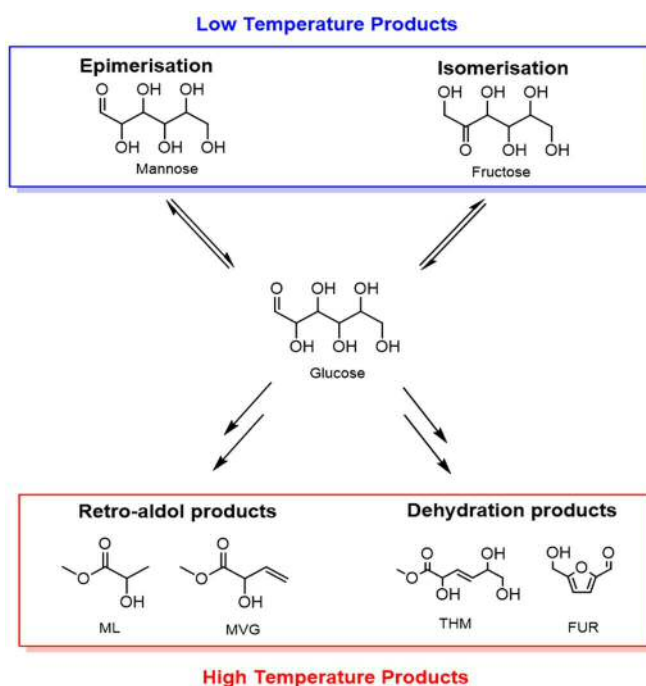


**Figure 3.** General scheme demonstrating the products that can be obtained by the catalytic conversion of sugars with Sn-Beta at both low (<140 °C) and high (>140 °C) temperature.

To date, the processing of glucose into valuable products is almost exclusively achieved by enzymatic catalysis, Xylose Isomerase being the most widely employed enzyme for this process.<sup>13</sup> Enzymatic processes, although being very selective, need to operate in a narrow operational window; temperature, pH, pressure, solvent purity, amongst others, need to be kept strictly under determinate parameters, the consequences of this being a very energy-demanding process, resulting in poor productivity and flexibility. Therefore, developing a solid heterogeneous process in order to convert glucose to different substrates would represent a breakthrough in the biomass valorisation.

It has been demonstrated in Chapter 4 and 5 that Sn-Beta possesses a high degree of stability when employed in continuous operation in organic media. However, the long-time

stability of Sn-Beta is as yet unknown when water is present in the system. Also the chelating configuration that glucose can assume during the transition state of the isomerisation is believed to possibly negatively impact the long-term stability of the active site. However, no evidence of this has been presented to date. Therefore, the main aim of this chapter is to study the stability of Sn-Beta when water is present, as a solvent or co-solvent, while performing glucose isomerisation. In addition to this, the high temperature route employed for the production of ML, will also be briefly explored in this chapter.

## 6.2 Results and discussion

### 6.2.1 Stability evaluation for glucose isomerisation in water and methanol

As shown during Chapter 3, the TH of CyO has been shown to be an effective model for this type of reactions, even though the reaction was tested only in organic media, and no information are available about the stability of the catalyst in the presence of water. However, the study of continuous TH of CyO permitted development of an experimental protocol that will be followed also in this study. As such, kinetic experiments will first be performed, and the stability of the catalyst during operation will be evaluated. Subsequently, adequate characterisation techniques will be used in order to try to correlate kinetics and structural properties.

To start investigating the stability of Sn-Beta during continuous GI, a solution of 1 wt.% of glucose in water and methanol has been reacted with 10Sn-Beta at 110 °C. This is the same temperature used by Moliner and co-workers,<sup>1</sup> and allows the reaction to proceed under otherwise benchmarked conditions. The choice of running the reaction both in water and in methanol was done in order to compare the stability of the catalyst in aqueous and organic media under similar reaction conditions. The reason why the concentration of glucose has been set to 1 wt.% is because of the low solubility of glucose in methanol, which prohibits the concentrations employed in Chapter 3 to be used when methanol is employed as solvent (10 wt. %). However, it must be said that such low concentration are unfavourable parameters for the economy and the efficiency of the process, because it will require to employ high amount of energy for downstream operation, for recovering the product, even if the reaction run at high selectivity. Therefore, the employment of such diluted solution is solely dictated by practical purpose.

Due to the thermodynamic equilibrium limitation of the reaction (60 % of glucose conversion at 110 °C), the contact time of the reactions were adjusted to start from a conversion between 35 - 40 %, to assure that the experiment were not performed close to the excess catalyst regime. The stability was evaluated by comparing the relative performance against the time on stream and the results are displayed in figure 4.

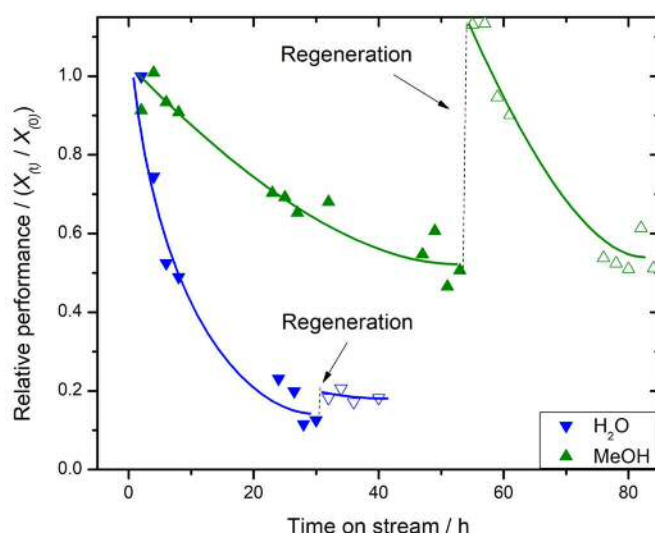


**Figure 4.** Relative performance of Sn-Beta during continuous glucose isomerisation in water (blue downward triangles) and in methanol (green triangles).

When performed in water, the isomerisation has experienced a very fast deactivation, with a loss of 90 % of its initial activity in the first 24 h. On the other hand, when the reaction was performed with methanol as solvent, the catalyst retained more than 50 % of its initial activity in 48h. Attempts to regenerate the catalyst were made after the reaction, following the heating protocol already successfully employed in the previous chapters. When the catalyst was used with methanol as solvent, it was possible to recover full activity by calcination. On the contrary, when water was used as solvent, the catalyst was still inactive after regeneration. At this point two main conclusion can be drawn: i) the rate of deactivation in the two systems are different, the use of water as solvent leading to a faster rate of deactivation, while in methanol a slower deactivation rate was observed; ii) the mechanism of deactivation is different in both cases. In particular it has been observed that while the catalyst could be regenerated after the reaction in methanol, when water was used as solvent the deactivation was permanent. In light of the latter observation, characterisation of the used catalysts bed were performed to gain a preliminary understanding on the phenomena involved.

### 6.2.2 Investigation of the deactivation causes after the reaction in water

Preliminary stability studies on GI in water and in methanol revealed that the deactivation in water was faster than in methanol and irreversible. Since such a remarked difference between the two system was observed, it was expected that the two materials showed a quite clear distinction in the structure. In first instance, it was hypothesised that the structure of the material could have been heavily damaged, as indicated by the permanent nature of the deactivation. Indeed, the stability of zeolites in hot liquid water is far from assured<sup>14</sup>. Therefore XRD on the used materials was performed and compared with the fresh one, the patterns are shown in figure 5.

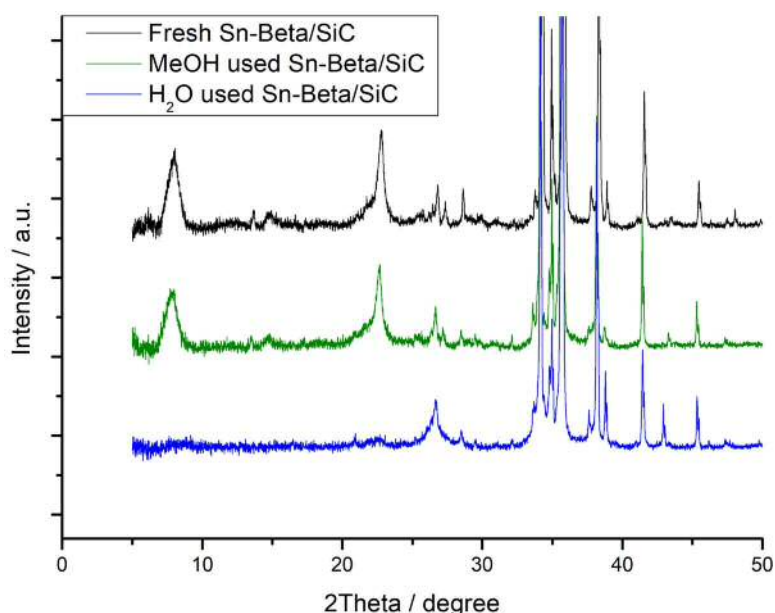


**Figure 5.** XRD patterns of fresh and used 10Sn-Beta samples before and after continuous glucose isomerisation.

of the BEA structure after the reaction of water, indicating severe damage (amorphisation) of the crystalline structure, in good agreement with what observed during the continuous operations. Since this evidence was sufficient to explain the fast and permanent deactivation of the catalyst in water, no further characterisation were performed on this catalyst.

### 6.2.3 Stability evaluation for glucose isomerisation performed in mixed solvents

Seeing that water lead to an irreversible deactivation of the catalyst within a day, while the use of methanol preserve half of the initial activity in 48 h of reaction, mixtures between methanol and water were explored in order to see at which level water lead to the permanent structural changes observed. To begin investigating the stability of glucose in mixture solvents, a solution of glucose in a mixture of 10 % in weight of water and 90 % of methanol was used, this solution will be called 10:90 H<sub>2</sub>O:MeOH. The results were compared with the reaction in pure methanol and water respectively under comparable condition. It is noted here that the contact was adjusted in order to start from a similar level of conversion in each case. The final results are presented in figure 6.

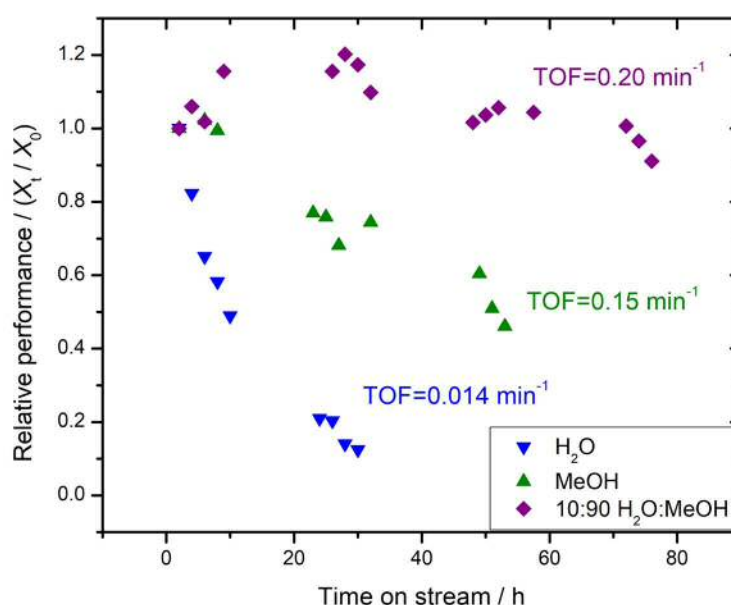


**Figure 6.** Influence of the solvent on the stability of Sn-Beta for low temperature glucose-fructose isomerisation. The initial level of conversion in all cases was between 33-40 %.

The analysis of the stability data was very surprising. Opposite of what was anticipated, the addition of 10 wt.% of water to methanol allowed to obtained a stable glucose conversion over the period of 80 h on stream, with a loss of just 10 % of the initial conversion (35.4 %) observed over this time. Further to its increased stability, the initial TOF (mol glucose converted mol<sup>-1</sup> (Sn) min<sup>-1</sup>) was found to be higher than the other two systems, reaching 0.20 min<sup>-1</sup> compared to 0.15 and 0.014 min<sup>-1</sup> for pure MeOH and pure water respectively. Clearly, the addition of water to the reaction feeds leads to improvements in activity, and more dramatically, improvements in stability. In order to evaluate better the deactivation of the catalyst, a linearisation of the conversion vs. time on stream have been made by applying the Levenspiel equation (shown in the Y axis), and is shown in figure 7.<sup>15</sup> In this

case, the slope of the best fitting line provides a value of a deactivation constant ( $k_d$ ). The evaluation of  $K_d$  allow a more precise numerical comparison of the deactivation extent observed for different system. Higher values of  $K_d$  correspond to higher deactivation rate.

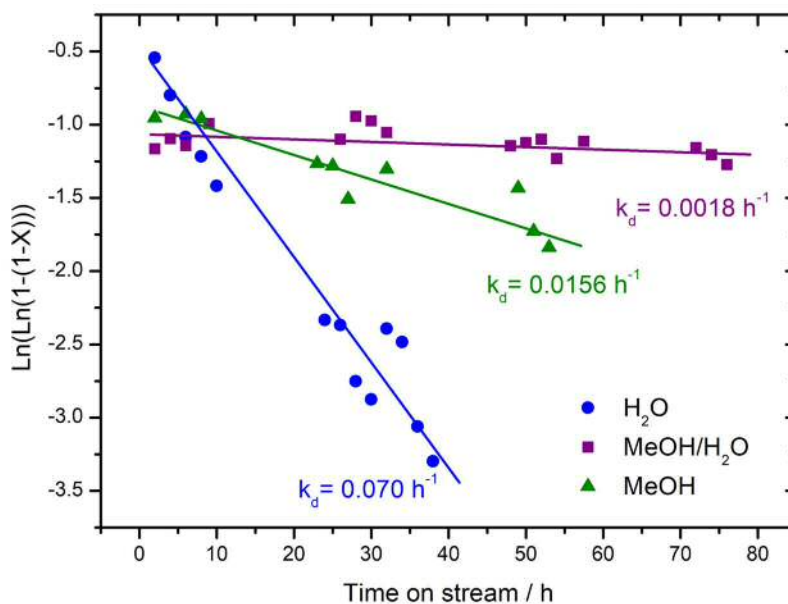


**Figure 7.** Conversion of glucose vs time on stream plotted in logarithmic form. The deactivation rate ( $K_d$ ) has been obtained from the slope of the line of best fit.

Looking at the value of  $K_d$  obtained, the increase of stability when water is added appears even more dramatic. The values of  $K_d$  so obtained are 0.070, 0.0156 and 0.0018  $\text{X}\% \text{ h}^{-1}$  for the systems in water, methanol and 10:90 water:methanol respectively. This showed that the increase in stability earned by using the mixture is 39 and 9 times higher than water and methanol respectively, despite water itself being a very unfavourable reaction solvent. In table 1 the product distribution of the reaction performed in pure methanol and 10:90  $\text{H}_2\text{O}:\text{MeOH}$  at 2 and 24 hours is shown.

n°	Conditions	$X_{\text{glucose}}$ (mol. %)	$Y_{\text{mannose}}$ (mol. %)	$Y_{\text{fructose}}$ (mol. %)	$\text{Sel}_{\text{fructose}}$ (mol. %)	$Y_{\text{methyl lactate}}$ (mol. %)
1	110°C, MeOH, 2 h TOS	35.4	5.2	15.3	43.2	1.2

**Table 1.** Conversion and yields of Gl in continuous flow after 2 and 24h of time on stream.

3	110°C, 10:90 H <sub>2</sub> O:MeOH, 2 h TOS	37.9	4.8	19.7	52.3	1.1
4	110°C, 10:90 H <sub>2</sub> O:MeOH, 24 h TOS	36.8	4.7	19.6	49.6	0.8

The data listed in the table shows higher selectivity in fructose of the mixed system compared to the only methanol one. Analysis of the distribution of the two main products, fructose and mannose, shows that introduction of water does not dramatically change the choice of the two catalytic pathways, with the isomerisation to fructose being the reaction and the epimerisation to mannose a secondary reaction, as demonstrated by the low yield in mannose (5 % at maximum glucose conversion). It is important to note that the methyl lactate detected is less than 2 % of yield, while it is the main product when the same reaction is performed at temperatures > 140 °C. This also confirms that the lactate formation is a catalytic pathway that is dependent on the temperature rather than the composition of the medium. However, the analysis of the data showed a very important effect, the selectivity of fructose, compared at iso-conversion, seems to have slightly higher values; 43 % compared to 52.3 %, for the only MeOH and 10:90 H<sub>2</sub>O:MeOH respectively. Therefore, further detailed studies focused on how water influences reactivity, other than stability, will be performed.

#### 6.2.4 Optimal operational window evaluation

To explore how the amount of water affects the catalysis, several glucose isomerisation continuous reactions have been performed changing the amount of water present in the solution. Precisely solutions of 1 wt.% of glucose with 50, 25, 10, 5, 1, and 0.5 wt.% of water were used as reaction feed. To have a better understanding of the effect of the water, the continuous flow reaction was conducted at the same contact time, so accordingly the initial conversion of this reaction. From each of these reactions the initial TOF and  $K_d$  were calculated and the values are plotted against the content of water in figure 8.

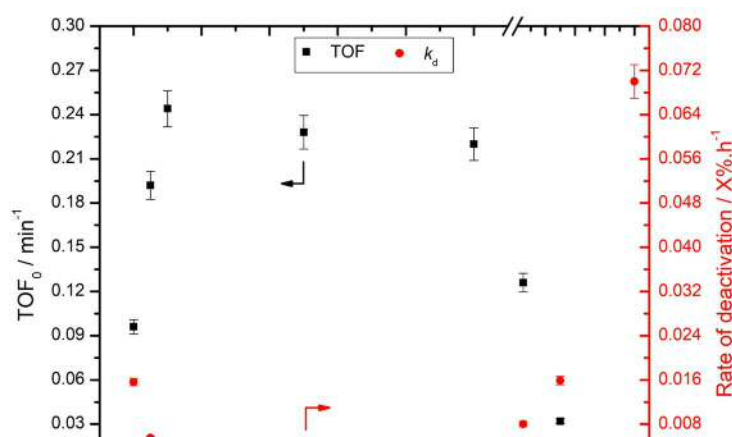




**Figure 8.** Influence of solvent composition in terms of activity ( $TOF_0$ ) and rate of deactivation ( $k_d$ ) during low temperature glucose-fructose isomerisation.

These results clearly indicate that the water has a huge impact on both stability and activity, as demonstrate by the plot. Following the  $K_d$  values (at which higher value correspond to slower rate of deactivation), from no content of water to only water solvent, the initial value of  $0.0156 \text{ X\% h}^{-1}$  gradually decrease to  $0.002 \text{ X\% h}^{-1}$ , and stays stable around that value until the content of water rise until 10 wt. %. Above that amount of water, the rate of deactivation increase again, until reaching is maximum value of  $0.07 \text{ X\% h}^{-1}$  when pure water is use. Surprisingly, when the  $TOF_0$  of the reactions are plotted against the same solvent composition, an analogous trend is observed, with the highest values reaching  $0.22 \text{ min}^{-1}$  when the water amount is between 1 and 10 wt. %.

From the analysis of this plot, it can be seen that there is an optimal operational window where the initial TOF is maximised and the and the  $K_d$  is minimise. This range of optimal values are found when composition of the water in the alcoholic solvent is between 1 and 10 wt.%. Operating the GI within this range of methanol/water mixtures allows having a productive process with the minimum level of deactivation. It also point out how a small quantity of water such 1 wt.% can dramatically improve the performance the reaction. However, it has briefly seen in 6.2.5 that the reaction run in the presence in water shown a slightly higher selectivity in fructose, for this reason this aspect will be study in deep in the next paragraph.

### 6.2.5 Selectivity as function of water content

The selectivity in fructose represent another key factor on the success of this process, in fact high selectivity always means less energy-demanding downstream separation, and also means less waste of valuable substrate. Therefore values of fructose selectivity as function of conversion for the reactions with different content of water (from 0.5 to 10 wt.% because

they show similar activity) have been compared with the reaction performed in pure methanol and pure water and shown in figure 9.

As it can be seen, when pure methanol was used, the selectivity dropped from 70 %, at conversion as low as 10 %, with typical values of  $\pm 40$  % when the conversion was between 30 and 40 %. At that range of conversion, selectivity above 45% was always detected when the amount of water present in the solution was  $> 1\text{wt.}\%$ . As a term of comparison, the selectivity as function of glucose conversion of the reaction performed in water is also shown. The selectivity in fructose is higher in this case than in any other system compared at the same level of conversion. However, this lower selectivity did not reflect into a higher selectivity of mannose or methyl lactate. It could be suggest that methanol induce to some side-reaction whose products were undetected by the analytical method used in this work. It has been seen that in methanol and in presence of some Brønsted acid residual, some methylglucoside or methylfructoside<sup>16</sup> can be formed, leading then to a lower selectivity by converting the substrate into “masked” substrates unnameable to further conversion. Alternatively, it can be proposed that fructose might undergo to some degradation reaction and form what are normally called humins, which are typical polymeric degradation products of sugars. Of course the reason behind the solvent composition-dependence of fructose selectivity will be investigate in future research. Now that the best condition to operate continuous isomerisation of fructose have been studied, optimisation studies on the reaction productivity can be attempted, in order to maximise not only stability but also STY, which is a key factor for a successful industrial process, and one of the typical weak points of enzymatic catalysis.

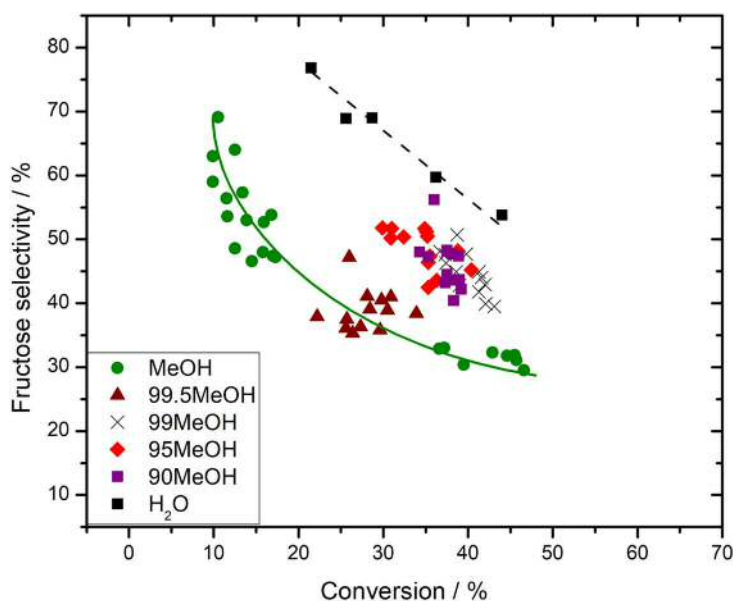


**Figure 9.** Influence of reaction solvent in terms of fructose selectivity, plotted as a function of glucose conversion. The reaction were run all in the continuous flow reactor at 100 °C and 1 wt. % of glucose.

### 6.2.6 Optimisation of the reaction

After having studied the effect of water and individuate the optimal operational window, attempts to optimise the system in term of maximising the space-time-yield (STY) were made. Between 1 and 10 wt. % of water content the performance of the system did not substantially change in term of activity selectivity and stability, therefore having 10 wt. % of water represent an advantage for two reason: i) it allows the boiling point of the solution to be increased, allowing to work at higher temperature at lower pressures, and ii) increase the solubility of the glucose. For these reason, the preliminary optimisation was made using the solvent composition of 10:90 H<sub>2</sub>O:MeOH. In particular, glucose concentration and reaction temperature have been changed in order to improve the performance of the reaction. The STY and relative lifetime of the optimised systems are summarised in Table 2.

**Table 2.** Optimisation of the low temperature GI system in terms of performance (space-time-yield) and lifetime, at various reaction conditions.

n°	Reactor	Conditions	Space-time-yield <sup>[a]</sup>	Relative lifetime <sup>[b]</sup>
1	Batch	H <sub>2</sub> O, 110 °C, 10 wt. %	1.2	-
2	Flow	H <sub>2</sub> O, 110 °C, 1 wt. %	2.7	1
3	Flow	MeOH, 110 °C, 1 wt. %	12.0	4.5
4	Flow	10:90 H <sub>2</sub> O:MeOH, 110 °C, 1 wt. %	15.9	41
5	Flow	10:90 H <sub>2</sub> O:MeOH, 110 °C, 4 wt. %	20.4	38
6	Flow	10:90 H <sub>2</sub> O:MeOH, 130 °C, 4 wt. %	186.4	14

Solubility test of glucose in the 10:90 H<sub>2</sub>O:MeOH solution found that the maximum solubility at room temperature was 4 wt.% of glucose. When the reaction was performed using a 4 wt.% solution at 110 °C a 20 % increase of the STY was observed compared to the reaction performed with the 1 wt.% solution. Successively, the temperature was increased from 110 to 130 °C. A STY value of 186.4 kg<sub>fructose</sub> kg<sub>cat</sub> cm<sup>-3</sup> h<sup>-1</sup> was calculated, 12 times higher than the

value calculated for the reaction at 110 °C. The lifetime measured ( $k_d = 0.0075 \text{ X\% h}^{-1}$ ) resulted four fold lower than the reaction run at 110°C and 1 wt. %. In order to check if some by-products were formed at high temperature and high glucose concentration, the selectivity of this reaction has been compared to the other reactions run in precedence and shown in figure 10.

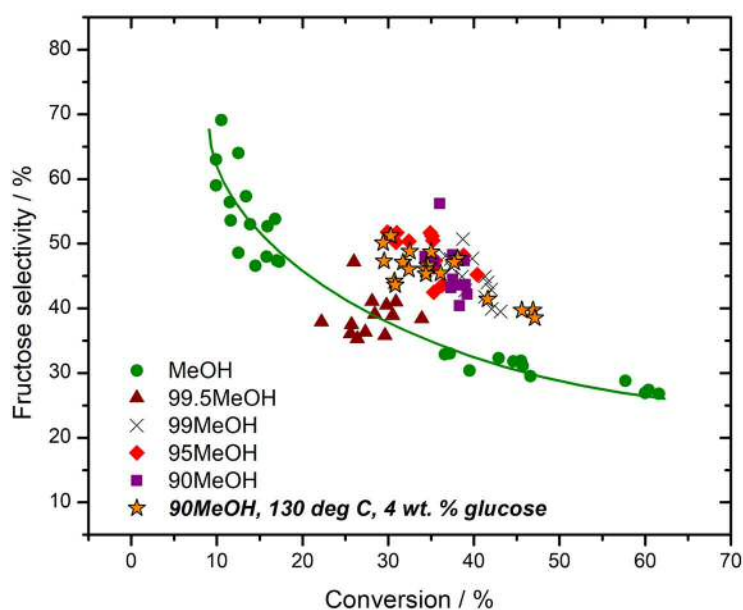


**Figure 10.** Influence of reaction solvent in terms of fructose selectivity, plotted as a function of glucose conversion. The reaction were run all in the continuous flow reactor at 100 °C and 1 wt. % of glucose. The optimised reaction (4 wt.%, 130 °C) is highlighted in the orange stars.

As it can be seen, the selectivity of the optimised reaction perfectly overlap with the values obtain when the reaction were performed at 110 °C with the same solvent composition, meaning that the increase of temperature at 130 °C do not impact the product distribution. However, even though a faster deactivation is observed, the superior STY greatly overcome its shorter lifetime. So far, it has been shown how the addition of small amount of water (1 – 10 wt. %) bring an global improvement during continuous glucose isomerisation. The beneficial effects regarded stability, activity and selectivity. However, still unknown is how universal is the effect of water, if this effect is related only the specific GI reaction, or if it is extended more generally to the catalyst, and is therefore applicable to different systems.

### 6.2.7 High temperature process: methyl lactate production

As described above, Sn-beta also catalyses retro-Aldol processes starting from glucose and fructose. This reaction is typically catalysed at high temperature ( $> 140\text{ }^{\circ}\text{C}$ ) and the products are methyl lactate (ML) and derivatives. These reactions can be both carried out in aqueous and alcoholic media, making them the main discriminant between the two pathways the operational temperature. This make the ML production a perfect reaction in which the effect of the water can be explored, to see if the beneficial effect that was manifested for GI is observed also under this different conditions.

To detect the universal applicability of the water effect, ML production has been carried out in a continuous flow reactor at  $160\text{ }^{\circ}\text{C}$  and in pure methanol to benchmark the kinetics and stability in absence of water. Furthermore, to selectively favour ML between many other products at high temperature, a solution of sugars containing alkali ( $\text{K}_2\text{CO}_3$  at  $2.5\text{ mg L}^{-1}$ ) has been used. Given its higher solubility in methanol at room temperature, fructose instead of glucose was chosen as substrate. This also allows the contribution of improved isomerisation in the co-presence of water to be excluded. Figure 11 describes the continuous conversion of fructose to ML, in pure MeOH.

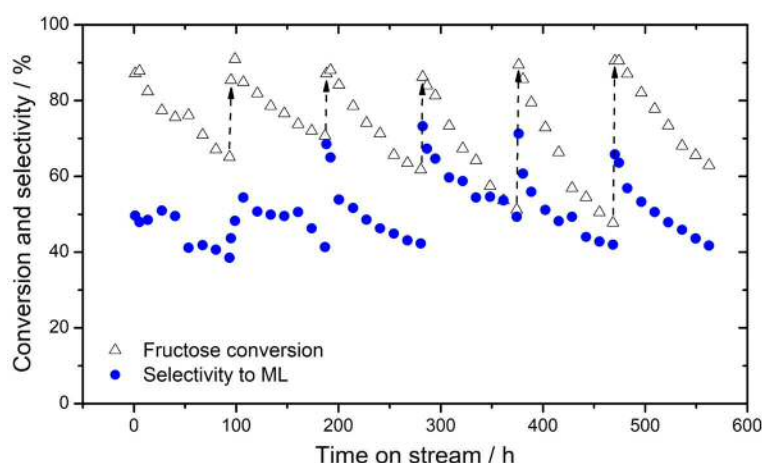


**Figure 11.** Time on stream data showing the selectivity towards methyl lactate (blue circles) and conversion of fructose (hollow triangles) using Sn-Beta at  $160\text{ }^{\circ}\text{C}$  in methanol. Regeneration by thermal treatment was performed every 96 h (dashed arrows).

Following the first 100 h on stream of the reaction performed in pure methanol, the conversion rapidly dropped from 87 % to 65 %. Deactivation of the catalyst is shown to be non-permanent, as demonstrated by the five regeneration procedures accomplished after every 100 h of reaction, realised by calcination at  $550\text{ }^{\circ}\text{C}$  for 3 h. Full activity could be restored, as indicated by the same initial conversion. However, the lower conversion reached in every successive cycle indicates that a faster deactivation for achieved at every

cycle, suggesting that an irreversible secondary deactivation might be present, along with a first reversible type. Interestingly, an increase of ML selective was also observed, starting from an initial selectivity of 50 % at the beginning of the first cycle, and finding a value of 70 % at the beginning of the last cycle. This is an indication that some rearrangement at the level of active site could have occurred.

To probe the effect of water, a continuous reaction was run with a methanol solution containing 1 wt. % of water, and a second reaction under otherwise identical conditions was performed. The time on stream data is shown in figure 12.

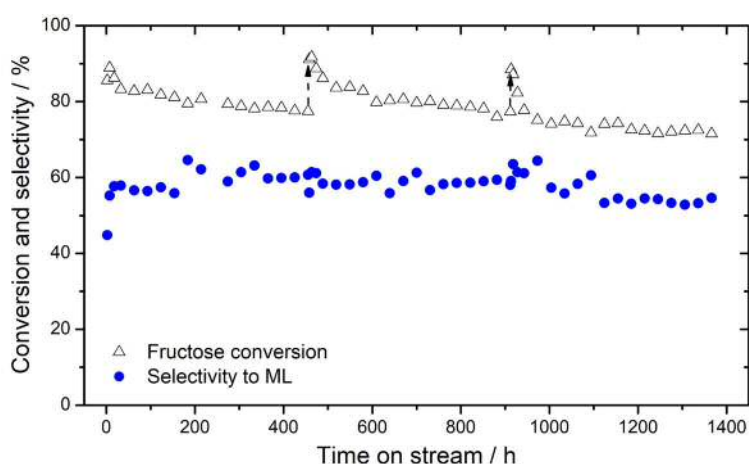


**Figure 12.** Time on stream data showing the selectivity towards methyl lactate (blue circles) and conversion of fructose (hollow triangles) using Sn-Beta at 160 °C in the presence of 1 wt.% water in methanol. The catalyst was regenerated periodically by thermal treatment (dashed arrows).

As observed earlier for the GI, also in this system, a little amount of water produces a dramatic increase in the stability of the catalyst. During the first cycle, the reaction run continuously for 450 h on stream, starting from an initial conversion of 90 % and dropping only to 75 %. In agreement with what has been observed in the low temperature system, the ML selectivity level in the presence of water stayed constantly in values  $\pm 60$  %. A comparison of the deactivation constants, calculated to be 0.23 and 0.008  $\text{X\%}\cdot\text{h}^{-1}$  for the process in pure methanol and in presence of water, respectively, illustrates that a decrease of 30 times on the rate of deactivation is observed upon the addition of only 1 wt.%  $\text{H}_2\text{O}$ . This result clearly demonstrates that the addition of water gives benefits to sugars conversion, independently from the reaction considered. However, the mechanism of how the water enhances stability, activity and selectivity is still unknown. Hence, characterisations are needed to shed a light on this outstanding and unified effect.

### 6.2.8 Leaching of Sn during continuous operation

The peculiar and universal role of water has given rise to many questions, especially for the dramatic effect that only a little amount of water can create. It has been observed that it improves activity, selectivity and stability of Sn-Beta during continuous valorisation of sugars, independently if it is glucose isomerisation or redox-aldol conversion of glucose to methyl lactate synthesis.

Leaching is often a cause of permanent loss of performance during continuous liquid catalysis. Therefore, the extent of Sn leached has been quantified by measuring the Sn concentration in the downstream of the flow system analysed by ICP-MS. The Sn detected by this analysis for the two systems is displayed in figure 13.

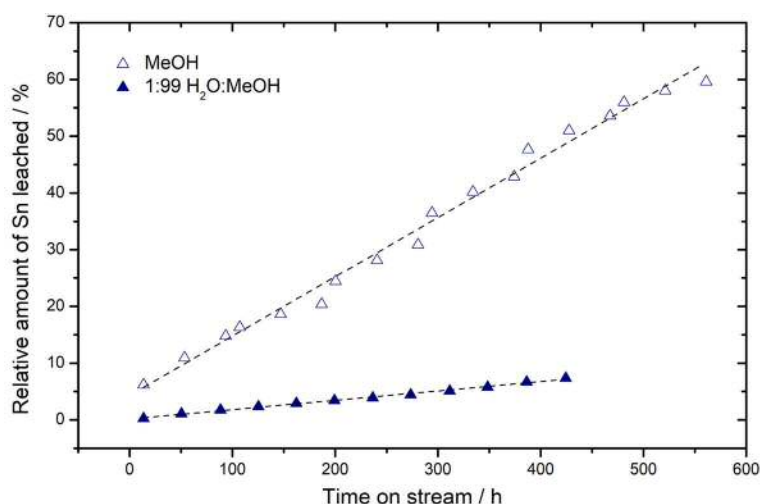


**Figure 13.** Comparison of the percentage of Sn recovered in the reaction effluent relative to the initial tin content in the Sn-Beta catalyst during operation in methanol and 1:99 H<sub>2</sub>O:MeOH, as determined by ICP-MS.

As it can be seen from the plot, two very different extents of leaching are found in presence and in absence of water. In the presence of water it has been detected a leaching of 7 % of the initial Sn over 450 h of reaction. When water is not present, almost 10 times more Sn is leached from the catalyst, making an average of 0.015 % of Sn<sub>leached</sub> h<sup>-1</sup>. Instead, a very different extent of leaching has been measured when ML production has been carried out in pure methanol. The total Sn leached calculated at the same time on stream (450 h) resulted of the 50 %, resulting in a leaching rate of 0.11 % Sn<sub>leached</sub> h<sup>-1</sup>, almost an order of magnitude higher than in the presence of 1 wt. % of water.

The effect of water on the leaching is undeniable; however, much care has to be taken before to correlate this effect to the deactivation of the catalyst. In fact, ICP cannot

discriminate between the type of Sn, therefore, active and inactive Sn species will be detected at the same way. In the case that inactive Sn species leached, like  $\text{SnO}_2$ , they will be detected by ICP-MS but their contribution to the catalysis is irrelevant. Besides, the fact that the reaction has been performed for 5 cycle and each cycle shows similar initial activity suggested that the Sn leached observed could not be all originated by the active site.

In order to explore the water effect on the Sn leaching during GI (the low temperature sugar process), ICP-MS analysis on the effluent has been performed as a single point analysis at the end of the flow process. In contrast to what was observed during the high temperature process, when the glucose isomerisation has been carried out very low amount of Sn leached in both system after 54 h on stream. In fact, only 0.0094 and 3.4 % of Sn leached has been measured for the system in 10:90  $\text{H}_2\text{O}:\text{MeOH}$  and pure methanol, respectively. This reveals an averaged leaching rate of  $0.00017 \text{ \% Sn}_{\text{leached}} \text{ h}^{-1}$  for the system in 10:90  $\text{H}_2\text{O}:\text{MeOH}$  and  $0.063 \text{ \% Sn}_{\text{leached}} \text{ h}^{-1}$  for the system in pure methanol. Despite the low values, it is revealing that also in this case the leaching rate in methanol is  $\pm 350$  times higher than the reaction made in the presence of water. However, a 3.5 % of Sn leached cannot account for more than the 50 % of loss in activity experienced in the only methanol system. Therefore more characterisation were carried out to determinate which effect water can have on the system.

By analysis of the leaching data obtained in the two different processes, two distinct conclusion can be made: i) the addition of water has an enormous impact in the observed leaching rate of the two systems, it has been calculated that the leaching in absence of water is relatively 10 and 350 times higher for the ML and GI system, ii) the temperature or the type of reaction involved greatly impacts the extent and rate of leaching. In fact the rate of Sn leaching for the ML process is found to be double that of GI in methanol.

However, if water has been proved to greatly reduce the leaching of Sn, consideration about the impact on the deactivation has to be done. In fact, during the GI in pure MeOH, 50 % of deactivation has been observed, while the total leaching of Sn (no information if is from active or inactive species) was measured to be of 3.4 %, hardly accountable for half of the loss of activity observed. Therefore, characterisation on the used catalyst must also be carried out.

### 6.2.9 Understanding the role of water



As observed in the previous paragraph, water can have several effects on the system, some of them very positive, like the reduce leaching observed during the ML reaction. However, the leaching observed in the two systems does not correlate well with the loss of activity.

Trying to rationalise the causes of this outstanding behaviour, several hypothesis can be made. The water could improve the stability of the system if: i) decreases the rate of restructuring of the zeolite; ii) decreases chemical poisoning of the active site by inhibited formation of, or *in situ* removal of, particular poisons; iii) it decreases/removes the accumulation of by-product and carbonaceous deposition, avoiding them pore fouling; and/or iv) it increases and maintains the presence of a specific type of active site. Therefore, to elucidate which of the above reasons can account for the kinetic observations, detailed spectroscopic study of the used catalyst have been performed.

XRD analysis (Figure 5) on the catalyst after reaction with pure water revealed the catalyst suffers a substantial loss of crystallinity in bulk water. This is in good agreement to the observation that the catalyst could not be regenerated following the first cycle, confirming that heavy structural damages (*i.e.* amorphisation of the crystalline structure) occurred during the reaction. Therefore, further characterisation of this system will not be explored. On the other hand, the catalyst used after the reaction performed in methanol preserved its initial crystalline structure, even though the activity dropped of half of its initial value. Further analysis on the catalyst used after the reaction performed with the 10:90 H<sub>2</sub>O:MeOH solution confirmed that the BEA structure is preserved even in the presence of moderate quantity of water, as it can be seen by the comparison of the XRD pattern of used catalyst after GI in pure methanol, and shown in Figure 14. Since the little amount of water does not damage the crystalline structure, the porosity of the used catalyst was explored, to see if water have an impact in reducing pore fouling, which has been demonstrated in Chapter 4 to be the main cause of deactivation of the TH of CyO, when conducted in organic media.

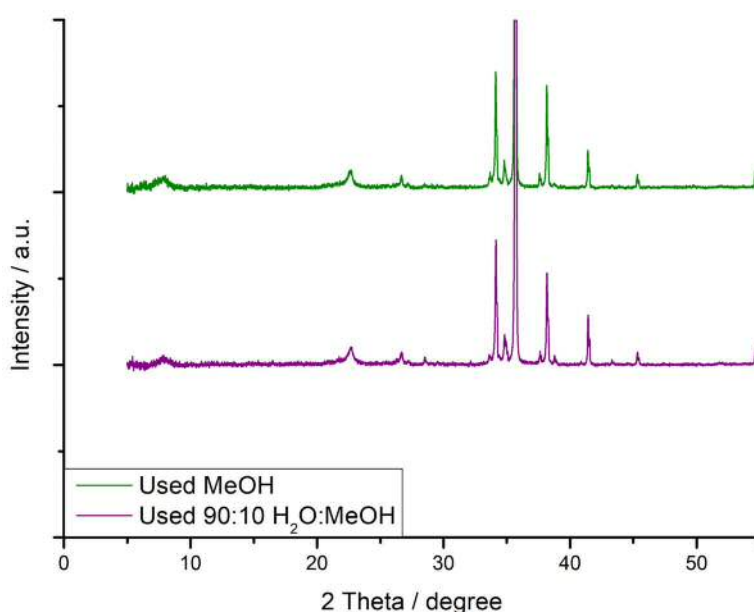


**Figure 14.** XRD patterns of Sn-Beta samples following reactions in MeOH and 10:90 H<sub>2</sub>O:MeOH, after 54 h on stream

Surface area and porosimetry analysis have been performed on the post-reaction catalysts in MeOH and 10:90 H<sub>2</sub>O:MeOH, and the results are shown in Table 3. Even though almost an order of magnitude of difference in stability was found between the two samples, little difference in the pore volume and surface area measurements could be spotted between the two used samples, showing almost identical values of BET surface area and total pore volume.

**Table 3 .** Porosimetry analysis of fresh and used samples of Sn-Beta after GI in MeOH and 10:90 H<sub>2</sub>O:MeOH for 54 h.

n°	Material	S <sub>BET</sub> (m <sup>2</sup> g <sup>-1</sup> )	V <sub>micro</sub> (cm <sup>3</sup> g <sup>-1</sup> )	Wt. % C (> 180 °C TGA)
1	Sn-Beta (fresh catalyst, undiluted)	421	0.28	
2	Sn-Beta/SiC (fresh catalyst, diluted in SiC)	75	0.048	-
3	Sn-Beta/SiC (used in MeOH)	53	0.035	1.2
4	Sn-Beta/SiC (used in 10:90 H <sub>2</sub> O:MeOH)	54	0.036	1.0

### 6.2.10 Poisoning studies

It has been shown that the main role of water is not in preserving the high crystalline structure of the zeolite and reducing the pore fouling, as demonstrated by XRD and porosimetry analysis, respectively. Therefore it was explored the possibility if some molecules could poison the active site and whether the role of water was in reducing their presence and their inhibition of the active sites. Obviously, the molecules chosen were particular compounds that are likely to be formed as by-product during sugars processing. Notably, the products chosen should also be formed in both systems. To do so, a series of batch reactions were performed in the presence of 10 mol % of by-product compared to the initial concentration of glucose (10 wt.%). Following reaction over the catalyst (10Sn-Beta)

the initial TOF was calculated for each reaction and compared to that of the fresh catalyst. The by-products tested were HMF, lactic acid, glyceraldehyde, dihydroxyacetone, glycolaldehyde and glycolic acid.

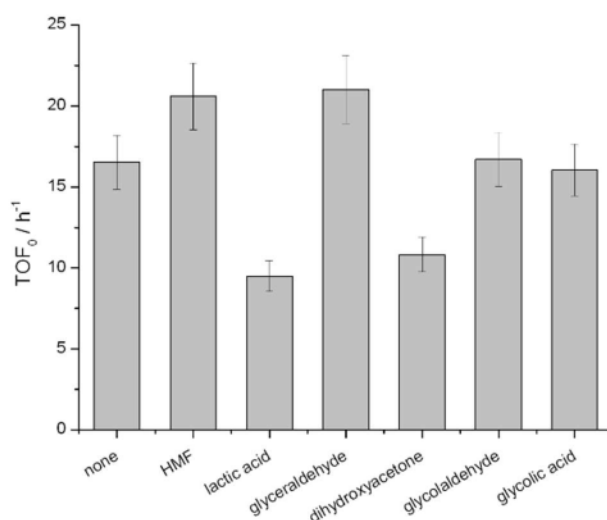


**Figure 15.** Impact of (by-)product addition on the initial rate of Sn-Beta for the isomerisation of glucose to fructose. Reaction conditions: 110 °C, 5 g of 10 wt. % glucose in water solution, 70 mg of catalyst, corresponding to a glucose/Sn molar ratio of 50. 10 mol. % of (by-)product was added to the vessel.

From Figure 15 it can be seen that only lactic acid and dihydroxyacetone produced a decrease in TOF of half of its original value. However, that happened when 10 mol % of by-product were introduced in the solution; during the continuous reaction, less than 1 mol % of lactic acid could be detected and no dihydroxyacetone was observed. Therefore, is very unlikely to attribute the loss of activity to the presence of poison under the operational conditions adopted. However, particular care must be taken when evaluating poisoning in continuous flow operation. Even though the poison molecule is present only in traces and well below the detectability limits of some analytical technique, the modality in which the continuous reactor run can make possible that the poison slowly accumulate on the catalyst, reaching then a critical concentration in which its effect can become quite relevant. Despite this, the results strongly indicate poisoning not to be relevant in this case.

#### 6.2.11 TGA and TPD-MS analysis

Pore volume measurements revealed that a consistent decrease of 30 % of the initial surface area was happening for both system, independently from the solvent composition, pointing

out that water cannot prevent reduction of pore volume. However, no qualitative information about the species that are deposited on the catalyst can be provided by surface area measurement. For this purpose, TGA and TPD-MS have been performed on the used catalysts. TGA allows an accurate quantification of specific species that desorbed from the catalyst at different temperature. Typically, different desorption temperature correspond to chemical species retained differently on the catalyst, so a semi-quantitative analysis can also be done. TGA spectra of the used catalysts after pure MeOH and 10:90 H<sub>2</sub>O:MeOH GI reaction are displayed in figure 16.

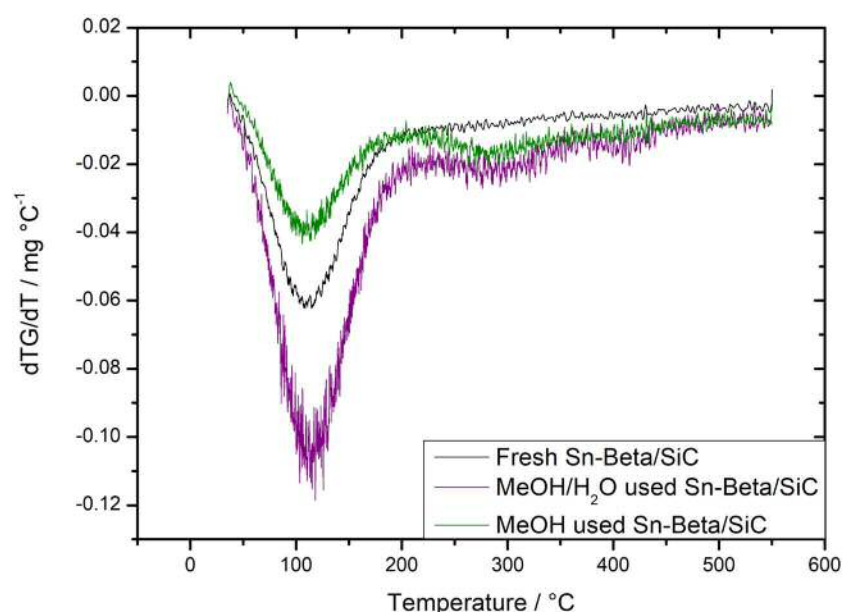


**Figure 16.** Thermo-gravimetric analysis of the fresh (top), the used in 10:90 H<sub>2</sub>O:MeOH (middle) and MeOH (bottom) catalyst. The relative mass loss (black line) and its derivative (blue line) are reported against the temperature.

Major mass losses in all samples at temperature below 180 °C were evident. Since the same mass losses were present in the fresh sample meaning that they did not come from any products of the reaction. Mass losses at temperature above 250 °C were detected as broad signals, meaning that a multitude of compounds could be present. However, the mass loss of this signal accounted only for less than 1.5 % in each used samples.

In order to identify the chemical nature of the desorbed component, a home-made TPD-MS system was used. A Praying Mantis DRIFTS cell was used as the heating element, while a continuous flow of air was used as carrier gas. The outlet of the cell was connected to a mass spectrometer in order to analyse the molecular mass of the desorbed compound present in

the effluent at various times. A similar ramping rate used for the TGA experiment was used for this experiment, in order to obtain a similar desorption profile. Figure 17 shows the fresh, used in MeOH and used in 10:90 H<sub>2</sub>O:MeOH TPD-MS spectra.

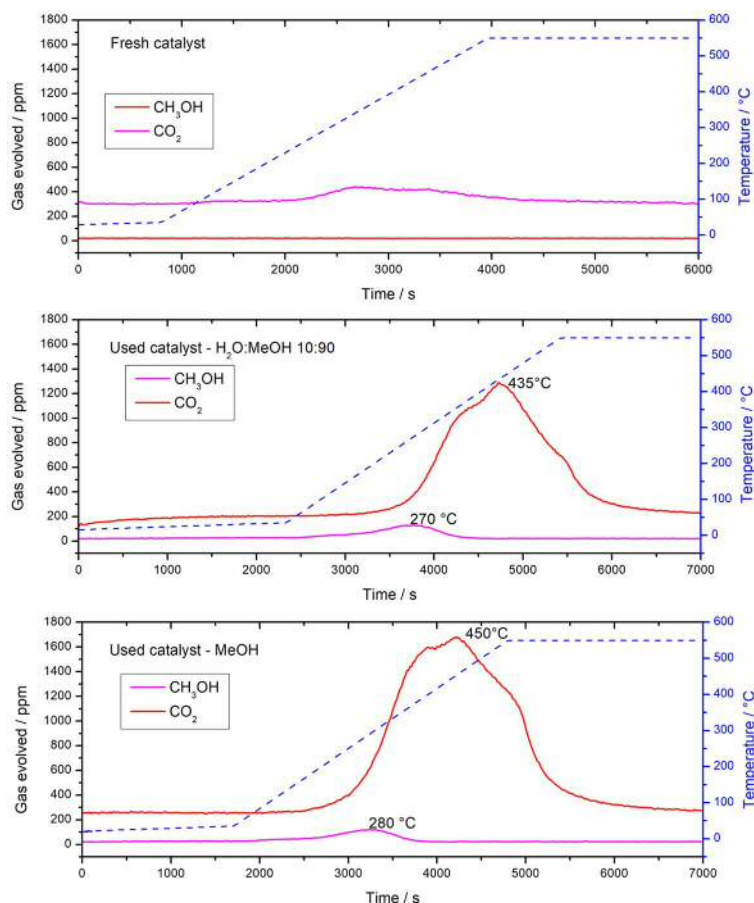


**Figure 17.** TPD-MS of the fresh(top), the used in 10:90 H<sub>2</sub>O:MeOH(middle)and MeOH(bottom)catalyst. percentage of the gases (left Y axis) and temperature ramp (right Y axis) are displayed in the graphic and plotted against the analysis time. Methanol and CO<sub>2</sub> evolution is monitored by means of the mass spectrometer detector.

The mass spectrometer detected two main gas species evolved from the catalyst upon heating, methanol and CO<sub>2</sub>, resulting in mass spectrometer signals of  $m/e = 32$  and  $44$ , respectively. In all the samples, species at lower desorption temperature (280 °C) were detected as methanol ( $m/e = 32$ ). Notably, these two mass are absent, or present at very low intensity, in a fresh samples run at the same condition, meaning that all the signal detected in the used samples come from the reaction. Interestingly, although the TGA is observed a mass loss centred at 250 °C, which was previously thought to derived from heavy carbon deposition, these results indicate that the broad signal found by TGA could be attributed to a strongly adsorbed solvent. At temperature higher than 300 °C all the mass

loss were detected as  $\text{CO}_2$  ( $m/e = 44$ ) meaning that all the species that were adsorbed into the catalyst were decomposing before desorption, so this signal could be related to carbon species deposited on the catalyst after the reaction, or to very strongly retained solvent molecules. In order to have a direct comparison of the amount of the  $\text{CO}_2$  evolved from the two used catalyst, the  $m/e = 44$  signals were plot together and shown in figure 18.

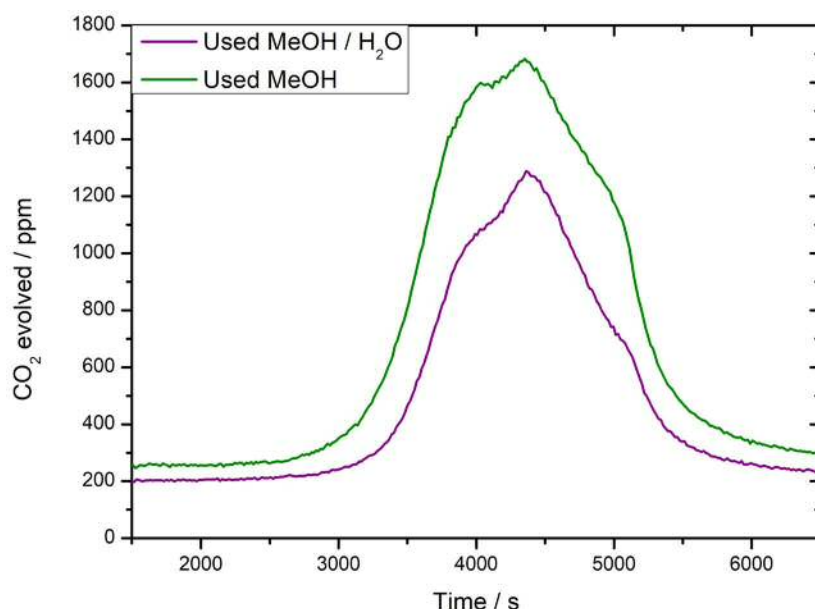


**Figure 18.** Comparison of the intensity of the  $m/e = 44$  signal from in the effluent from the TPD-MS analysis of Sn-Beta following operation in MeOH (green) and 10:90  $\text{H}_2\text{O}$ :MeOH (purple).

It can be seen that differences in the total type and quantity of carbonaceous species are present in both used catalytic materials. In fact, the used catalyst after the pure methanol reaction present higher quantity of  $\text{CO}_2$ , even though the difference of the amount evolved from the used sample in 10:90  $\text{H}_2\text{O}$ :MeOH is less than 50 %. However, it is unlikely that a decrease of 20-30 % of the carbonaceous species can lead to an increase of an order of magnitude of the stability, especially it has been demonstrated that this accumulation is not related to a decrease of the pore volume, since the same extent of pore volume reduction was observed for both systems. In addition, it cannot explain the higher initial TOF observed when water is present. At this point, structural properties of the catalyst, Sn leaching, active site poisoning and accumulation of species on the catalyst have been explored, but none of them gave convincing evidence of the observed univerval and beneficial effect of water. Therefore, in order to try to find a correlation between presence of water and higher stability, activity and selectivity, attempts to explore the nature of the active site prior to, and following, operation were made.

### 6.2.12 Restructuring of active site investigated by $^{119}\text{Sn}$ MAS NMR

Investigations on the nature of the beneficial effect of water performed by multiple techniques did not yet provide a clear answer. However, none of the techniques used so far could investigate directly the active sites of the catalyst. In fact, one cause of deactivation that has not been explored yet is active site restructuring. In light of the time on stream data of GI and ML continuous processes, it can be hypothesised that water impacts the form of the active site, or can preserve the true active site form during continuous operation. For example, it could influence the ratio between open and closed sites, by hydrolysing Sn-O-Si bonds. It is strongly supported in the literature that open sites, where one Sn-O-Si bond is hydrolysed, represents the most active form of the catalyst for glucose conversion, therefore, conditions that could favour its formation could be reflected in the better performance observed by in the continuous flow reaction when water was present.

To investigate if water could effected the restructuring of the active site,  $^{119}\text{Sn}$  MAS NMR was applied on the used samples after 54 h of GI reaction in MeOH and 10:90  $\text{H}_2\text{O}$ :MeOH. A fresh sample was also included as a comparison. It is known, and examples are shown in the previous chapters, that  $^{119}\text{Sn}$  MAS NMR suffers from disadvantages associated to the low abundance of  $^{119}\text{Sn}$ .<sup>17,18</sup> To overcome this issue, the spectra were acquired with a different method, very recently published by Ivanova group.<sup>19</sup> A Carr-Purcell-Meiboom-Gill (CPMG) sequence was used to acquire the spectra instead of the conventional single echo acquisition. This method consists of a different pulse sequence acquisition and a successive modelling of the obtained spectra to reconstruct the NMR signal. Substantially high S/N spectra per unit time are therefore acquired, at the expense of some chemical shift resolution. CPMG (acquired in direct excitation and cross polarisation) and a single Hahn echo spectra of as prepared (fresh) 10Sn-Beta are shown in figure 19.

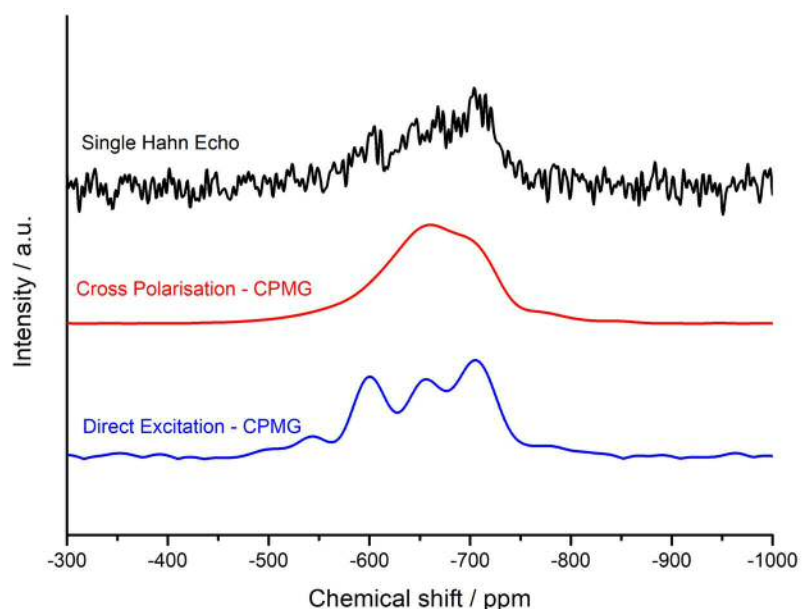


**Figure 19.**  $^{119}\text{Sn}$  MAS NMR spectra of 10 Sn-Beta acquired with different modalities: (from top to bottom):  $^{119}\text{Sn}$  MAS NMR single Hahn echo spectra;  $^{119}\text{Sn}$  CPMG MAS NMR in cross polarisation and  $^{119}\text{Sn}$  CPMG MAS NMR in direct excitation..

Furthermore, the CPMG spectra were acquired in two different methods, in direct excitation (DE) and in cross-polarisation (CP). Direct excitation methods, as implied by the name, directly excite the Sn nuclei at its own radiofrequency. Cross polarisation instead relies on the transferring of the magnetic polarisation from an excited heteronuclei (in this case  $^1\text{H}$ ) to the target nuclei, which is  $^{119}\text{Sn}$ . The transfer of the spin can happen only if the two nuclei are in spatial proximity; therefore, the presence of hydrogen nuclei around Sn is a necessary condition. In Figure 20 the CPMG  $^{119}\text{Sn}$  MAS NMR spectra acquired in DE and CP of fresh catalyst, used in methanol and used in 10:90  $\text{H}_2\text{O}:\text{MeOH}$  are displayed.

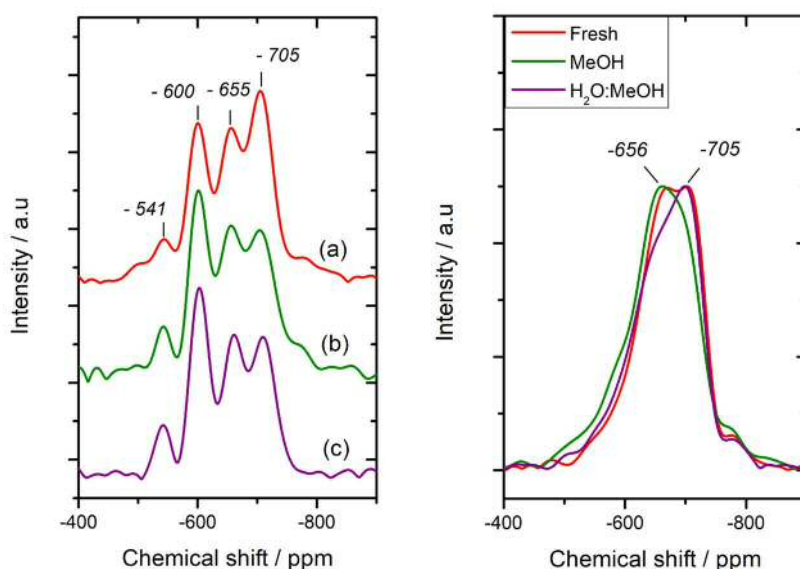


**Figure 20.** (Left)  $^{119}\text{Sn}$  DE-CPMG MAS NMR spectra of 10Sn-Beta prior to (a) and following reaction in pure methanol (b) and 10:90  $\text{H}_2\text{O}:\text{MeOH}$  (c). (Right)  $^{119}\text{Sn}$  CP-CPMG MAS NMR spectra of 10Sn-Beta prior to and following reaction in pure methanol and 10:90  $\text{H}_2\text{O}:\text{MeOH}$ .

$^{119}\text{Sn}$  DE-CPMG MAS NMR spectra (Figure 18 Left) show clearly that at least four main Sn species are present in the samples. As indicated in detailed MAS NMR studies available in the literature, the peaks at -541 and -600 ppm are indicative of penta-coordinated Sn in the framework, and  $\text{SnO}_2$ -like species, respectively.<sup>20</sup> The peaks at -605 and -705 ppm are in the



region of the framework hydrated Sn active site. It is important to say that any quantification of the species cannot be done since their relaxation time  $t_1$  is unknown. However, semi-quantitative analysis based on the relative ratio of the peaks is possible. Examining the three different DE spectra, it can be seen that there is a growth of the  $\text{SnO}_2$  signal in both samples after reaction. However, surprisingly the ratio of the signals of the two framework species is very similar after both reactions, suggesting that no additional restructuring of Sn happened in the absence of water during the GI reaction.

A very different situation was observed in the CP spectra. In fact, the broad signal of the sample reacted in MeOH, highlighted a major contribution from the peak at -655 ppm, while opposite situation was observed in the spectra of 10:90  $\text{H}_2\text{O}:\text{MeOH}$  samples, where the major contribution at the signal seems to arise from the peak at -705 ppm. It is also important to underline that in the fresh samples the peaks at -655 and -705 ppm seem to contribute equally to the overall signal, meaning that actual changes happened during the reaction. Clearly, having protons in the surroundings of the Sn site at -705 ppm is a necessary conditions for the site to be active, in fact, when the samples is deactivated, the intensity of this signal is much lower, almost absent. By combining the DE and CP spectra it can be suggested that during the two reactions the speciation of the Sn species does not change dramatically, as indicated by the same ratio of -655 and -705 ppm signal in DE. However, a change in the local environment, for example a second coordination sphere around specific active site, and this can give rise to the differences observed in the CP spectra.

It is know from the literature, that Sn site with hydrogen donor group in the vicinity (from a silanol or a coordinated water molecule) are more active for sugar isomerisation.<sup>21,22</sup> It can therefore be proposed that having a proton in that specific active site (-705 ppm) helps to preserve the activity of the reaction. Of course, the presence of water in the stream could help to maintain that proton in place. However, the nature of the loss of that proton is not possible to be defined by this technique, therefore only speculation can be made at this stage. Reasonably, in the absence of water, it can be proposed that a ligand exchanged, or an alkoxylation of a  $\text{Sn}-\text{OH}$  to  $\text{Sn}-\text{OCH}_3$ , or a condensation of an open form with a vicinal silanol to form  $\text{Sn}-\text{O}-\text{Si}$  could occur. Following this model, it can be hypothesised that the true active form is the open form, and having a constant stream of water obviously helps to maintain the Sn site in this form. On the other hand, when methanol is the only solvent, the possibility of this “continuous maintenance” of the active form is inhibited. In order to verify the viability of this hypothesis, which is that water favour the formation of Sn-OH sites, <sup>29</sup>Si

MAS NMR has been employed. In fact, when Sn-O-Si is hydrolysed, two hydroxyl species are formed, one being Sn-OH, the second being Si-OH.  $^{29}\text{Si}$  MAS NMR is an established technique for identifying the degree of hydrolysis or the Si-O-Si bonds. Around -110 ppm are normally located resonances called  $Q_4$  and are characteristic of  $\text{Si}(\text{OSi})_4$ , hence a non-hydrolysed tetrahedral silica species. In contrast,  $Q_3$  species present one bond hydrolysed and are then depicted like  $\text{Si}(\text{OSi})_3(\text{OH})$ , their resonances can be found around -100 ppm.<sup>23</sup> The three samples analysed by  $^{119}\text{Sn}$  MAS NMR were successively analysed also by  $^{29}\text{Si}$  MAS NMR and the spectra are overlaid, normalised against the highest signal, and shown in figure 21.

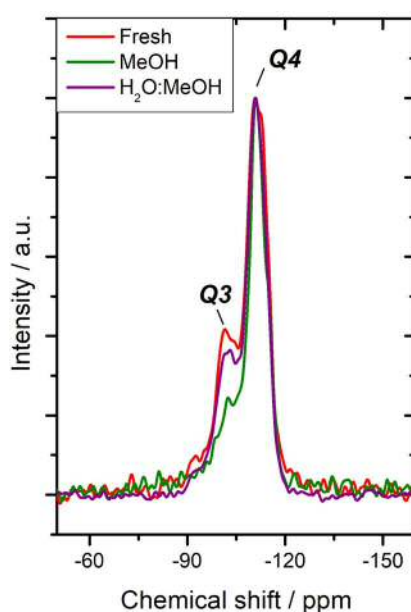


**Figure 21.**  $^{29}\text{Si}$  MAS NMR of Sn-Beta, prior to reaction, and following GI in MeOH and 10:90 H<sub>2</sub>O:MeOH.

It can be clearly seen that the fresh sample shows the two features,  $Q_4$  and  $Q_3$ , with the first being clearly the major species, as expected since most of the tetrahedral silicon unites are connected between them in the zeolite framework by Si-O-Si bonds. When the used samples are analysed, the first thing that can be noticed is a decreasing of the  $Q_3$  signal, which is related related to  $\text{Si}(\text{OSi})_3(\text{OH})$  species. It is important to say that a when this silicon is adjacent to a framework Sn site, that Sn must be present as the open form. It can be seen from the spectra that the  $Q_3$  signal is remarkably decreased after the reaction in pure methanol, whilst in the presence of water most of its intensity is preserved.

The decreased of  $Q_3$  feature indicates a loss of a silanols, and there a are two ways this feature it can be lost: i) the silanol can be lost by condensation, to form a  $Q_4$  type, or ii) it can be lost by alkoxylation to form a  $\text{Si}(\text{OSi})_3\text{OR}$ . Even though the real cause of this loss cannot be determined at this stage, these findings are in very good agreement with the “loss of a

proton" observed by  $^{119}\text{Sn}$  CP-CPMG MAS NMR. Indeed, it can indicate that, in an analogous way of the silicon species, Sn can lose a vicinal proton by condensation with a silanol or be alkoxylation by a methanol molecules, leading to a loss of the -705 ppm signal. However, it must be taken in consideration the fact that the DE spectra of the Sn remain unchanged. This would be possible if the open and closed form would have the same chemical shift. Otherwise, it can be hypothesised that the Sn speciation does not change, but what it might changed is the local environment, such as the second coordination sphere of active site. It can be proposed that water can preferentially surrounded the active site, without changing its chemical nature, but in some way having a beneficial effect in terms of catalytic performance. However, more detailed NMR studies, by groups dedicated to MAS NMR spectroscopy, are clearly required to make a more detailed conclusion regarding the ultimate active site structure.

#### 6.2.13 Washing regeneration

If the deactivation of the catalyst happened by condensation of the open Sn sites, or alkoxylation due to the absence of water, then re-introduction of water should in principle restore the original active form, or the original local chemical environment. Indeed, it has been reported that the dissociative adsorption of water to form Sn-OH and Si-OH species is facile in Sn-Beta, particularly at the reaction temperatures employed in this study. Therefore, to prove from a mechanistic point of view this hypothesis, a set of experiments, consisting in washing the deactivated catalyst with different solvents and solvent mixture were carried out, and the activity after the washing treatment was measured.

After 50 h of GI reaction performed in MeOH, the catalyst was washed with four different treatments: i) 12 h washing with pure MeOH, ii) 12 h washing with 10:90  $\text{H}_2\text{O}$ :MeOH, iii) 20 h washing with 10:90  $\text{H}_2\text{O}$ :MeOH and iv) 2 h washing with pure water. Same flow rate and same temperature of the reactor (110 °C) were kept during the washing. Once the washing was terminated, the 1 wt. % glucose in pure methanol solution was reintroduced over the catalyst, and the reaction was carried out normally for a second cycle. Figure 22 shows the glucose conversion versus time on stream plot of the washing experiments. As can be seen, almost full regeneration of the catalyst can be achieved by low temperature solvothermal regeneration. However, only in the case of the washing with 10:90  $\text{H}_2\text{O}$ :MeOH the activity was recovered; partially in the case where washing was carried out for 12 h, and fully when the reaction was performed for 20 h. On the other hand, no activity was performed when

pure methanol and pure water were employed as solvents. These experiments pointed out the reversible nature of the deactivation and the fact that re-introducing water after reaction can restore the initial activity could suggest that having water present while the reaction is performing can act as an *in situ* regeneration of the active site.

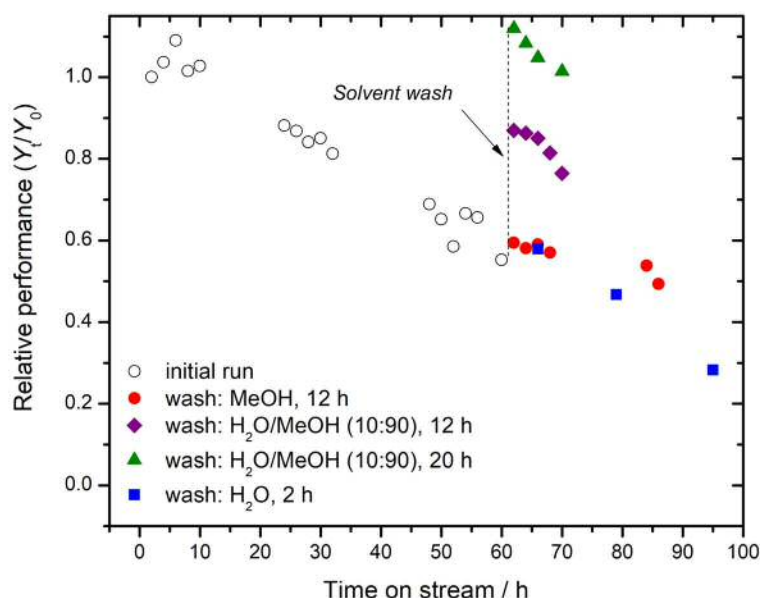


**Figure 22.** Regeneration of Sn-Beta performed by washing the catalytic bed with different solvents/mixture for different time, following an initial reaction of GI in pure methanol. Second cycles were also performed in pure methanol.

In order to have a better insight about the Sn speciation before and after the washing,  $^{119}\text{Sn}$  MAS NMR was performed on the used and the regenerated by washing catalysts and shown in figure 23.

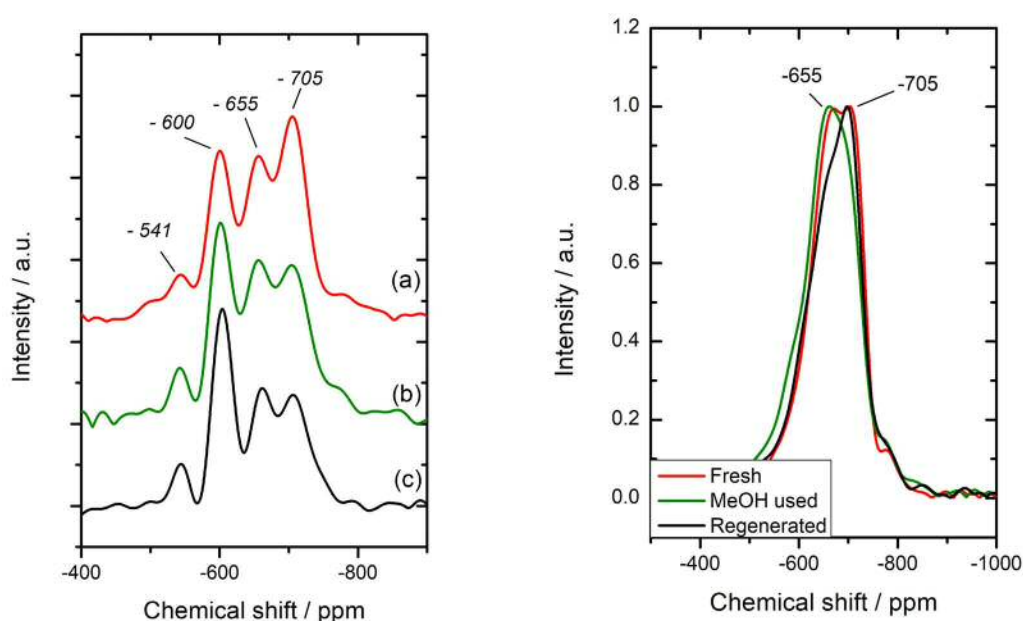


**Figure 23.**  $^{119}\text{Sn}$  CPMG MAS NMR spectra of 10 Sn-Beta (a) fresh, (b), used in Methanol and (c) regenerated by washing with 10:90 H<sub>2</sub>O:MeOH, acquired in (Left) direct excitation and (Right) cross polarisation.

As in the previous case, no difference in Sn speciation can be observed by  $^{119}\text{Sn}$  DE-CPMG MAS NMR, in fact the ratio of the three Sn species remains substantially unchanged, before and after the washing. However, when  $^{119}\text{Sn}$  CP-CPMG MAS NMR was performed on the catalyst series, it clearly shows that the NMR signal at -655 ppm decreased in order to favour the signal at -705 ppm, as observed when the reaction was carried out in the mixture solution. This experiment clearly shows that water, also when is introduced after the reaction, brings about a positive effect. The fact that it regenerates the sample at the same reaction condition strongly suggests that having water during the reaction can mitigate the deactivation of the active site. Preliminary  $^{29}\text{Si}$  and  $^{119}\text{Sn}$  MAS NMR study suggests that water do not change the Sn speciation, as demonstrated by the unchanged DE Sn spectra, but may have an effect on the coordination sphere of the active site, as suggested by the change in the CP signal, which is only possible when proton are in the vicinity of the Sn.

### 6.3 Conclusions

This work showed the outstanding effect of the presence of water during sugars conversion in continuous flow, both for glucose isomerisation and methyl lactate formation, underlining the universality of the effect, since the two reaction are performed under very different condition (temperature and contact time). Quantities as low as 1 wt.% of water could increase the stability of the process by an order of magnitude; besides, activity and selectivity were also positively affected.

Characterisations on the used catalysts were performed in order to indicate a cause of deactivation consequent effect of water. Although many techniques, like TGA, TPD-MS, XRD, porosimetry analysis, were used, no major difference between the samples could be find. In fact, the textural properties were identical in the presence or not of small amount of water. A slightly higher accumulation of carbonaceous deposition was found when the MeOH alone was used. However, the extent of this effect was not sufficient to be solely responsible for the differences observed in stability. All this negative response pointed toward to a more subtle effect occur during continuous operation.

With the use of more sophisticated techniques, such as  $^{119}\text{Sn}$  MAS NMR, with ability to probe directly the Sn, a clearer picture could be drawn. Sn NMR indicated that the speciation of active site was changed at the end of the two reactions, but a remarked difference was possibly found in the local environment of the Sn. In fact cross polarisation  $^{119}\text{Sn}$  NMR and  $^{29}\text{Si}$  NMR suggested that a loss of a proton near the Sn could occurred during the reaction performed in pure MeOH, while the same proton is retained when water is present. However, the exact nature of this proton(s) is not yet apparent. It can be hypothesise that it belongs to the oxygen atom present in the open form of the Sn active site, believed by many to be the most active form of Sn in the catalyst. However, this is only a speculation, and no characterisation studies made so far can really identify the real nature of the active site. However, it was understood that the presence of small quantity of water could preserved in the optimal way the surrounding of the active site, acting as a *in situ* form of catalyst regeneration procedure. In fact, by washing a partially deactivated catalyst with a solution of water, activity of the catalyst could be almost totally recovered.

Nevertheless, many points are still uncovered. The biggest of all, is what water does at a mechanistic and molecular level to the active site. To achieve this insight, however, development of *in operando* techniques are clearly essential, and will evidently need to be the focus of future research studies.

## References

- <sup>1</sup> Y. Román-Leshkov, M. Moliner, J. A. Labinger, M. E. Davis, *Angew. Chem. Int. Ed.*, 2010, **49**, 8954.
- <sup>2</sup> US Department of Agriculture. (<https://www.ers.usda.gov/topics/crops/sugar-sweeteners/background/>)
- <sup>3</sup> L. T. Fan, M. M. Gharpuray, Y.-H. Lee, *Cellulose Hydrolysis*, Springer, Berlin, 1987.
- <sup>4</sup> W. S. Mok, M. J. Antal, G. Varhergyi, *Ind. Eng. Chem. Res.*, 1992, **31**, 94.
- <sup>5</sup> M. Moliner, Y. Román-Leshkov, M E. Davis, *Proc. Nat. Acad. Sci.*, 2010, **107**, 6164.
- <sup>6</sup> A. A. Rosatella, S. P. Simeonov, R. F. M. Frade, C. A. M. Alfonso, *Green Chem.*, 2011, **13**, 754
- <sup>7</sup> E. De Jong, M. A. Dam, L. Sipos, G.-J. M. Gruter, *ACS Symposium Series*, 2012, **1105**, 1.
- <sup>8</sup> J. D. Lewis, S. Van der Vyver, A. J. Crisci, W. R. Gunther, V. K. Michaelis, R. G. Griffin, Y. Román-Leshkov, *ChemSusChem*, 2014, **7**, 2255
- <sup>9</sup> Y. Román-Leshkov, C. J. Barret, Z. Y. Liu, J. A. Dumesic, *Nature*, 2007, **447**, 982.
- <sup>10</sup> M. S. Holm, S. Saravanamurugan, E. Taarning, *Science*, 2010, **328**, 602.
- <sup>11</sup> S. Tolborg, I. Sádaba, C. M. Osmundsen, P. Fristrup, M. S. Holm, E. Taarning, *ChemSusChem*, 2015, **8**, 613.
- <sup>12</sup> A. Sølvhøj, E. Taarning, R. Madsen, *Green Chem.*, 2016, **18**, 5448.
- <sup>13</sup> S. Bhosale, M. Rao, V. Deshpande, *Microbiol. Rev.*, 1996, **60**, 280.
- <sup>14</sup> R. M. Ravenelle, F. Schubler, A. D'amico, N. Danilina, J. A. Van Bokhoven, J. A. Lercher, C. W. Jones, C. Sievers, *J. Phys. Chem. C*, 2010, **114**, 19582.
- <sup>15</sup> O. Levenspiel, *Chemical Reaction Engineering*, John Wiley & sons, New York, 3<sup>rd</sup> edn., ch. 21, pp. 473.

- 
- <sup>16</sup> S. Saravanamurugan, A. Riisager, E. Taarning, S. Meier, *ChemCatChem*, 2016, **8**, 3107.
- <sup>17</sup> S.-J. Hwang, R. Gounder, Y. Bhawe, M. Orazov, R. Bermejo-Deval, M. E. Davis, *Top. Catal.*, 2015, **58**, 435.
- <sup>18</sup> W. R. Gunther, V. K. Michaelis, M. A. Caporini, R. G. Griffin, Y. Roman-Leshkov, *J. Am. Chem. Soc.*, 2014, **136**, 6219.
- <sup>19</sup> Y. G. Kolyagin, A. V. Yakimov, S. Tolborg, P. N. R. Vennestrom, I. I. Ivanova, *J. Phys. Chem. Lett.*, 2016, **7**, 1249.
- <sup>20</sup> A. V. Yakimov, Y. G. Kolyagin, S. Tolborg, P. N. R. Vennestrom, I. I. Ivanova, *J. Phys. Chem. C*, 2016, **120**, 28083
- <sup>21</sup> G. Li, E. A. Pidko, E. J. M. Hensen, *Catal. Sci. Technol.*, 2014, **4**, 2241
- <sup>22</sup> W. N. P. Van der Graaff, G. Li, B. Mezari, E. A. Pidko, E. J. M. Hensen, *ChemCatChem* 2015, **7**, 1152–1160
- <sup>23</sup> J. Dijkmans, M. Dusselier, W. Janssens, M. Trekels, A. Vantomme, E. Breynaert, C. Kirschhock, B. Sels, *ACS Catal.*, 2016, **6**, 31.

## ***7. Conclusions and pertaining challenges***

### **7.1 Conclusions**

Sn-Beta have been extensively studied for almost 20 years, during which period many different aspects of its chemistry have been covered, from its reactivity for a variety of reactions, to the methods of its synthesis. This extended investigation appointed Sn-Beta as being one of the most promising materials for biomass valorisation processes. Despite its academic success and attention, however, Sn-Beta has not yet found any employment in any commercial process. After a detailed analysis of the existing literature (Chapter 1), this can be attributed to the absence of essential information relevant to an accurate evaluation of its feasibility as a catalyst. In particular, not enough emphasis has been placed on the productivity, the stability, and the reaction engineering elements of this material throughout its history. For this reason, the focal point of this thesis has been to study the crucial parameters necessary for developing intensified biomass valorisation processes catalysed by Sn-Beta.

One of the main bottlenecks during the development of Sn-Beta has been its difficult synthesis. In particular, the classical hydrothermal synthesis requires long times, highly hazardous reactants and can only proceed at low metal contents. Together, these have greatly discouraged its production at larger scales. For this reason, many years of research of Sn-Beta have been focused on the search of alternative synthetic methods to the classical



hydrothermal synthesis. Post synthetic preparations of Sn-Beta have recently become a first choice alternative to the classical synthesis, and they have been proven to overcome the main drawbacks of the first synthetic method. Amongst these, SSI has been shown to be fast and scalable, and capable of incorporating high metal contents of Sn. All of these characteristics have made this material very appealing from a commercial point of view. Despite the great promises held by Sn-Beta made by SSI, no detailed studies were carried out in order to establish its catalytic potential for biomass conversion reactions. Therefore, the first part of this thesis has focused great attention in investigating the intrinsic activity of a series of Sn-Beta with metal loading content between 2 and 10 wt. %. The study was carried out by probing the intrinsic kinetic behaviour of the material for the transfer hydrogenation (TH) of cyclohexanone (CyO) to cyclohexanol (CyOH), and for the isomerisation of glucose to fructose (GI). For both reactions, it has been found that the intrinsic activity was relatively constant for catalysts with metal loadings between 2 and 5 wt. % (denoted as XSn-Beta, where X is the Sn loading in wt. %). However, at higher loadings the activity constantly decreased. To relate the observed catalytic behaviour with structural characteristic of the materials, several characterisation techniques were performed on the catalyst series. Particularly, from  $^{119}\text{Sn}$  MAS NMR spectroscopy, it was observed that in the materials containing up to 5 wt. % of Sn, the speciation of Sn remained relatively consistent, with the major fraction of Sn being in the active, framework form Sn, and a smaller fraction being present as inactive  $\text{SnO}_2$  sites. However, at increasing loadings a more consistent growth of the inactive  $\text{SnO}_2$  phase was observed. The increasing amount of inactive  $\text{SnO}_2$  at increasing Sn loadings was found to be in very good agreement with to the kinetic data observed. In particular, when the most (2Sn-Beta) and the least (10Sn-Beta) active samples are compared, the calculated intrinsic activity of the lowest loading material was found to be approximately double that of the highest metal loading catalyst. However, due to its five-fold higher content of material, 10Sn-Beta was found to be the most productive material, in terms of activity per unit mass of catalyst, making this catalyst the most suitable for intensification of the reaction.

Along with the difficult material synthesis, another bottleneck in the research of Sn-Beta was evident from the absence of intensification studies during biomass valorisation reactions. In particular, almost no information was available about the lifetime of this catalyst at the commencement of this thesis, which is one of the main parameters used in order to determine the actual industrial potential of the material. In order to fill this knowledge gap, a series of stability studies were carried out employing continuous flow reactors, which

allowed the stability of the catalyst to be studied at high turnover numbers. The study was carried out with an increasing gradient of challenges, starting from the stability study of Sn-Beta performing the model TH reaction of CyO to CyOH in organic media, moving to TH of furfural (FF) and its consecutive etherification to 2-(butoxymethyl)furan (BMF), and finally exploring the most challenging GI reaction performed in mixed solvents, both organic and aqueous media.

In Chapter 4 the stability of Sn-Beta for the TH of CyO has been studied in continuous flow. It has been shown that the catalyst possesses an exceptional stability, being able to perform the reaction continuously for more than 23 days with only 40 % of loss of its initial activity. After this period of time, investigations on the causes of deactivation were carried out employing several characterisation techniques on the used bed. These demonstrated that during the reaction, the crystalline structure was preserved and no major restructuring of active sites occurred. In contrast, evidence of deactivation was found by porosimetry analysis, TGA and NMR extraction studies. A 50 % decrease of the pore volume was observed by porosimetry, in good agreement to TGA and NMR found that the product, CyOH, was preferentially retained in the material during the reaction. This effect is commonly referred as pore fouling and is one of the most common modes of deactivation of zeolites. To indirectly confirm these findings, thermal regeneration was carried out on the catalyst by heating it to 550 °C, and full activity was recovered, showing the reversible nature of the deactivation. Having identified the main contribution of deactivation, experiments aimed of its mitigation were applied. In particular, the temperature of the reaction was increased in order to favour desorption of the CyOH product, thus minimising its accumulation. It was found that the treatment was effective and other than enhancing the catalyst lifetime, the productivity was substantially increased.

Encouraged by the positive results of found during the TH of CyO, a different reaction was then probed in continuous flow. The TH of FF was carried out at similar conditions and in the same organic medium, and it was observed that following the TH step to form FA, the reaction proceeded further through etherification of the alcohol to form BMF, a molecule belonging to a class of potential bio fuels. However, it was found that when performing the reaction in continuous flow, the etherification step suffered a much more dramatic deactivation compared than the TH step, resulting in a very low selectivity of the BMF at high substrate turnover. In order to obtain a more selective process for BMF, introduction of Brønsted acid functionality was explored, as such species are known to be superior in activity towards etherification reaction. Different ways to introduce Brønsted functionality

were investigated. Firstly, physical mixtures of Sn-Beta and H-Beta were explored. The optimal ratio between the two materials were studied in batch mode, and successively tested in continuous flow. Unfortunately, the utilisation of a physical mixture did not bring any obvious advantage in terms of continuous BMF selectivity. TGA analysis indicated that the presence of H-Beta led to a very fast formation of high molecular weight compounds that could have likely lead to the deactivation of the material. A different approach was followed in order to make a bifunctional catalyst containing Sn and Al in the same material. Such a catalyst was initially obtained by performing SSI of Sn into a partially de-aluminated Beta zeolite. A dramatic improvement of BMF selectivity (increased to 75% vs. the original 35 % of the only Lewis acid material, after 800 substrate turnovers) was observed in the continuous flow reaction of TH/tandem reaction. However, very low TH activity was observed.  $^{119}\text{Sn}$  MAS NMR revealed that incorporation of Sn in a partial de-aluminated material was not effective, as indicated by a big fraction of inactive  $\text{SnO}_2$  being observed in the NMR spectrum. To overcome this issue, Sn and Al were incorporated by SSI together into a totally de-aluminated Beta framework. Finally, a material with high TH activity and BMF selectivity was obtained, and under optimised conditions it could run with BMF selectivity higher than 70 % for more than 2000 substrate turnover, showing to be the most stable catalyst in literature for this kind of tandem reaction.

Sn-Beta has shown that it can performed excellently well in continuous operation in organic media. However, to date there are no experimental evidence that continuous operation are possible when the media is water or when water is present in certain amount in the reaction stream. Sn-Beta was initially reacted with glucose solutions in water and methanol (MeOH) as solvents. While it preserved 50 % of its activity after 48 h of reaction in MeOH, in water the loss of activity was dramatic, and full deactivation was found after just 24 h. Even more concerning were the results found after attempting to regenerate the catalyst post water reaction, in which case no activity was recovered, though full activity was recovered in the case of the MeOH reaction. X-ray diffraction analysis confirmed that the zeolite structure was severely damaged after the reaction in water, while it was found intact in the case of the reaction in MeOH. Successively, it was explored the effect of presence of water in methanol. It was observed that introduction of 10 wt. % or less of water in MeOH, greatly improved the stability of the catalyst. The extent of deactivation was quantified by calculating a deactivation constant ( $k_d$ ) and it was found that the improvement in stability upon introduction of small quantity of water (1 – 10 wt. %) was of 1 order of magnitude compared to the reactions performed in pure MeOH. Furthermore, the addition of water

increased also the selectivity to fructose, showing a full beneficial effect. More astonishing was when these results were compared with the ones found by project collaborators at Haldor Topsøe. The same catalyst was employed in the high temperature conversion of sugars, in which the retro-Aldol reaction is exploited for the continuous production of methyl lactate. They found that introduction of 1 wt. % of water in the methanol solution improved substantially the stability of the reaction, suggesting that the effect of water applied on the catalyst rather than on the specific reaction. Successively, several characterisations techniques were employed in order to rationalise the observed water-effect. Even though a conclusive answer could not be formulated,  $^{119}\text{Sn}$  NMR spectroscopy suggested that the water might have a big impact in hydrating and maintaining hydration of certain active sites, while the Sn speciation looked like unchanged during the process with and without water. By exploiting this characteristic it was possible to regenerate the catalyst after the reaction performed in methanol by simply washing the catalyst with a MeOH/H<sub>2</sub>O mixture, which was convenient because it could be done at a low temperature and with no need of remove the reactor from the plug flow reactor.

## 7.2 Pertaining challenges and final remarks

Despite the fact that many challenges have been tackled and solved during this work, many new questions have also been generated. SSI methodology resulted in a fast and reproducible method for synthesising Sn-Beta catalyst. However, it has been observed that the efficiency of Sn incorporation becomes poorer as the metal loading increases, leading to the formation of inactive SnO<sub>2</sub>. The cause of this behaviour has not been explored. Therefore, a mechanistic study on this phenomenon would be necessary to shed light on the process in act. In particular, *in situ* techniques, such as DRIFT, DRUV-Vis, Raman and XRD could be employed in order to follow the process of incorporation of the metal in the framework before and during the calcination step, and ideally would be crucial to individuate at which conditions SnO<sub>2</sub> formation starts to become relevant. Furthermore, different solid sources of Sn could be employed, such as commercially available Sn(IV)acetate and the Sn(IV)chloride pentahydrate. This would be done in order to explore how the organic ligand and the molecule size would make a difference in the incorporation of the metal in the zeolite framework.

In addition, the use of different methodology for silanol formation could be explored. In fact, acid treatments remove predominantly Al atoms from the framework. On the other hand, it is known that alkaline treatment instead removes Si atoms from the framework, making new silanol sites in which Sn could be inserted. In this way, the silanol nests as created might be located in different part of the framework, having thus a possible different effect on the metal incorporation efficiency. Such a method could also be used as a possible synthesis of bifunctional catalyst, which has been shown to possess superior performance in tandem reactions. In fact, by de-silicating an aluminosilicate material, it could be possible to remove Si atoms and leave behind Al in the framework. Successively, addition of Sn could be attempted in order to see if, by creating different kind of silanol nest, the incorporation of the Lewis acid could be more efficient.

Although it was shown that Sn-Beta possesses an excellent stability during continuous processes in organic media, most of biomass valorisation processes required to be run in water or with a certain amount of water present. On this regard, it has been shown that up the stability during GI is excellent with up to 10 wt. % of water present in MeOH solvent. However, this is true for post-synthetic Sn-Beta made by SSI. At this point, two big research topics might be necessary and complementary to this work: to study the influence of type of synthesis and to study the influence of the type of structure. It is well established that post synthetic and hydrothermal stannosilicates possess different characteristics; one above all is the different hydrophilicity. In fact, hydrothermal synthesis of Sn-Beta leads to a material with higher hydrophobicity, due to the lower number of structural defect *i.e.* silanol groups.<sup>1</sup> Even though the use of the hydrothermal synthesised material is not desirable for its problematic synthesis (see 1.6.1), the comparison of the stability during GI reaction with the post-synthetic material could be crucial to understand how hydrophobicity and hydrophilicity play a role in determining the stability of the catalyst when water is present. Other than using hydrothermal material to probe the effect of hydrophobicity, increased hydrophobicity could also be introduced to the post synthetical material by silylation.<sup>2</sup>

Other parameters that could be explored in order to probe the stability of GI process is the type of zeolite structure. Some examples are present in literature where Sn has been incorporate inside a zeolite with a different structure of the Beta.<sup>3</sup> However their stability under hydrothermal conditions is unknown. For this work many parameters have to be considered, such as the efficiency of Sn incorporation and the diffusion of sugars in the pore of the zeolite, therefore cutting off some structure characterised by small pore aperture, such MFI. Besides, in order to improve the diffusive properties of the zeolite, and to mitigate

possible pore blocking, hierarchical zeolite could represent a solution, as they already shown to be beneficial during the continuous flow performance of BVO reaction.<sup>4</sup>

Ultimately, it would be greatly helpful and insightful the development of suitable *in operando* reactors, in order to monitor the changes happening to the catalyst under real reaction conditions, in order to have a direct relationship between structural changes and kinetics. Techniques such as UV-Vis, Raman, FT-IR are all suitable to be used *in operando* reactors and would give very indicative evidence on the catalyst changes and hopefully they could relates back with changes in kinetics. However, an accurate design of the reactor is needed and many considerations have to be taken. An optical window installed on the reactor have to be transparent to the radiation and at the same time it has to possess mechanical and chemical strength in order to resist to chemicals and to the moderate pressure required for extended periods of time. Despite all the challenges that the development of this dedicated reactor required, it is widely accepted that the development and usage of such apparatus would bring new and stronger knowledge in the deactivation mechanism of heterogeneous catalysts during liquid phase processes.

To conclude, this thesis work adds an important piece of research on Sn-Beta that was almost completely unexplored before. In fact, it has been demonstrated that Sn-Beta is capable to perform as a catalyst for relative long amounts of time during continuous operation in organic media. Contrary to very common beliefs that this material is water tolerant, GI reaction in aqueous media showed that it is definitely not, and water is actually not a good solvent for continuous operation. Despite its deleterious effect when it is alone, water has been proven to increase dramatically the stability of the catalyst when it is present in small quantities permitting for the first time to perform GI continuously without suffering extensive deactivation.

## References

<sup>1</sup> J. C. Vega-Vila, J. W. Harris, R. Gounder, *Journal of Catalysis*, 2016, **344**, 108.

<sup>2</sup> P. A. Zapata, Y. Haung, M. A. Gonzalez-Borja, D. E. Resasco, *Journal of Catalysis*, 2013, **308**, 82.

<sup>3</sup> W. N. P. van der Graaf, C. H. L. Tempelman, E. A. Pidko, E. J. M. Hensen, *Catal. Sci. Technol.*, 2017, **7**, 3151.

<sup>4</sup> A. Al-Nayili, K. Yakabi, C. Hammond, *J. Mater. Chem. A*, 2016, **4**, 1373.

## **Acknowledgements**

In first place, I would like to thank Ceri for giving me the opportunity to do my PhD in his group. Without his advices and constant guidance the quality of my work would have not been the same. But most of all, I thank him for the enjoyable time and for the positive atmosphere that he created within the group.

A special thanks also to Nikos, whose support and scientific (and not) advices have been useful and valuable during this period.

Also thanks to the Haldor Topsøe team, which fruitful collaboration and long meetings have been very inspiring for my work.

Finally, big thanks to all the people whom I worked side by side every day and that contributed, some directly and some indirectly, to this work.